



University  
of Glasgow

Teka, Ibrahim (2011) *Diamidine transporters of Trypanosoma brucei*. PhD thesis.

<http://theses.gla.ac.uk/2640/>

Copyright and moral rights for this thesis are retained by the author

A copy can be downloaded for personal non-commercial research or study, without prior permission or charge

This thesis cannot be reproduced or quoted extensively from without first obtaining permission in writing from the Author

The content must not be changed in any way or sold commercially in any format or medium without the formal permission of the Author

When referring to this work, full bibliographic details including the author, title, awarding institution and date of the thesis must be given

# **Diamidine Transporters of Trypanosoma brucei**

**Ibrahim Ali Teka**

Thesis submitted in fulfilment of the requirements for  
the degree of Doctor of Philosophy

**Institute of Infection, Immunity & Inflammation  
College of Medical, Veterinary & Life Sciences  
University of Glasgow**

**March 2011**

## Abstract

Human African trypanosomiasis (HAT), a lethal disease caused by infection with *Trypanosoma brucei rhodesiense* or *Trypanosoma brucei gambiense*, affects a significant number of people in sub-Saharan Africa. Related trypanosome species are also responsible for veterinary trypanosomiasis in many species of domestic and wild animals, causing disruption to agricultural and economic development in one of the world's poorest areas. Current control and management of the disease mainly relies on a handful of trypanocides that have been in use for over 50 years. The treatment is associated with numerous of limitations such as drug toxicity, affordability and, most worryingly, increasing rates of treatment failure due to spread of parasites resistant to the existing drugs. Therefore, development of new drugs against Human African Trypanosomiasis is much needed.

Trypanosomes are incapable of *de novo* synthesis of the purine rings, and since purines are essential for many cellular functions (e.g. nucleic acid synthesis, energy metabolism) this means the parasites have an absolute requirement for exogenous purines. Several nucleoside and nucleobase transporters have been identified in *T. brucei brucei*, including the P1 and P2 adenosine. These transporters have recently received a great deal of interest as potential drug targets as possible determinants of drug resistance.

The P2 nucleoside transporter is one of the best-studied transporters and it has been shown to facilitate entry of arsenical and diamidine trypanocides, such as melarsoprol and pentamidine. Loss of this transporter appears to confer resistance to some of these drugs *in vitro*. It has been shown that pentamidine is taken up by two additional transporters named high affinity pentamidine transporter (HAPT1) and low affinity pentamidine transporter (LAPT1). These transporters have been studied based on their kinetic role of drug uptake and neither has been characterised at the molecular level.

The main aims of the project were to study the HAPT1 transporter in detail, including identification of substrate recognition determinants, involvement in

transport of diamidine trypanocides other than pentamidine, and the cloning of the genes coding for HAPT1 and /or LAPT1 from *T. b. brucei*.

It was found that the main veterinary drug, the diamidine diminazene, was also transported by HAPT1, albeit much less efficiently than pentamidine. This provided new insights into the causes of drug resistance for African trypanosomes, in particular, the well-documented cross-resistance between melaminophenyl arsenical drugs and diamidines.

A large number of diamidine analogues and other compounds were tested for inhibition of HAPT1 and their inhibition constants were determined. This identified the essential characteristics for high affinity interaction between substrate and the transporter-binding pocket. This study will aid the design of new ligands and inhibitors for this drug transporter.

Furthermore, the gene for HAPT1 was identified as AT-E, a close analogue of TbAT1, which encodes for the P2 transporter. Two distinct alleles, named AT-E1 and AT-E2, were identified in wild-type *T. b. brucei*, probably representing a single gene locus. Knockdown of AT-E expression using RNAi significantly decreased HAPT1 in both bloodstream forms and procyclics. Expression of AT-E was reduced in the B48 pentamidine resistant line that lacks HAPT-mediated drug uptake. This project has greatly increased our understanding of the biochemical and molecular nature of HAPT1 transporters in *T. b. brucei*.

# Table of Contents

<b>1</b>	<b>General introduction.....</b>	<b>1</b>
1.1	Human African trypanosomiasis .....	2
1.2	History overview and epidemiology .....	3
1.3	The clinical manifestations of the disease .....	5
1.4	Parasite biology .....	7
1.4.1	Plasma membrane .....	8
1.4.2	Glycosomes.....	9
1.4.3	Mitochondrion.....	9
1.4.4	Acidocalcisomes.....	10
1.5	Taxonomy.....	10
1.5.1	Salivaria trypanosomes .....	11
1.5.2	Stercoraria trypanosomes.....	11
1.6	Lifecycle.....	11
1.7	Diagnosis.....	14
1.8	The control of HAT.....	14
1.9	Treatment of HAT .....	16
1.9.1	Pentamidine .....	17
1.9.1.1	Pentamidine in relation to T. brucei Mitochondrial Membrane Potential (MMP) .....	19
1.9.2	Suramin.....	21
1.9.3	Melarsoprol.....	22
1.9.4	Eflornithine .....	23
1.9.5	Diminazene aceturate.....	25
1.9.6	DB-75.....	26
1.9.7	Nifurtimox .....	26
1.10	Trypanosome molecular biology .....	27
1.11	RNA Interference & Gene Knockout.....	29
1.12	The nucleoside and nucleobase salvage and transportation .....	33
1.12.1	Equilibrative nucleoside transporter (ENT) Family .....	34
1.12.2	Concentrative nucleoside transporter (CNT) Family.....	35
1.13	Structure activity relationship study of the nucleoside and nucleobase transporters .....	36
1.14	Drug Uptake via Nutrient Transporters .....	37
1.15	Overview of the TbAT1/P2 molecular study and its role in drug transportation .....	42
1.16	The molecular basis of the HAPT1 and LAPT1 transporters .....	44
1.17	Transport of pentamidine across the plasma membrane.....	45
1.18	Drug resistance .....	47
<b>2</b>	<b>Materials and methods.....</b>	<b>51</b>
2.1	Cell culture.....	52
2.1.1	Trypanosomes .....	52
2.1.1.1	Growth and maintenance of bloodstream form trypanosomes (BSF) <i>in vitro</i> .....	52
2.1.1.1	Growth and maintenance of procyclic form trypanosomes (PCF) <i>in vitro</i> .....	53
2.1.2	Bacterial strains.....	53
2.2	Preparation of stabilates .....	54
2.3	Monitoring <i>in-vitro</i> cell growth and drug sensitivity .....	56
2.3.1	In-vitro drug sensitivity using Alamar Blue dye.....	56
2.3.2	In-vitro drug sensitivity using propidium iodide assay .....	57
2.3.3	Drug sensitivity by using cell count.....	57
2.4	Transport assays in trypanosomatids .....	58
2.4.1	Collection and purification of bloodstream form T. b. brucei from rat .....	58

2.4.2	Collection and purification of bloodstream and procyclic form <i>T. b. brucei</i> from culture	59
2.4.3	Radiolabeled Uptake Assay in <i>T. brucei</i>	60
2.4.4	Analysis of transport assays data	61
2.4.5	Chemicals used in the transport assays	62
2.5	Selection for high Pentamidine concentrations	63
2.6	Determination of the mitochondrial membrane potential	63
2.7	Molecular techniques	64
2.7.1	Isolation of genomic DNA from <i>T. b. brucei</i>	64
2.7.2	Isolation of total RNA from <i>T. brucei</i>	65
2.7.3	Determination of DNA/ RNA concentration	66
2.7.4	Polymerase chain reaction (PCR)	66
2.7.5	Primer design	67
2.7.6	Agarose electrophoresis of DNA	69
2.8	Cloning techniques	69
2.8.1	Ligation into pGEM-T Easy vector	69
2.8.2	Creation of A-overhang of PCR products	70
2.8.3	Cloning into destination vectors (RNAi vectors)	71
2.8.4	Preparation of chemically-competent <i>Escherichia coli</i>	71
2.8.5	Transformation of <i>E. coli</i>	72
2.8.6	Colony-screening PCR	72
2.8.7	Purification of plasmid DNA	72
2.8.8	DNA sequencing	73
2.9	RNA Interference in <i>T. brucei</i>	73
2.9.1	RNAi fragment design and construction	73
2.9.2	RNAi in <i>T. brucei</i> Bloodstream forms	75
2.9.3	RNAi in <i>T. brucei</i> procyclic forms	77
2.9.4	Transfection of BSF Trypanosomes	78
2.9.5	Transfection of PCF Trypanosomes	79
2.9.6	Selection of RNAi clones	80
2.9.7	Cloning by serial limiting dilution	81
2.9.8	Analysis of Growth Rates	81
2.9.9	Preparation of cDNA	82
2.9.10	Reverse Transcriptase PCR	82
2.10	Southern blot analysis	83
2.10.1	Preparation of the gel, blotting and transfer onto nylon membrane	84
2.10.2	Membrane probe labelling	85
2.11	Software and web resources	86
<b>3</b>	<b><i>The diamidine diminazene aceturate is a substrate for the High Affinity Pentamidine Transporter: implications for the development of high resistance levels in trypanosomes.</i></b>	<b>87</b>
3.1	Introduction	88
3.2	Generation of a new clonal line resistant to high levels of diminazene aceturate	89
3.3	Alamar blue drug sensitivity assays	90
3.4	Transport assays	90
3.5	Results and discussion	90
3.5.1	Pentamidine transport in procyclic <i>Trypanosoma brucei</i> as a model for bloodstream forms	90
3.5.2	Transport of diminazene aceturate in procyclic trypanosomes	94
3.5.3	Resistance profile of a highly diminazene-resistant cell line, ABR	95
3.5.4	Diamidine transport in drug resistant trypanosomes	98
3.6	Conclusion	102
<b>4</b>	<b><i>Structure / Activity relationships of the <i>T. b. brucei</i> High Affinity Pentamidine transporter</i></b>	<b>104</b>

4.1	Introduction.....	105
4.2	Characterisation of HAPT1 recognition motif.....	107
4.3	Results.....	107
4.3.1	Drug Sensitivity Assays .....	107
4.3.2	Drug Uptake Assays.....	109
4.3.3	Structure-activity relationships.....	110
4.3.4	HAPT1 recognition motif.....	111
4.3.4.1	The affect of the two amidine groups on binding.....	111
4.3.4.2	The affect of the position of amidine groups on binding.....	112
4.3.4.3	The effect of the benzene rings on binding .....	114
4.3.4.4	The effect of linker on binding.....	115
4.4	Discussion .....	123
<b>5</b>	<b><i>Development and characterisation of a clonal line resistant to 1 <math>\mu</math>M pentamidine.....</i></b>	<b>127</b>
5.1	Introduction.....	128
5.2	Results.....	129
5.2.1	Induction of resistance.....	129
5.2.2	Cloning out .....	130
5.2.3	In-vitro monitoring cell growth.....	131
5.2.4	Alamar Blue assay and in vitro drug profile.....	132
5.3	Stability of resistance phenotype .....	135
5.4	Pentamidine transport in P1000 cell line.....	136
5.5	Kinetic characterisation.....	136
5.6	Study of Mitochondrial Membrane Potential (MMP) .....	137
5.7	Effect of pentamidine adaptation on expression of AT-E gene and sequencing analysis .....	142
5.8	Discussion .....	144
<b>6</b>	<b><i>Cloning, sequencing, and analysis of the AT-like transporter genes from multiple <i>T. b. brucei</i> lines.....</i></b>	<b>147</b>
6.1	Introduction.....	148
6.2	Identification of AT-like genes.....	150
6.2.1	Polymerase chain reactions and cloning of AT-like sequences.....	151
6.2.2	Sequence analysis .....	154
6.2.3	Southern blot analysis .....	158
6.2.4	Expression of AT-like genes in P1000 in comparison to 427-WT and TbAT1-B48 160	
6.3	Discussion .....	161
<b>7</b>	<b><i>Validation of AT-E as a candidate diamidine transporter.....</i></b>	<b>163</b>
7.1	Introduction.....	164
7.2	Results.....	165
7.2.1	RNAi in bloodstream forms.....	165
7.2.1.1	Plasmid construction and cloning selection.....	167
7.2.1.2	Ligation of the sense fragment .....	167
7.2.1.3	Second step of cloning (insertion of antisense fragment) .....	169
7.2.1.4	Plasmid DNA preparation .....	170
7.2.1.5	Growth Curve after Tetracycline induction .....	172
7.2.1.6	Reverse Transcriptase -PCR showing knockdown of AT-E .....	172
7.2.1.7	[ <sup>3</sup> H]-Pentamidine uptake in bloodstream forms .....	174
7.2.1.8	Drug profile and in vitro drug sensitivity.....	176
7.2.2	RNAi in procyclic forms.....	177
7.2.2.1	Cloning of RNAi/AT-E Constructs.....	178
7.2.2.2	Tetracycline induction and Analysis of growth curve.....	181
7.2.2.3	Reverse Transcriptase -PCR showing knockdown of AT-E.....	182
7.2.2.4	Uptake Assays .....	183
7.2.2.5	Propidium iodide and pentamidine resistance.....	185
7.3	Discussion .....	187

**8 General discussion..... 191**  
**Appendices..... 199**  
**References..... 224**

## List of Figures

Figure 1.1. Distribution Human African trypanosome.....	2
Figure 1.2. Diagram showing the principal structures of the <i>Trypanosoma brucei</i> bloodstream form.....	8
Figure 1.3. Life cycle of <i>Trypanosoma</i> in both mammalian and tsetse fly.....	13
Figure 1.4. General structures of the most commonly used trypanocidals compounds that are licensed for use against African trypanosomiasis.....	17
Figure 1.5. Diagram represents RNAi mechanism in trypanosomatids.....	30
Figure 1.6. Purine transporters in the bloodstream form of the <i>Trypanosoma b. brucei</i> and their substrates.....	38
Figure 1.7. Purine and pyrimidine transporters in the procyclic form of the <i>Trypanosoma b. brucei</i> and their substrates.....	39
Figure 1.8. Phylogenetic tree of protozoan and human ENT family transporters..	41
Figure 1.9. Diagram presents the main pentamidine transporters present in the trypanosomes membrane and their substrates as well as their coding genes. Reproduced from (Bray <i>et al</i> , 2003).....	45
Figure 1.10. Current model showing mechanisms for drug uptake in the trypanosome. TbAT1/P2, <i>T. brucei</i> adenosine transporter 1 (code for P2 activity). HAPT1, High Affinity Pentamidine Transporter. LAPT1, Low Affinity Pentamidine Transporter. TbMRPA, <i>T. brucei</i> multidrug resistance protein A. PTD, pentamidine. MeIB, melarsoprol. MO, Melarsen oxide. T, trypanothione. MeIT, melarsoprol-trypanothione complex. N, nucleus. K, kinetoplast. M, mitochondria. Reproduced from (de Koning, 2008). .....	47
Figure 2.1. Diagram summarises the uptake assay in trypanosomes.....	62
Figure 2.2. Primers designed to amplify AT-A like putative genes.....	67
Figure 2.3. Map of the pGEM-T-Easy plasmid.....	70
Figure 2.4. Sense and antisense RNAi primers were designed to pick a fragment within the AT-E. The sense primer contains KpnI- <i>Bam</i> HI and the antisense primer contains <i>Xba</i> I- <i>Apal</i> .....	75
Figure 2.5. Forward and reverse for the RNAi/AT-E primers. ....	75
Figure 2.6. 411 bp RNAi fragment was amplified with unique primers (bold and underlined).....	76
Figure 2.7. Cartoon presents the RNAi/AT-E construct for blood stream form. ....	76
Figure 2.8. The structure of RNAi vector p2T7Ti.....	78
Figure 2.9. Sequence from a portion of pT27T1 with RNAi/ AT-E insert highlighted in yellow. ....	78
Figure 2.10. Cloning by serial limiting dilution. ....	81
Figure 2.11. DNA is transferred into nylon membrane through capillary transfer..	85
Figure 3.1. Transport of 1 $\mu$ M [ $^3$ H]-pentamidine by <i>T. b. brucei</i> s427WT procyclic forms.....	91
Figure 3.2. Uptake of low and high concentrations of [ $^3$ H]-Pentamidine in procyclic form.....	92
Figure 3.3. Characterisation of High affinity pentamidine transport.....	93
Figure 3.4. Transport of 1 $\mu$ M [ $^3$ H]-diminazene in procyclic trypanosomes. ....	95
Figure 3.5. PCR amplification results to confirm identity of <i>T. brucei</i> <i>tbat1</i> <sup>-/-</sup> .....	96
Figure 3.6. Selection for diminazene resistance in the <i>tbat1</i> <sup>-/-</sup> cell line cultured under drug pressure.....	96
Figure 3.7. Transport of [ $^3$ H]-pentamidine in wild-type and ABR cell lines. ....	99
Figure 3.8. Transport of 1 $\mu$ M [ $^3$ H]-diminazene in the s427WT (A), <i>tbat1</i> <sup>-/-</sup> (B), B48 (C) and ABR (D) cell lines.....	100

Figure 3.9. Transport of 1 $\mu$ M [ $^3$ H]-pentamidine (filled bars) or 1 $\mu$ M [ $^3$ H]-diminazene (open bars) in four different cell lines.....	100
Figure 3.10. Saturation plot of [ $^3$ H]-diminazene transport in bloodstream forms of the <i>tbat1</i> <sup>-/-</sup> cell line.....	101
Figure 4.1. The natural substrate for P2 transporter and some trypanocides. ....	106
Figure 4.2. EC <sub>50</sub> values of pentamidine and some RT compounds. ....	109
Figure 4.3. High Affinity Pentamidine Transporter-mediated uptake of $^3$ H-pentamidine (RT05/RT08). ....	114
Figure 4.4. Images produced with Chem3D Ultra software version 10 (CambridgeSoft) after minimization of energy.....	117
Figure 4.5. High Affinity Pentamidine Transporter Mediated Uptake of $^3$ H-pentamidine (RT02/RT18). ....	120
Figure 4.6. 3-D images after minimization of energy shows that presence of a third oxygen atom on the linker obviously reduces affinity to HAPT1 (panel A). ....	121
Figure 4.7. Positioning of Amidine group that confers highest affinity for the High Affinity Pentamidine Transporter.....	124
Figure 4.8. Graph represents the relationship between the length of the linker and affinity to the HAPT1 transporter. The study involved the benzofuranamidine compounds (panel A) and benzamidine compounds (panel B).....	125
Figure 4.9. Recognition motif model for HAPT1.....	126
Figure 5.1. A diagram representing the steps involved in creating the pentamidine resistant cell line. ....	129
Figure 5.2. Creation of P1000 cell line.....	130
Figure 5.3. The Effect of pentamidine adaptation on growth of P1000 cell line <i>T. b. brucei</i> S427 and TbAT1-B48. ....	131
Figure 5.4. Pentamidine sensitivity in four clones of P1000.....	133
Figure 5.5. Drug profile of P1000 compare to 427 wild type and TbAT1-B48. ....	135
Figure 5.6. Inhibition of 1 $\mu$ M [ $^3$ H]-pentamidine uptake by P1000 bloodstream forms.....	137
Figure 5.7. The Effect of 500 nM pentamidine on the mitochondrial membrane potential in drug sensitive and resistant <i>T. brucei</i> bloodstream forms as measured by fluorescence of TMRE.....	140
Figure 5.8. Reverse transcriptase PCR (RT-PCR) result.....	142
Figure 6.1. PCR amplification of AT-A (lane1), AT- E (lane2) and AT-G (lane 3) from the three strains of blood stream form <i>T. b. brucei</i> . ....	152
Figure 6.2. <i>EcoRI</i> digestion releases AT-A insert (1449 bp) from the pGEM-T Easy.....	153
Figure 6.3. <i>EcoRI</i> digestion releases AT-E insert (1389 bp) from the pGEM-T Easy.....	153
Figure 6.4. <i>EcoRI</i> digestion releases AT-G insert (1449bp) from the pGEM-T Easy. ....	154
Figure 6.5. Electrophoresis gels representing some of the <i>EcoRI</i> digest of the purified plasmid DNA containing the AT-like inserts. ....	154
Figure 6.6. Southern blot 1. ....	159
Figure 6.7. Southern blot 2. ....	159
Figure 7.1. Map of pHDK02. ....	166
Figure 7.2. Amplification of the RNAi/AT-E fragment corresponding to 411 bp of AT-E gene of <i>T. brucei</i> (lane1).....	167
Figure 7.3. Confirmation of correct restriction sites in the RNAi/AT-E fragment after transformation. ....	168
Figure 7.4. Digestion of pGEM-T-Easy + RNAi/AT-E construct with KpnI and BamHI.....	168
Figure 7.5. Required digestion for second step ligation. ....	169

Figure 7.6. Confirmation of complete ligation and correct orientation of the RNAi-AT-E cassette. ....	170
Figure 7.7. Digestion of pHDK02 prior to transfection into bloodstream form cell line (2T1). ....	171
Figure 7.8. Growth curve of bloodstream form RNAi/AT-E cell line (IT.BERi). ....	172
Figure 7.9. Reverse Transcriptase -PCR analysis in the RNAi/AT-E in bloodstream form cell line (IT.BERi). ....	173
Figure 7.10. Time course for the uptake of low and high concentrations of [ <sup>3</sup> H]-pentamidine in IT.BERi cell line. ....	175
Figure 7.11. Pentamidine profile in RNAi/AT-E bloodstream form cell line (IT.BERi). ....	176
Figure 7.12. Digestion with <i>Bam</i> HI and <i>Hind</i> III release the RNAi/AT-E fragment of 411 bp from the pGEM-T-easy (lane1). Lane 2. Uncut p2T7Ti plasmid. ....	179
Figure 7.13. Digestion of p2T7Ti vector with <i>Bam</i> HI and <i>Hind</i> III releases the GFP gene at 760 bp (lane 1). ....	179
Figure 7.14. Map of pHDK07, derived from the p2T7Ti vector. ....	180
Figure 7.15. Confirmation of correct ligation of the RNAi/AT-E in p2T7Ti vector. ....	180
Figure 7.16. Growth curve of procyclic form RNAi/AT-E cell line (IT.CERi). ....	181
Figure 7.17. Reverse transcriptase –PCR analysis of the RNAi/AT-E knockdown in procyclic form (IT.CERi). ....	183
Figure 7.18. Time course for the uptake of low concentration of [ <sup>3</sup> H]- pentamidine in procyclic forms of RNAi cell line (IT.CERi). ....	184
Figure 7.19. Time course for the uptake of high concentration [ <sup>3</sup> H]- pentamidine in procyclic forms of RNAi cell line with and without tetracycline RNAi induction. .	185
Figure 7.20. Pentamidine profile in RNAi/AT-E procyclic form cell line (IT.CERi). ....	186

## List of Tables

Table 2.1. Cell lines that are being used in the project and their features.....	55
Table 2.2. Oligonucleotide primers used in this study.....	68
Table 2.3. Enzymes used in digestion for southern blot.....	83
Table 2.4. Examples of plasmids created in the lab during this project.....	84
Table 3.1. Comparison of [ <sup>3</sup> H]-pentamidine transport parameters in bloodstream and procyclic <i>T. brucei</i> .....	92
Table 3.2. EC <sub>50</sub> values for the four different trypanosomes strains used in this study. ....	97
Table 4.1. Represents EC <sub>50</sub> values and resistance factors for selected RT compounds (RT01, RT05 and RT18) in WT-427 and <i>TbAT1-KO</i> , <i>TbAT1-B48</i> and P1000. ....	108
Table 4.2. The effect of the symmetrical amidine groups on affinity to HAPT1 transporter.....	112
Table 4.3. The importance of amidine group position in interaction with HAPT1 transporter.....	113
Table 4.4. The roles of the two benzene rings in binding to HAPT1 transporter. ....	115
Table 4.5. The effect of rigid structure and flexibility of the molecule on affinity to HAPT1 transporter. ....	116
Table 4.6. The effect of length of the linker on affinity to <i>T. b. brucei</i> HAPT1 transporter.....	119
Table 4.7. The role of the two oxygen residues on the linker in binding to the HAPT1 transporter. ....	122
Table 5.1. Resistance phenotypes of the P1000 clones. ....	133
Table 5.2. The averages of EC <sub>50</sub> values of various trypanocides determined by using alamar blue assays. ....	134
Table 5.3. <i>In vitro</i> susceptibility, comparing resistance phenotypes of the pentamidine resistance cell line P1000 to WT s427 and <i>TbAT1-B48</i> . ....	136
Table 5.4. Summary of the MMP results.....	141
Table 6.1. Alternative nomenclature for the AT like genes.....	151
Table 6.2. Summary of the polymorphic nucleotides in AT-E genes.....	158
Table 6.3. Southern blot analysis.....	160
Table 7.1. Forward and reverse primers for RNAi/AT-E amplification.....	166
Table 7.2. RNAi knockdown of pentamidine transport activities in <i>T. b. brucei</i> bloodstream forms (IT.BERi).....	176
Table 7.3. The EC <sub>50</sub> of pentamidine and PAO in (IT.BERi). ....	177
Table 7.4. RNAi knockdown of pentamidine transportations in <i>T. b. brucei</i> procyclic form (IT.CERi).....	184
Table 7.5. The EC <sub>50</sub> of pentamidine and PAO in IT-CERi cell line.....	186

## Acknowledgement

I greatly acknowledge my supervisor Dr. Harry de Koning, for his trust, guidance, encouragement and his invaluable support throughout these three years of PhD. I also would like to thank my assessors, Dr. R. McCulloch and Dr Lisa Ranford-Cartwright, for their advice and support, and all the people who contributed to this project.

Very special thanks to my family back in Libya for their endless support during my study; my beloved wife for her support and for being patient (for the long nights I spent away at work). Most Important my two boys Abdulrahman and Ali for the laughter and great time I had with them (and for the many sleepless nights).

I would like to thank all the fellow students and staff of GBRC, level 5 and level 6, Division of Infection and Immunity (University of Glasgow) in particular those in H. de Koning group (previous current members), Abdualsalam, Anne, Antonius, Gordon, Hssan, Matt, Mohammed, Nasser, Neils, , Manal, Jane for their support and encouragement, of course I will not forget Chris.

Many thanks to M. Barrett's group and those I shared the office with: Isabel, Sharon (Cora), Dhilia, Abhinav.

Special thanks to David, Federica, Edward, (Abdulrahman Abdi, Carloine, Lucio and Mechael - from level 6) for their help with the molecular work and Prof. Mike Turner and Nushin Emami for helping me with the stistaical analysis.

This work would have not been possible without the financial support of "the Libyan Government", to whom I am very grateful.

The list of the acknowledgements would not be complete without mentioning the family of the medical genetics deptment University of Glasgow, Including Dr Douglas Wilcox and Anne Theriault for always being a second family and all other firendss from out side the University, specially Abdulmajid Ayad, Tareg Abulifa, Mohammed abdalwahab, Kate Adams, Tatiana Purdikova, Jim (Ji Junzhe) for being very special friends.

## Publications

1. Teka, I., Kazibwe, A., El-Sabbagh, N., Al Salabi, M.I., Ward, C.P., Eze, A.A., Munday, J.C., Mäser, P., Matovu, E., Barrett, M.P. and De Koning, H.P. (2011) The diamidine diminazene aceturate is a substrate for the High Affinity Pentamidine Transporter: implications for the development of high resistance levels. *Molecular Pharmacology*, submitted
1. Munday, J.C., Teka, I., Eze, A.A., Burchmore, R.J.S., Barrett, M. P. and De Koning, H.P. (2011) Kinetoplastid Molecular Cell Biology 2011, Woods Hole, USA, April 8 - 12, 2011.
2. Munday, J., Teka, I. and De Koning, H.P. (2010) Molecular analysis of drug transporters in *Trypanosoma brucei*: insights into drug resistance. 5<sup>th</sup> Northern UK Kinetoplastid Meeting, Hull, Dec 8<sup>th</sup>, 2009. [oral presentation]
3. Munday J.C., Ibrahim Teka, I., Burchmore, R.J.S., Michael P Barrett, M.P. and De Koning, H.P. (2010) Molecular analysis of drug transporters in *Trypanosoma brucei*: insights in drug resistance. *Epithelial Biology 2010*. Dundee, Scotland, 2-3 September 2010. [oral presentation]
4. Munday J.C., Ibrahim Teka, I., Burchmore, R.J.S., Michael P Barrett, M.P. and De Koning, H.P. (2010) Molecular analysis of pentamidine transporters in *Trypanosoma brucei*. British Society for Parasitology Spring Meeting, Cardiff, March 30 - 1 April 2010.
5. Teka, I.A. and De Koning, H.P. (2010) Structure-activity relationship of the High Affinity Pentamidine Transporter in *Trypanosoma brucei*. British Society for Parasitology Spring Meeting, Cardiff, March 30 - 1 April 2010
6. Teka, I., Al-Sabbagh, N., and De Koning, H.P. (2009) 4<sup>th</sup> Northern UK Kinetoplastid Meeting, Glasgow, Dec 8<sup>th</sup>, 2009. [oral presentation]
7. Teka, I., El-Sabbagh, N., Al-Salabi, M. and De Koning, H.P. (2008) Annual Conference of the Consortium for Parasitic Drug Design, Atlanta, Georgia, USA. Oct 30 - Nov 1, 2008. [oral presentation]

## **Author's Declaration**

I declare that the results presented in this thesis are my own work, except when stated otherwise, and that this work has not been submitted for a degree at another institution.

Ibrahim Ali Teka

March 2011

## Abbreviations

ABR	Adapted <i>tbat1</i> <sup>-/-</sup> <i>T. b. brucei</i> to a high concentration of diminazene
ACT	actin
AMP	ampicillin resistance marker ( $\beta$ -lactamase)
ATP	adenine triphosphate
BBB	blood- brain barrier
BSF	bloodstream form
bp	base pairs
BSA	bovine serum albumin
dsRNA	double-stranded RNA
CATT	card agglutination test for trypanosomiasis
CBSS	Carter's balanced salt solution
cDNA	Complementary DNA
CIAP	calf intestinal alkaline phosphatase
CNS	central nervous system
CNT	concentrative nucleoside transporter
CSF	cerebrospinal fluid
dH <sub>2</sub> O	distilled water
ddH <sub>2</sub> O	double distilled water
DDT	Dichlorodiphenyltrichloroethane
DFMO	$\alpha$ -difluoromethylornithine (eflornithine)
DMSO	dimethylsulfoxide
DNA	deoxyribonucleic acid
dNTPs	deoxynucleotide triphosphates
dsRNA	double stranded RNA
E	epimastigotes
<i>E. coli</i>	<i>Escherichia coli</i>
EDTA	ethylenediaminetetraacetic acid disodium salt dehydrate
EC <sub>50</sub>	Effective concentration inhibiting 50% cell proliferation
ENT	equilibrative nucleoside transporter
f	forward
FBS/FCS	Foetal bovine serum/foetal calf serum
g	gram
gDNA	genomic DNA
GFP	green fluorescent protein
h	hour
H	hypoxanthine transporter
HAPT1	high affinity pentamidine transporter
HAT	human African trypanosomiasis
Hyg	hygromycin
<i>HYG</i>	hygromycin resistance gene (hygromycin phosphotransferase)
IC <sub>50</sub>	median inhibition concentration
IT-BERi	<i>T. brucei</i> cell line with RNAi/AT-E (BSF)
IT-CERi	<i>T. brucei</i> cell line with RNAi/AT-E (PCF)
kb	kilobase
kDa	kilodalton
kDNA	kinetoplast DNA
K <sub>i</sub>	inhibition constant
K <sub>m</sub>	Michaelis-Menten constant
KO	knockout
IAEA	International Atomic Energy Agency

L	litre
LAPT1	low affinity pentamidine transporter
LB	luria bertani
LDL	low density lipoprotein
LdNT2	<i>Leishmania donovani</i> nucleoside transporters
LED	light-emitting diode
LS	long slender bloodstream form
M	molar
MMP ( $\psi_m$ )	Mitochondrial membrane potential
min	minute
ml	millilitre
mM	millimolar
mmol	millimole
mRNA	messenger RNA
MT	metacyclic trypomastigotes
MW	molecular weight
ND	not determined
NE	no effect
NEO	neomycin resistance gene (neomycin phosphotransferase)
ng	nanogram
nM	nanomolar
NT	nucleoside transporters
o/n	overnight
°C	degrees Celsius
OD	optical density
ODC	ornithine decarboxylase enzyme
ORF	open reading frame
ORI	origin of replication
PAC	puromycin resistance gene (puromycin <i>N</i> -acetyltransferase)
PARP	procyclic acidic repetitive protein
PAO	Phenyl Arsine Oxide
PBS	phosphate-buffered saline
PCF	procyclic form
PCR	polymerase chain reaction
PI	propidium iodide
pre-mRNA	precursor-mRNA
PSG	phosphate-buffered saline with glucose
r	reverse
RFLP	restriction fragment length polymorphism
rRNA	ribosomal RNA
RNAi	RNA Interference
RISC	RNA-induced silencing complex
RT-PCR	Reverse Transcriptase-PCR
SAR	structure activity relationship
SAT	sequential aerosol technique
SDS	sodium dodecyl sulfate
SIT	sterile insect technique
siRNA	short interfering RNAs
ssRNA	single-stranded RNAs
<i>T. b.</i>	<i>Trypanosoma brucei</i>
<i>TbAT1</i>	<i>Trypanosoma brucei</i> Adenosine Transporter 1 gene
<i>tbat1<sup>-/-</sup></i>	TbAT1 gene deletion
<i>TbNT</i>	<i>Trypanosoma brucei</i> Nucleoside Transporters

TbNBT	<i>T. b. brucei</i> nucleobase transporters
Tet	tetracycline
TMRE	Tetramethylrhodamine ethyl ester
U	unit
UV	ultraviolet
V	volt
v	volume
V <sub>max</sub>	maximum velocity
VSG	variant surface glycoprotein
w	weight
w.t.	wild type
wb	whole blood
WHO	World Health Organisation
μl	microlitre
μg	microgram
μM	micromolar

# **1 General introduction**

## 1.1 Human African trypanosomiasis

Human African Trypanosomiasis (HAT), otherwise known as African sleeping sickness is considered as a disease with one of the highest mortality rates and affects the world's poorest population. In sub-Saharan African countries the disease is caused by a protozoan parasite known as *Trypanosoma brucei*, of which two subspecies (*T. b. rhodesiense* and *T. b. gambiense*) cause human infection (Luscher *et al*, 2007; Brun *et al*, 2010; Hotez & Kamath, 2009). Meanwhile, the third subspecies, *Trypanosoma brucei brucei*, causes disease only in animals (Barrett *et al*, 2003). Trypanosomiasis is a fatal disease if left untreated; according to the World Health Organisation (WHO) between 300,000 to 500,000 are at risk with an estimated 30,000 individuals people currently infected with the disease ([www.who.int/trypanosomiasis\\_african/en/](http://www.who.int/trypanosomiasis_african/en/)), ([www.who.int/mediacentre/factsheets/fs259/en/](http://www.who.int/mediacentre/factsheets/fs259/en/)).

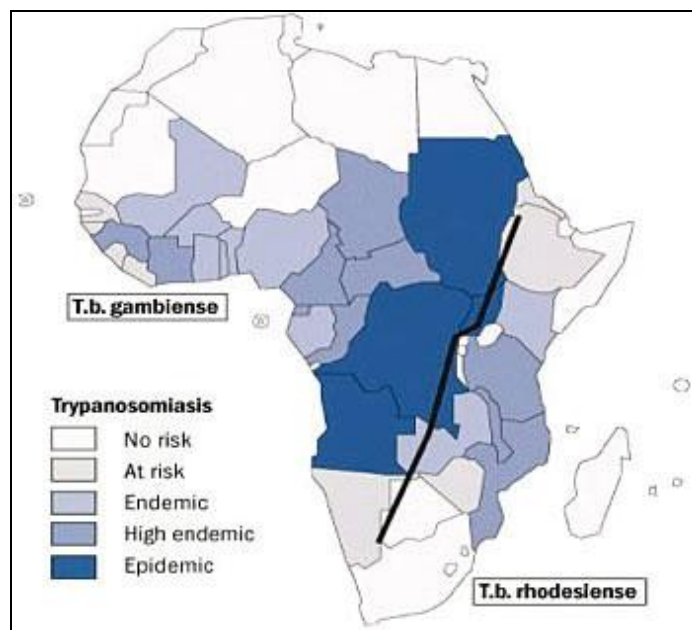


Figure 1.1. Distribution Human African trypanosome.

Map shows the epidemiological status and distribution of two strains of the *Trypanosoma brucei* responsible for HAT in Sub-Saharan Africa.

(Quoted from [http://www.medicalecology.org/diseases/d\\_african\\_trypano.htm](http://www.medicalecology.org/diseases/d_african_trypano.htm))

*T. b. rhodesiense* and *T. b. gambiense* have different geographical distributions (Figure 1.1). *T. b. rhodesiense* is found in wooded areas of East and Southern Africa and responsible for the acute form of the disease and the absence of medical care will lead to death within a maximum of six months in 80% of the cases. However, *T. b. gambiense* is generally known as the cause of a chronic

form of the disease and found in the tropical areas of West and Central Africa (WHO, 2000; Simarro *et al*, 2008; Simarro *et al*, 2010).

The third subspecies *T. b. brucei* is responsible for the disease in animals which is known as Nagana. In addition the veterinary disease is also caused by *T. congolense* (sub-genus *Nannomonas*) and *T. vivax* (sub-genus *Dutonella*). Trypanosoma species are believed to be responsible for the death of an estimated 3 million cattle annually (Luscher *et al*, 2007). Moreover, such an infection is responsible for a decrease in reproduction by 20% as well as a decrease in milk production by 25% (Kuzoe, 1993).

Besides being human-infective agent; *T. b. rhodesiense* can infect both wild and domestic animals. However, *T. b. gambiense* is transmitted mainly from human to human, although there is increasing evidence of animals acting as host reservoirs of this parasite as well (Welburn *et al*, 2001; Hotez & Kamath, 2009; Brun *et al*, 2010).

Ever since trypanosomes have been recognised as human pathogens, trypanosomiasis has been counted as one of the most devastating health and economic development problems in sub-Saharan Africa. In order to control the disease, many ideas and methods have been employed to limit the expansion of the disease in humans and livestock. Some of these ideas proved to be practical and continue to work to the present day. Those methods include chemotherapy and the control of parasite spreading by controlling the parasite vector. Unfortunately, vector control still has limited sustainability and has not fully integrated into practice leaving chemotherapy as the other choice especially with the lack of vaccination against the parasite. Chemotherapy, however, is also associated with some problems such as extreme toxicity, affordability and the emergence of resistance (Maudlin, 2006; Bacchi, 2009; Hannaert, 2010). Therefore the generation of new potential chemotherapies that are effective and affordable to the public and small farm holders is urgently needed.

## 1.2 History overview and epidemiology

Human sleeping sickness occurs in Africa affecting specific foci, and has reached epidemics levels within these foci a number of times in recorded history (Hide,

1999). It is believed to have existed in Africa for many centuries; and was noticed long before knowing the cause of the disease. Atkins described its characteristics in 1742 as “sleepy distemper”, and in 1857 David Livingstone called it the “fly disease” as he believed that flies in the area carry some toxins in their bite (Hide, 1999). The Europeans drew attention to it soon after their arrival to Africa in the late 19th century, and slave traders were refusing to buy slaves with swollen necks, an early sign of sleeping sickness (Barrett *et al*, 2003).

In 1895 Sir David Bruce proved a link between the tsetse fly vector and the animal infection Nagana, and in 1896 he reported African trypanosomes to be pathogenic agents. Later the species was named after him *Trypanosoma brucei*. In 1902 Dutton managed to isolate the parasite *Trypanosoma gambiense* from an English man's blood who was working on the river Gambia and he was unsuccessfully treated for malaria (Hide, 1999; Maudlin, 2006; Kennedy, 2004), and in 1910 Stephens and Fantham first described *Trypanosoma brucei rhodesiense*, which is responsible for Rhodesian disease in East and South Central Africa (Kennedy, 2004).

Between 1896 and 1908, about 1 million people died in East Africa as a result of HAT infection (Seed, 2001). In the year 1930 about 33,562 human cases were reported in Zaire (now the Democratic Republic of Congo) (Ekwanzala *et al*, 1996). A further HAT epidemic occurred in Africa between 1920 - 1930 (WHO, 1998).

During the middle of the 20<sup>th</sup> century, the incidence decreased substantially; this was due to an improved ability of screening and treatment of the population, fighting the tsetse flies using insecticides, and the limitation animal reservoirs (Seed, 2001; Kuzoe, 1993). In Angola for example, the number of cases dropped dramatically from 5000 cases in early 20<sup>th</sup> century, to 3 cases only reported in a screening program that was carried out in 1974 and involved 471,588 people (Delespoux & de Koning, 2007).

In the last three decades HAT has struck back. According to WHO reports the incidence increased to reach 500,000 cases and about 66,000 deaths each year ([www.who.int/mediacentre/factsheets/fs259/en/](http://www.who.int/mediacentre/factsheets/fs259/en/)). In 1998 a total of 6,610 cases out of 154,700 people screened were found to suffer from sleeping sickness infections in Angola (Delespoux & de Koning, 2007). In 2003, countries

such as Angola and the Democratic Republic of Congo reported to WHO 3 000 and 11 000 new cases respectively.

According to WHO, ([www.who.int](http://www.who.int)) during the year 2005 there was an outbreak of HAT across the southern part of Sudan and Chad, through Uganda and Congo to Angola and Tanzania, putting over 60 million people at risk in those areas. Very recently, a 19-year-old Sudanese refugee, who had lived for about 10 years in refugee camps in Uganda, was diagnosed with late stage of Human African trypanosomiasis (Cherian *et al*, 2010).

The re-emergence of HAT is in part attributed to the instability of political landscapes and to social disturbances in sub-Saharan Africa, which caused disturbance in the rhythm of life including health services. On the other hand the lack of surveillance and the poor access to clinical examination and diagnostic methods, and also the difficulty of vector control in some countries, have all contributed to the current surge in HAT cases (Kuzoe, 1993; Welburn *et al*, 2001; Jannin & Cattand, 2004; Lutje *et al*, 2010; Cherian *et al*, 2010).

### **1.3 The clinical manifestations of the disease**

It is known that human sleeping sickness has a focal distribution (Figure 1.1), mainly sub-Saharan Africa (Hide, 1999). It noticeably affects poor areas with populations who live under the poverty line. Besides being a life-threatening factor, it has negative impact on economic development as it mainly affects the most productive age group between 15 to 45 years ([http://www.who.int/trypanosomiasisafrican/resources/afro\\_tryps\\_strategy.pdf](http://www.who.int/trypanosomiasisafrican/resources/afro_tryps_strategy.pdf)).

Although an accurate number of the affected cases and the number of endemic countries is unknown. The recent (WHO) HAT Atlas indicated that sleeping sickness was present in at least 23 sub-Saharan African countries in the period 2000 - 2009 (Simarro *et al*, 2010).

As mentioned above, the two causative species of HAT give rise to forms of clinical conditions with slightly differing symptoms. The disease found in East and South Central Africa, caused by *Trypanosoma b. rhodesiense*, is the cause for the acute form of Rhodesian sleeping sickness and the onset of noticeable symptoms can occur within a few weeks from the initial infection with the

parasite. If the condition is left untreated it can lead to death usually within a year or even within a few weeks after onset of the disease (Rodgers, 2009). *T. b. gambiense* generally produces a chronic form of Gambian sleeping sickness and clinical signs in this case do not show immediately as the condition gradually develops severity from the almost asymptomatic incubation period of the first few months, to the severe neurological problems and terminal coma after a prolonged period, sometimes up to several years (Welburn *et al*, 2001; Maudlin, 2006d; Rodgers, 2009).

Clinically, during the early stage the infected person will experience non-specific symptoms, including headaches, unstable fever, weakness, sweating and pain in the joints. More complicated symptoms may appear, such as myocarditis with congestive heart failure, pulmonary oedema and pericardial effusion. If the infection is due to *Trypanosoma b. rhodesiense* the untreated condition usually develops quickly and can be fatal in few weeks.

Human African Trypanosomiasis (HAT) is characterised by the presence of parasites that live extracellular in the bloodstream and lymphatic system. Soon after the infected vector bites the victim the parasite enters the blood stream and as an obligatory parasite it uses the host environment as a source of essential nutrients for its biochemical activities. The metacyclic stage of the parasite makes its way from the bite site into the bloodstream, lymph and peripheral organs and starts differentiating and proliferating, marking the onset of early stage HAT. This stage of infection is also known as the haemolympathic stage or stage one (Barrett *et al*, 2003; Barrett, 2006; de Koning *et al*, 2005; Bentivoglio & Kristensson, 2007).

During the hemolympathic stage the patient develops a primary chancre at the site of the tsetse fly bite (Moore *et al*, 2002). Nonspecific symptoms could be seen in many patients including irregular or intermittent fever, tiredness, aching joints and headache. The parasites then invade all organs of the body including the heart and spleen (World Health Organisation, 2001; Barrett *et al*, 2003).

The untreated condition will develop to the late or encephalitic stage, where the parasite has crossed the blood- brain barrier (BBB), proliferates in the cerebrospinal fluid (CSF), and finally invades the central nervous system (CNS) causing a wide range of neurological disorders including severe headaches and

sleeping disorders; encephalopathy resulting from alterations in brain function leads to an inversion of the sleep-wake condition. Later the patient falls into a deep coma and eventually dies if not treated (Barrett *et al*, 2003; Maudlin, 2006; Kennedy, 2006; Rodgers, 2009; Lutje *et al*, 2010).

## 1.4 Parasite biology

*Trypanosoma* are eukaryotic species that belong to the order Kinetoplastida with a maximum  $15 \times 4 \mu\text{m}$  in dimension (Figure 1.2). It is a unicellular flagellate with a nucleus situated near the centre of the cell; the flagellum of the protozoan arises from a small round organelle called kinetoplast, consisting of a fibrous mitochondrial DNA network. Under the light microscope this round shape stains with the same colour as the nucleus (Overath *et al*, 1986; Shlomai, 2002).

Morphologically, the bloodstream form trypomastigotes of *T. b. gambiense* and *T. b. rhodesiense* are identical, which makes it difficult to tell them apart. Some changes in their characteristics may occur depending on the life cycle stage and the environment surrounding them (Vickerman, 1969).

The flagellum exits the cell through the flagellar pocket, situated near the posterior end of the cell in close proximity to the kinetoplast. The flagellum and main body of the cell are covered with a plasma membrane and the flagellum extends the length of the cell within a sheath forming an undulating membrane attached to the body of the cell. The free part of the flagellum extending beyond the anterior end of the cell swivels freely and moves the cell through the medium (Vickerman, 1969; Vickerman, K. *et al*, 1993).

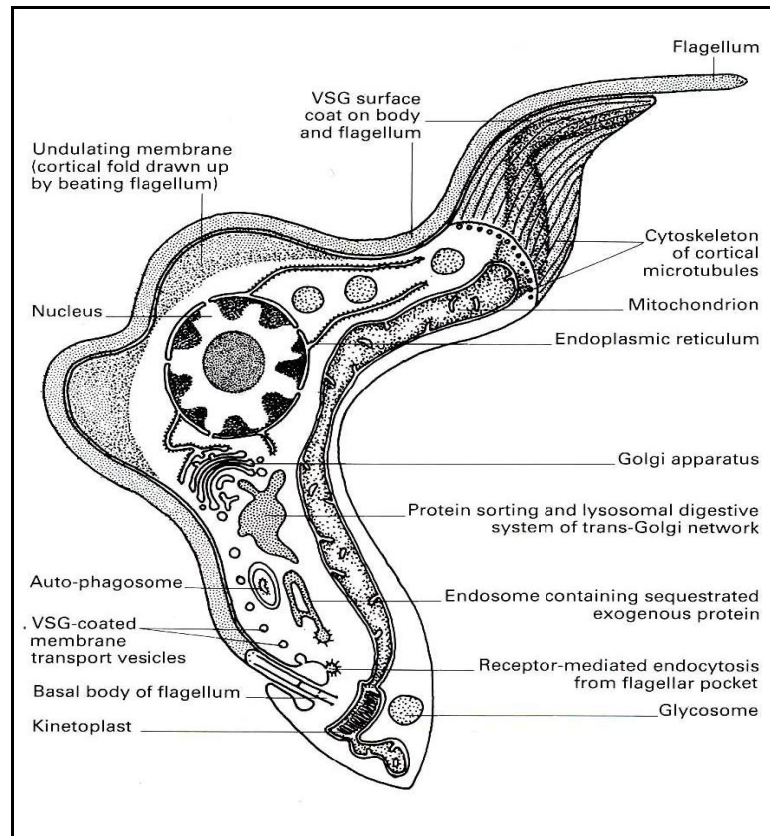


**Figure 1.2. Diagram showing the principal structures of the *Trypanosoma brucei* bloodstream form.**

Reproduced from Vickerman, K. *et al*, 1993.

The cell body and flagellum of the metacyclic and bloodstream forms are covered with a dense coat known as Variant Surface Glycoprotein (VSG) which is extruded from the flagellar pocket after synthesis in the Golgi apparatus and transportation through the cytosol in vesicles (Vickerman, K. *et al*, 1993). This coat acts to protect the trypanosome from the innate and acquired immune response of the mammalian host (Turner, 1999; Mansfield & Paulnock, 2008).

### **1.4.1 Plasma membrane**

As a typical eukaryote, *Trypanosoma* cells are enclosed by the plasma membrane which separates them from the surrounding environment. It is composed of phospholipids, cholesterol, glycolipids, and proteins all of which go to form a bilayer surface coat that separates the parasite cell from the surrounding environment. The surface of the bloodstream and metacyclic forms are covered by VSG, which helps to avoid the action of the immune system (Overath *et al*, 1986; Vickerman, 1969).

The plasma membrane also contains proteins like receptors and essential nutrient transporters. These include nucleoside/nucleobase transporters and amino acid transporters, among others, which are critical for metabolic functions. These transporters play an important role in delivering nutrients and other metabolic compounds into the parasite cell. The plasma membrane transport system is now widely used in investigations towards new chemotherapy, particularly to mediate the entry of drugs into the cell (de Koning, 2001; Bridges *et al*, 2008).

### **1.4.2 Glycosomes**

These are round or oval-shaped microbodies found in all major members of trypanosomatidae family with a general diameter between 0.2 and 0.8  $\mu\text{m}$  surrounded by a single membrane (Opperdoes *et al*, 1984). Glycosomes contain important enzymes for pyrimidine biosynthesis. Glycosomes play an important role in cell energy supply, as they contain a number of enzymes that are important in converting glucose to 3-phosphoglycerate plus glycerol (Michels *et al*, 2000).

### **1.4.3 Mitochondrion**

Each cell contains a single mitochondrion, replication of which is closely linked to the cell division cycle. The *T. brucei* mitochondrion has its own genome, representing 10-20% of the total DNA of the cell. It has an irregular shape as it changes depending on the cell cycle stage. In the bloodstream form (BSF) the mitochondrion is poorly developed forming a single canal without inner membrane foldings. The mammalian stage of the cell is characterised by the absence of both krebs cycle and the classical respiratory chain are absent, whereas in procyclic forms (PCF) both the respiratory chain and Krebs cycle are active and the mitochondrial system take the shape of a network forming inner membrane foldings (Vickerman, 1985; van Weelden *et al*, 2003).

The mitochondrial membrane potential and nuclear and kinetoplast DNA are believed to be strongly involved in the accumulation of diamidines in trypanosomes (de Koning, 2001).

### 1.4.4 Acidocalcisomes

Acidocalcisomes are membrane-bound structures which possess an electron dense content. These acidic organelles contain high calcium concentrations as well as phosphorus and other cations. Their membrane contains a number of pumps and channels important for material and ion exchange. In particular acidocalcisomes are strongly involved in the process of calcium ion exchange via calcium pumps, which are considered targets for potential trypanocidal agents (Moreno & Docampo, 2003; Docampo *et al*, 2010).

## 1.5 Taxonomy

The trypanosomatidae family belongs to the order of Kinetoplastida and consists of a group of pathogens able to infect a wide range of hosts. Based on morphological features and host range trypanosomatids have been classified to a number of genera, some of which have only one host, and are known as monoxenous such as, *Leptomonas*, *Crithidia* and *Blastocrithidia*, for which the hosts are usually invertebrates. Others are classified as heteroxenous and have different hosts depending on their life-cycle stage such as *Trypanosoma* and *Leishmania*, which are transmitted by insect vectors and are infectious to many vertebrate species. (Kreier & Baker, 1987).

The three subspecies of *Trypanosoma brucei* have always been of a concern due to their clinical and economical aspects. According to Vickerman (1996) the three subspecies of *T. brucei* are morphologically indistinguishable, but recent studies using various molecular techniques such as isoenzyme analysis, restriction fragment length polymorphism (RFLP) and minisatellite marker analysis enable identification and the isolation of each of them (Gibson, 2002; Njiru *et al*, 2004).

Of the three *T. brucei* sub-species only *T. b. brucei* does not infect humans but is responsible for disease in animals (Nagana). The reasons why only *T. b. gambiense* and *T. b. rhodesiense* are human infectious and not *T. b. brucei* is because the latter is sensitive to a trypanolytic factor (TLF) which is Apol1 molecule present in human serum, whereas *T. b. gambiense* and *T. b. rhodesiense* both appear to be resistance to this serum constituent (Raper *et al*,

2001; Smith *et al*, 1995; Kieft *et al*, 2010). Another subspecies, named *Trypanosoma cruzi*, is only found in South and Central America. This parasite causes a medical condition known as Chagas disease (Barrett *et al*, 2003; Njiru *et al*, 2004).

The genus *Trypanosoma* is also subdivided into two main groups depending on the mode of transmission, the Stercoraria trypanosomes and the Salivaria trypanosomes (Hoare, 1972).

### **1.5.1 Salivaria trypanosomes**

These are mainly found in Africa, they developed in the mid-gut of the insect vector and transform to a mammal-infective form in their salivary glands. They are transmitted in the saliva by the vector bite. This group includes the HAT causative agents (*T. brucei gambiense* and *T. brucei rhodesiense*), as well as the animal infective agents (*T. b. brucei*, *T. evansi*, *T. vivax* and *T. congolense*) (Kreier & Baker, 1987; Barrett *et al.*, 2003).

### **1.5.2 Stercoraria trypanosomes**

The causative agent for Chagas' disease (*T. cruzi*) is the foremost parasite of this group. In this group trypanosomes develop into a mammalian infective form, in the hind-gut of their insect vectors and are transmitted via contaminated insect faeces (Vickerman, 1985).

## **1.6 Lifecycle**

*T. brucei* is di-geneic (Figure 1.3) as it is obliged to infect a mammalian host and an insect vector in order for it to complete their life cycle. During each stage of the life cycle the cells undergo different biochemical and morphological transformations. This includes changes to the shape of the parasite, the orientation and location of some of the organelles such as the kinetoplast in relation to the nucleus, obvious changes in the mitochondrial system and changes of the surface of the cell (Vickerman, 1969; Vickerman *et al*, 1988).

The life cycle of *Trypanosoma* takes about 3 weeks within the vector. The parasite firstly replicates by binary fission and elongates into the procyclic forms (PCF) in the vector midgut, changes in the surface coat from VSG to procyclin and develops the mitochondrial system. In contrast to bloodstream forms, PCF are characterised by a fully developed mitochondrion, high levels of metabolic activity and protein synthesis, and the formation of a procyclin coat surrounding the parasite cell (Figure 1.3). Also observed are high levels of mRNA associated with the polysomes (Vickerman, 1985; Vickerman *et al.*, 1988).

The parasite subsequently invades the salivary gland of the tsetse fly and transforms into epimastigotes (E) and continues to replicate by binary fission. Some of the epimastigotes transform into non-dividing metacyclic trypomastigotes (MT), which are highly motile and characterised by the lack of a free flagellum (Vickerman, 1985; Brecht & Parsons, 1998).

The lifecycle in humans starts when the infected tsetse fly takes a blood meal (Figure 1.3) and deposits some of its saliva, which carries the parasite, pre-adapted, metabolically, for life inside a mammalian host. Once inside the mammalian host the metacyclics differentiate to form trypomastigotes, or 'slender bloodstream forms' and proliferate rapidly in the blood and lymph (Roberts, L. S. and Janovy, J., 2000; Bogitsh *et al.*, 2005).

In the mammalian host, the bloodstream form of the parasite undergo three phases of transformation (Figure 1.3), each with certain biochemical characteristics including cell cycle arrest and the reduction of protein levels, as well as various antigenic changes (Vickerman, 1985).

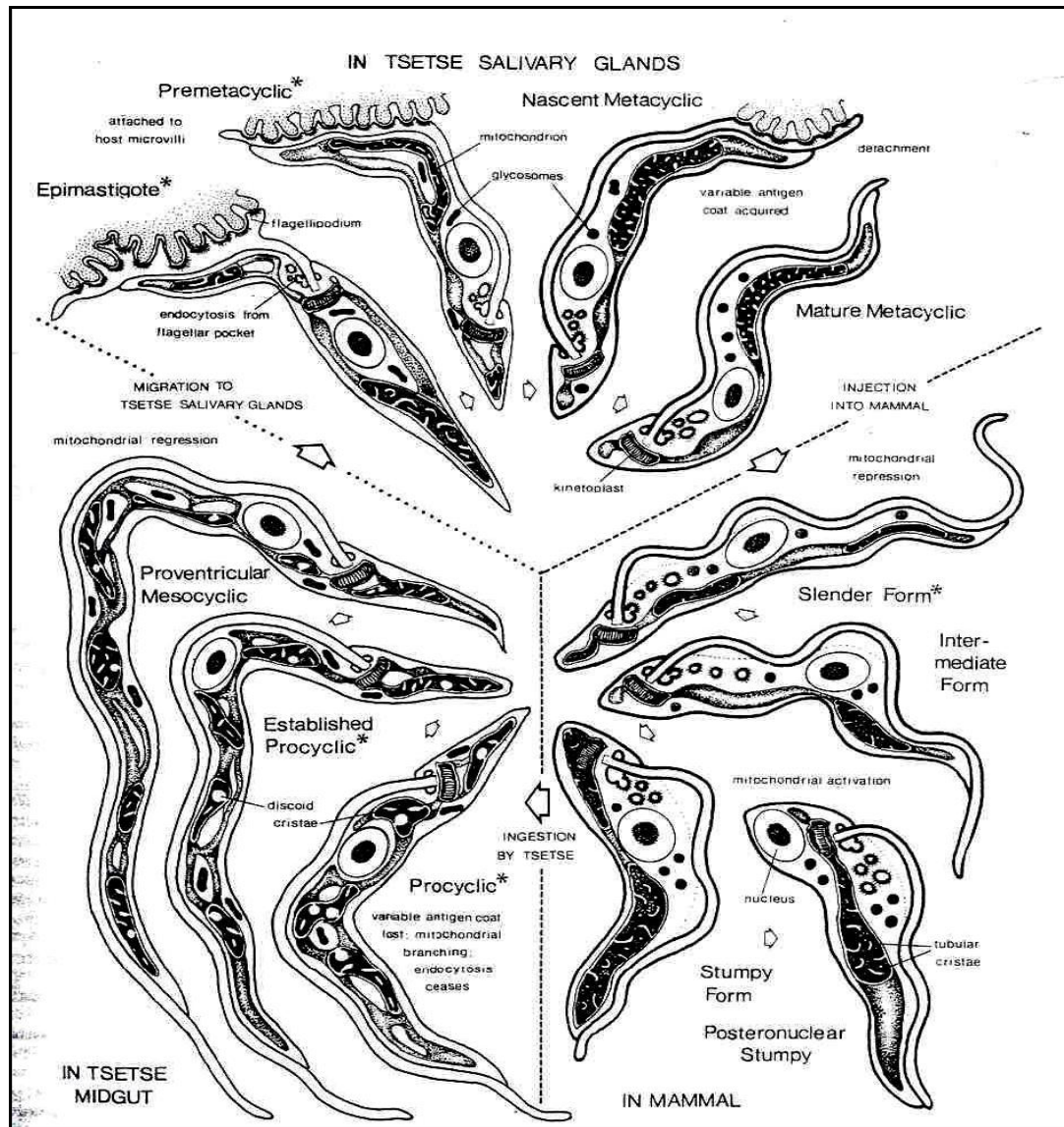


Figure 1.3. Life cycle of *Trypanosoma* in both mammalian and tsetse fly.

Reproduced from (Vickerman, 1985)

After the vector bites the victim, the parasite reaches the lymphatic fluid and transforms into human-infective long slender bloodstream form (LS), with a free flagellum extending from the undulating membrane. They replicate by binary fission and their number doubles within 6 hours, and transform into an intermediate form that will subsequently develop to the third stage, which is the short stumpy (SS) form (Vickerman, 1985). The stumpy forms appear, like their name suggests, shorter and thicker than the slender bloodstream forms, with their flagellum greatly shortened so that it barely protrudes past the main body of the cell (Figure 1.3). In order to overcome the immune system of the host, other changes occur, involving the variation of the surface coat, which will result in variable level of parasitemia (Vanhamme *et al*, 2001). Within a few days, the parasite will spread throughout the body. At some point it reaches the

cerebrospinal fluid and penetrates the central nervous system (CNS), resulting in the cerebral stage of the disease.

## 1.7 Diagnosis

Good progress has been made in the field of screening and diagnosis of HAT. In the acute form of the disease generally the level of parasitemia is high and the diagnosis of *T. b. rhodesiense* is easily achieved by microscopy using thin or thick films of the peripheral blood to detect the presence of the parasites (Kennedy, 2006). However, the diagnosis of the disease form caused by *T. b. gambiense* is not easy as the clinical presentations of early stage HAT are easily confused with other tropical diseases such as malaria, typhoid and other febrile diseases (Gilles, H. M., 1999). The best diagnostic method is by serological analysis methods using the card agglutination trypanosomiasis test (CATT). This is the preferred test for screening potential *T. b. gambiense* cases as it is a quick and easy method and also enables the use of dried blood samples on filter-paper for future serological analysis.

In deciding on a course of treatment it is of critical importance to determine whether the patient is in stage one of the infection or if the trypanosomes have crossed into the cerebrospinal fluid (CSF) to initiate stage two. The only way to do this reliably is to examine the CSF by lumbar puncture, after a single dose of suramin or pentamidine in order to avoid contamination during the sampling procedure by clearing the parasites from the blood.

Other methods can still be used to detect the late stage of HAT, although these methods are not easily applicable in this field including PCR, raised CSF proteins, EEG abnormalities, and the presence of intrathecal IgM synthesis (Kennedy, 2006).

## 1.8 The control of HAT

The control of the disease can be scaled be divided into two areas: the control of the disease by medical treatment, or by limiting the transmission of the disease by controlling the vector. Given the fact that there is no vaccination to prevent the disease the only options left to manage the disease is via

chemotherapeutic regimes, disease surveillance and vector control (Stich *et al*, 2003).

However, the chemotherapeutic aspect for HAT is still unsatisfactory due to the high cost of some of the drugs and, more importantly, the side effects of these drugs. Another aspect that is now extremely worrying is the increase of parasitic resistance as a result of continuous use of these few drugs, which in some cases means that the disease becomes incurable. This is true especially for melarsoprol, which is the most effective drug for late stage HAT (de Koning, 2001).

The disease is transmitted by the tsetse fly (*Glossina* spp.), spreading over 8.5 million km<sup>2</sup> of Africa. Aside from chemotherapy, disease limitation by controlling its transmission is an important option and can offer a long-term solution for reducing the incidence of trypanosomiasis. Historically, many methods have been successfully used especially by livestock holders, is by avoiding the tsetse-infected areas. In the early 20th century, game animals were killed and large tracts of woodland destroyed to stop the breeding of tsetse fly (Allsopp, 2001b; Schofield & Maudlin, 2001).

The discovery of insecticides such as DDT opened a new door for tsetse control, and ground spraying became an effective technique for more than half a century ([www.who.int](http://www.who.int)). Such a solution became the main line of defense against the tsetse fly, and in Nigeria alone; using this technique 230,000 km<sup>2</sup> of ground was cleared of tsetse flies. A new spraying protocol named sequential aerosol technique (SAT) in which aircrafts were used to spray low doses of insecticides was first used in the early 1940s in South Africa. In Cameroon this technique kept trypanosomiasis under control for 18 years in conjunction with ground spraying. (Allsopp, 2001; Schofield & Maudlin, 2001).

In the later years of the 20th century new methods have been used, including bait technique, which involves attracting tsetse to fabric traps where they can be captured or killed. The last developed form of the bait technique has also given good results; in this new form, the artificial traps are replaced with live baits such as cattle from which the tsetse takes their meal. In this technique non-toxic pyrethroid insecticide is applied in animal dips or by spraying them with pour-on formulations (Allsopp, 2001).

Lately, the International Atomic Energy Agency (IAEA) has proposed the sterile insect technique (SIT) to decrease tsetse population consisting of the release of sterilised tsetse males. This technique has many advantages such as being insecticide-free and is environmentally friendly, but its cost-effectiveness is disputed (Allsopp, 2001; Vreysen, 2001).

## 1.9 Treatment of HAT

Soon after David Bruce identified the pathogenic trypanosomes, Paul Ehrlich led the scientific investigation in the field of trypanocide discovery and development. A 100 years of effort have only produced a handful of effective drugs that have worked well in treating HAT condition (Luscher *et al*, 2007). Unfortunately, there have been some drawbacks associated with the use of those drugs, such as toxicity and high cost. The most alarming issue is the increase of the treatment failure due to the rise of resistance, as in the case of melarsoprol used in late-stage sleeping sickness.

The drugs that are currently in use in the treatment of Human African trypanosomiasis are pentamidine, melarsoprol, suramin, nifurtimox and DFMO. Whereas the drugs of choice for the treatment of African animal trypanosomiasis (Nagana) are diminazene aceturate (Berenil<sup>®</sup>), isometamidium chloride (Trypamidium<sup>®</sup>), and ethidium (Homidium<sup>®</sup>) and cymelarsan.

Treatment of HAT involves different strategies using various therapeutic agents according to the stage of the disease. Suramin and pentamidine are the drugs of choice for the early stage of the disease (haemolympathic trypanosomiasis), which is caused by *T. b. rhodesiense* and *T. b. gambiense*, respectively. Once the CNS is involved the late stage of the disease is treated with drugs that are able to cross the blood-brain barrier (BBB) such as melaminophenyl arsenical drug melarsoprol (Denise & Barrett, 2001).

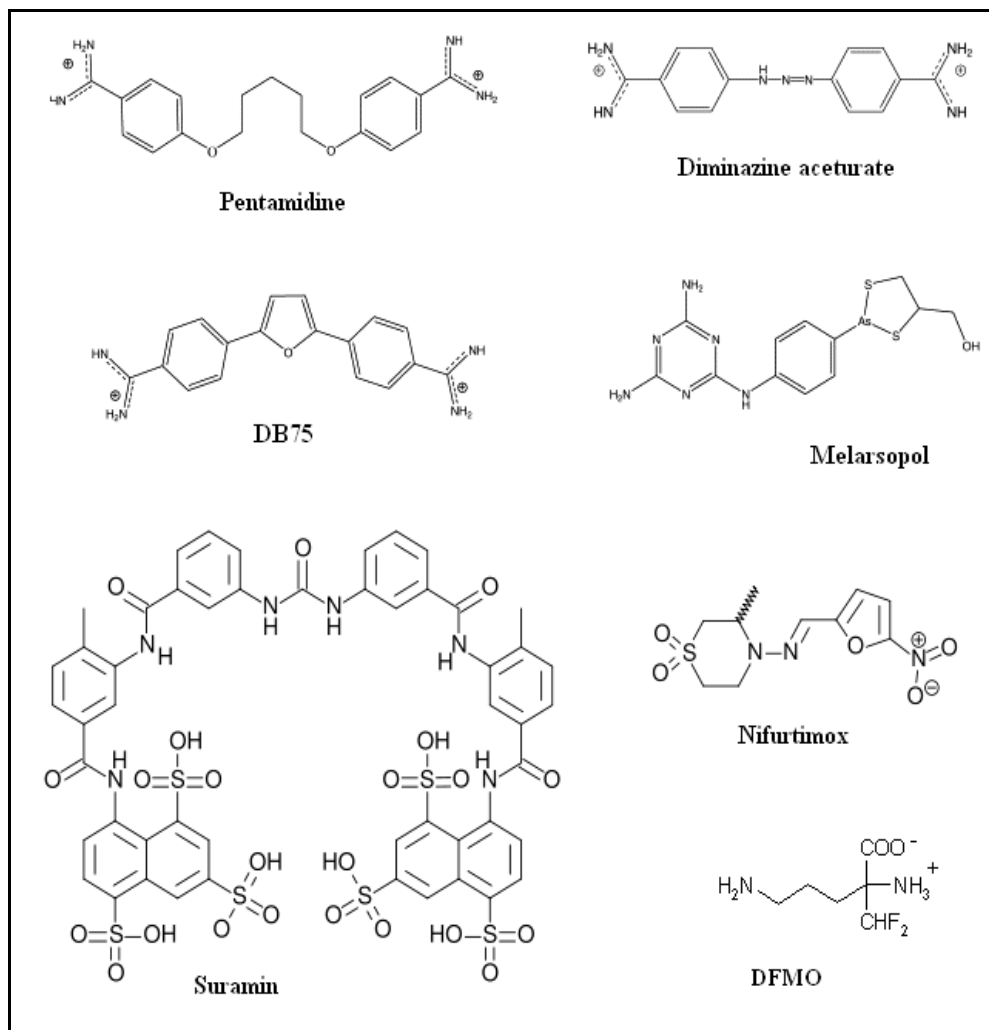


Figure 1.4. General structures of the most commonly used trypanocidal compounds that are licensed for use against African trypanosomiasis.

### 1.9.1 Pentamidine

Pentamidine is an aromatic diamidine (Figure 1.4) that has been used as an effective chemotherapy in the early stage of human trypanosomiasis caused by *T. b. gambiense* since 1937. Stilbamidine was initially used in the 1930s but was insufficiently stable under tropical conditions. Other diamidines such as Berenil (diminazine aceturate) are licensed against the veterinary form of trypanosomiasis. Pentamidine is a di-cation at physiological pH; therefore it cannot cross bio-membranes, including the blood brain barrier (BBB), and is only efficient against the first stage of sleeping sickness (Denise and Barrett, 2001).

However, it was recently found that pentamidine actually does have a significant uptake across the BBB, which must be carrier-mediated, but is excluded by ABC transporters (Sanderson *et al.*, 2009). The experimental diamidine CPD0801 is currently under consideration for treatment of cerebral sleeping sickness, owing

to its highly promising cure rates in the murine late stage model (Wenzler *et al.*, 2009). Pentamidine is a water-soluble compound and is taken up by the parasite to intracellular concentration in excess of 1mM, while the bloodstream concentration ranges from 0.5 to 2.5  $\mu$ M after the standard dose of 4 mg/kg (Bray *et al.*, 2003; Jannin & Cattand., 2004). The mode of action of pentamidine remains unclear, but it is known that transporters play an important role in the drug action and as explained in Section 1.15, pentamidine accumulation into *T. brucei* relies on a minimum of three distinct transporters (Figure 1.9) (de Koning, 2001).

Numerous intracellular targets have been suggested for pentamidine, but without proof which is thought to be the main one. Pentamidine binds tightly to the minor groove of DNA at AT-rich sites, suggesting that pentamidine exert its anti-trypanosomal activity by inhibiting DNA-dependent enzymes perhaps leading to direct obstruction to the transcription process (Wilson *et al*, 2005; Gillingwater *et al*, 2010). It was also linked to subsequent destruction of the kinetoplast as it binds strongly to the network of minicircular DNA molecules that comprise the kinetoplast (kDNA) (Tevis *et al*, 2009). The millimolar intracellular pentamidine concentrations indicate that the drug could act on multiple targets. For instance, pentamidine can affect the mitochondrion by acting as an uncoupler of oxidative phosphorylation, inhibit the S-adenosyl methionine decarboxylase (Ado-MetDC) enzyme perhaps preventing polyamine synthesis, and interfere with trypanothione metabolism (Wang, 1995; Fairlamb, 2003; Nok, 2003; Bacchi, 2009).

Nephrotoxicity and diabetes mellitus are among the adverse effects caused by the use of pentamidine. Diamidines are thought to act directly against the parasites, independently of their physiological action against the host. The diamidines were in fact designed to induce hypoglycaemia, as chemical analogues of insulin, and so starve the trypanosomes of energy (Williamson, 1970). It is fortunate that the compounds proved better trypanocides than insulin receptor agonists.

Pentamidine is only effective in early stage treatment, as the compound does not penetrate the CNS and it is given as an intramuscular injection at a recommended dosage of 4 mg/kg either daily or on alternating days for a total

of seven to ten administrations (Jannin & Cattand, 2004; Bacchi, 2009). Some unpleasant side effects may occur when using pentamidine include nausea, abdominal pain, tachycardia (a rapid heart rate). Lowering of blood glucose levels and arterial hypotension has been observed in some 10% of treated cases. However, treatment with pentamidine can leave serious and long-termed problems including nephrotoxicity, damage to the pancreas and liver enzyme abnormalities (Legros *et al*, 2002; Barrett *et al*, 2007; Kennedy, 2008).

Despite the fact that Pentamidine resistance is inducible in the laboratory and by stepwise exposure to sub-lethal pentamidine concentrations *in vitro* or *in vivo*, resistance to pentamidine does not appear to be a major problem to treatment, even after long time of use in the treatment of HAT (Fairlamb, 2003; Bridges *et al*, 2007). This is because of the multiple transporters used to accumulate the drug (De Koning, 2001); alteration or loss of one of these transporters would not lower the intracellular concentration to a sub-therapeutic level. This was confirmed by the disruption of the TbAT1 purine transporter, which resulted in only a minor loss of sensitivity to the drug (Matovu *et al*, 2003). *In vitro* adaptation of the cells lacking the TbAT1/P2 transporter to gradual increasing concentration of pentamidine showed that cells lost the transport activity associated with HAPT1. This cell line appeared to be less infective to mice, possible indicating a growth disadvantage *in vivo*. Pentamidine treatment failures have certainly been reported for cases of *T. b. gambiense* infections in the field (Pepin & Khonde, 1996) but are generally assumed to reflect incorrect early-stage diagnosis of what may have been late stage cases (Delespoux and De Koning, 2007).

#### **1.9.1.1 Pentamidine in relation to *T. brucei* Mitochondrial Membrane Potential (MMP)**

Two different mechanisms could be responsible for mitochondrial dysfunction, including a direct mechanism such as membrane damage, and anoxia or indirect mechanisms such as intracellular ion disruption and enzyme inhibition. Mitochondria consist of an outer membrane, an inner membrane which is folded into cristae, and the inner matrix. The inner membrane contains the enzymes for electron transport and oxidative phosphorylation that are important for cellular function. Therefore maintenance of inner mitochondrial membrane

integrity is essential for cellular energy homeostasis and its normal function. According to the chemiosmotic theory of oxidative phosphorylation the electrochemical gradient across the inner mitochondrial membrane is the driving force behind oxidative phosphorylation. For that reason, the mitochondrial membrane potential must be protected in order to provide a normal cellular function. However, the chemical dissipation of the electrochemical gradient would lead to a marked decrease in the rate of oxidative phosphorylation and a depletion of cellular energy levels (Rahn *et al*, 1991). Measurements of the mitochondrial membrane potential (MMP) are used to understand the functioning of mitochondria in normal cell function and in processes leading to cell death (Skarka & Ostadal, 2002).

Not all laboratory-induced drug resistance in African trypanosomes can be attributed to loss of drug transporters. The mitochondrion status and the mitochondrial membrane potential and their role as drug targets and in drug resistance have been studied in the field of trypanosomiasis. For instance, pentamidine has been reported to target the mitochondrion in various species. A study using some fluorescent pentamidine analogues on *Leishmania* parasites showed that they accumulate strongly in mitochondria, causing mitochondrial damage and subsequently cell death. Pentamidine resistance in *Leishmania donovani* was also proven to be associated with a reduction in the mitochondrial membrane potential (Mukherjee *et al*, 2006; Barrett *et al*, 2007).

In *Trypanosoma*, the study of fluorescent analogues of the diamidine DB99, using simple fluorescence microscopy, revealed that they accumulate rapidly in the kinetoplast as well as the nucleus (Stewart *et al*, 2005). Such a study was not possible with pentamidine, due to its non-fluorescent nature; however it was possible to study whether a correlation between pentamidine resistance levels and membrane potential exists. During this project we were able to confirm that mitochondria are a target for pentamidine and resistance to the drug appears to coincide with a significant reduction in the mitochondrial membrane potential (see chapter 5).

### 1.9.2 Suramin

Suramin is also available under several trade names (Bayer 205, Antrypol, Germanin, Moranyl, Naganin) (Delespaux & de Koning, 2007). Chemically, it is a colourless polyanionic sulfonated naphthylamine (Figure 1.4); it was modified from the Trypan Red dye that was used by Paul Ehrlich and was first used as a trypanocide in the early 1920s. It is only effective in the treatment of early stage *T. b. rhodesiense* and *T. b. gambiense* human disease. It is the drug of choice for the treatment of early stage *T. b. rhodesiense* sleeping sickness in East Africa (World Health Organisation, 1995) because it is more effective than pentamidine, the drug of choice for *T. b. gambiense* (Pepin & Milord, 1994).

Suramin is strongly negatively charged (six negative charges) at physiological pH (Delespaux & de Koning, 2007). The charged nature of the drug may explain the mode of entry into the cell as it binds strongly to plasma proteins including low-density lipoproteins (LDLs) which are a main source of sterols for bloodstream trypanosomes. Trypanosomes recognise and eagerly endocytose LDL through specific membrane receptors allowing the bound suramin to be accumulated through the same process (Barrett *et al*, 2007; Bacchi, 2009).

The drug can be injected as it is a highly water soluble substance and it is administered slowly by intravenous infusion to reduce the risk of anaphylactic shock and other side-effects. It is usually given in a dose of 5 mg/kg test dose on day one to check for allergic reactions, followed by 10 mg/kg on day 3 of treatment. 20 mg/kg is given on days 5, 11, 23, and 30 (Legros *et al*, 2002). Suramin has a long half-life of 44-54 days and can still be detected in the blood between five and eight months after the final injection. Again this is probably due to its high charge therefore it is very effective drug in the early stage caused by *T. b. rhodesiense* as it clears the blood rapidly of the parasite (Pepin & Milord, 1994; Bacchi, 2009).

The mode of action in killing the parasite is still completely unknown; some studies suggested that its action involves inhibition of various glycolytic enzymes in *T. b. brucei* and also other enzymes, including those of the pentose phosphate pathway (de Koning, 2001; Barrett *et al*, 2007; Fairlamb, 2003). The compound also binds to other enzymes, such as thymidine kinase, consequently inhibiting

them. Therefore it is very possible that suramin's action may be caused by the inhibition of several of these enzymes (Bacchi, 2009).

Some side effects are quite common in the treatment with suramin, including renal toxicity, fever, perhaps due to the lysing of the trypanosomes, nausea, vomiting. In rare cases the side effects may develop into jaundice, severe diarrhoea or anaphylactic anaemia. Severe delayed reactions include kidney damage, and in some cases it might cause death (Pepin & Milord, 1994; de Koning, 2001; Fairlamb, 2003).

Despite being in use for over eighty years the resistance phenotype to suramin is reported stable in field strains. In laboratory and field strains suramin has not shown any cross-resistance with arsenicals, diamidines, quinapyramine or isometamidium (Delespaux & de Koning, 2007).

### **1.9.3 Melarsoprol**

Melarsoprol belongs to the melaminophenyl arsenical compounds (Figure 1.4) and has been the drug of choice for second-stage HAT caused by either *T. b. gambiense* or *T. b. rhodesiense* since the late 1940s. Melarsoprol is soluble in lipids and therefore it can cross the blood brain barrier (Nok, 2003; Fairlamb, 2003) As it is not water-soluble the drug is given as an intravenous injection after being dissolved in propylene glycol. This solvent is a highly irritant agent that causes tissue damage and anti-inflammatory drugs such as prednisolone are used in conjunction to minimise the impact of such side effects (Delespaux & de Koning, 2007; Fairlamb, 2003).

There is no standard protocol for dosage or length of treatment with melarsoprol, but the most commonly used strategy is made up of three stages, between seven and ten days apart, of three- or four-day courses at a dosage of 3.6 mg/kg per day by single intravenous injection. Melarsoprol is active against both early and late stage infections, but because the treatment is usually associated with several dangerous side effects the most serious being that up to 10% of patients suffer from a serious reactive encephalopathy resulting in death in 50% of those cases, treatment with melarsoprol requires hospitalization of the patient. For this reason the drug is only used for late stage trypanosomiasis as

other less toxic drugs are available for stage one, such as pentamidine (Pepin & Milord, 1994; Lutje *et al*, 2010).

Melarsoprol is the only arsenic-based compound that is currently used against trypanosomosis in humans; other drugs belonging to the same class of compounds are widely used in the livestock form of the disease. Cymelarsan is one good example and is used in the treatment of *T. evansi* infections, which is the cause of a wasting disease called Surra in many domestic animals and some wild animals. Very recently, it was successfully used in the treatment of livestock after a new outbreak of *T. evansi* that occurred in mainland Spain, after the importation of camels from the Canary Islands. The investigation at the place of the outbreak showed that 76% of the camels, 35% of the donkeys and 2% of the horses were infected. The animals were isolated and treated using Cymelarsan (0.5 mg/kg). After treatment, the blood analysis revealed negative results (Tamarit *et al*, 2010). This follows another recent outbreak of surra in France (Dequesnes *et al.*, 2008).

In the recent years there have been reports of high percentages of treatment failures using melarsoprol, especially its use against *T. b. gambiense* in areas with high transmission rates such as in the Democratic Republic of Congo, southern Sudan, Uganda and Angola. This increase requires more attention especially with the continuously increasing rate of resistance in many areas (Delespaux & de Koning, 2007).

#### **1.9.4 Eflornithine**

Eflornithine ( $\alpha$ -difluoromethylornithine, DFMO) (Figure 1.4) was originally developed as an anti-tumour drug. It was licensed for human use recently as a less-toxic alternative treatment for melarsoprol-refractory sleeping sickness. After being approved as safe for human use it was first introduced for the treatment of HAT in 1990 against *T. b. gambiense* even in the late stage of infection. It acts as a specific and irreversible inhibitor of the ornithine decarboxylase (ODC) enzyme. Its action takes place at the first step of polyamine biosynthesis by disrupting the formation of polyamine (Denise & Barrett, 2001; Delespaux & de Koning, 2007).

The low turnover rate of human ODC made it ineffective as an anti-tumour drug, whereas it is very effective against *T. b. gambiense* as its ODC is more stable and has a longer half-life. However DFMO has low efficacy: only 225  $\mu\text{M}$  is toxic to *Trypanosoma gambiense* and it is completely ineffective against human *T. b. rhodesiense* infections. *T. b. rhodesiense* has a higher overall ODC activity and its ornithine decarboxylase enzyme has a shorter half-life than in *T. b. gambiense* (Delespaux & de Koning, 2007; Denise & Barrett, 2001d). A study with radiolabelled DFMO did not show any difference in uptake levels by both strains. Bacchi *et al* (1993) attributed that to the possible interaction of AdoMet metabolism in increasing tolerance to DFMO (de Koning, 2001).

Carrillo and colleagues have studied *in vitro* the turnover rate of DFMO in various cells including *L. mexicana* promastigotes, *Crithidia fasciculata*, *Phytomonas* and ODC-transformed *T. cruzi* as the genomic project of the later showed that the polyamine auxotrophic organism *T. cruzi* does not contain ornithine decarboxylase (ODC). It was found that DFMO was able to arrest proliferation in both *L. mexicana* and *T. cruzi*, but in *Crithidia fasciculata* and *Phytomonas* the drug had no effect. ODC metabolic turnover measurements showed that the enzymes from *Crithidia* and *Phytomonas* have a short half-life of 20-40 min, while ODC from *Leishmania* and transgenic *T. cruzi* are more stable with a 6 hours half-life (Carrillo *et al*, 2007). Under different growth conditions DFMO decreases the levels of putrescine and spermidine in parasites with high ODC turnover, but spermidine levels were higher in parasites with slow ODC turnover rates (Carrillo *et al*, 2000; Delespaux & de Koning, 2007).

Some disadvantages have limited the use of DFMO in treatment for example being expensive drug and its short half-life of about 3 hours in the plasma following intravenous injection with 80% of the drug excreted unchanged in urine after 24 hours makes it difficult to administrate. For successful treatment the drug must be given in high doses of about 400 mg kg<sup>-1</sup> per day in four daily infusions every 2 hours for 7 or 14 days. Additionally, treatment using eflornithine is associated with several unpleasant reactions including anaemia, leucopenia, pancytopenia, gastroenteric symptoms, headaches, and sometimes seizures (Lutje *et al*, 2010).

It has been proposed that the entry of DFMO into the target cells proceeds by passive diffusion (Denise & Barrett, 2001; de Koning, 2001). A recent study has shown that resistance to DFMO can be induced relatively easily. It only took around 60 days for the bloodstream form *T. b. brucei* 427 strain to become resistant to eflornithine using the simple approach of growing the sensitive cells in increasing concentrations of drug. The mechanism of resistance to eflornithine was investigated and was shown to be accompanied by loss of a specific amino acid transporter. The transporter is coded by a single gene designated *TbAAT6* and PCR analysis showed that the resistance cell line lacks this gene. This was confirmed by complementation of the gene into the resistant line and restoring sensitivity. Parasites lacking *TbAAT6* are viable in animals and retain the resistance phenotype, indicating that parasite populations could easily develop resistance. Therefore, it will be critical to monitor the status of this gene within parasite populations in endemic areas especially with the increased use of eflornithine in trypanosomiasis therapy (Vincent *et al*, 2010). In an effort to prevent the loss of DFMO as an effective treatment, a combination therapy with nifurtimox was recently introduced.

### **1.9.5 Diminazene aceturate**

Diminazene aceturate, otherwise known as Berenil, belongs like pentamidine to the class of aromatic diamidines. It is widely used as a veterinary trypanocide in the treatment of livestock trypanosomiasis. The advantage of being relatively cheap and effective in the treatment of other animal infections makes it the drug of choice in treating sick cattle in sub-Saharan Africa. In recent years an increasing level of resistance to the drug in the field has been reported creating real problems, especially with the occurrence of cross-resistance with the only alternative drug, Isometamidium.

Diamidine is a highly charged compound, and requires specific carriers to migrate across cell biomembranes and the absence of these transporters will reduce the uptake of diminazene (Fairlamb, 2003; Delespaux & de Koning, 2007). In *T. b. brucei*, diminazene was found to display high affinity for the P2 aminopurine transporter, with a  $K_i$  value of  $2.4 \pm 0.5 \mu\text{M}$  (de Koning & Jarvis, 1997). This was verified by a study of the phenotype of a strain from which the P2/TbAT1 single gene had been deleted. The *tbat1*<sup>-/-</sup> line displayed high levels of

resistance to diminazene (Matovu *et al.*, 2003). The continued sensitivity of this strain to approximately 1  $\mu$ M diminazene aceturate led to speculation about residual uptake through a secondary system. This was investigated in detail and reported in Chapter 3 of this thesis.

In experimental studies and /or when other drugs were unavailable, diminazene been used in the treatment of human *rhodesiense* and *gambiense* early stage HAT, even though it has never been licensed for human treatment (Fairlamb, 2003; Delespaux & de Koning, 2007).

### **1.9.6 DB-75**

DB-75 (furamidine) is also one of the aromatic diamidine compounds with broad-spectrum antimicrobial action (Fairlamb, 2003; Delespaux & de Koning, 2007). Despite some studies that suggest that DB75 inhibits mitochondrial function, its antimicrobial action mechanism is still not clear. DB75 is active in animals only if given as an injection whereas its amidoxime prodrug DB289 (pafuramidine) is orally active. The drug uptake profile appears to be like diminazene principally dependant upon the P2 transporter, but with measurable uptake still evident in TbAT1-KO cells line (Lanteri *et al.*, 2004; Barrett & Gilbert, 2006). Pafuramidine is the only new chemical entity to enter clinical trials for HAT in decades; these were ultimately not successful due to nephrotoxicity, although the drug was sufficiently efficacious against early stage *gambiense* sleeping sickness (Paine *et al.*, 2010).

### **1.9.7 Nifurtimox**

Nifurtimox (Lampit®) belongs to the 5-nitrofurans compound group, and has been used as an anti-protozoal since the 1960s in South America to treat the acute form of Chagas disease and recently in Africa against late stage of *T. b. gambiense* but no evidence of efficacy against *T. b. rhodesiense* has been shown. The advantages of this drug are that it is orally available and relatively cheap. No cross-resistance with other drugs has been reported but as a monotherapy the duration of administration is too long and causes unacceptable toxicity. To overcome this disadvantage the dose was reduced and a shorter

course of treatment, together with eflornithine introduced as treatment regime (Delespaux & de Koning, 2007; Lutje *et al*, 2010; Yun *et al.*; 2010).

## 1.10 Trypanosome molecular biology

It is clearly understood that Trypanosomes are obligatory parasites and that they are totally reliant on the host environment to obtain many essential materials for cellular functions. For instance, purine and pyrimidines are essential compounds for nucleic acid synthesis in every living cell. Trypanosomes as well as all other protozoan parasites are unable to synthesize purine nucleobases *de novo*, and totally rely on the host environment as a source of purine (de Koning *et al*, 2005). In contrast, apart from *Giardia lamblia*, *Tritrichomonas foetus* and *Trichomonas vaginalis*, parasitic protozoa are able to synthesize the pyrimidine ring *de novo*, and are also able to salvage some pyrimidines such as thymidine or uracil (de Koning *et al*, 2005).

The biochemical characteristics of trypanosomes have highlighted that, in order for the parasite to salvage these nutrients, they must employ specific transport systems. There are many proteins associated with the cell surface that facilitate directly or indirectly in migration of nutrient compounds across the membrane. Since purine uptake requires the activity of specific nucleoside and/or nucleobase transporters located in the plasma membrane of the parasite, these transporters and the role they play in parasite viability have been well studied. Trypanosoma species as well as many other protozoan species possess at least two nucleoside transport activities at some stages of their life cycle; these transporters can also transport other components, especially those that share some chemical features with their natural substrate (de Koning *et al*, 2005; de Koning & Diallinas, 2000).

With the development of the molecular biology it is now possible to use biochemical characteristics in conjunction with aspects of their molecular biology such as gene expression, antigenic variation, and genetic diversity to understand the roles of these transporters in the parasite lifecycle and in their potential to mediate the uptake of selective drugs.

The parasite is covered on the surface membrane with a dense surface coat composed of a unique protein known as the variant surface glycoprotein (VSG) (Turner, 1999). Recognition of this surface coat by the host immune system will result in killing of the parasite. Because the parasite frequently switches to a different VSG it avoids being targeted by antibodies (Barry, 1979). This process of variation is what gives rise to the relapsing parasitemia seen in patients of sleeping sickness. The molecular mechanisms by which the parasite effects the periodic changes in the VSG coat has been well studied (Barry & McCulloch, 2001). The trypanosome genome codes for about 1000 different VSG genes (VSGs) and pseudo-VSGs which are scattered throughout the trypanosome genome. Only one variant is expressed at a time with certain VSGs associated with metacyclic populations and others making an appearance early in the course of infection (Turner, 1999; Barry & McCulloch, 2001; Barry *et al*, 2005). It is estimated that trypanosomes are capable of making  $10^{-6}$ - $10^{-2}$  switches of VSG per doubling time of 5-10 hours (El Sayed *et al*, 2000).

All expressed VSGs are located at the telomere, suggesting that VSG genes are translocated into these specific sites (Donelson, 2003). There are other molecular mechanisms that could be involved in the introduction and removal of VSG genes from these sites, but not all have been accurately characterised. Regulation of antigenic variation is as complex as the event itself (Donelson, 2003) as only one VSG is expressed at a time there must be a mechanism which the parasite developed in order to silence the other expression sites, as well as specific transcription at a particular site. Suggestions have been made for the presence of a modified base (base J) being involved in the stabilisation of repression of expression sites (Ulbert *et al*, 2004; Hertz-Fowler *et al*, 2008).

Base J is a hypermodified base found in eukaryotic DNA, it was first identified in the nuclear DNA of *Trypanosoma brucei* in 1993. It was also confirmed to be present in all kinetoplastid flagellates analyzed and some unicellular flagellates closely related to trypanosomatids, but it has not been found in other protozoa or in metazoa. J is invariably present in the telomeric repeats of all organisms analyzed (Borst & Sabatini, 2008).

All the VSG genes that have been identified by genome sequence so far are located towards the telomeric ends of chromosomes. Of all the identified VSG

genes, 95% do not properly encode protein, 5% are fully functional for example encode all recognizable features of known functional VSGs, 9% are atypical which means they are complete genes but may not encode all elements for accurate folding or post-translational modification, 62% are full-length pseudogenes as they contain stop codons and/or frame shifts, and 19% are gene fragments (Barry *et al*, 2005).

However, the procyclic form of the African trypanosome do not express the VSG coat as they possess a glycoprotein coat composed of procyclins. Procyclins are encoded by genes that are organised in tandem arrays of two or three copies on two pairs of chromosomes. They are first expressed in the midgut of the tsetse fly, upon bloodstream form differentiation to the procyclic form. The fact that expression of the procyclin coat is coupled to the loss of the VSG coat suggests that there is a tightly regulated system is involved in the expression process (Roditi & Clayton, 1999).

## 1.11 RNA Interference & Gene Knockout

RNA Interference (RNAi) is another name for double-stranded RNA (dsRNA). It was first discovered by Fire and Mello and collaborators in the roundworm *C. elegans* (Fire *et al*, 1998) and resulted in the silencing of specific gene expression (Hannon, 2002). RNAi is a powerful and flexible technique to characterize the mechanisms of eukaryotic gene regulation in which a short sequence of double-stranded RNA (dsRNA) is formed targeting a specific gene (Kent & MacMillan, 2004).

In general, gene expression within the eukaryotic cell involves two main steps, which are transcription and translation. These steps involve synthesis, maturation, and degradation of protein-coding messenger RNA (mRNA). Transcription occurs when precursor-mRNA (pre-mRNA) molecules are produced due to the action of RNA polymerase II in the nucleus. This process involves some steps including the removal of non-coding intron sequences in a process known as splicing. Then the cap is added to the 5' end and the poly-A tail to the 3' end of the fragment, after which it is transported to the cytoplasm and subsequently to the ribosome, where translation takes place. The final outcome of mature mRNA is different depending on the requirement and the type of translated

product needed by the cell. Gene expression can be controlled by hybridizing an anti-sense RNA to mRNA; this can be achieved in two possible ways (i) by blocking the translation process or (ii) degradation of the mRNA\_anti-sense duplex through RNase H (Kent & MacMillan, 2004).

RNAi is a reliable method that enables the process of knocking down expression levels of a specific gene product and allows the investigator to monitor the effect of the targeted gene on the phenotype of a single cell or whole organism. The mechanism of RNAi is rapid, simple and specific, and the introduction of the dsRNA can be preceded through a number of sequential steps. Firstly, there is cleavage of the dsRNA by the RNase III enzyme DICER into shorter 21- 23 nucleotide dsRNA pieces termed short interfering RNAs (siRNA) (Figure 1.5).

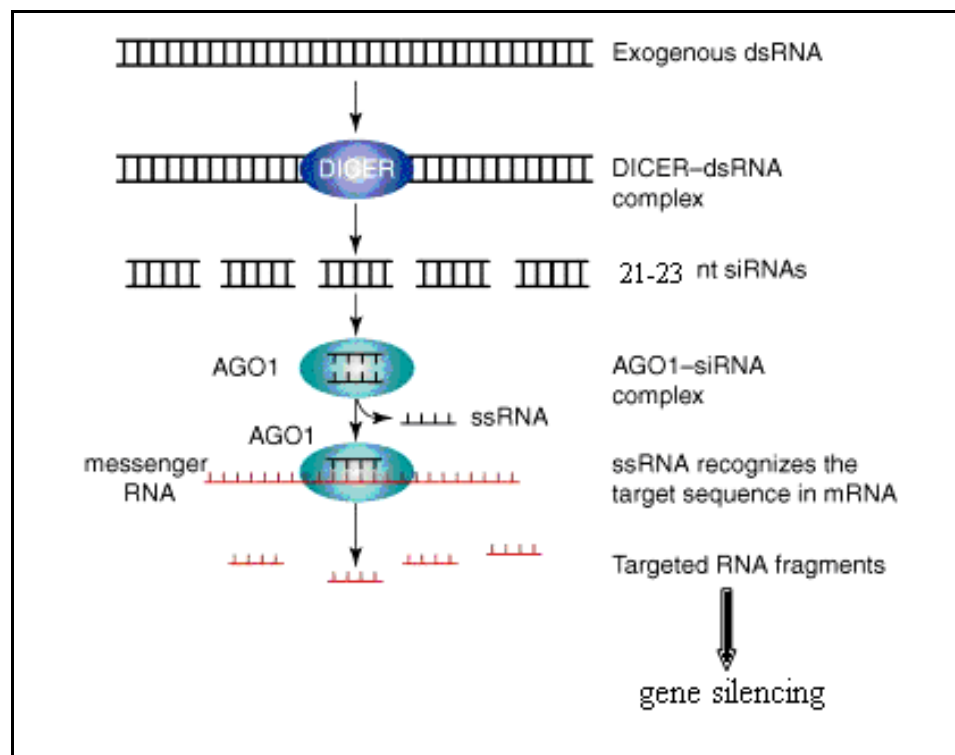


Figure 1.5. Diagram represents RNAi mechanism in trypanosomatids.

(Reproduced from (Balana-Fouce & Reguera, 2007).

These siRNAs have a characteristic phosphorylated 5' end and a two-nucleotide overhang at the 3'OH end. The siRNAs then enter a RNA-induced silencing complex (RISC). A helicase, belonging to the argonaute (AGO1) family or Slicer, unwinds the two strands of the siRNA to form single-stranded RNAs (ssRNA), and RISC scans the mRNAs in the cytoplasm and cleaves the molecules that are found complementary to the RISC-contained siRNA. The siRNA guides its cognate mRNA into an RNA-induced silencing complex, which rapidly cleaves the target

mRNA resulting in down regulation of mRNA transcript and gene silencing (Carmichael, 2002).

The early use of the RNAi technique in *Trypanosoma brucei* has provided a convenient method to generate a specific gene (sequence) knockout phenotypes (Ngo *et al*, 1998). It is now considered as an informative method and is widely used to study *Trypanosoma* at the molecular level. Rusconi and coworkers carried out one early example of RNAi use on *Trypanosoma brucei* to knockdown the *TbPFR2* gene to study the phenotypic effect on the flagella motility function. This study established that functional complementation could be achieved by using RNAi experiments to observe the phenotypic effects due to specific silencing of the targeted gene (Rusconi *et al*, 2005). RNAi has now become one of the preferred tools to study the function of some of the *Trypanosoma* organelles in molecular details, for example it was recently used to identify genes that are associated with mitochondrial membrane potential (Verner *et al*, 2010).

Some requirements must be taken into count when considering the use of RNAi in a study, including the length of the RNA fragment, which should be between 400 and 1000 bp. The other important requirement is the sequence composition of the targeted RNA. RNA-mediated interference required a specific sequence in the interfering RNA or target RNA to avoid miss targeting, especially the downregulation of genes with similar sequence (Parrish *et al*, 2000).

Many vectors have been constructed; the most commonly used are recently developed tetracycline-regulated vectors for production of dsRNA. The first RNAi experiments in *Trypanosoma brucei* used electroporation of dsRNA into cells, leading to potent but transient phenotypes (Motyka & Englund, 2004). The utility of RNAi was greatly enhanced with the production of vectors that stably integrate into the genome and express dsRNA in an inducible manner. The first such vector used a tetracycline-inducible promoter to drive RNA expression. More recently newer vectors were developed, which surround a fragment of the gene between two opposing tetracycline-inducible T7 promoters (Wang *et al*, 2000; LaCount *et al*, 2000). The double T7 promoter system has two major advantages, one is it works for both the procyclic and bloodstream forms of the parasite. Secondly, the ability of using a single construct to carry multiple

genes, allowing simultaneous targeting (Motyka & Englund, 2004). However, some reports shown that the two-promoter system may not work for all genes (La Count *et al.*, 2000). This led to the construction of new vectors such as the recently developed stem loop RNAi vector for inducing expression of stem loop RNA in *T. brucei* under tetracycline control (Alsford & Horn, 2008). Occasionally mutant phenotypes may not be detectable, this could be due to the targeted genes are non essential or because they have overlapping functions in other proteins, or not completely down-regulated.

Designing primers to amplify the flanking sequences for the purpose of gene knockdown by homologous recombination has become straightforward, especially after the completion of the sequence of the megabase chromosomes of *Trypanosoma brucei* (ten Asbroek *et al*, 1990). In general biology, homologous recombination has important implications for growth, development and adaptation of all organisms. It has roles in DNA damage repair, for the generation of genetic diversity and to ensure chromosomal segregation at meiosis (van Gent *et al*, 2001; Modesti & Kanaar, 2001). In African trypanosomes homologous recombination also has implications in the antigenic variation processes. Recombination is used to move new VSG genes into specialised bloodstream VSG transcription sites. Genetic and molecular evidence has suggested that antigenic variation uses homologous recombination; however the detailed reaction pathways are yet to be elucidated (Conway *et al*, 2002; Burton *et al*, 2007).

The natural homologous recombination phenomenon has been widely used so support stable transformation and has been successfully applied to trypanosomes (ten Asbroek *et al*, 1990). Linearised DNA constructs, transfected into the cell, allows replacement of a gene to occur by homologous recombination. This means highly specific targeting of a chosen genomic locus. In *T. brucei* a number of selectable marker genes are now employed to achieve stable transformations for instance using the neomycin, puromycin and hygromycin B antibiotic resistance genes (ten Asbroek *et al*, 1990; Vara *et al*, 1986; Lee & van der Ploeg, 1991; Clayton *et al*, 2000). RNAi was successfully used during this project in both bloodstream and procyclic forms of *T. b. brucei* (see Chapter 7).

## 1.12 The nucleoside and nucleobase salvage and transportation

Purine nucleosides are important requirement for the growth and development of all protozoans as they are necessary for the synthesis of biomolecules such as DNA and RNA, act as cofactor for many enzymes, and as activated sugar intermediates, the purine ring is integral to ATP, essential for energy metabolism (Gherardi & Sarciron, 2007).

Trypanosomes are unable to synthesise purines *de novo* so they rely entirely on the extracellular environment to obtain these nutrients from their host (de Koning *et al*, 2005). Due to the hydrophilic nature of most nucleosides and nucleobases, they cannot easily diffuse across the lipid bilayer of the plasma membrane. Therefore, the parasite developed specific transport proteins integrated in the cell membrane for their translocation (Cohn & Gottlieb, 1997; de Koning *et al*, 2005). Salvage of purine nucleobases or nucleosides in protozoa is mediated by various transporters, which are localised in the plasma membrane of the parasites (Landfear *et al*, 2004). Some protozoans have been shown to possess two nucleoside transporters in addition to one or more transporters for the salvage of nucleobases (de Koning *et al*, 2003). All the nucleoside and nucleobase transporter genes identified in protozoa to date have been found to belong to the equilibrative nucleoside transporter family, which is described in detail in section 1.9.1. Studies of these transporters at the molecular level have allowed for a better understanding of the physiology of the parasites (de Koning *et al*, 2005).

Molecular studies in mammals as well as protozoa revealed that transmembrane proteins which are involved in uptake and release of free nucleosides and nucleobases across the eukaryotic plasma membrane possess two major nucleoside transporter families; (i) equilibrative nucleoside transporter (ENT) and (ii) concentrative nucleoside transporter (CNT) (de Koning *et al*, 2005).

### 1.12.1 ***Equilibrative nucleoside transporter (ENT) Family***

The equilibrative nucleoside transporters are a family of proteins that mediate facilitated diffusion of nucleosides, such as adenosine, down their concentration gradients across cell membranes. In other words they mediate nucleoside transport in both directions depending on the nucleoside concentration gradient across the plasma membrane (Hyde *et al*, 2001; Acimovic & Coe, 2002; de Koning *et al*, 2005). This transport system is reported to be present in various cell types including mammals, plants, yeast, insects, nematodes and protozoa among others (Hyde *et al*, 2001; Acimovic & Coe, 2002; Podgorska *et al*, 2005).

For instance in the malaria parasite *Plasmodium falciparum* genetic studies have shown that they play an essential function in the transport of all naturally occurring purine nucleosides and nucleobases across the parasite plasma membrane after crossing the human erythrocyte cell membrane (Molina-Arcas *et al*, 2006; Downie *et al*, 2010).

All the protozoan nucleoside transporters cloned to date, including from *T. b. brucei*, are members of the ENT family. Beside their specificity in nucleoside transportation they have been reported to transport nucleobases in addition to pyrimidine nucleosides and some cytotoxic drugs from the extracellular environment across the cell membrane of human and protozoan cells. Some of them are specific for purines, whereas others recognize both purines and pyrimidines. (Acimovic & Coe, 2002; de Koning *et al*, 2005; Zhou *et al*, 2010). However, no pyrimidine-specific transporters have been cloned from protozoa or mammalian organisms, and it is unclear whether such transporters are encoded by ENT-family genes (De Koning, 2007). A study of nucleoside transporters (NT) using radiolabelled-ligand uptake and genetic analyses found that (NT1) and (NT2) of *Leishmania donovani* are excellent examples of this dual-selectivity phenomenon. This study found that LdNT2 is specific for purines because it has a high affinity and selectivity for inosine, guanosine and xanthosine, whereas LdNT1 transports adenosine in addition to pyrimidine nucleosides with reasonable efficiency (Bellofatto, 2007).

Many protozoan ENT transporters are proton symporters. The first protozoan nucleoside transporter confirmed to be a proton symporter was P1 (de Koning, *et*

*al.*, 1998). Several other purine and pyrimidine transporters from *Leishmania donovani* and *T. brucei* have also been shown to be proton symporters (reviewed in De Koning *et al.*, 2005). The proton-dependence of the *T. b. brucei* purine transporters is in contrast with the transporters in mammalian cells and tissues. Purine uptake in animal cells is by one of two mechanisms: facilitated diffusion/equilibrative transport or alternatively sodium-dependent active transport (Plagemann, *et al.*, 1988; Griffith & Jarvis, 1996). It is hoped that such fundamental differences in the function of the transport processes can be exploited to target trypanocides selectively to the trypanosome (Landfear, *et al.*, 2004).

The specification of the equilibrative nucleoside transporter (ENT) and their role in purine and pyrimidine uptake is now widely used in chemotherapeutics investigation and of possible delivery of drugs across cell membranes (de Koning *et al.*, 2004; de Koning *et al.*, 2005).

### **1.12.2 Concentrative nucleoside transporter (CNT) Family**

The concentrative nucleoside transporters (CNT) are Na<sup>+</sup>-dependent, as they facilitate the movement of nucleoside by pairing to sodium ion regardless of its concentration gradient. In contrast to the equilibrative nucleoside transporters which are present in most cell types, (CNT) are only expressed in a tissue-specific fashion (Gray *et al.*, 2004; Baldwin *et al.*, 2004; de Koning *et al.*, 2005).

This family is classified according to their substrate specificities to three sodium-dependent members: the CNT1 or (SLC28A1) which is responsible mostly for pyrimidine-nucleoside transportation, CNT2 or (SLC28A2) responsible purine-nucleoside transportation and CNT3 or (SLC28A3) transports both pyrimidine and purine nucleosides. They transport both naturally occurring nucleosides and synthetic nucleosides, and this ability can be used in the treatment of various diseases (Gray *et al.*, 2004; Aymerich *et al.*, 2005). No members of the CNT-family have been found in protozoan genomes analysed to date. However, some of the protozoan ENT-family transporters are energy-dependent, being H<sup>+</sup> rather than Na<sup>+</sup>-symporters (De Koning *et al.*, 1997; De Koning *et al.*, 1998; Stein *et al.*, 2003).

## 1.13 Structure activity relationship study of the nucleoside and nucleobase transporters

Two purine nucleoside transport activities are known in African trypanosomes: P1 expressed in both bloodstream and procyclic form of the *T. brucei*, and P2 expressed only in the bloodstream (Figure 1.6 & Figure 1.7). Briefly, both transporters have been kinetically characterized; the P1 transporter displayed a higher affinity and capacity for adenosine ( $K_m$  of  $0.38 \pm 0.10 \mu\text{M}$  and a  $V_{\text{max}}$  of  $2.8 \pm 0.4 \text{ pmol} \cdot 10^7 \text{ cells}^{-1} \cdot \text{s}^{-1}$ ) than the P2 transporter ( $K_m$  of  $0.92 \pm 0.06 \mu\text{M}$  and a  $V_{\text{max}}$  of  $1.12 \pm 0.08 \text{ pmol} \cdot 10^7 \text{ cells}^{-1} \cdot \text{s}^{-1}$ ). This difference in substrate affinity has been explained by De Koning and Jarvis in 1999 when they identified the recognition motif of both transporters (de Koning & Jarvis, 1999).

This was achieved after determining the affinity of purines analogues for the transporter by measuring the inhibition constant of each on [ $^3\text{H}$ ]-adenosine uptake. From data thus obtained, a structure activity relationship study was performed and the energy contribution to binding of each part of the molecule was determined. The recognition motif of each transporter clearly explains why P2 recognises only aminopurines but does not recognize oxopurines: mainly because the main interaction of adenosine with the P2 transporter is suggested to be via hydrogen bonds to the N1 and the 6-amino group of the purine ring, without involvement of the ribose moiety for ligand binding. In contrast, the P1 recognizes both amino- and oxopurines because the P1 transporter appears to form hydrogen bonds with N3 and N7 of the purine ring as well as with the 3' and 5' hydroxyl groups of the ribose moiety (see figure 4.1 in this thesis). This model also shows that diamidines such as pentamidine or melarsoprol share the P2 recognition motif but not the one of P1 and thus it explains their uptake by P2 but not by P1 (de Koning & Jarvis, 1999).

The same method will be followed to study the recognition motif for HAPT1 transporter which is one of the aims of this PhD project. This is a continuation of a study that has been ongoing for several years; during this period a number of compounds have been tested in our laboratory in order to investigate the HAPT1 recognition motif, and inhibition constants ( $K_i$ ) have been determined for most.

The current project has substantially increased the dataset, allowing for a formulation of testable relationships between structure and binding affinity.

## 1.14 Drug Uptake via Nutrient Transporters

The transporters and their role in nutrient transportation have received much interest in recent times as they could serve as potential targets for novel drugs to help overcome the difficulties in the treatment of HAT (de Koning *et al*, 2005; Barrett & Gilbert, 2006).

In comparison to the other protozoa such as *Leishmania* (amastigotes) and *Plasmodium falciparum*, which reside intracellularly, *Trypanosoma brucei* reside extracellularly and potential drugs do not have to cross mammalian cell membranes prior to reaching their target (de Koning *et al*, 2005).

A number of plasma membrane purine transporters in *Trypanosoma brucei brucei* have been identified so far, each facilitate in different stages of the cell cycle, three in the procyclic form, four in the long-slender bloodstream form and one during the short-stumpy form. Apart from *Trichomonas vaginalis*, *Tritrichomonas foetus*, and *Giardia lamblia* most protozoa are able to synthesize pyrimidines, and few studies have addressed pyrimidine uptake in protozoa, unless both pyrimidines and purines happen to use the same transporters. Purine transporters are competitively inhibited by some pyrimidines. The cases of adenosine transporters NT1 of *Crithidia fasciculata* and TgAT2 of *Toxoplasma gondii* are good examples as they are competitively inhibited by uridine, thymidine, and cytidine (de Koning *et al*, 2005; Gudin *et al*, 2006). However, to date no specific pyrimidine transporters have been identified in trypanosomatids or other eukaryotic cell types at the molecular level (de Koning *et al*, 2003).

*T. b. brucei* also expresses several different purine nucleobase transporters according to life-cycle stage. These transporters designated H1 and H4 hypoxanthine transporters, have been identified in the procyclic stage (Figure 1.7). The H1 transporter has a high affinity for purine nucleobase permeants but was proved to be unable to transport pyrimidines (de Koning & Jarvis, 1997). The other transporter was named TbNBT1 or H4 mediates the uptake of natural

purine nucleobases in addition to uracil and allopurinol across the cell membrane (Burchmore *et al*, 2003).

Uptake of purine nucleobases in the *T. b. brucei* bloodstream form was linked to the activity of two distinct transporters which were designated the H2 and H3 hypoxanthine transporters (Figure 1.6). H2 was found to mediate the uptake of hypoxanthine with a  $K_m$  value of 123 nM, furthermore it was found to be affected by a range of purine nucleobases and pyrimidines, and was inhibited by guanosine with a  $K_i$  of 10.9  $\mu$ M. At low concentrations, the H2 transporter was found to be responsible for the uptake of about 90% of hypoxanthine, whilst the H3 transporter was responsible for the remaining 10% of transport. The lower affinity H3 hypoxanthine transporter was more specific and was found to display micromolar affinity for the four natural purine nucleobases (hypoxanthine, adenine, guanine, and xanthine) with affinities that range between 4.7  $\mu$ M to 28.8  $\mu$ M but none of the other purines or pyrimidines was found to inhibit the transporter (de Koning & Jarvis, 1997).

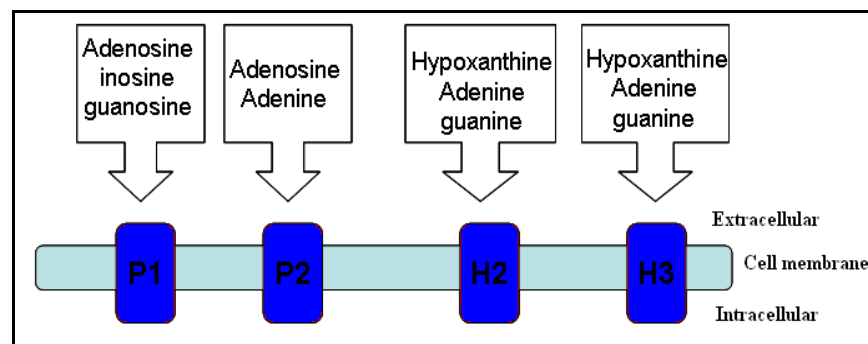


Figure 1.6. Purine transporters in the bloodstream form of the *Trypanosoma b. brucei* and their substrates.

In addition to the previous transporters the *T. b. brucei* procyclic form express the U1 transporter (Figure 1.7) which is strongly linked to the uracil transportation at this life stage (de Koning & Jarvis, 1997; Burchmore *et al*, 2003).

The purine nucleoside P1 transporter is expressed in the procyclic form (PF) and the bloodstream form (BSF) (Figure 1.6; Figure 1.7). The gene encoding this transporter, designated *Trypanosoma brucei* Nucleoside Transporter 2 (TbNT2), was cloned and expressed in *Xenopus* oocytes and confirmed to mediate the

uptake of adenosine, inosine and guanosine (Sanchez *et al*, 1999; Landfear, 2001).

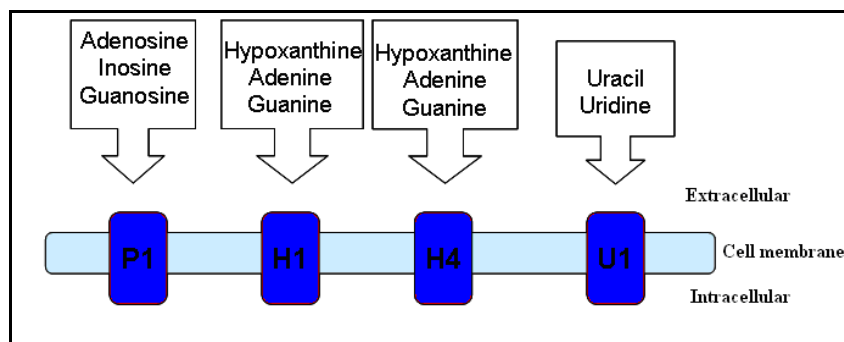


Figure 1.7. Purine and pyrimidine transporters in the procyclic form of the *Trypanosoma b. brucei* and their substrates.

Kinetic studies have shown that the P1 transporter displayed very high affinity for [<sup>3</sup>H] adenosine with a  $K_m$  value of 0.15  $\mu\text{M}$  and could be inhibited by other purine nucleosides but had very little affinity for the purine nucleobases. The P1 transporter was also found to be responsible for up to 80% of the adenosine flux in *T. b. brucei* bloodstream forms (Carter & Fairlamb, 1993; De Koning & Jarvis, 1999). Addition of 1  $\mu\text{M}$  melarsen oxide or melarsoprol failed to inhibit uptake of adenosine by the P1 transporter, indicating that this transporter was not involved in the uptake of these chemotherapeutic agents (Carter & Fairlamb, 1993).

The P2 transporter (Figure 1.6) is only expressed in bloodstream forms (Mäser *et al*, 1999). In addition to aminopurines, the P2 transporter also mediates the cellular uptake of non-purine trypanocides of clinical importance, especially those that share the structural recognition motif with adenosine such as melaminophenyl arsenicals and diamidines, (see chapter 4) (Mäser *et al*, 1999; Sanchez *et al*, 1999; Landfear, 2001; de Koning *et al*, 2005). In contrast to the P1 transport component, P2-mediated uptake of adenosine was inhibited by the addition of melarsen oxide or melarsoprol, implicating this transporter in uptake of trypanocidal agents (Carter and Fairlamb, 1993; De Koning and Jarvis, 1999). The role of the P2 transporter in drug delivery and resistance was first observed in 1993 by Carter and Fairlamb after adaptation of *Trypanosoma brucei* wild type to high concentrations of melarsen. This selection resulted in the loss of the P2 transporter and cloned cells lacking the P2 transporter were found to be 67 fold more resistant to melarsoprol *in vitro* when compared to the parental

cell line (Carter & Fairlamb, 1993). Furthermore, it was demonstrated using melarsen resistant *T. brucei* bloodstream forms that the P2 purine transport system was implicated in the reduced import of the diamidine pentamidine, leading to the suggestion of its involvement in pentamidine resistance (Carter *et al*, 1995).

Two further pentamidine transport activities have been characterised. Extensive kinetic studies of pentamidine uptake in bloodstream forms highlighted two adenosine-insensitive transporters that were involved in its transport. These transporters were designated High Affinity Pentamidine Transporter (HAPT1) and Low Affinity Pentamidine Transporter (LAPT1). Both transporters were insensitive to inhibition by purines and pyrimidines; their genetic identities have not been formally established, though a preliminary report (Ortiz *et al*, 2008) and phylogenetic analysis both speculated that previously uncharacterised members of the ENT family might encode HAPT1 and LAPT1 (de Koning, 2001; de Koning *et al*, 2005).

Several genes belonging to the ENT family members from the nucleotide transporters have been identified and named TbNT3 to TbNT9. The study of their functional expression in *Xenopus oocytes* found that some are high affinity purine transporter genes with products displaying characteristics highly similar to those of TbNT2 (Landfear *et al*, 2004; Landfear, 2001; Ortiz *et al*, 2009). In 2004 Sanchez and colleagues identified TbNT10 within the short stumpy form of the life cycle, which is pre-adapted for infection of the tsetse fly. In the yeast *Saccharomyces cerevisiae* the TbNT10 gene expressed transporter able to mediate the uptake of adenosine, guanosine and inosine (Al Salabi *et al.*, 2007; Spoerri *et al*, 2007).

However, three genes that belong to the 11<sup>th</sup> and 12<sup>th</sup> members of the *Trypanosoma brucei* ENT family were allocated by De Koning (2005) as the TbAT-like genes (discussed in details in chapter 6). These three genes are located in the same phylogenetic subgroup (group 1) of the ENT phylogenetic tree (Figure 1.8).

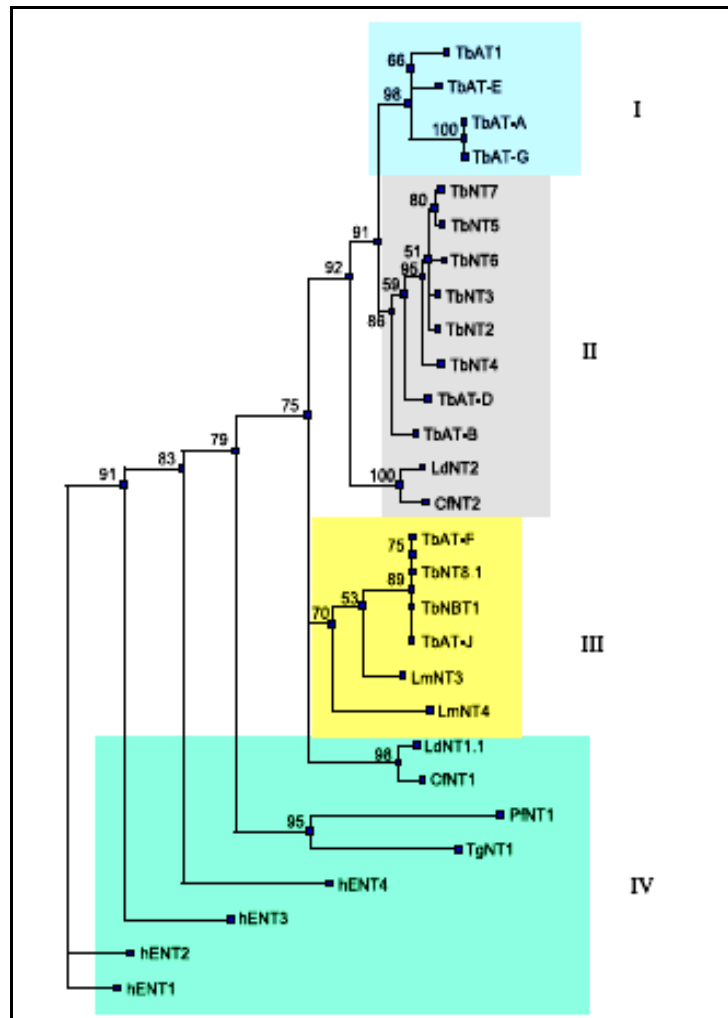


Figure 1.8. Phylogenetic tree of protozoan and human ENT family transporters.

The tree shows the close relation between the *T. brucei* adenosine transporter (TbAT1) gene (which also mediates pentamidine uptake) and the AT-A and AT-E like genes (Group I). Group II. Nucleoside transporter genes. Group III. Nucleobase transporter genes. Group IV. Nucleoside transporter genes (human and other protozoa). Reproduced from (de Koning *et al*, 2005)

The transporter genes are designated TbAT-A, TbAT-E and TbAT-G and share 58%, 58% and 66% similarity with TbAT1 at amino acid level, respectively, and the Gene DB systematic identifiers of these genes are Tb09.244.2020 for AT- A, Tb09.V4.0106 for AT- G and Tb927.3.590 for AT- E. A preliminary study of TbAT-A found that it was capable of diamidine uptake when expressed in yeast but did not mediate transport of purines or pyrimidines (de Koning *et al*, 2005).

Ortiz and colleagues have studied these genes recently and they have named them differently: AT-A = TbNT11.1, AT-G = TbNT11.2 and AT-E = TbNT12. In this study, the genes were expressed in a mutant *Leishmania* cell line that is deficient in purine nucleoside or nucleobase uptake. Based on their function both genes were identified as high-affinity purine nucleobase transporters. On

the other hand the expression of transporters in *Xenopus oocytes* revealed that they may also be capable of transporting the diamidine drug pentamidine which is the major drug in treating early stage of human African trypanosomiasis (Ortiz *et al*, 2009). However, this study left many questions open and did not attempt to identify either gene as a candidate for HAPT1 or LAPT1.

## 1.15 Overview of the TbAT1/P2 molecular study and its role in drug transportation

Studies of a *T. b. brucei* melarsen resistant clone provided the first evidence of the involvement of the adenosine P2 transporter in drug uptake as melarsen oxide and melarsoprol inhibited P2-mediated adenosine transport (Carter & Fairlamb, 1993). Soon after, Carter and colleagues showed that loss of P2 transporter also led to reduced import of pentamidine, leading to the suggestion of its involvement in pentamidine resistance (Carter *et al*, 1995). The P2 adenosine transport system was further found to be present in *T. equiperdum* where the P2 transporter of a berenil resistant clone, cross-resistant to melarsoprol, displayed reduced activity and possibly decreased affinity for the main P2 substrate, adenosine compared to the drug sensitive clone (Barrett *et al*, 1995).

A revolution in molecular genetics has brought a new era in the study of trypanosome transporters, as many of their coding genes have now been identified. Molecular characterisation of the gene encoding TbAT1 has played a major role in understanding the mechanisms underlying drug resistance in *T. brucei* (Mäser *et al*, 1999). *TbAT1* is a single copy gene and encodes a protein of 463 amino acids with 11 predicted transmembrane domains. Sequence analysis of TbAT1 gene showed that it shares up to 30% identity with to *Leishmania donovani* nucleoside transporter *LdNT1* at the amino acid level (Vasudevan *et al*, 1998; Mäser *et al*, 1999). *In vitro* studies have revealed that loss or alterations in P2 adenosine transport is indeed associated with the development of resistance to melaminophenyl arsenicals and diamidines (Mäser *et al*, 1999; Matovu *et al*, 2003; Bridges *et al*, 2007). Definitive verification came with the generation of a TbAT1 knock out (KO) line, which showed a significant reduction in sensitivity to various arsenicals and diamidines. This result confirms how cross-resistance

between these two classes of drugs can arise (de Koning, 2001; Mäser *et al*, 2003; Delespaux & De Koning, 2007).

A *TbAT1* gene cloned from a melarsen-resistant clone designated (STIB 777R) had ten nucleotide differences in its cloned *TbAT1* open reading frame (ORF) compared to the *TbAT1* of the melarsen-sensitive clone designated (STIB 777S). The trypanosomes genome is considered to be diploid; therefore a copy of this gene should be present on each of the two chromosomes and sequencing analysis of STIB 777S strain suggested the possibility that it was homozygous for the sensitive allele. The expression of the *TbAT1* gene cloned from the melarsen-resistant clone (STIB 777R) in yeast did not increase the uptake of adenosine and, moreover, did not confer susceptibility to melarsen-oxide, confirming its lack of activity. In the same study a PCR/ RFLP (Restriction fragment based polymorphism) method using the *Sfa NI* enzyme enabled the distinguishing between the *T. brucei* melarsen sensitive (STIB 777S) and melarsen resistant clone (STIB 777R) by displaying different allele patterns, 566 bp & 111 bp for the wild type *TbAT1* and 435 bp and 242 bp for the mutated *TbAT1*. The method was used to demonstrate the presence of a mixed banding pattern in patient samples which were either infected with trypanosomes homozygous for both the sensitive and resistant *TbAT1* alleles or heterozygous for the sensitive or resistant *TbAT1* alleles (Matovu *et al*, 2001). A total of 10 point mutations have been identified in the melarsen resistant clone and some of these mutation caused changes at amino acid levels. For instance, the change of a base G to A at position 532 converted alanine (Ala) to threonine (Thr) which eliminated the *Sfa NI* site present in the wild type *TbAT1*. Another mutation led to amino acid alteration with the change of a base A to G at position 857 causing conversion of asparagine (Asn) to serine (Ser), leading to a new *Sfa NI* site 325 bp further downstream (Mäser *et al*, 1999).

In general, exploitation of nutrient transport systems for delivery of new drugs needs to adhere to several key conditions; namely selectivity and efficacy. More specifically, there needs to be high affinity of the trypanocide for the particular transporter, coupled with low affinity for the mammalian transporter. Furthermore, there needs to be low abundance of competing substrates and ideally there needs to be concentrative rather than equilibrative uptake (de Koning & Jarvis, 1999; Barrett & Fairlamb, 1999). The P2 purine transporter,

thus far, appears to satisfy these two conditions but has one major disadvantage: the fact that the parasite can lose this transporter without compromising viability (Matovu *et al*, 2003). Therefore, identification of new routes for successful drug delivery is essential.

## **1.16 The molecular basis of the HAPT1 and LAPT1 transporters**

The traditional biochemical techniques that have been used in the study of the transportation systems in trypanosomes had many disadvantages, particularly as the multitude of transporters with overlapping specificities can confound efforts to dissect the function of the individual carrier. It has been well documented that trypanosomes express two pentamidine transport activities in addition to P2: the High Affinity Pentamidine Transporter (HAPT1) and the low affinity Pentamidine Transporter (LAPT1). HAPT1 and LAPT1 transporters have been detected biochemically using radiolabelled permeants (de Koning, 2001) but have yet to be characterised at the molecular level and the understanding of their molecular basis is now needed to study their contributions to drug uptake and, in particular, to drug resistance.

As mentioned above a functional study of the NT11 and NT12 genes (AT-A, E, G) by Ortiz and co-workers suggested that these genes are high-affinity purine nucleobase transporters when expressed in a null background purine nucleoside or nucleobase uptake *Leishmania* model. On the other hand the expression of these transporters in *Xenopus oocytes* revealed that they displayed high affinity to pentamidine (Ortiz *et al*, 2009).

The coding gene for P2 adenosine transporter has already been identified to be TbAT1 (Figure 1.9). Since the three closely related genes have been confirmed to be able to transport pentamidine, the question now is whether the TbAT like genes will prove to be the code for the HAPT1 or/and LAPT1. This is the major aim of my PhD project.

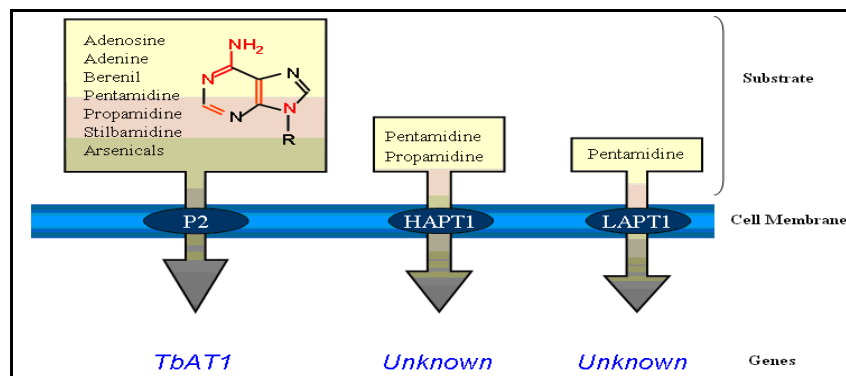


Figure 1.9. Diagram presents the main pentamidine transporters present in the trypanosomes membrane and their substrates as well as their coding genes. Reproduced from (Bray *et al*, 2003).

## 1.17 Transport of pentamidine across the plasma membrane

The possibility of using transporters to mediate drug uptake into cells has been under consideration for many years. Noticeably to date, the treatment of African trypanosomiasis in both animals and humans is still dependent on diamidines and melaminophenyl arsenicals (de Koning, 2008). Pentamidine is taken up by trypanosomes via P2 transporters as observed in early studies which linked the loss of P2 transporter through arsenical adaptation and resistance to diamidines (Barrett & Fairlamb, 1999; de Koning *et al*, 2000; de Koning, 2001; de Koning *et al*, 2004). This was supported to some extent by the study of TbAT1/P2 gene knock-out and how it could cause reduced susceptibility of *T. brucei* to melaminophenyl arsenicals and diamidines.

The TbAT1 gene deletion (*tbat1*<sup>-/-</sup>) resulted in only a 2-3 fold resistance for melarsoprol and pentamidine suggesting alternative routes of drug uptake might lead to higher levels of resistance to other diamidines (Matovu *et al*, 2003). This finding was later confirmed by a kinetic study which demonstrated that, unlike the transport of diminazene which is almost entirely accumulated through P2 (de Koning *et al*, 2004), pentamidine is taken up and concentrated by at least two additional transporters named HAPT1 and LAPT1 (de Koning & Jarvis, 2001; de Koning, 2001). The presence of multiple transporters in the trypanosomes makes it difficult to develop resistance to pentamidine. TbAT1/P2 has also been demonstrated to play a major role in the uptake of the newly developed diamidine drug DB75 (otherwise known as furamidine) as the *tbat1*<sup>-/-</sup> cell line

was found to be 10-fold resistance compare to the wild type 427 strain (Barrett & Gilbert, 2006; Ward *et al*, 2010).

Bridges and colleagues recently developed a new strain, designated TbAT1-B48, by subjecting the *TbAT1* knockout strain to high concentrations of pentamidine *in vitro*. The characterization of the new TbAT1-B48 strain demonstrated loss of HAPT1 activity but not of LAPT1 and showed high levels of pentamidine resistance compared to the wild type strain (Bridges *et al*, 2007). HAPT1 loss in TbAT1-B48 strain also resulted in cross resistance to melarsoprol. In contrast, *T. brucei* lacking only the *TbAT1* gene were previously shown to be 18-fold resistant to diminazene compared to wild type *T. brucei*, with hardly any detectable transport of radiolabeled diminazene (Matovu *et al*, 2003; de Koning *et al*, 2004), and no further increase in diminazene resistance was observed in B48. Based on those observations a number of conclusions were made, first of all *in vitro* exposure to pentamidine led to a massive increase of resistance to the drug, leading to concerns for the emergence of resistance in the field. The TbAT1-B48 cell line lost HAPT1 due to pentamidine adaptation, confirming HAPT1 as a second route for pentamidine. The high level of cross-resistance with arsenical drugs indicates involvement in melarsoprol uptake as well. Although the *tbat1*<sup>-/-</sup> strain displayed significant resistance to diminazene and DB75, it is still sensitive to approximately 1  $\mu\text{M}$  diminazene, suggesting other routes of entry.

Adaptation of the *tbat1*<sup>-/-</sup> *T. b. brucei* to a high concentration of diminazene aceturate and resulted in new cell line, designated ABR (Anne Kazibwe, PhD thesis, University of Glasgow).

The kinetic study showed that uptake of radiolabeled pentamidine in the ABR strain was significantly reduced and this was shown to be the result of loss of HAPT1 activity, whereas LAPT1 activity was unchanged. However, transport of radiolabeled diminazene was still detectable at 1  $\mu\text{M}$  [<sup>3</sup>H]-diminazene in the ABR line, although the rate was very much reduced compared to wild-type, suggesting the existence of yet a third route of entry for this drug, at least at high concentrations. The findings from this study revealed that *T. brucei* line lacking TbAT1/P2 transport by selection for high concentration of diminazene resulted in the loss of HAPT1 indicating that HAPT1 is a secondary route for

diminazene transport. This will be further investigated in Chapter 3. The findings of this study change the previous model which considered the P2 as the only route of entry for diminazene uptake and instead the new model shows HAPT1 as a secondary route (Figure 1.10).

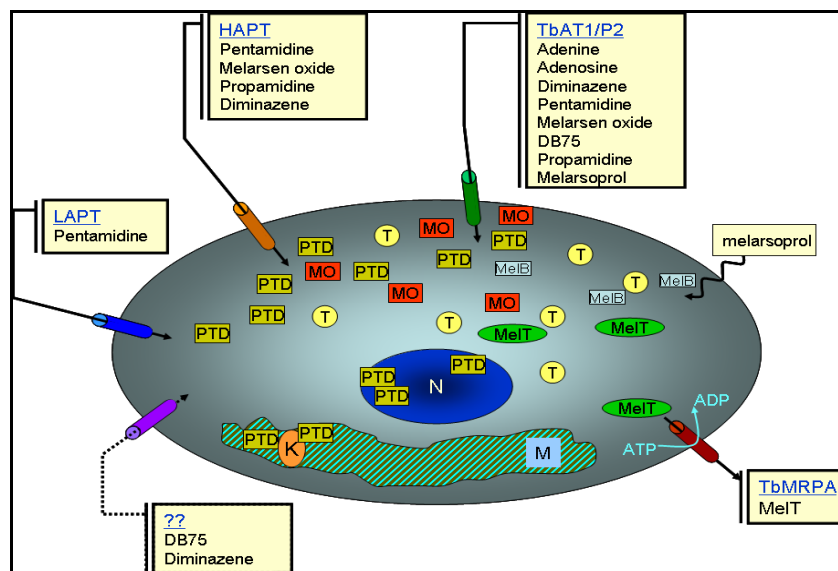


Figure 1.10. Current model showing mechanisms for drug uptake in the trypanosome. TbAT1/P2, *T. brucei* adenosine transporter 1 (code for P2 activity). HAPT1, High Affinity Pentamidine Transporter. LAPT1, Low Affinity Pentamidine Transporter. TbMRPA, *T. brucei* multidrug resistance protein A. PTD, pentamidine. MeIB, melarsoprol. MO, Melarsen oxide. T, trypanothione. MeIT, melarsoprol-trypanothione complex. N, nucleus. K, kinetoplast. M, mitochondria. Reproduced from (de Koning, 2008).

## 1.18 Drug resistance

Treatment failure is a major issue when combating sleeping sickness especially in cases caused by *T. b. gambiense* (Brun *et al*, 2010). Causes are not always parasite-related, and may include extreme toxicity of some of the drugs and affordability (Legros *et al*, 2002). Considering the fact that the treatment of both human and animal African trypanosomiasis relies on only few drugs, treatment failure due to emergence of parasite resistance is the most threatening issue in disease control. Resistance may arise as a result of the ability of the parasites to survive in high drug concentrations that are toxic to the host, for example; *T. b. rhodesiense* is naturally refractory to eflornithine and therefore cannot be treated with this. Another reason could be a cause of treatment failure is poor metabolism of the drug by the patient (Matovu *et al*, 2001).

Unfortunately, the last few years have seen a gradual increase in resistance against the drugs used in the treatment of trypanosomiasis leading to treatment failure. A thorough understanding of the mechanism of resistance and possible cross-resistance to certain drugs in single isolates from the field will help to develop a new formulation of compounds that could be more effective in trypanosomiasis treatment.

Drug transporters have received much interest recently for being involved in developing resistance. The early studies have linked the P2 transporter to the uptake of arsenical drugs and it was shown that an arsenical-resistant strain had lost the P2 transport function (Carter & Fairlamb, 1993). It was also observed that arsenical-resistant parasites accumulated lower levels of diamidines and other drugs gave an indication that resistance could be due to reduced uptake of the trypanocides (Carter *et al*, 1995). Following the identification of the TbAT1 gene it was discovered that an arsenical-resistant strain contained several point mutations in the gene which resulted in the alteration of the transporter protein at 6 amino acid positions. The altered P2 transporter was unable to mediate normal uptake of adenosine, adenine and its presence in yeast led to a reduced sensitivity to arsenicals compared to that seen when the wild-type transporter was expressed (Mäser *et al*, 1999). A study of parasite isolates derived from patients in whom melarsoprol therapy had failed to bring about a cure showed that many possessed similar point mutations in the TbAT1 sequence (Matovu *et al*, 2001).

Although several studies have also implicated the P2 transporter in the uptake of diamidine drugs (Carter *et al*, 1995) the identification of the (HAPT1) and (LAPT1) pentamidine transporters has added complexity to the model for uptake of diamidines in *Trypanosoma* species (De Koning, 2001). The high level of cross-resistance between the arsenicals and the veterinary diamidine berenil is a consequence of the two drugs sharing the same main route of uptake through the P2 transporter (Witola *et al*, 2004; de Koning *et al*, 2004) although there is some evidence for a residual uptake of arsenicals via HAPT1 (Matovu *et al*., 2003; Bridges *et al*., 2007). Surprisingly, the arsenical-resistant parasites described earlier as having lost the P2 transport function were hardly resistant to pentamidine at all (Fairlamb *et al*, 1992) could be explained by the transport of pentamidine by the additional two transporters even in the absence of the P2

transporter (De Koning, 2001). A *tbat1*<sup>-/-</sup> clonal line showed only a 2 - 3-fold loss in pentamidine sensitivity relative to its control (wild type) strain (Matovu *et al*, 2003). This is because of some diamidines use only TbAT1/P2 to pass into the cell, whereas some others as well as melaminophenyl arsenicals have at least one additional transmission route (de Koning, 2008). Cross-resistance between some drugs such as melaminophenyl arsenicals and diamidine in *T. b. brucei* has been noticed in both field isolates and laboratory strains, in addition finding that multiple factors may impact the level of resistance to the drugs. It seems that only the simultaneous loss of P2 and HAPT1 causes high levels of resistance to melaminophenyl arsenicals *in vitro* (Bridges *et al*, 2007).

High levels of treatment failure with melarsoprol associated with well-documented phenomenon of arsenical-diamidine cross-resistance have been reported in some foci of West Africa. There are also many reports of resistance to diminazene aceturate from across Africa. The possibility that arsenical resistance is the result of zoonotic transmission of diminazene-resistant parasites to humans cannot be discounted (De Koning, 2001). Although experimental induction of pentamidine resistance is relatively easy, reports of pentamidine resistance in the field have so far been either anecdotal or attributed to misdiagnosis of late-stage HAT (Bridges *et al*, 2007; de Koning, 2008).

In order to make best possible use of the nutrient transport systems for delivery of new drugs both selectivity of the transporter and efficacy of the drug must be considered. More specifically, there needs to be high affinity of the trypanocide for the particular transporter, coupled with low affinity for the mammalian transporter. Furthermore, there needs to be low abundance of competing substrates and ideally there needs to be concentrative rather than equilibrative uptake (de Koning & Jarvis, 1999; Barrett & Fairlamb, 1999). The P2 purine transporter, thus far, appears to meet these two requirements, however it has one major disadvantage and that is the parasite can lose this transporter without compromising viability (Matovu *et al*, 2003). Therefore, identification of new routes for successful drug delivery is essential to the introduction of new therapies to the field.

This Ph. D. project was initiated with the issues stated above very much in mind. The main focus of the project was to improve our knowledge of previously-identified transport components in *T. brucei* with particular emphasis on pentamidine-specific transporters, mainly LAPT1 and HAPT1. This also led us to investigate the possibility of losing LAPT1 activity via exposure to higher pentamidine concentrations. The initial aims were to quantitatively characterise the substrate recognition motifs of the *T. brucei* HAPT1 transporter. Circumstances also allowed us to explore any novel uptake route for the diamidine compounds diminazene aceturate. Another primary aim was to identify and clone the *T. brucei* genes that encode the HAPT1 and/or LAPT1 transporters.

## **2 Materials and methods**

## 2.1 Cell culture

### 2.1.1 Trypanosomes

The *Trypanosoma brucei brucei* strains and cell lines used during this project for biochemical and molecular studies are shown in Table 2.1. Bloodstream and procyclic form *T. b. brucei* were used for various stages of the study as appropriate. Two TbAT1-B48 strains which were recently transfected with either copy of the AT-E gene were used in the study of mitochondrial membrane potential where they were designated B48+AT-E1 and B48+AT-E2 (Section 5.6). Growth conditions were kept constant throughout this project except where explicitly stated. Strains were maintained in liquid nitrogen, prepared as described in section 2.2.

#### 2.1.1.1 Growth and maintenance of bloodstream form trypanosomes (BSF) *in vitro*

Bloodstream form *Trypanosoma brucei brucei* were cultured in HMI-9 medium (Hirumi & Hirumi, 1989) supplemented with 10% heat-inactivated Fetal Calf Serum (FCS (PAA)) and 14  $\mu$ l of  $\beta$ -mercaptoethanol (Sigma) / Litre, pH 7.4 at 37 °C and 5% CO<sub>2</sub>, unless otherwise stated. Four clonal lines of BSF of trypanosomes were used in this study: *Trypanosoma brucei brucei* wild type strain (s427- WT); TbAT1 knock out (KO) derived from s427- WT in which the TbAT1/P2 aminopurine transporter has been replaced with selection cassettes by homologous recombination, resulting in resistance to several important trypanocides (Matovu *et al.* 2003); the pentamidine-adapted clonal line (B48) which is lacking HAPT transporter activity (Bridges *et al.*, 2007); P1000, derived from B48 by further adaptation to pentamidine (growth in 1  $\mu$ M; this thesis); and TbAT1- KO-ABR, which is TbAT-KO lacking HAPT through adaptation to 0.8  $\mu$ M diminazene aceturate (Anne Kazibwe, PhD thesis, University of Glasgow).

Cultures were passaged into fresh medium at least three times a week, and cell densities of cultures were typically kept between  $1 \times 10^4$  and  $2 \times 10^6$  cells per ml. Bloodstream forms of *T. brucei* strain 2T1, derived from 427 and designed for use in combination with the pRP<sup>aiSL</sup> vector (Alsford & Horn, 2008) were generously donated by David Horn. Transgenic trypanosomes were grown in

HMI-9 supplemented with 10% FCS and 0.5 µg/ml phleomycin (Sigma) to maintain the tetracycline repressor (TetR) constructs and 0.2 µg/ml of puromycin (Sigma) for selection of correct integration. After transfection puromycin was replaced with 2.5 µg/ml Hygromycin B (Roche) as the drug resistance marker for selection. To induce the RNAi effect, tetracycline (Sigma-Aldrich) was added to the medium at a concentration of 1 µg/ml.

#### **2.1.1.1 Growth and maintenance of procyclic form trypanosomes (PCF) *in vitro***

*T. b. brucei* procyclic form (PCF) strains 427 and various derivatives were cultivated at 25-28 °C in SDM-79 medium (Brun & Schonenberger, 1979); supplemented with 10% (v/v) heat inactivated Fetal Calf Serum (FCS (PAA)). A typical culture was started at 10<sup>5</sup> cells/ml, which reached mid-log phase (10<sup>6</sup> cells/ml) after approximately 3 days and stationary phase (10<sup>7</sup> cells/ml) after 6-7 days.

For RNAi experiments, *T. b. brucei* PCF strain 29-13 (Wirtz *et al*, 1999) was used. These were maintained by addition of 15 µg/ml G418 (Sigma) and 25 µg/ml Hygromycin B (Roche) to the medium, and 25 µg/ml Phleomycin (Sigma) as selection marker after transfection. RNAi effect was induced by adding 100 ng/ml tetracycline (Sigma-Aldrich) was added to the culture. Growth was monitored by microscopy and cell numbers were determined by using an improved Neubauer haemocytometer (Weber Scientific).

#### **2.1.2 Bacterial strains**

The chemically competent JM109 or XL1 strains of *Escherichia coli* were used for routine cloning and subcloning of *T. b. brucei* genomic sequences. Competent cells were purchased from Stratagen initially but were subsequently prepared in-house using the method described in section 2.8.4.

Non-recombinant competent *E. coli* cells were kept as glycerol stabilates at -80 °C. Transformed cells were grown in LB broth (Sigma) supplemented with 100 µg/ml of ampiciline (Sigma-Aldrich) for selection at 37 °C overnight under vigorous shaking (250 pm).

## 2.2 Preparation of stabilates

Routinely, stabilates were made from all parasitic strains used in this project. Cell cultures with a density between  $1 \times 10^6$  -  $2 \times 10^6$  were diluted 1:1 in HMI-9 with 30% glycerol (Riedel-de Haen), then aliquots of 1 ml were immediately transferred to ice and slowly frozen to  $-80$  °C in a box isolated with cotton to allow a gradual reduction in the temperature over a period of 24 hours. Vials were then transferred to liquid nitrogen for long-term storage.

Vials of frozen parasites (stabilates) were recovered by thawing at room temperature for about three minutes. Cells were then harvested by centrifugation (10 min,  $3000 \times g$  at  $21$  °C) and resuspended in fresh relevant medium. Some cultures required the presence of chemicals such as antibiotics. Recovery of stabilates was assisted by resuspending in fresh medium for at least 24 hours before the addition of antibiotics, concentrations of which were increased subsequently by 25% per passage until the desired concentration was reached.



## 2.3 Monitoring *in-vitro* cell growth and drug sensitivity

### 2.3.1 *In-vitro* drug sensitivity using Alamar Blue dye

The Alamar blue assay (Rüz *et al.*, 1997; Gould *et al.*, 2008) functions as an indicator for cell health and is used to determine the relative number of live cells in a certain population. In this assay many compounds were screened for activity against bloodstream form trypanosomes to check for effects on cell growth following the Alamar Blue method.

The Alamar blue test was performed in 96 well-plates and is based on the ability of the metabolically active cells to reduce resazurin (non-fluorescence blue dye) to resorufin (intensely pink and fluorescent). The ability to inhibit cell growth was proportional to the intensity of fluorescence produced by the surviving trypanosomes after 48 hours of incubation with the test compound. Wells where parasites were killed by a particular concentration of compound will produce the least fluorescence whereas wells with cells that survived lower concentrations of compounds will produce higher levels of fluorescence.

BSF trypanosomes at a density of  $10^4$  cells per 100  $\mu$ l were incubated for 48 hrs in 96-well flat-bottomed white microtiter plates, then for a further 24 hours after addition of 20  $\mu$ l of 125  $\mu$ g/ml Alamar blue dye (resazurin, Sigma). Drug concentration started at 100  $\mu$ M, unless otherwise stated, and decreased in doubling dilution across two rows in the plate, with the final well receiving no drug, as a control for maximum cell growth and fluorescence. All experiments were performed on at least three independent occasions. Fluorescence was measured in a FLUOstar OPTIMA fluorimeter (BMG Labtech) at wavelengths 530 nm for excitation and 590 nm for emission. To calculate the  $EC_{50}$  value (Effective Concentration that inhibits growth by 50%), the relative fluorescence was plotted against the log of the test compound concentration to give a sigmoidal dose response curve using GraphPad Prism software version 4.0 or 5.0.

Alamar Blue (Resazurin sodium salt) was prepared by the addition of 12.5 mg of Resazurin (Sigma-Aldrich) in 100 ml of Phosphate Buffered Saline ((PBS) Sigma-Aldrich) at pH 7.4 and filter-sterilized for use in the experiments. This material can be stored in the dark at 4 °C for up to 2 months or frozen at -70 °C (Rüz *et*

*al.*, 1997). All the drug dilutions were freshly prepared in the respective medium on the day of the assay. Tested compounds were prepared as stock solutions in 100% DMSO (Riedel-de Haen); the final concentration of DMSO never exceeded 1% which did not affect the growth of parasites (personal observation in many experiments).

### **2.3.2 *In-vitro* drug sensitivity using propidium iodide assay**

PCF trypanosomes, as well as both the BSF and PCF RNAi cell lines, were not able to reduce Alamar blue dye sufficiently to generate an adequate fluorescent signal within the standard incubation time. Therefore propidium iodide (PI; Sigma) assays were performed using 96-well plates using the appropriate medium: HMI-9 for bloodstream forms and SDM-79 for procyclic form. Propidium iodide is a method based on monitoring the fluorescence of propidium iodide when bound to DNA, which provides end-point  $EC_{50}$  values that are directly comparable to those established by the standard resazurin reduction assay (Gould *et al.*, 2008). Drug concentrations and dilutions were performed under the same conditions described above for the Alamar blue assay. Final cell density of  $10^5$  per 100  $\mu$ l were incubated with drugs for 48 hours followed by 1 hour in the presence of 18  $\mu$ M of Propidium iodide. Digitonin (Sigma-Aldrich) at 40  $\mu$ M was added together with the PI, in order to permeabilise the cells to propidium iodide (Gould *et al.*, 2008).

The plates were then read using the FLUOstar OPTIMA fluorimeter (BMG Labtech) at 544 nm excitation and 620 nm emission. To determine  $EC_{50}$  values the reads were analyzed using Prism software.

### **2.3.3 Drug sensitivity by using cell count**

For unknown reasons the BSF of the RNAi/AT-E (IT-BERi) cell lines did not metabolise Alamar blue dye sufficiently to use for  $EC_{50}$  determinations, the PI-based assay was used instead and it gave satisfying results. The cell survival in various drug concentrations was monitored directly using cell count with an improved Neubauer haemocytometer (Weber Scientific) after 48 hours of incubation of the cells with the tested drugs in order to check accuracy of the  $EC_{50}$  values that obtained from using PI assay. In this experiment, 100  $\mu$ l of the

stocks of the drugs of interest were prepared in the appropriate medium at 2 times the desired concentration and were added to 96 well plates in doubling-dilution format down two rows. Cells from each strain were added to a final density of  $1 \times 10^5$  cells / well. After 48 hours of incubation at 37 °C, cell numbers were determined by microscopy using a haemocytometer. This experiment was repeated twice and involved the count of twelve selected wells for each drug (counting every second well, starting from the high to the lower concentrations of drug). The drug-free well was also included in the counting as control for maximum growth. Percentage of survival was plotted to a sigmoidal curve using Prism software (data not shown), yielding accurate  $EC_{50}$  values identical to those obtained from the PI assay.

## 2.4 Transport assays in trypanosomatids

### 2.4.1 *Collection and purification of bloodstream form T. b. brucei from rat*

Strain 427-WT *T. b. brucei* was retrieved from stabilate storage and used to inject female Wistar rat intraperitoneally. After up to 72 hours from the injection, and at peak parasitaemia, the circulating blood was withdrawn by cardiac puncture under terminal anaesthesia using a syringe loaded with a small volume of Carter's balanced saline solution (CBSS; Appendix A) containing 100 U/ml heparin to avoid blood coagulation. The whole blood was stored on ice until centrifuged at  $1,250 \times g$  for 15 minutes resulting in separation of the sample into three different layers. The white Buffy coat containing the parasite will form as a layer between the red blood cells and the plasma layer. The Buffy layer was carefully removed using a plastic Pasteur pipette and resuspended in a small volume of phosphate-buffered saline with glucose (PSG, pH = 8.0; Appendix A), a procedure that inevitably also transfers some red blood cells.

To isolate the parasite from the red blood cells, the parasite/PSG suspension was washed through a column of DEAE cellulose (DE-52, Whatman). To prepare the column, a 50 ml syringe was filled with 5 cm of DEAE cellulose, placed on the top of a glass-wool cushion to prevent cellulose loss. The cellulose column was washed with 200 ml of PSG. The cellulose column was prepared at pH 8.0 because the trypanosomes are more positively charged and the rat red blood cell

surfaces are more negatively charged at the range of pH 6-9. Thus, pH 8.0 will allow the parasite to pass through the column at this pH but not the red cell. The "Buffy coat" suspension was gently mixed and loaded onto the top of the column and run through by refuelling the column with PSG for several times (Lanham, 1968, and Lanham & Godfrey, 1970). The purification was carried out as rapidly as possible since pH 8.0, although necessary for the correct functioning of the column, is can be detrimental to the parasites if maintained for an extended period.

Parasites collected from the cellulose column were washed twice in the assay buffer (pH 7.4), by centrifugation (10 minutes at  $1000 \times g$ ), and resuspended in assay buffer at  $10^8$  cells/ml. The cells were usually left for 15-20 minutes at room temperature before use to allow suspension to adapt to the conditions of the experiment (Figure 2.1).

#### ***2.4.2 Collection and purification of bloodstream and procyclic form *T. b. brucei* from culture***

Uptake assay requires high number of cells; therefore cultures were grown in large quantities. For BSF trypanosomes a culture of 300 ml in HMI-9 medium (Invitrogen) or appropriate medium and incubated at  $37^\circ\text{C} + 5\% \text{CO}_2$  for 48 hours or until culture reach mid-log phase of growth. At this stage of growth, parasites were harvested by centrifugation at  $1000 \times g$  for 10 minutes and washed twice with assay buffer (see Appendix A). Cells were harvested just before the start of the experiment. After the second wash the pellet containing parasites was resuspended in assay buffer at the density of  $1 \times 10^8$  cells/ml. Cells were then allow to reach room temperature before use (Figure 2.1).

RNAi / BSF cell line were cultivated in HMI-9 plus antibiotic and cells hereafter are named Tet-induced for the RNAi induced cells, and Non-induced when RNAi was not induced with tetracycline.

PCF trypanosomes for transport assays were grown in 250-ml cultures at  $25^\circ\text{C}$  in SDM-79 (Invitrogen) until the mid-log stage of growth is reached. The cultures were then harvested and treated as described in bloodstream forms. Cells were also grown in Tet-Induced and Non-induced conditions using SDM-79 plus

antibiotics. Cells were checked by microscopy at the end of each experiment to ensure that cells were viable throughout the experiment.

### **2.4.3 Radiolabeled Uptake Assay in *T. brucei***

Uptake of radiolabelled [ $^3\text{H}$ ] Pentamidine ( $^3\text{H}$ -Pent) and [ $^3\text{H}$ ] diminazene aceturate ( $^3\text{H}$ -DA) (both Amersham, UK) was determined using a derivation of the rapid-stop/oil-spin protocol described previously (Carter & Fairlamb, 1993; de Koning & Jarvis, 1997). The molar concentration of the permeants was adjusted according to the transporter of interest in order to study the activity of each transporter individually. This is because of the differences in kinetic parameters, especially the  $K_m$  of each transporter. HAPT1, for example, has a high affinity to pentamidine, with a published  $K_m$  value of  $36 \pm 6$  nM (De Koning, 2001), and fully saturated at submicromolar concentrations. In contrast, LAPT1, displays a low affinity to pentamidine ( $K_m = 56 \pm 8$   $\mu\text{M}$ ; De Koning, 2001) and it requires millimolar concentrations to saturate. Therefore, when HAPT1 is tested using 30 nM [ $^3\text{H}$ ]-penta or less, the contribution of LAPT1 activity to the total flux will be insignificant, and at 1  $\mu\text{M}$  [ $^3\text{H}$ ]-penta only LAPT activity is measured (De Koning, 2001; Bridges *et al.*, 2007; Bray *et al.*, 2003). When pentamidine transport was studied in the presence of the TbAT1/P2 transporter (i.e. in s427-WT), the P2 transporter must be blocked with 1mM adenosine, which is added to the radiolabel solution for this purpose.

Transport assays were initiated with 100  $\mu\text{l}$  of trypanosome suspension ( $\sim 10^7$  cells) being mixed with 100  $\mu\text{l}$  assay buffer containing radiolabelled compounds at a specific concentration, sometimes mixed with various concentrations of other test compounds / inhibitors. Some test compounds were made as stock solutions in 100% DMSO (Riedel-de Haen); the final concentration of DMSO in the assays was maximum 1%.

All transport assays were performed in triplicate and all parameters were determined at least three times independently unless otherwise stated. Using a 1.5 ml microcentrifuge tube 100  $\mu\text{l}$  solution with radiolabeled permeants (at two times the desired concentration) was layered over 300  $\mu\text{l}$  oil mix (dibutyl-phthalate oil (Merck) / mineral oil (Sigma), 7:1 (v/v)). Then 100  $\mu\text{l}$  of the cell suspension was added to the microcentrifuge tubes and incubated with the

permeants for a predetermined time at room temperature. Uptake was terminated by adding 1 ml of ice-cold stop (solution of unlabelled permeant in Assay Buffer, usually at 1 mM) followed by rapid centrifugation at 13,000 rpm for 30 seconds, pelleting the cells below the oil layer and separating them from radiolabel not internalised. The microfuge tubes were then flash-frozen in liquid nitrogen and the bottom, containing the cell pellet, cut off and collected in numbered scintillation vials containing 300  $\mu$ l of 2% of sodium dodecyl sulphate (SDS, Sigma-Aldrich). Vials were left for 30 minutes at room temperature to allow solubilisation of the pellet. This was followed by addition of 3 ml Ecoscint scintillation fluid (PerkinElmer) and the accumulated radioactivity was measured in the 1450 Microbeta Liquid Scintillation and Luminescence Counter (PerkinElmer Lifesciences) (Figure 2.1).

Non-mediated uptake of the respective permeant was assessed by determining the rate of uptake of the radiolabeled permeant in the presence of 1mM unlabelled permeant as well as with cells and permeant at 0 °C.

#### **2.4.4 Analysis of transport assays data**

All assays were performed in triplicate and IC<sub>50</sub> values were based on a minimum of 5 data points over the relevant range. For the time course uptake experiments, the rate of uptake of the permeant was obtained from a plot of permeant concentration against time using Prism 4.0 or 5.0, GraphPad software. Using linear regression, correlation coefficients were obtained for the linear phase of uptake. F-tests and Runs tests (Prism) showed significance of deviation from zero uptake and from linearity, respectively.

Inhibition and kinetic constants (IC<sub>50</sub>, V<sub>max</sub> and K<sub>m</sub>) were generated by non-linear regression curve using GraphPad Prism version 4.0 or 5.0. K<sub>i</sub> values were calculated using the Cheng-Prusoff equation  $K_i = IC_{50}/(1+(L/K_m))$  (Cheng & Prusoff, 1973), where L is the permeant concentration; this equation is valid only for competitive inhibition. The K<sub>m</sub> and V<sub>max</sub> values were obtained for the transporter using the Michaelis-Menten equation  $v = (V_{max} \times L)/(K_m + L)$  (Stein, 1986).

### 2.4.5 Chemicals used in the transport assays

[<sup>3</sup>H] Diminazene and [<sup>3</sup>H] Pentamidine were purchased from Amersham Pharmacia Biotech (UK). Compounds used as competitive inhibitors in uptake experiments were obtained mainly from Sigma unless where stated otherwise. Other test compounds were synthesised by collaborators. ‘DB’ compounds were received from David W. Boykin, Georgia State University, Atlanta, USA. ‘CHI’ compounds were from Paul O’Neil, University of Liverpool, UK. ‘RT’ compounds were synthesised by Dr. Richard Tidwell, University of North Carolina, Chapel Hill, USA.

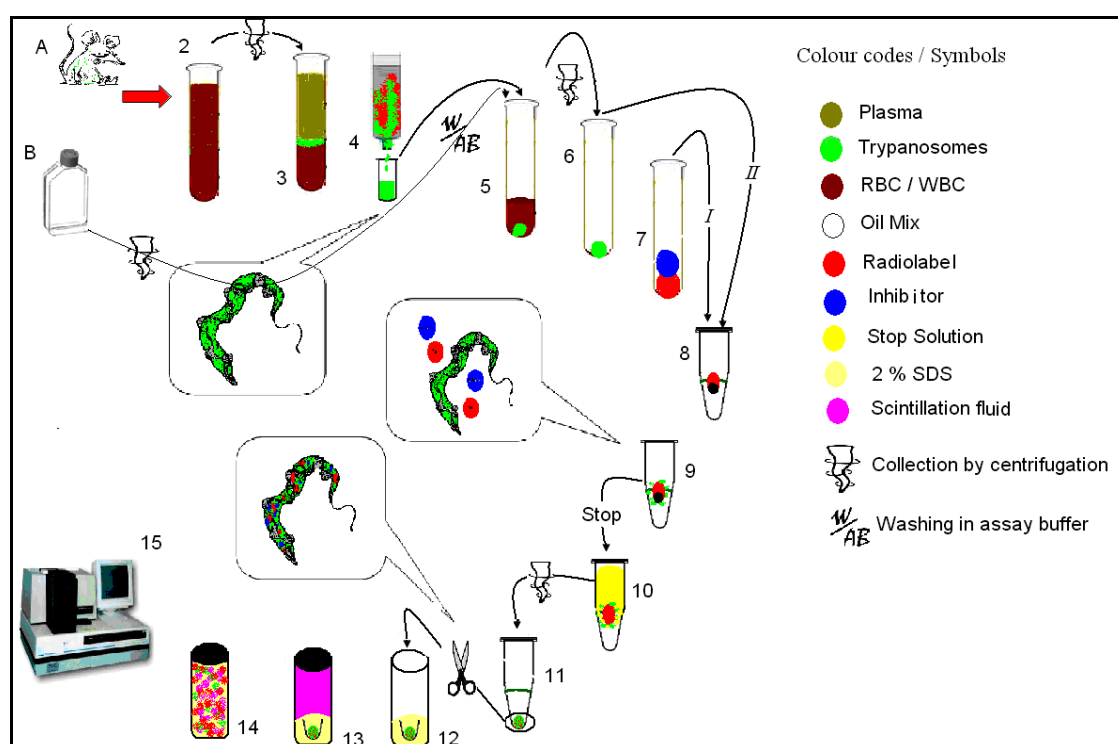


Figure 2.1. Diagram summarises the uptake assay in trypanosomes.

(1) Source of parasites (A) *in vivo* and (B) *in vitro* (2). Blood collected from a rat by cardiac puncture. (3) Three different layers; plasma (top), white Buffy coat containing the parasites (middle) and red blood cells (bottom). (4) The Buffy layer was carefully removed, resuspended in PSG and cellulose. From this point, parasites from either source (A) *in vivo* or (B) *in vitro* are treated in same way. (5) Cells are washed twice in the assay buffer. (6) Cells are resuspended in assay buffer at  $10^8$  cells/ml. (7) 100  $\mu$ l 1:1 (v/v) radiolabeled / inhibitor is added (single bubble 7. I). (8) 100  $\mu$ l of the cell suspension (7.II) is added, starting the uptake. (9) Incubation for pre-determined time. (10) 1 ml of ice cold stop solution is added. (11) Tube is flash frozen in liquid nitrogen and pellet is cut into scintillation vial. (12) 300  $\mu$ l of 2% SDS for 30 minutes. (13) 3 ml of scintillation fluid is added. (14) O/N incubation at room temperature. (15) Read by scintillation counter.

## 2.5 Selection for high Pentamidine concentrations

*TbAT1*-B48 was obtained from *TbAT1*-KO by *in vitro* selection for high levels of resistance to pentamidine, resulting in a loss of HAPT1 but not LAPT1 transport, with 130-fold resistance to the drug compared to the 427-WT cell line (Bridges *et al*, 2007). In this project, we tried to select B48 cell line to higher concentration of pentamidine, in order to create a resistant cell line and possibly a strain lacking LAPT1. Creating a trypanosome strain with null pentamidine uptake would aid the study and characterise these transporters at molecular levels.

The selection was carried out *in vitro*. Cells were passaged every two days in HMI-9 with 10% FCS, supplemented with the correct concentration of pentamidine (freshly made) in a stepwise manner with a gradual increase of the drug when required (see relevant section). Having obtained, after a minimum of 95 passages (about 12 months) a cell line able to grow at a near-normal rate in 1000 nM pentamidine, cells were passaged for several weeks at this concentration to check for stability of growth. Then a 10 ml culture of cells was grown for two days and subsequently cloned by limiting dilution on three 96 well plates, starting at a density of 1000 cells/ well (Section 2.9.6).

After seven days of incubation with 1  $\mu$ M of drug at 37 °C + 5% CO<sub>2</sub>, 5 unique colonies were isolated and tested for susceptibility to pentamidine (Sigma) using Alamar blue. One clone was selected for further work and designated P1000. A drug sensitivity profile for the selected clone was created.

## 2.6 Determination of the mitochondrial membrane potential

Fluorescence Activated Cell Sorting Technology (FACS) was used to investigate the influence of pentamidine pressure on mitochondrial membrane potential (MMP) in several *T. b. brucei* lines.

Four different cultures were setup for each cell line and incubated with or without pentamidine, Valinomycin (100 nM; Sigma) and Troglitazone (10  $\mu$ M; BIOMOL International). The latter two were included as controls in the

experiment as they induce a rapid reduction or increase, respectively, in the mitochondrial membrane potential (Ibrahim *et al.*, 2011). A 10-ml volume of each culture was started at  $1 \times 10^6$  cells/ml in HMI-9 with 10% FCS and incubated at 37 °C and 5 % CO<sub>2</sub> for 24 hours with and without test compounds. Samples were taken at various predetermined intervals, at which time 1 ml from each culture was transferred to microcentrifuge tubes and centrifuged for 10 minutes at 2500 × g, and then washed once in 1 ml PBS. Subsequently, the pellet was resuspended in 1 ml PBS containing 25 nM of Tetramethylrhodamine ethyl ester (TMRE, Invitrogen), and incubated at 37 °C for 30 minutes (Figarella *et al.*, 2006; Denninger *et al.*, 2007; Ibrahim *et al.*, 2011). The samples were then kept on ice and analyzed with flow cytometry using the FL2-Height detector and CellQuest software.

## 2.7 Molecular techniques

### 2.7.1 Isolation of genomic DNA from *T. b. brucei*

Phenol-chloroform method described by Sambrook and co-authors, was the method employed in this study for genomic DNA extraction as it results in high purity DNA which is suitable for restriction digestion (Sambrook *et al.*, 1989).

*T. b. brucei* were grown in a 50 ml culture for 48 hours. After 48 hours  $1 \times 10^8$  cells were harvested by centrifugation at 1,500 × g for 10 minutes at 4 °C. Supernatant was discarded and the pellet was washed at least once in 1 ml PBS (Appendix A). The cell pellet was resuspended in 500 µl of lysis buffer (Appendix A). To digest the protein component within the suspension 1 µl of Proteinase K solution (Sigma) (10 mg/ml in dH<sub>2</sub>O) was added to the suspension. The lysis reaction was kept overnight at 50 °C to allow complete lysis of the cells.

A 500 µl volume of liquid phenol (Sigma-Aldrich) was added to the lysis reaction followed by gentle inversion of the tube for 1 minute. The solution was centrifuged at 4000 × g for 10 minutes resulting into two separate phases, of which the clear top phase was transferred to a fresh sterile tube. To this, 500 µl of phenol:chloroform (1:1) (Sigma-Aldrich) was added, and the sample was mixed thoroughly and centrifuged as before. The upper aqueous layer was again removed into a fresh tube, and 500 µl of chloroform was added, followed by

gentle inversion for 1 minute and centrifugation. The upper layer was added to a final clean tube. The DNA was precipitated by adding a 1/10<sup>th</sup> volume of sodium acetate (3 M) and 1 ml of ice-cold 100% ethanol (Sigma-Aldrich). The solution was mixed gently and placed at -20°C for 30 minutes. DNA was collected by centrifugation at 4000 × g for 10 min and washed in 1 ml 70% ethanol. After centrifugation (4000 × g, 5 min) the ethanol was carefully removed and the tube containing DNA pellet was air-dried. Finally, the DNA was resuspended in 50 µl of distilled water and incubated with 1 mg / ml RNase (Sigma) for 1 hour at 37 °C to remove contaminating RNA, samples were then stored at 4 °C for future work.

### **2.7.2 Isolation of total RNA from *T. brucei***

Total RNA was isolated from different strains of *T. b. brucei* using TRIzol reagent (Invitrogen). TRIzol reagent is a mono-phasic solution composed of phenol and guanidine isothiocyanate. For this purpose cells were harvested at 1,500 × g for 10 min at 4 °C. Supernatant was discarded and the pellet was resuspended in 1 ml TRIzol reagent (Sigma) and incubated at room temperature for 5 minutes. 200 µl of chloroform (Sigma-Aldrich) was added to the lysate and mixed by gentle inversion and incubated for 2 min at room temperature. This was followed by centrifugation at 12.000 × g for 15 min at 4 °C resulting in separation of organic and aqueous phases. The upper clear aqueous phase (containing the RNA) was transferred to a fresh microfuge tube and 0.5 ml of isopropyl alcohol was added. This mixture was incubated for 10 min at room and then centrifuged (10 min, 4 °C) and the RNA pellet was washed with 1 ml of 75% ethanol and centrifuged again for 2 min at 4°C. The ethanol was gently removed; the pellet was air-dried for 10 min tube was left open in sterile air flow for 10 minutes and resuspended in RNase-free dH<sub>2</sub>O. Samples were stored at -70 °C.

All the work in this project was carried out using RNase-free reagents, solvents and equipment including plastic ware and filter tips. All solutions including RNase-free water were made freshly. RNase-free water was prepared by treatment with 0.01% (v/v) diethylpyrocarbonate (DEPC). Treated bottles were left overnight at room temperature, then autoclaved. RNaseZap solution (Invitrogen) was used to decontaminate other plastic and glass surfaces and create an RNase-free environment.

### **2.7.3 Determination of DNA/ RNA concentration**

DNA and RNA concentrations were measured using Nanodrop technology (The NanoDrop® ND-1000 spectrophotometer NanoDrop Technologies, Inc., Rockland DE). A volume of 1 µl of the sample is used to provide the concentration in ng/µl. DNA yielded after gel extraction was estimated by comparing the DNA band with the corresponding band of a reference marker. This was achieved by loading a volume of 5-10 µl of the purified gel alongside with same volume of 2-Log DNA molecular weight marker (Quick-Load® 2-Log DNA Ladder / New England Biolabs).

### **2.7.4 Polymerase chain reaction (PCR)**

PCR was used to amplify segments of DNA from *T. b. brucei* for various molecular procedures. Genes were identified using the genome sequence for *Trypanosoma brucei* strain TREU927 from GeneDB as a reference sequence, since that of the 427 strain had not been completed. Published Gene ID numbers were used to identify the AT-like genes sequences used in this study, (Tb09.244.2020) for AT-A, (Tb09.V4.0106) for AT-G and (Tb927.3.590) for the AT- E.

*Taq* Polymerase (Promega) was used for routine PCR screening, where *KOD* hot start DNA polymerase (Novagen) was used in PCR reaction used in all cloning strategies including gene sequencing because of its proofreading capability. PCR reactions were performed at a total volume of 25 µl containing 200 µM of dNTPs (Promega), 2.5 µl of 10× buffer, 3.5 µl 25 mM MgSO<sub>4</sub>, forward and reverse primers each at a final concentration of 0.15 µM, up to 500 ng of genomic DNA and 0.5 unit of *KOD* hot start DNA polymerase. When *Taq* polymerase was used the reaction mixture was identical except the replacement of MgSO<sub>4</sub> with 1.5 mM of MgCl<sub>2</sub>, and 1 Unit *Taq* polymerase. The mixture was made up to the required volume with DNase and RNase-free dH<sub>2</sub>O treated with 0.001% DEPC filtered through a 0.2 µm filter and autoclaved. The amplification was performed using a thermal cycler (PTC200 DNA Engine Thermal Cycler, MJ Research Incorporated, USA) under differing conditions.

In general, the PCR was performed in three stages: cycle 1, 95 °C for 2 minutes followed by 29 cycles composed of a denaturation step at 95 °C for 20 seconds,

the annealing temperature (dependent on the primers pairs) for 30 seconds, and an amplification step which varied based on the primers pairs and the polymerase enzyme used in the reaction; (*KOD*: 70 °C for 30 seconds) and (*Taq*: 72 °C for 2 minutes), a final extension at 70°C - 72°C for 5 minutes. Correctly sized products were isolated by electrophoresis on a 1% agarose gel stained with 10 µl of SYBR safe DNA gel stain (10,000× concentrate in DMSO, Invitrogen) then purified using a QIAquick gel extraction kit according to manufacturer's instructions (Qiagen).

### 2.7.5 Primer design

All primers were synthesised by Eurofins MWG Operon, generally two primers were designed specifically to known regions of DNA. One primer in the 5'-3' direction (sense) and the other is in the complementary direction 3'-5' direction of the DNA (antisense) (Figure 2.2). When required, primers were designed to incorporate particular restriction sites to enable a subsequent ligation of the PCR fragment into a particular vector.

The oligonucleotide primers used in this study are listed below in Table 2.2, and they were designed for cell line genotyping, amplification of AT-A, AT-G and AT-E genes, colony screening by PCR sequencing amplification of RNAi fragment of AT-E gene and to check for the presence of the drug markers and the correct orientation of particular fragments.

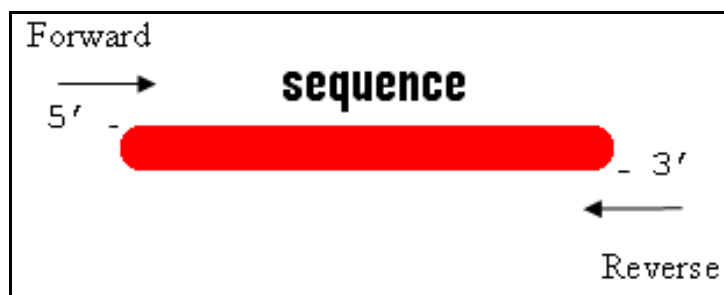


Figure 2.2. Primers designed to amplify AT-A like putative genes.

Primer pair	Sequence (5'-3')	Fragment sizes (Minimum)
AT-A Forward	5' GGATGCTTGGCTTCGGTCT 3'	1449 bp
AT-A Reverse	5' ACTGTGACTCATCTTTCCGGG 3'	
AT-E Forward	5' AGAATGATGCTCGGGTTCGAA 3'	1389 bp
AT-E Reverse	5' TTGAGGAAGTCCCTCCTTGA 3'	
AT-G Forward	5' ATGCTTGGCTTCGGTCTGT3'	1449 bp
AT-G Reverse	5' TTA CTGTGACTCATTTTTTCG 3'	
Actin Forward	5'CCGAGTCACACAACGT 3'	456 bp
Actin Reverse	5' CCACCTGCATAACATTG 3'	
TbAT1 Forward	5' GCCCGGATCCGGCTGGTTTTTAGACAA AAGTGAT 3'	677 bp
TbAT1 Reverse	5' GCCCCTCGAGCCGCATGGAGTAAGTCTGA 3'	
T7 primer	5' TAATACGACTCACTATAGGG 3'	411 bp
SP6 primer	5' CATTAGGTGACACTATAG 3'	
RNAi/AT-E Forward For BSF	5' AC <b>GGGCCC</b> <b>GGTACC</b> <b>AAGCTT</b> GATCCCTCTGGCTGTTC GAC 3' Key to restriction sites: <b>GGGCCC</b> = <i>Apal</i> , <b>GGTACC</b> = <i>KpnI</i> <b>AAGCTT</b> = <i>HindIII</i>	411 bp
RNAi/AT-E Revers For BSF	5' AC <b>CTCGAG</b> <b>GGATCC</b> TCTGCTGCATACTTCATGGC 3' Key to restriction sites: <b>CTCGAG</b> = <i>XhoI</i> <b>GGATCC</b> = <i>BamHI</i>	411 bp
RNAi/AT-E Forward For PCF	5' TACG <b>GGATCC</b> GATCCCTCTGGCTGTTCGAC 3' Key to restriction sites: <b>GGATCC</b> = <i>BamHI</i>	411 bp
RNAi/AT-E Reverse For PCF	5' TACG <b>TTCGAA</b> AGACGACGTATGAAGTACCG 3' Key to restriction sites: <b>TTCGAA</b> = for <i>Hind III</i>	411 bp

Table 2.2. Oligonucleotide primers used in this study.

Restriction endonuclease recognition sites are coloured.

### **2.7.6 Agarose electrophoresis of DNA**

DNA was separated on the basis of differences in molecular size by electrophoresis through agarose gel prepared by adding 1% (w/v) agarose (Invitrogen) to 1× TAE buffer (Appendix A) and boiling the solution in a microwave to allow the agarose to dissolve. Once the mixture had cooled to 40-50 °C, SYBR safe (Invitrogen, 1:10,000) or ethidium bromide (Sigma, 0.5µg/ml) was added. DNA samples were mixed with 6× DNA loading buffer (Promega), and loaded into the wells alongside DNA ladder (Promega). Electrophoresis was performed at 100-120 V in 1× TAE buffer. The bands were visualised under UV illumination in a Gel Doc system (Bio-Rad).

The band corresponds to a desired DNA fragment was excised using a clean scalpel and transferred into a sterile microcentrifuge tube. The band was then extracted from the gel using the Qiagen Gel Extraction Kit following manufacturer's instructions.

## **2.8 Cloning techniques**

### **2.8.1 Ligation into pGEM-T Easy vector**

All PCR products were initially cloned into the pGEM-T-Easy (using the Promega Vector System I kit) for verification of DNA sequence before being sub-cloned into their destination vector. Successful cloning into this vector was achieved by taking advantage of the presence of the single thymidine residue at both 3' ends (Figure 2.3). The T-overhangs at the insertion site greatly improve the efficiency of ligation of any PCR product (insert) containing a compatible overhang (A-overhang) that is usually generated by the *Taq* polymerases enzyme.

Poly-A tailed PCR fragments were cloned into the pGEM-T vector using a 3-fold molar excess of the insert DNA over the vector. The ligation reaction was performed under the following conditions: final concentration of 1× ligation buffer, 1 µl vector (20-50 ng/µl), 3 µl PCR product, 1 µl T4 DNA Ligase (1 U/µl, Promega). The reaction was incubated at room temperature for up to 5 hours or 4 °C overnight. A positive control (control insert DNA) and a background control (digested vector without insert DNA) were used to assess ligation of the vector.

Once the plasmid had been purified and the presence of insert verified by restriction digest (*EcoRI*), the PCR products were digested, isolated, and cloned into various other vectors.

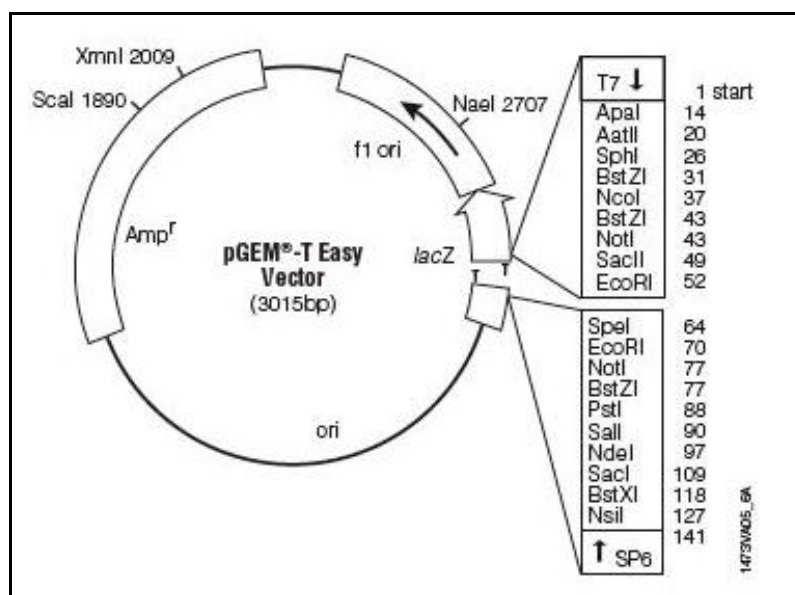


Figure 2.3. Map of the pGEM-T-Easy plasmid.

This figure shows the important features of the pGEM-T-Easy cloning plasmid (Promega). The plasmid contains a single 3' terminal thymidine at each end, providing compatible overhangs for the insertion of PCR products amplified by *Taq* polymerases. Inserts were identified by sequencing using the primers T7 and SP6, which bind to the T7 and SP6 RNA polymerase promoters, flanking the multiple cloning region. Figure taken from the Promega website ([www.promega.com](http://www.promega.com)).

### 2.8.2 Creation of A-overhang of PCR products

The use of KOD hot start polymerase (Novagen) in PCR amplification resulted in products with blunt ends, requiring the creation of 5'- adenosine overhangs for the PCR product into pGEM-T Easy. To this end, PCR products were incubated with *Taq* polymerase (Promega), which adds adenosine residues to the end of the DNA in a template-independent manner. 7  $\mu$ l of gel-purified product was mixed with 1  $\mu$ l of 10 $\times$  *Taq* reaction buffer, 0.2 mM dATP and 5 units of *Taq* polymerase; final volume was brought to 10  $\mu$ l with sterile dH<sub>2</sub>O. This was incubated at 72 °C for 30 min. Ligation to pGEM-T Easy was performed as described above.

### **2.8.3 Cloning into destination vectors (RNAi vectors)**

Verified correct sequences in pGEM-T-Easy clones were cloned into destination vectors where a good RNAi fragment is recommended to be about 400 - 600 bp in size (Redmond *et al.*, 2003). In this project, a fragment of 411 bp from the original AT-E fragment, ligated into pGEM-T-Easy (pIT.03), was amplified by PCR using specific primers containing appropriate restriction enzyme linkers added onto the actual primers sequences in order to enable digestion/ ligation of the PCR fragment vector using same restriction enzymes.

PCR product and the destination plasmid were linearized using the same restriction endonucleases. The digests were separated by agarose gel electrophoresis and the inserts and plasmids were excised from the gel under UV illumination and purified using the Qiagen gel extraction kit (Qiagen).

The insert sequence was ligated into the destination plasmid in a 10  $\mu$ l ligation reaction containing 5 units of T4 DNA ligase (Promega), 1 $\times$  DNA ligase reaction buffer and a range of molar ratios of vector to insert. Ligated plasmids were transformed into chemically competent *E. coli* (JM109 or XL1) and plated on LB agar plates containing the appropriate antibiotics. Colony PCR screen was used to identify colonies containing the correct insert. Plasmid DNA was produced from these colonies, analysed by restriction endonuclease digestion and verified by sequencing.

To prevent self ligation of the vector, after digestion, linearised vector was dephosphorylated with calf intestinal alkaline phosphatase (CIAP, Promega). CIAP phosphatase stock (Promega) was obtained at 1U/ $\mu$ l and diluted 25 times in ddH<sub>2</sub>O. A 1 - 2  $\mu$ l volume of the diluted stock was added to the digestion mix and incubated for 30 minutes prior to ligation process; the enzyme was then inactivated by incubation at 65°C for 10 minutes.

### **2.8.4 Preparation of chemically-competent *Escherichia coli***

*E. coli* competent cells type JM109 or XL1 were purchased from (Stratagene) and further stocks were prepared in the laboratory using the calcium chloride method (Sambrook *et al.*, 1989). The efficiency of the competent cells was

tested prior to use and was typically higher than  $1 \times 10^7$  colony-forming units per  $\mu\text{g}$  of transformed plasmid DNA.

To inoculate a culture from glycerol stock, a scraping was taken from the frozen tubes and streaked on LB agar plate containing particular antibiotics. Plates were then incubated overnight at  $37^\circ\text{C}$  and an individual colony was picked to inoculate in 5 ml of L broth medium.

### **2.8.5 Transformation of *E. coli***

The heat-shock method was used for the transformation of *E. coli* competent cells (Sambrook *et al*, 1989). After transformation cells were spread onto LB plates supplemented with  $100 \mu\text{g/ml}$  of ampicillin. Plates were incubated at  $37^\circ\text{C}$  overnight. Colonies were picked and screened for the insert by PCR. A positive control was included in all transformation experiments, where competent cells were transformed with DNA provided with the pGEM-T Easy kit (Promega). A negative control was always included where non-transformed cells were treated in the same way of the transformed cells.

### **2.8.6 Colony-screening PCR**

Bacterial colonies transformed with a ligation mixture were spread on agar plates with antibiotic selection. Those bacteria able to grow were screened by PCR to see which colonies contained plasmids with ligated inserts of the correct size. Using a clean sterilized tip, a number of colonies were picked (used as the template) off the agar plate individually and lightly dipped into the corresponding PCR tubes. The remaining streak of the colony was transferred to a 5-ml volume of LB and incubated overnight at  $37^\circ\text{C}$ . Cultures of the colonies showing positive PCR products were used in further experimental studies.

### **2.8.7 Purification of plasmid DNA**

Single bacterial colonies containing the correct size of insert were used to inoculate 5-ml cultures of LB medium containing  $100 \mu\text{g/ml}$  ampicillin for selection and grown at  $37^\circ\text{C}$  overnight in a shaking incubator. Cells were then harvested by centrifugation at  $1,250 \times g$  for 10 min at room temperature.

Plasmid purification was achieved using the QIAprep spin miniprep Kit (Qiagen). The presence of the cloned PCR fragment in the purified plasmid was screened by restriction enzyme digestion and by sequencing.

### **2.8.8 DNA sequencing**

The sequencing part of the project was performed on DNA from 427-WT and its derived cell lines (B48 and P1000) based on independent PCR amplifications of the AT-A, AT-G and AT-E genes.

Twelve individual bacterial colonies, transformed with pGEMTeasy containing the insert of interest for AT-A, AT-G and AT-E genes, were first checked by restriction endonuclease digestion after purification using a Qiagen miniprep kit and sent away for sequencing using MWG's standard T7 and SP6 sequencing primers.

Sequencing was carried out for the following reasons: to confirm the presence of the gene coding for a particular transporter within the strain's genome; to confirm the presence of a particular fragment in the construct during the cloning process; to verify whether the sequences matched that listed in GeneDB; and finally to check for any point-mutations and estimate the copy number of a particular gene.

## **2.9 RNA Interference in *T. brucei***

RNA interference (RNAi) refers to the introduction of homologous double stranded RNA (dsRNA) to specifically target a gene product mRNA, resulting in "null" phenotype (La Count *et al.*, 2000).

### **2.9.1 RNAi fragment design and construction**

For the RNAi constructs, gene fragments of around 400-600 bp in size were amplified by PCR from *T. b. brucei* s427 genomic DNA using specific primers containing appropriate restriction enzyme linkers.

The TbAT-E sequence Tb927.3.590 (GeneDB) was originally identified by BLAST search with TbAT1 (De Koning *et al.*, 2005). After sequencing multiple copies of *T. b. brucei* s427 AT-E, a fragment of 411 bp was selected based on the multiple alignment. This fragment had little sequence divergence, and TrypanoFAN: RNAi software (Redmond *et al.*, 2003) was used in the identification of a 411bp RNAi fragment specific for AT-E (Figure 2.4 & Figure 2.5).

In order to enable compatible ligation of the RNAi fragment and the vector, primers were designed to incorporate restriction sites so the PCR product could subsequently be cloned into the vector. Restriction sites for *KpnI-BamHI* enzymes (Promega) were incorporated into the forward and *XbaI-ApaI* (Promega) into the reverse primer used to amplify RNAi/AT-E fragment, this allowed subcloning to the vector pRPa<sup>SLi</sup> (see Table 2.2 and Figure 2.6).

Two sets of primers, different from the one above for cloning into the BSF vector pRPa<sup>SLi</sup>, were designed with the addition of specific enzymatic restriction sites in order to amplify the same 411bp RNAi fragment from pIT.03 (pGEM-T easy + AT-E insert) for cloning into the PCF vector p2T7Ti. The forward primer contained a *BamHI* (Promega) restriction site, whereas the reverse contained a *HindIII* (Promega) restriction site (Figure 2.9). The creation of the RNAi/AT-E construct pHDK07 was achieved by the digestion of both PCR product and the vector with the same enzymes followed by ligation.

After successful ligation, competent *E. coli* bacteria were transformed with the ligation mixture using the standard heat shock method described above (section 2.8.5). Cells containing the construct were selected for growth on LB agar plate containing 100 µg/ml ampicillin. Positive colonies were picked and grown in LB medium containing ampicillin (100 µg/ml). The plasmid was purified using QIAprep Miniprep kit (Qiagen). Correct integration of the construct was checked by restriction digest and by PCR.

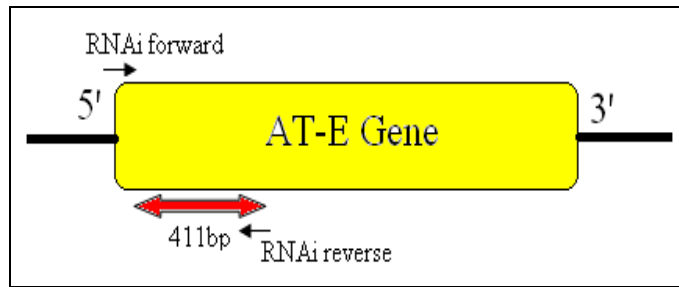


Figure 2.4. Sense and antisense RNAi primers were designed to pick a fragment within the AT-E. The sense primer contains *KpnI-BamHI* and the antisense primer contains *XbaI-ApaI*.

```

tgcggaggatcaaaggttttgaataacgtcttcacgtactacaatgccacgacgttccttgtggagttccttctga
ctttattcatgctgacaaatcttgaaggcggatcccctctggctgttcgactcgggtgccggtctcatccttcaatt
ttggcagttttcgtcgtgataatggtcaccataataaaaaacaacagaaaccggcgcgaaggtaacgattatgctc
gtcgggtgatcaatgggtgttcggcaacactttgtgacaccggaaacgggtgcccttattagcccgttcctataa
aattttcagcggcgttgtgtgggtgtcgcagtttgggtatcatcacatcgttcttctctatcgtaataaaagcat
ctatggagagcaactacgaaagcatgttgacacagtcccgaattttcttggcttgggtgtccttcttgaagtggttt
cctgcatcctcttgggtgcttctgaggaagaaccatacgccatgaagtatgcagcagagtttcggtacgccgcaa
gggaaaggaccaatgcttgtgaaaacaagaaagtggcgcacaaatggcccagcagaacaagatgaagactc

```

Figure 2.5. Forward and reverse for the RNAi/AT-E primers.

Primers were designed (bold / underlined) to amplify the 411bp for the RNAi/AT-E (highlighted in yellow) from the AT-E gene. Linker containing restriction sites required for appropriate ligation into vectors.

### 2.9.2 RNAi in *T. brucei* Bloodstream forms

The RNAi/AT-E construct was based on the pRPa<sup>iSL</sup> plasmid (Alsford & Horn, 2008) in which the RNAi fragment was ligated twice (sense and antisense) into a stem-loop construction with *Tet*-inducible promoter. This resulted in pHDK02, providing a stem-loop construction optimal for RNAi. Vector pRPa<sup>iSL</sup> was designed to complete a partial hygromycin sequence in 2T1 cells upon transfection, while introducing puromycin sensitivity by destroying a puromycin resistance coding sequence in 2T1 cells (Alsford & Horn, 2008).

The correct ligation of the two fragments was achieved in a two-step digest: (A) both RNAi/AT-E fragment and the vector were digested by *Kpn-BamHI* (Promega) and ligated in the sense direction. (B) The second step of ligation involved the digestion of the construct from step (A) and another fragment of RNAi/AT-E with

*Apal-XbaI* (Promega). The resulting bands corresponding to the correct size of each fragment were extracted from the 1% agarose gel. The RNAi/AT-E is ligated into the linearised vector obtained in step (A) in antisense direction. Successful ligation resulted in pHDK02.

```

gggcccggtaccaagcttgatccctctggctgttcgactcggtgccggtctcatcctcaatttggcagtttcgctgataatg
gtcaccataataaaaaaacagaaaccggcgccaaggtaacgattatgctcgtcgggtgatcaatgggtgtgcccgaacactttgt
gacaccggaacggtgcccttattagcccgttcctacaaaattttcagcgccgttggtggggtgctgcagtttggtgtcatcac
atcgttctctctatcgaataaaagcatctatggagagcaactacgaaagcatgttgacacagtcccgaatttctttggcttggtgtc
cttcttgaagtgtttctgcatcctcttgggtcttctgaggaagaactcatacgcatgaagtatgcagcagaggatccgagctc

```

Figure 2.6. 411 bp RNAi fragment was amplified with unique primers (bold and underlined). A linker was attached to each primer containing restriction sites; (**ggtacc**) *KpnI* and (**gggccc**) *Apal* (forward), and a reverse includes (**gagctc**) for *BamHI*, (**gagctc**) for *XbaI* (complementary). This fragment was inserted twice in pRPa<sup>ISL</sup> Vector in sense and antisense manner after digestion with the appropriate enzymes each time, as shown in Figure 2.7.

Competent *E. coli* bacteria were transformed with pHDK02 using the standard heat shock method. The presence of the two inserts was confirmed using a restriction digest and by sequencing. Prior to transfection, the construct was linearised with *Ascl*, and the resulting cassette was used in the transfection of the 2T1 cell line (Figure 2.7). Correct integration of the cassette was checked by PCR using specific primers designed to amplify the drug resistance marker.

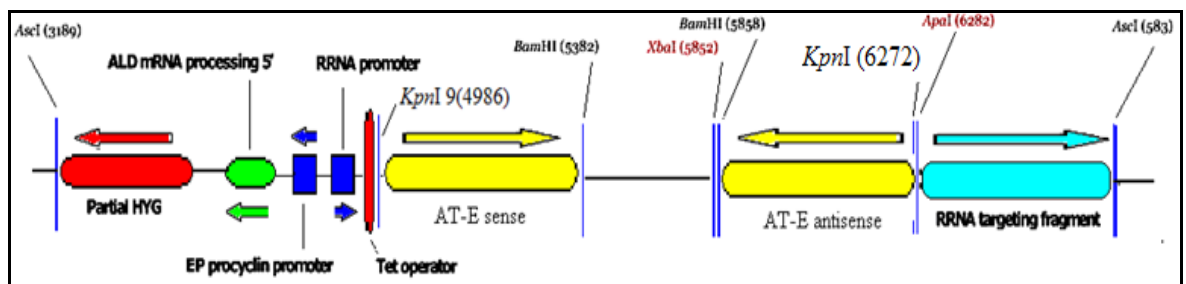


Figure 2.7. Cartoon presents the RNAi/AT-E construct for blood stream form.

Linearization of pHDK02 with *Ascl* resulted in RNAi cassette (two fragments inserted in sense and antisense direction). This was transfected into the 2T1 cell line, and tetracycline induction was designed to result in the reduction of AT-E mRNA levels due to RNAi knockdown.

### 2.9.3 RNAi in *T. brucei* procyclic forms

The construct for RNAi study in PCF *T. b. brucei* is based on the placing of the RNAi/AT-E fragment between opposing T7 promoters within the p2T7Ti vector construct (Figure 7.14) (LaCount *et al.*, 2000). The vector's backbone consists of an rRNA spacer that is required for the integration into the rRNA locus of the parasite's genome, a tetracycline inducible operator, and a drug resistance gene for selection (phleomycin). The vector is only used in a cell line derived from EATRO 427-WT cell line named *T. b. brucei* 29-13, which expresses bacteriophage T7 RNA polymerase and the *Tet* repressor from bacteriophage.

Two sets of primers, different from the ones used in BSF, were designed with the addition of specific enzymatic restriction sites in order to amplify the 411bp RNAi fragment. The forward primer contained a *Bam*HI restriction site, whereas the reverse primer contained a *Hind*III restriction site. The creation of the RNAi/AT-E construct pHDK07 was achieved by the digestion of both PCR products and the vector with the same enzymes followed by ligation. Competent *E. coli* were transformed with pHDK07 and the plasmid was purified and stored at 4 °C until use in the transfection process. The presence of the RNAi/AT-E insert was confirmed by restriction digest and sequencing.

Prior to transfection of the 29-13 cell line, the construct was linearized with *Not*I (Figure 2.8). Correct integration of the cassette was checked by PCR using specific primers designed to amplify the drug resistance marker.

The T7 polymerase and the tetracycline repressor constructs were maintained in the 29-13 cell line (La Count *et al.*, 2000) by the addition of 15 µg/ml G418 and 25 µg/ml Hygromycin B to the medium. To induce the RNAi effect, tetracycline was added at a concentration of 100 ng/ml. Without tetracycline, the *Tet* repressor expressed in the cells binds to the *Tet* operator to inhibit transcription from the integrated construct. With the addition of tetracycline, the repressor is bound and its action prevents binding to the operator, allowing transcription to take place.

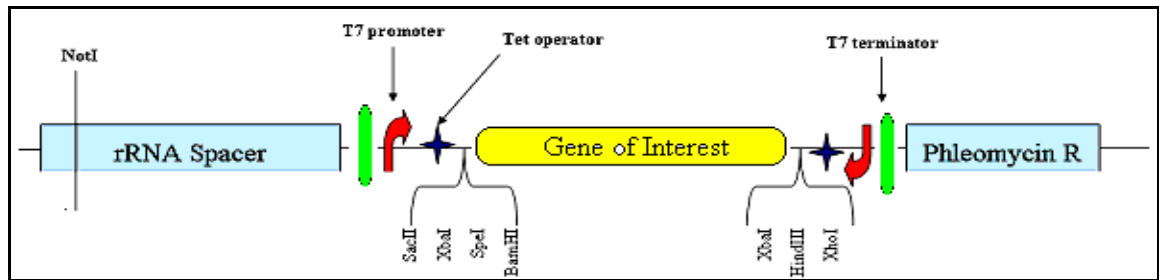


Figure 2.8. The structure of RNAi vector p2T7Ti.

The yellow section represents the RNAi fragment of the gene of interest placed between two Inducible T7 promoters. Phleomycin R is the resistance gene, used as a selective marker.

```

agttggaaaattatacagaatgtctttggcaacacaccgcctgattaatacgaactcactataggagatctcccta
tcagtgatagagatctagccgcggtggcggccggccgctctagaactagtggatccgatccctctggctgttcga
ctcggtgccggtctcatcctctcaattttggcagtttctgcgtgataatggtcaccataataaaaacaacagaaa
ccggcgccaaggaacgattatgctcgtcgggtgatcaatgggtgtgaggcaacactttgtgacaccggaacg
gtgcccttattagcccgttcctacaaaatttcagcgccgttgtgtgggtgtcgcagtttgggtgtcatcacat
cgttcttctatcgtataaaagcatctatggagagcaactacgaaagcatgttgacacagtcgccgaatctctt
ggcttgggtgtccttctgaagtggtttctgcacctcttgggtcttctgaggaagaactcatacgccatgaagtat
gcagcagaaagcttatcgataccgtcgacctcgagggggggccggggagatctctatcactgataggagatct
ccctatagtgagtcgtattaatcaggaacggtgtgttgccaaagacattctgtataatcttccaactaccctaacc

```

Figure 2.9. Sequence from a portion of pT27T1 with RNAi/ AT-E insert highlighted in yellow. Primers used to amplify the RNAi fragment are bold and underlined, restriction sites were added to the sequence of the primers for digestion and ligation proposes. (**GGATCC**) for Bam HI and (**AAGCTT**) for Hind III.

#### 2.9.4 Transfection of BSF Trypanosomes

In order for the spherical RNAi/AT-E vectors to penetrate the host cell, they have to be linearised. In the BSF case pHDK02 was linearised using *Ascl*. Low voltage (30V) agarose gel electrophoresis DNA migration resulted in two distinct fragments: one corresponded to the RNAi cassette and the second to the vector backbone. The cassette was extracted from the gel using the Qiagen extraction kit and used in the transfection process. To minimise the possibility of degradation, linearised plasmid DNA was added to the cells just before electroporation. Transfection of 2T1 (Alsford & Horn, 2008) was performed using an Amaxa Nucleofector II (Lonza, Germany) under strictly sterile conditions.

An amount of  $5 \times 10^7$  cells at mid-log phase was harvested by centrifugation at  $1500 \times g$  and resuspended in 100  $\mu$ l of human T-cell Nucleofector solutions and transferred to an electroporation cuvette (0.2 cm). 10  $\mu$ l of sterilized H<sub>2</sub>O containing 10  $\mu$ g linearised RNAi/AT-E cassette was added to the mixture and the cells were transfected by electroporation using program X-001 (Burkard *et al.*, 2007). Cells were transferred into pre-warmed HMI-9 with 10% FCS without antibiotics and incubated at 37 °C. Hygromycin B and Phleomycin, at 2.5  $\mu$ g/ml and 0.2  $\mu$ g/ml, respectively, were added after 16 hours recovery in fresh HMI-9 medium and the culture was distributed with 10-fold dilutions into four 24 wells plates. Positive wells arose from single resistant cells after 5 days; these wells were selected and the cells cloned by limiting dilution in 96-well plates (see section 2.9.7).

RNAi-AT-E cassette and the tetracycline repressor constructs were maintained within the transfected cells by addition of 0.2  $\mu$ g/ml puromycin and 0.5  $\mu$ g/ml phleomycin to the medium. After transfection, puromycin was replaced, with addition of 2.5 $\mu$ g/ml Hygromycin-B as drug resistance marker for selection. To induce the RNAi effect, tetracycline was added to the medium at a concentration of 1  $\mu$ g/ml.

### **2.9.5 Transfection of PCF Trypanosomes**

For stable transfection of the procyclic host strain 29-13 via integration into an rDNA spacer region, the RNAi constructs were linearised by *NotI* digestion (Wirtz *et al.*, 1999) The digestion of plasmid DNA was carried out in a volume of 40  $\mu$ l using 1 unit of *NotI*, 4  $\mu$ l of 10 $\times$  buffer and 10  $\mu$ g of plasmid DNA and incubated at 37 °C for 2 h. After the addition of 1 further unit of the restriction enzyme, the reaction was re-incubated overnight, with the final digest checked by agarose gel electrophoresis.

The linearised DNA plasmid was sterilised by ethanol precipitation after an inactivation of the enzyme at 65 °C for 20 minutes, then air dried in a sterile hood and resuspended in 20  $\mu$ l of sterile water. Agarose gel electrophoresis was used to assess proper linearization of the vector. For the transfection, PCF 29-13 cells were grown to mid-log phase ( $5 \times 10^6$  cells/ml).  $5 \times 10^7$  cells were collected by centrifugation at  $1,500 \times g$  for 10 min at room temperature, washed twice in

10 ml of ZPFM buffer (Appendix A) and resuspended in 100  $\mu$ l human T-cell Nucleofector solution. This mix was then transferred to an electroporation cuvette (0.2 cm) and 10  $\mu$ g of the construct in 10  $\mu$ l of distilled H<sub>2</sub>O was added to the cells/T-Cell mix. Cells were electroporated using an Amaxa Nucleofector II (Lonza, Germany) program X-001. Immediately following transfection, cells were transferred into fresh pre-warmed SDM-79 medium with 10% FCS supplemented with 15  $\mu$ g/ml of G418 and 25  $\mu$ g/ml Hygromycin B. Drug selection was started the next day after allowing cells to recover. After 24 hours 10  $\mu$ g/ml of phleomycin was added to the culture, the culture was distributed with 10-fold dilutions into four 24 wells plates and incubated at 27 °C. Positive wells were observed between 10 to 15 days after incubation; the wells were selected and the cells cloned by serial limiting dilution in a 96-well plate.

### **2.9.6 Selection of RNAi clones**

In order to obtain unique clones, cells of positive wells were cloned out by serial limiting dilution in a 96-well plate. This was carried out by culturing the positive BSF cells in HMI-9 supplemented with 10% FCS and 2.5  $\mu$ g/ml hygromycin B and 0.2  $\mu$ g/ml phleomycin. For PCF 25% conditioned SDM-79 medium with 10% FCS supplemented with 15  $\mu$ g/ml of G418 and 25  $\mu$ g/ml Hygromycin B and 10  $\mu$ g/ml phleomycin was used. The conditioned medium was prepared by growing wild-type 427 PCF cells from early to late log phase of growth (7-9  $\times$  ampicillin 10<sup>6</sup>/ml) then pelleted at 1500  $\times$  g and the supernatant sterilized by filtration. This was added to fresh SDM-79 (25%, v/v). Drug-resistant cells were selected between 7 - 10 days for BSF and between 10 to 15 days for PCF.

Once clonal lines were obtained, cells were maintained in the presence of drugs. For each clone, cell culture, in log phase, was aliquoted in relevant medium plus 30% glycerol (v/v) and stored in liquid nitrogen.

Growth curves in the presence and absence of tetracycline were carried out. Cell counts were combined with RNA extraction at various time points, in order to generate cDNA to assess AT-E mRNA levels relative to un-induced controls. This was checked using Reverse Transcriptase PCR (RT-PCR). Unique clones with successful RNAi knockdown were used in further investigations including uptake assays and the creation of drug profiles for each clone.

### 2.9.7 Cloning by serial limiting dilution

This technique involves seeding the cells in 200  $\mu$ l of growth medium supplemented with the selection marker starting at 1000 cells in the first well of the 96 wells plate and subsequently doubly diluted across the plate. This was followed by incubation of the plates in suitable conditions. The time before observation of positive wells depends on the strain being used. Unique clones are picked from the positive well that are predicted to have contained less than 1 parasite ( $> 0.97$  cell/well) during the dilution procedure (Figure 2.10).

	1	2	3	4	5	6	7	8	9	10	11	12
A	1000	500	250	125	62.5	31.25	15.62	7.81	3.9	1.95	0.97	0.49
B	500	250	125	62.5	31.25	15.62	7.81	3.9	1.95	0.97	0.49	0.24
C	250	125	62.5	31.25	15.62	7.81	3.9	1.95	0.97	0.49	0.24	0.12
D	125	62.5	31.25	15.62	7.81	3.9	1.95	0.97	0.49	0.24	0.12	0.06
E	62.5	31.25	15.62	7.81	3.9	1.95	0.97	0.49	0.24	0.12	0.06	0.03
F	31.25	15.62	7.81	3.9	1.95	0.97	0.49	0.24	0.12	0.06	0.03	0.015
G	15.62	7.81	3.9	1.95	0.97	0.49	0.24	0.12	0.06	0.03	0.015	0.075
H	7.81	3.9	1.95	0.97	0.49	0.24	0.12	0.06	0.03	0.015	0.075	0.0375

**Figure 2.10. Cloning by serial limiting dilution.**

96 wells plate were used starting at 1000 cells (well A-1) then doubly diluted across the plate (transfer 100 $\mu$ l to A-2 and 100 $\mu$ l to B-1). Unique clones will rise from below 1 cell / well parasitemia. This table presents the levels of parasitemia per well after dilution (total volume of 200 $\mu$ l / well).

### 2.9.8 Analysis of Growth Rates

Growth rate analysis was also used to assess the effect of RNAi tetracycline induction on the growth of BSF and PCF trypanosomes. For RNAi, cell lines growth was determined in the presence and absence of tetracycline, and was grown in 24 well plates using a total volume of 1ml of relevant medium supplemented with relevant antibiotic. BSF cultures (IT.BERi) were typically started at a density of  $2 \times 10^4$  cells/ml, in HMI-9 medium / 10% FCS in the presence and absence of tetracycline. PCF cultures (IT.CERi) were commonly initiated at a starting density of  $5 \times 10^4$  cells/ml in SDM-79 medium/10% FCS. Parasite numbers were measured by counting with an improved Neubauer haemocytometer (Weber Scientific), and cell counts were taken over time points for up to 10 passages/per strain.

### **2.9.9 Preparation of cDNA**

The synthesis of cDNA was carried out using the classical method using oligo (dT) primers (random primers - Qiagen). A total of 5 µg of RNA (extracted as described in section 2.7.2) was used as a template to generate a full length double stranded cDNA. All the reagents were obtained from Invitrogen and the synthesis process followed the protocols provided by the manufacturer unless stated otherwise.

The SuperScript® III Reverse Transcriptase (Invitrogen) was used to synthesize the first strand of cDNA. In an RNase-free tube, the reaction contained 1 µl of oligo-dT (300 µg/µl), 5 µg of total RNA (same RNA concentration was used for instant control), and 1 µl of dNTP mix (10mM). The volume was brought to 13 µl by adding DEPC-treated distilled water. The mixture was incubated at 65 °C for 5 min to remove any secondary structures and then placed on ice for 1 min. The content of the tube was collected by brief centrifugation, and 4 µl of 5× First-Strand buffer, 1 µl of DTT (0.1 M) and 1 µl RNaseOUT Recombinant RNase Inhibitor (40 U/µl) were added. The mix was incubated at 42 °C for 2 min followed by addition of 1 µl Superscript III Reverse Transcriptase (200 U). The solution was then incubated at 42 °C for 50 min. One tube was treated in the exact way, except for the addition Superscript III Reverse Transcriptase and was included as a control during cDNA synthesis to test for any DNA contamination. The reaction was then inactivated by heating at 70 °C for 15 min before chilling on ice for 2 min. The cDNA was used immediately for PCR or stored at -20 °C for further work.

### **2.9.10 Reverse Transcriptase PCR**

Reverse Transcriptase polymerase chain reaction (RT-PCR) was used to investigate any changes in mRNA levels upon induction of tetracycline pressure in RNAi cell lines. The reaction is performed on cDNA made from RNA extracted from a cell line without and after RNAi tetracycline induction. The methodology is very similar to the typical PCR reaction (Section 2.7.4), with the difference of using cDNA as a template. A 1 µl volume of each template (+/- Tetracycline and +/- RT) at equal concentrations and *Taq* polymerase (Promega) along with gene-specific primers were used in the amplification process. The PCR product of the

tetracycline induced sample would show as a lower density band, compared to the non-induced sample, if knockdown of the specific gene occurred.

AT-E, AT-A and P2-specific primers were used to investigate whether RNAi reduced AT-E mRNA levels and whether the knockdown of the AT-E sequence by tetracycline induction affected the expression of the other two genes. Superscript III Reverse Transcriptase-untreated samples were also included as a negative control for DNA contamination.

## 2.10 Southern blot analysis

The Southern blot technique was used in this project to investigate the copy number of the AT-E gene within the genome of *T. b. brucei* (s427). It was performed on 427-WT genomic DNA using 13 restriction endonuclease enzymes chosen to provide a diagnostic pattern of bands detectable on a Southern blot. Some of the restriction enzymes will cut within the region flanking the gene whereas others will cut within the gene. One enzyme that did not cut anywhere was included as a control (Table 2.3).

Enzyme	Cutting Site	Fragment Size	Enzyme	Cutting Site	Fragment Size
Bcl I (promega)	In/ Out of the gene	2022 bp	Nco I (promega)	Out of the gene	11318 bp
Bgl II (promega)	Out of the gene	19253 bp	Pst I (promega)	In/ Out of the gene	2091 bp / 1672 bp
Cla I (promega)	Out of the gene	4105 bp	Sac I (promega)	Out of the gene	9042 bp
EcoR I (promega)	Out of the gene	7481 bp	Sal I (promega)	Out of the gene	5158 bp
EcoR V (promega)	Out of the gene	4385 bp	Xba I (promega)	Out of the gene	> 10 kb
Kpn I (promega)	Out of the gene	11000 bp	SnaB I (ROCH)	Out of the gene	8322 bp
Mlu I (promega)	Out of the gene	19283 bp			

**Table 2.3. Enzymes used in digestion for southern blot.**

Since the genome sequencing project for 427-WT of *T. b. brucei* is not complete we used the genome sequence for *Trypanosoma brucei* strain TREU927 from GeneDB as a reference in the restriction digest with the chosen enzymes. Vector NTI software was used to design a map for the restriction sites on 42 Kb (20 Kb

added to each side of AT-E). Restriction site were also confirmed on the s427 AT-E sequences ligated into pGEM-T Easy (pIT.03, pIT.04) (Table 2.4).

Laboratory name of plasmid	Origin	Applications	Insert (gene) / Size	Source of the insert	Source of the vector
pIT.01 pIT.02 pIT.03 pIT.04	pGEM-T Easy	Intermediate cloning vector / Sequencing of relevant insert	AT-A (1449bp) AT-G (1449bp) AT-E1 (1389bp) AT-E2 (1389bp)	427-WT gDNA 427-WT gDNA 427-WT gDNA 427-WT gDNA	Promega
pHDK02	pRPa <sup>iSL</sup>	cloning vector for RNAi knockdown in BSF	RNAi/AT-E 411 bp	pIT.03	Prof. Mike Barret (University of Glasgow)
pHDK07	p2T7Ti	cloning vector for RNAi knockdown in PCF	RNAi/AT-E 411 bp	pIT.03	Dr. Mechael Swedrski (University of Glasgow)

**Table 2.4.** Examples of plasmids created in the lab during this project.

Digestions were performed in 13 tubes where each tube contained a 100 µl-volume of digestion mix: 10 µg of s427 gDNA, 10 µl of restriction enzyme buffer, 50 U restriction enzyme (brought to 100 µl with ddH<sub>2</sub>O). The digestion was performed overnight at 37 °C, and then 50 U from each enzyme were added, followed by further 1-hour incubation.

### **2.10.1 Preparation of the gel, blotting and transfer onto nylon membrane**

The digested DNA was mixed with an appropriate volume of 6× DNA loading buffer, and loaded into wells of a 1% (w/v) agarose gel. Electrophoresis was

performed at 23V, and monitored by UV illumination to optimise band separation.

The gel was then submerged in depurination solution (0.125 M HCl) and agitated gently for 10 minutes. In order to produce single-stranded DNA, gel was denatured *in situ* by gentle agitation in denaturation solution (1.5 M NaCl, 0.5 M NaOH) for 30 minutes. The gel was then immersed in neutralisation solution (1.5 M NaCl, 1 M TrisHCl pH7.5) for 30 minutes with gentle agitation. These steps were separated by rinsing with ddH<sub>2</sub>O.

The DNA was then transferred from the gel to a Hybond-N nylon membrane (Amersham Pharmacia Biotech) according to the Southern method (1975) (re-described by Sambrook *et al*, 1989) and depicted in Figure 2.11.

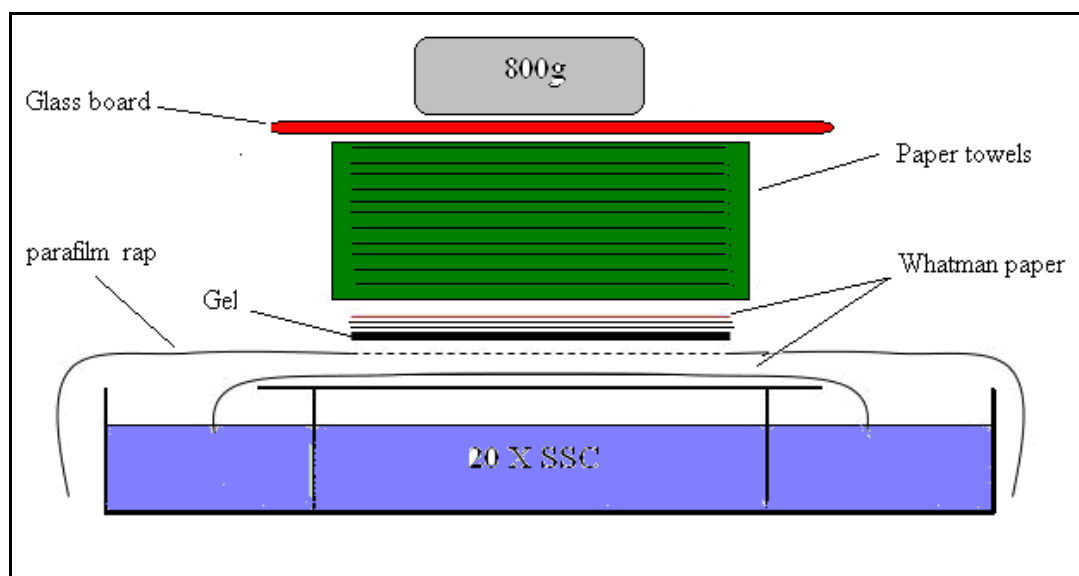


Figure 2.11. DNA is transferred into nylon membrane through capillary transfer

### 2.10.2 Membrane probe labelling

The membrane carrying the DNA fragments was labelled with a <sup>32</sup>P-labelled probe using the Prime It® II Random primer labelling kit (Stratagene), where 10 µl of random primers were added to 25 ng of DNA in a total reaction volume of 37 µl. The mixture was heated to 95 °C for 5 min in order to denature. A brief centrifugation was followed by the addition of 10 µl of 5× dATP primer buffer, 50 µCi α <sup>32</sup>P dATP and 1 µl of Exo Klenow enzyme (Stratagene) (5 U/µl), and the mixture was incubated for 10 min at 37 °C .

Prehybridisation process was carried out for 2 h in a rotating hybridization oven (Stratagene) at 42 °C, where the membrane was placed in tube containing hybridisation solution (50% Formamide, 5× SSC, 10× Dendhart's solution, 0.1% SDS, 20 mM NaH<sub>2</sub>PO<sub>4</sub>, pH 6.5 and 0.2 mg/ml salmon sperm DNA). The probe was denatured for 5 min at 95 °C and immediately added to the tube containing the membrane in hybridisation solution, and the hybridisation was allowed to proceed overnight at 42 °C.

The membrane was stripped by washing for 2 minutes in 0.5× SSC buffer, and washing twice for 10 min each in 0.1% SDS at 55 °C and then exposed at - 80 °C for 24 hours to autoradiography film (Kodak medical X Ray film, or membrane Hyperfilm ECL from GE Healthcare). Film was developed using a Compact X4 developer (X-ograph Imaging systems).

## 2.11 Software and web resources

Vector NTI was used to analyse DNA and protein sequences as well as in primer design where it was also used to locate the open reading frames within translated nucleotide sequences and restriction enzyme sites. The AlignX programme of the Vector NTI package was also used in the alignments of related nucleotide and amino acid sequences. ContigExpress was used to align overlapping sequences to form contiguous sequences. Final multiple sequence alignment presented in (Appendix D) was created using CLC software CLC Genomics Workbench 4.0.3.

Other databases and websites used during to project are listed below:

<http://www.ncbi.nlm.nih.gov/>

<http://www.tigr.org/tdb/>

<http://tritypdb.org/tritypdb/>

[http://www.sanger.ac.uk/Projects/T\\_brucei/](http://www.sanger.ac.uk/Projects/T_brucei/)

<http://www.genedb.org/genedb/tryp/index.jsp>

<http://trypanofan.path.cam.ac.uk/software/RNAit.html>

**3 The diamidine diminazene aceturate is a substrate for the High Affinity Pentamidine Transporter: implications for the development of high resistance levels in trypanosomes**

### 3.1 Introduction

One of the many diseases that plague sub-Saharan Africa is trypanosomiasis, a disease complex formed by several species infecting domestic and wild animals (mostly *Trypanosoma congolense*, *T. vivax* and *T. brucei brucei*) and humans (*T. b. rhodesiense* and *T. b. gambiense*) and transmitted by tsetse flies. In addition *T. vivax* and the closely related animal parasites *T. evansi* and *T. equiperdum* can also be transmitted sexually or by other biting insects, which has spread the disease to large regions of Southern Asia and South America. The infection is known as sleeping sickness in humans, nagana in cattle, dourine in horses, and as surra in camels and other high-value livestock such as buffalo. The human disease is invariably fatal if left untreated and the veterinary condition causes enormous damage to economies and food production. The only option for control of trypanosomiasis is chemotherapy as insect control on the necessary scale is prohibitively expensive and vaccine development appears practically impossible due to the high rate of antigenic variation of African trypanosomes.

However, the choice of chemotherapeutic agents is very limited and those available suffer from many shortcomings such as high levels of host toxicity, parenteral administration, and perhaps most importantly increasing levels of treatment failure due to drug resistance. For treatment of the late or cerebral stage sleeping sickness has led to the replacement of melarsoprol with eflornithine in many foci (Balasegaram *et al*, 2009) and the recent introduction of eflornithine/Nifurtimox combination therapy (Priotto *et al*, 2009; Yun *et al*, 2010). The early or haemolymphatic phase is still treated with the aromatic diamidine compound pentamidine, introduced in the 1930s (Delespaux & de Koning, 2007).

For the veterinary condition the situation is even more serious with many reports of resistance to the two principal drugs of isometamidium (a phenanthridine) and diminazene aceturate (aromatic diamidine) (Geerts *et al*, 2001; Delespaux & de Koning, 2007), and no alternative treatments in development. The paucity of new drug development for both the human and veterinary diseases makes understanding of the spreading resistance phenotypes an absolute priority. Resistance markers are required for epidemiological studies to assess the real spread of resistance, and an insight into the causes of resistance and the

patterns of cross-resistance must underpin rational strategies to limit the impact and further spread of the problem.

It has been known for considerable time that trypanosomes resistant to melaminophenyl arsenicals such as cymelarsan (used against surra in camels) and melarsoprol is associated with cross-resistance to at least some of the aromatic diamidines (Williamson & Rollo, 1959; de Koning 2008). We now know that pentamidine is salvaged by three distinct transport entities in bloodstream trypanosomes, the P2 aminopurine transporter, the High Affinity Pentamidine Transporter (HAPT1) and the Low Affinity Pentamidine Transporter (LAPT1) (de Koning & Jarvis, 2001; de Koning, 2001; Matovu *et al*, 2003; Bridges *et al*, 2007). P2 is encoded by the ENT-family gene *TbAT1* (Mäser *et al*, 1999) but the genes encoding HAPT1 and LAPT1 are still unknown and the identification of these transporters is made more difficult by the complexity of the three influx routes for the drug under study, the relatively low rate of uptake by HAPT1 and the lack of specific inhibitors for LAPT1. We thus decided to investigate [<sup>3</sup>H]-pentamidine transport in procyclic *T. b. brucei*, in the hope to obtain a simpler model.

We found that procyclic cells lack the adenosine-sensitive P2-mediated pentamidine transport but that two pentamidine uptake systems, indistinguishable from HAPT1 and LAPT1 in bloodstream forms, were expressed. This allowed us to characterise P2-independent diminazene uptake in detail and determine that this is mediated by the procyclic high affinity pentamidine transporter (PPT1), a finding we subsequently verified in bloodstream forms. This gives a rationale for the continued sensitivity of trypanosomes without functional P2 transporter to diminazene at concentrations around 1  $\mu$ M and increases our understanding of cross-resistance between arsenical and diamidine trypanocides.

### **3.2 Generation of a new clonal line resistant to high levels of diminazene aceturate**

The generation process was performed by previous PhD student Anne Kazibwe using *in vitro* drug selection on *T. brucei* bloodstream trypanosomes from the *tbat1*<sup>-/-</sup> cell line (Matovu *et al*, 2003), using small, stepwise increments of

diminazene. The actual induction process is described in the University of Glasgow PhD thesis of Anne Kazibwe (2008). Briefly, the selection process was initiated using the doubling dilution method on a 96 well plate. The drugs were prepared by dissolving in sterile water. Diminazene aceturate was prepared as stock solution in sterile water and used at a start concentration of 1.6  $\mu\text{M}$ , equivalent to its  $\text{IC}_{50}$  value.

### **3.3 Alamar blue drug sensitivity assays**

Drug sensitivities were determined using the Alamar blue assay exactly as described (Gould *et al.*, 2008), measuring fluorescence in 96-well plates with a FLUOstar Optima (BMG Labtech) at wavelengths 544 nm for excitation and 620 nm for emission. Alamar Blue assays were performed as described in chapter 2, using cell density of  $10^5$  cells / ml and incubation time of 48 hours with the drugs followed by 24 hours incubation with alamar blue dye.  $\text{IC}_{50}$  values were calculated by non-linear fitting of the data to a sigmoidal dose-response curve with variable slope (Prism 5.0, GraphPad).

### **3.4 Transport assays**

Transport assays with procyclic and bloodstream form trypanosomes were performed as described previously in chapter 2. Kinetic parameters were calculated using the appropriate linear and non-linear regression equations in Prism 5.0 (GraphPad). All experiments were performed in triplicate on at least three independent occasions see chapter 2.

## **3.5 Results and discussion**

### ***3.5.1 Pentamidine transport in procyclic *Trypanosoma brucei* as a model for bloodstream forms***

It has previously been reported that procyclic *T. brucei* express a high affinity pentamidine transport system, which was designated PPT1 (Procyclic Pentamidine Transporter 1) and displayed similar properties to the HAPT1 transporter in bloodstream forms (de Koning, 2001). However, no conclusion was then reached as to whether PPT1 might be identical to HAPT1 and the presence

or absence of a low affinity component in procyclics, equivalent to LAPT1 in bloodstream forms, was not investigated. We report here additional data on the high affinity transport of diamidines in both life cycle stages, and the first characterisation of low affinity pentamidine transport in procyclic trypanosomes.

The linearity of [ $^3\text{H}$ ]-pentamidine uptake in s427 WT procyclics was first investigated. Uptake of 1  $\mu\text{M}$  pentamidine was linear for at least 450 s (linear regression, 6 points over 450 s;  $r^2 = 0.98$ ) with a rate of  $0.037 \pm 0.002 \text{ pmol}(10^7 \text{ cells})^{-1}\text{s}^{-1}$  and fully inhibited by 1 mM unlabelled pentamidine (slope not significantly different from zero; F-test) see (Figure 3.1). All [ $^3\text{H}$ ]-pentamidine experiments were performed using 60 s incubations, very much within the linear phase of uptake.

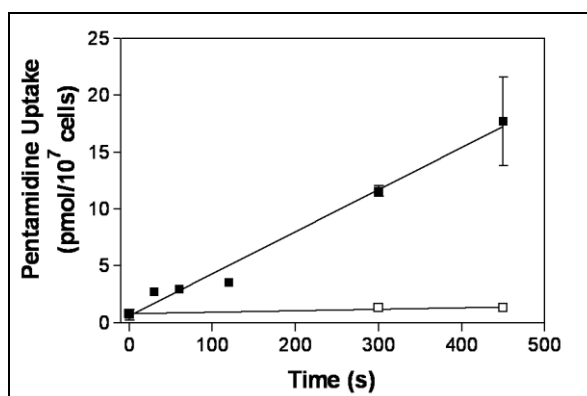


**Figure 3.1.** Transport of 1  $\mu\text{M}$  [ $^3\text{H}$ ]-pentamidine by *T. b. brucei* s427WT procyclic forms. Uptake measured in the presence (□) or absence (■) of 1 mM unlabelled pentamidine. The experiment was performed in triplicate and error bars indicate SEM; when not shown fall within the symbol.

Procyclic s427, like bloodstream forms, displayed separate high and low affinity transport entities for [ $^3\text{H}$ ]-pentamidine; when transport was measured at 25 nM radiolabel unlabelled pentamidine inhibited the flux at concentrations above 10 nM and fully saturated the transporter at 1  $\mu\text{M}$  (Figure 3.2, A), whereas uptake of 1  $\mu\text{M}$  [ $^3\text{H}$ ]-pentamidine was inhibited only by concentrations over 10  $\mu\text{M}$  (Figure 3.2, B). Michaelis-Menten constants ( $K_m$ ) were determined at  $0.030 \pm 0.003$  and  $33 \pm 10 \mu\text{M}$ , respectively, consistent with the HAPT1/LAPT1 system observed in bloodstream forms of the same strain. The maximum uptake rate at saturation ( $V_{\text{max}}$ ) for low affinity pentamidine transport was virtually identical in both life

cycle forms but, interestingly, the  $V_{max}$  for the high affinity component was 10-fold higher in procyclic forms (Table 3.1).

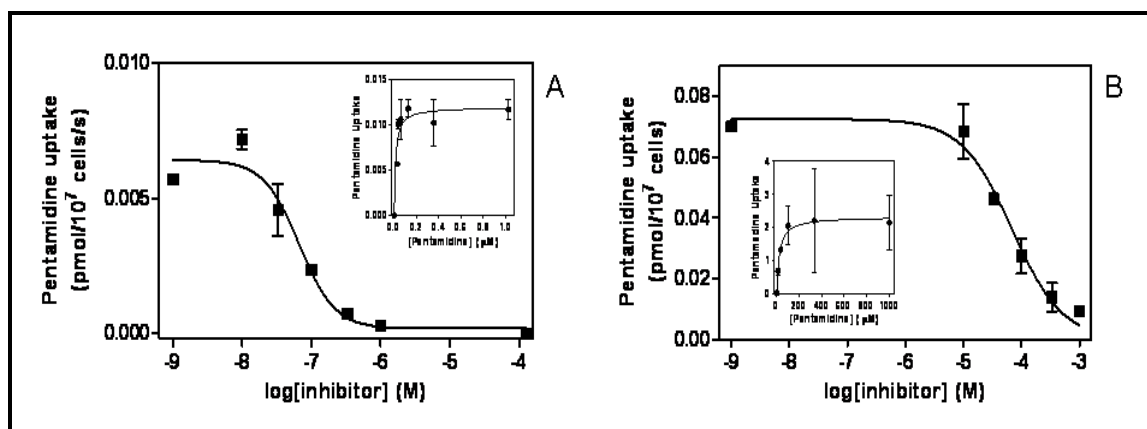


Figure 3.2. Uptake of low and high concentrations of [ $^3$ H]-Pentamidine in procyclic form. [ $^3$ H]-Pentamidine uptake in procyclic s427 trypanosomes at a permeant concentration of (A) 30 nM and (B) 1  $\mu$ M. Cells were incubated with [ $^3$ H]-pentamidine for 60 seconds in the presence or absence of various concentrations of unlabelled pentamidine as indicated. The insets depict the conversion of the inhibition plots to Michaelis-Menten saturation plots. Both graphs are representative of at least 6 independent experiments, each performed in triplicate. The data shown represent the average of these triplicate determinations  $\pm$  SEM. When not shown, error bars fall within the symbols.

		Bloodstream forms	Procyclic forms
High affinity transport	Pentamidine $K_m$	$0.035 \pm 0.005$	$0.030 \pm 0.003$
	Pentamidine $V_{max}$	$0.0028 \pm 0.0006$	$0.031 \pm 0.07$
	Propamidine $K_i$	$4.6 \pm 0.7$	$3.7 \pm 0.4$
	Diminazene $K_i$	$63 \pm 3$	$54 \pm 16$
	DB820	$43 \pm 10$	$45 \pm 18$
	CPD0801	$40 \pm 8$	$16 \pm 4$
Low affinity transport	Pentamidine $K_m$	$56 \pm 8$	$33 \pm 10$
	Pentamidine $V_{max}$	$0.75 \pm 0.15$	$0.78 \pm 0.12$
	Propamidine $K_i$	$316 \pm 3$	$429 \pm 180$
	Diminazene $K_i$	$160 \pm 50$	$180 \pm 20$

Table 3.1. Comparison of [ $^3$ H]-pentamidine transport parameters in bloodstream and procyclic *T. brucei*.

High affinity transport of [ $^3$ H]-pentamidine was measured at concentrations of 25 – 40 nM radiolabel, or 12.5 nM for the determination of  $K_m$  values; Low affinity transport was assayed at 1  $\mu$ M [ $^3$ H]-pentamidine. Data given are the average of at least three independent experiments, each performed in triplicate, and Standard Errors. Bloodstream forms were isolated from the blood of infected rats whereas procyclics were cultured in standard SDM79 medium. Units are  $\mu$ M for  $K_m$  and  $K_i$  values, and pmol per  $10^7$  cells per second for  $V_{max}$ . Some of the values have previously been reported in De Koning (2001).

The inhibitor profile of high affinity pentamidine uptake was also highly similar in both stages. In addition to the previously reported inhibition constants ( $K_i$ ) for propamidine and diminazene aceturate (de Koning, 2001) we further compared

inhibition by the furamide analogues DB820 and CPD0801 (formerly known as DB829) (Mathis *et al*, 2007). Again very similar activities on high affinity [<sup>3</sup>H]-pentamidine transport in procyclic and bloodstream forms were found (Figure 3.3 and Table 3.1). No reliable  $K_i$  values for DB820 and CPD0801 could be determined in relation to low affinity pentamidine transport due to lack of inhibition in the soluble range of these compounds. Indeed, no substrate or inhibitor with higher affinity than pentamidine has yet been identified for this transport activity. However, we report here LAPT1  $K_i$  values for propamidine and diminazene, which were similar in both trypanosomal stages (Table 3.1).

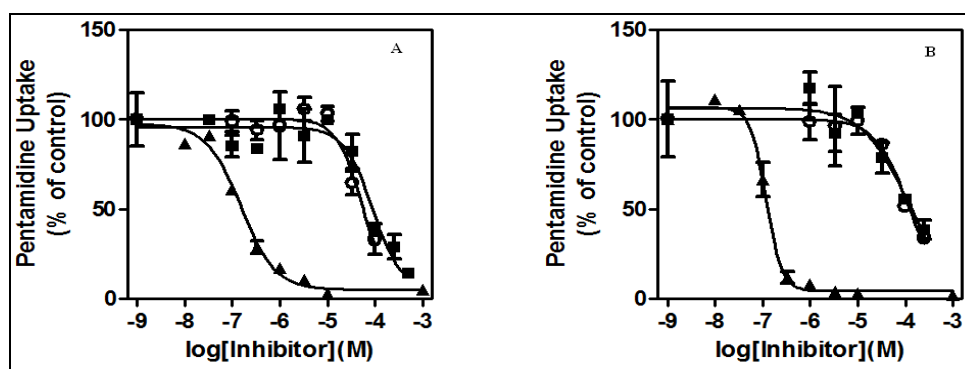


Figure 3.3. Characterisation of High affinity pentamidine transport.

High affinity pentamidine transport in bloodstream (A) and procyclic (B) forms of *T. b. brucei* in the presence of various concentrations of unlabelled inhibitors: ▲, pentamidine; ○, DB820; ■, CPD0801. [<sup>3</sup>H]-pentamidine concentration was 25 nM and incubation time was 60 s. The experiments shown are representative of at least three independent experiments, each performed in triplicate. Error bars are Standard Errors.

The kinetic data available are thus consistent with the HAPT1 and LAPT1 transporters of bloodstream forms (de Koning, 2001; Matovu *et al*, 2003; Bridges *et al*, 2007) being expressed also in procyclic forms, although definitive proof will require molecular studies. Although the procyclic high affinity pentamidine transporter was previously designated PPT1, we will now for the sake of clarity refer to them it as HAPT1, and the low affinity transporter LAPT1.

The procyclic forms make a convenient model to study diamidine transport due to the non-expression of the P2 aminopurine transporter (de Koning *et al*, 1998) which also transports pentamidine (Carter *et al*, 1995; de Koning & Jarvis, 2001) diminazene (de Koning *et al*, 2004) and other diamidines (Lanteri *et al*, 2006; Collar *et al*, 2009; Ward *et al*, 2010). In addition, the much higher rate of uptake through PPT1, compared to HAPT1, clearly aids the study of diamidine transport at the low label concentrations required.

### 3.5.2 Transport of diminazene aceturate in procyclic trypanosomes

While pentamidine is transported efficiently by bloodstream forms in the absence of P2 and the deletion of the P2-encoding gene *TbAT1* alone does not confer more than marginal pentamidine resistance (Matovu *et al*, 2003), other therapeutically important diamidines such as diminazene aceturate (de Koning *et al*, 2004), DB75 (furamidine) (Lanteri *et al*, 2006) and its aza analogues DB820 and CPD0801 (Ward *et al*, 2010) rely overwhelmingly on P2 and display moderately high levels of resistance in *tbat1*<sup>-/-</sup> trypanosomes. Notwithstanding these observations, it is evident that those diamidines are also taken up by a non-P2 mechanism, as *tbat1*<sup>-/-</sup> trypanosomes remain sensitive to approximately 1  $\mu\text{M}$  of these diamidines *in vitro* (Matovu *et al*, 2003; Lanteri *et al*, 2006) and infections with *tbat1*<sup>-/-</sup> *T. b. brucei* can be cured using increased doses of DB75. In order to understand drug uptake and resistance mechanisms for these therapeutically important diamidines it is thus critical to identify and characterise the non-P2-mediated uptake systems.

The absence of a P2 transporter in procyclic cells, and the much higher expression of a high affinity transporter, presumably HAPT1, allowed us to study how the diamidines are accumulated in the absence of P2. Unlike in *tbat1*<sup>-/-</sup> bloodstream trypanosomes (de Koning *et al*, 2004), [<sup>3</sup>H]-diminazene uptake was readily measured in procyclics of the same strain (s427). Uptake was linear over 10 min with a rate of  $0.0075 \pm 0.0006 \text{ pmol}(10^7 \text{ cells})^{-1}\text{s}^{-1}$  and was fully saturated by 1 mM unlabelled diminazene (Figure 3.4, A). This transport was not mediated by either the P1 or P2 adenosine transporters, as neither adenine nor inosine (inhibitors of P2 and P1, respectively (Carter & Fairlamb, 1993; de Koning & Jarvis, 1999; Al Salabi *et al*, 2007)), had any effect on diminazene accumulation (Figure 3.4, B). Likewise, up to 1 mM adenosine had no effect on diminazene uptake (not shown). Transport of [<sup>3</sup>H]-diminazene aceturate displayed simple Michaelis-Menten kinetics consistent with a one-transporter model and a moderate affinity with a  $K_m$  value of  $28 \pm 5 \mu\text{M}$  and a  $V_{\text{max}}$  of  $0.59 \pm 0.11 \text{ pmol}(10^7 \text{ cells})^{-1}\text{s}^{-1}$  ( $n = 4$ ) (Figure 3.4, C). Interestingly, this transport phenomenon was very potently inhibited by pentamidine (Figure 3.4, B), with a  $K_i$  value of  $0.033 \pm 0.004 \mu\text{M}$  ( $n = 3$ ), which led us to hypothesise that at least in procyclic trypanosomes, diminazene aceturate is transported by HAPT1. This

conjecture is strongly supported by the reciprocal inhibition of the two diamidines: the  $K_m$  value for diminazene is similar to the  $K_i$  value of diminazene inhibiting high affinity [ $^3\text{H}$ ]-pentamidine transport, and the pentamidine  $K_m$  for procyclic HAPT1 is identical to the  $K_i$  of pentamidine inhibiting [ $^3\text{H}$ ]-diminazene uptake.

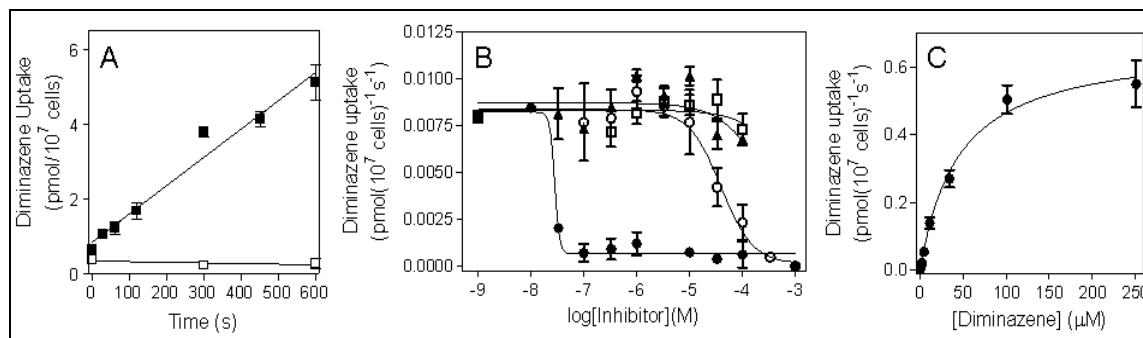


**Figure 3.4. Transport of 1  $\mu\text{M}$  [ $^3\text{H}$ ]-diminazene in procyclic trypanosomes.**

**(A)** Procyclic s427 were incubated for the indicated times with radiolabel in the presence (□) or absence (■) of 1 mM unlabelled diminazene acetate. The correlation coefficient for the 1  $\mu\text{M}$  line was 0.97 and it was highly significantly different from zero ( $P < 0.00001$ ; F-test) whereas the 1 mM line was not significantly different from zero ( $P = 0.50$ ; F-test). **(B)** Inhibition of [ $^3\text{H}$ ]-diminazene transport by various concentrations of pentamidine (●), unlabelled diminazene (○), adenine (▲) and inosine (□). **(C)** Michaelis-Menten saturation curve for [ $^3\text{H}$ ]-diminazene in procyclic cells, representative of four independent experiments. All experiments were performed in triplicate and error bars indicate SEM.

### 3.5.3 Resistance profile of a highly diminazene-resistant cell line, ABR

The hypothesis that non-P2-dependent diminazene is mediated by HAPT1 in procyclics and thus presumably by HAPT1 in bloodstream forms was investigated using a strain adapted from the *tbat1* $^{-/-}$  clonal line by *in vitro* exposure to increasing diminazene concentrations; the identity of the *tbat1* $^{-/-}$  line was confirmed prior to adaptation (Figure 3.5). Adaptation in the presence of incremental diminazene concentrations was performed over 6 months as depicted in (Figure 3.6).

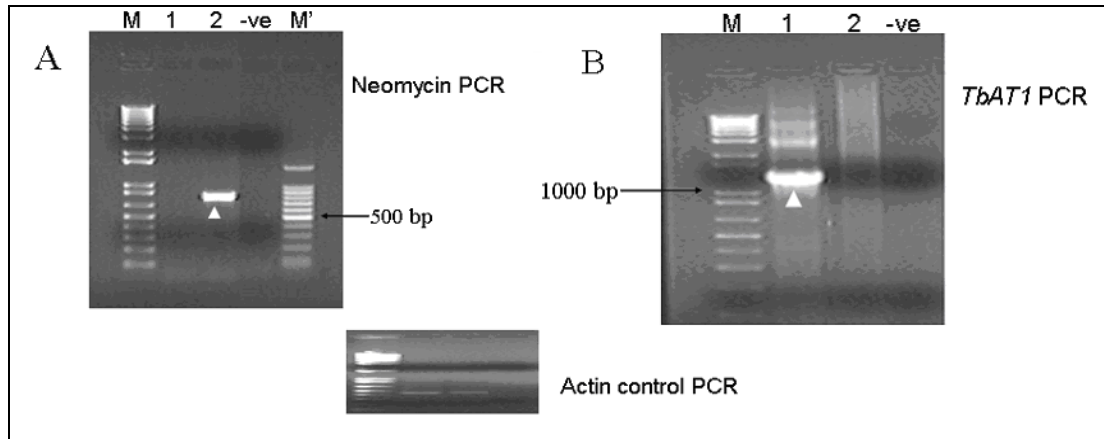


Figure 3.5. PCR amplification results to confirm identity of *T. brucei* *tbat1*<sup>-/-</sup>.

Panel A, neomycin 800 bp PCR product (white arrow head). Panel B, *TbAT1* 1400 bp PCR product (white arrow head). Lane 1, *T. brucei* s427 (wild type with P2 activity). Lane 2, *tbat1*<sup>-/-</sup> (mutant lacking P2 activity). -ve, no template (water) control. M, 1 Kb plus DNA size marker (Invitrogen, Life technologies, USA). M', 100 bp DNA size marker (Promega). Adapted from the study of Anne Kazibwe / previous PhD student (University of Glasgow) with permission.

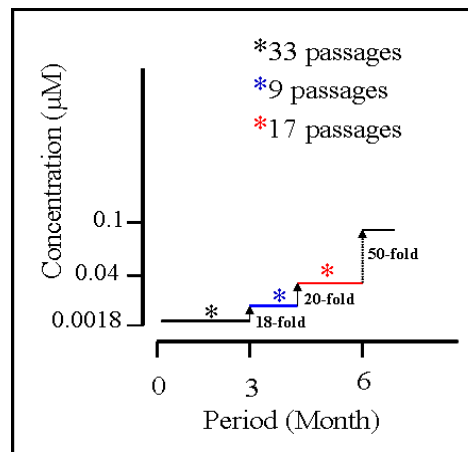


Figure 3.6. Selection for diminazene resistance in the *tbat1*<sup>-/-</sup> cell line cultured under drug pressure.

Observed increments in resistance in the *tbat1*<sup>-/-</sup> cell line in comparison to wild type s427 when cultured in increasing drug concentrations over a 6 month period are indicated. This work was done by Anne Kazibwe / previous PhD student (University of Glasgow)

The *tbat1*<sup>-/-</sup> cell culture selected against high level resistance to diminazene was cloned out by limiting dilution and the resulting clonal line (designated ABR) was tested for its susceptibility to diminazene aceturate using the Alamar Blue assay, after a total of 55-60 passages. At this stage, immediately following the adaptation to diminazene, the ABR line was found to be more resistant compared to wild type strain 427 and the *tbat1*<sup>-/-</sup> parent strain (data not shown) and a full resistance profile was made after a further 27 passages in drug free

medium over a period of three months to ensure stability of the resistance phenotype (Table 3.2).

	s427WT		<i>tbat1</i> <sup>-/-</sup>			B48			ABR		
	EC <sub>50</sub> (nM)	n	EC <sub>50</sub> (nM)	n	RF	EC <sub>50</sub> (nM)	n	RF	EC <sub>50</sub> (nM)	n	RF
Pentamidine	6.8 ± 1.1	12	15 ± 6	11	2.2	570 ± 200	6	83	340 ± 97	5	50
Diminazene	629 ± 132	12	5780 ± 1560	12	9.2	2670 ± 510	4	4.2	14600 ± 3900	5	23
DB75	212 ± 60	12	1670 ± 460	10	7.9	360 ± 110	5	1.7	4560 ± 1560	5	22
Cymelarsan	4.1 ± 0.4	12	13 ± 2	12	3.2	62 ± 15	6	15	27 ± 4	6	6.6
PAO	0.69 ± 0.13	8	0.76 ± 0.09	8	1.1	0.54 ± 0.14	4	0.8	0.82 ± 0.14	4	1.2

**Table 3.2. EC<sub>50</sub> values for the four different trypanosomes strains used in this study.**

RF, resistance factor relative to wild-type (s427WT). n, number of repeats. Statistical significance for the presence of resistance was calculated using a one-way ANOVA test (GraphPad Prism 5.0) in which the strains were grouped (a,b,c) according to significant difference ( $p < 0.05$ ) or not ( $p > 0.05$ ); see Appendix E.

Table 3.2 lists EC<sub>50</sub> values for the diamidines pentamidine, diminazene and DB75, and for the arsenical compounds Cymelarsan and Phenylarsine oxide (PAO). Cymelarsan is a water-soluble member of the melaminophenyl arsenical class of trypanocides, a close homologue of the lipophilic drug melarsoprol, and used against veterinary trypanosomiasis; PAO is included as a known trypanocide that rapidly crosses the plasma membrane by passive diffusion (Carter & Fairlamb, 1993; Bridges *et al*, 2007).

All the drug sensitivity experiments were performed with 4 different cell lines in parallel: wild-type s427, the *tbat1*<sup>-/-</sup> line derived thereof, B48 derived from *tbat1*<sup>-/-</sup> by adaptation to pentamidine in vitro (Bridges *et al*, 2007), and the ABR line derived from *tbat1*<sup>-/-</sup> by adaptation to diminazene. Resistance factors (RF; EC<sub>50</sub> of derived line divided by EC<sub>50</sub> of wild type line) are indicated in Table 3.2. The EC<sub>50</sub> values and resistance levels of the first three lines closely follow previously reported patterns: *tbat1*<sup>-/-</sup> displays a minor loss of sensitivity to pentamidine and melaminophenyl arsenicals and a significant level of resistance to DB75 and diminazene (Matovu *et al*, 2003; Lanteri *et al*, 2006); in B48 resistance to Cymelarsan and pentamidine is greatly increased due to loss of HAPT1 activity (Bridges *et al*, 2007). Of interest is that in many assays we observe a certain reversal of DB75 and diminazene resistance levels in B48, though this did not reach statistical significance. In contrast to B48, the ABR line

did display a significant increase in diminazene and DB75 resistance relative to the parental *tbat1*<sup>-/-</sup> line (P<0.02 and P<0.05, respectively; one-way ANOVA test) and while also displaying increased resistance to pentamidine and cymelarsan, this increase was less pronounced than in B48 (though the different sensitivities in B48 and ABR reached statistical significance only for cymelarsan; P=0.05, one-way ANOVA test). These results indicate that the adaptation to diminazene either uses a different mechanism than adaptation to pentamidine, or that the adaptation to such high levels of resistance is multifactorial. As the adaptation of B48 was attributed to the loss of HAPT1 activity (Bridges *et al*, 2007), it was next investigated whether activity of the pentamidine transporters had changed in the ABR line.

### **3.5.4 Diamidine transport in drug resistant trypanosomes**

Assessment of [<sup>3</sup>H]-pentamidine transport activity in the ABR line found no evidence of high affinity uptake (assessed at 30 nM radiolabel): whereas transport was readily inhibited by submicromolar pentamidine concentrations in wild-type cells (Figure 3.7, A), in ABR cells this flux was of a much lower level and sensitive only to concentrations higher than 10 μM pentamidine (Figure 3.7, B). Likewise, the high affinity component in wild-type cells was sensitive to propamidine as described for HAPT1 (de Koning, 2001), which had no effect on uptake in ABR cells (Figure 3.7, B).

The most straightforward interpretation of the data is a complete absence of HAPT1 activity in ABR cells, with the 30 nM [<sup>3</sup>H]-pentamidine taken up by the one remaining pentamidine transporter, LAPT1. Assessment of LAPT1 function at 1 μM [<sup>3</sup>H]-pentamidine did reveal a wild-type pattern of low-affinity uptake that was insensitive to propamidine in ABR cells (Figure 3.7, D).

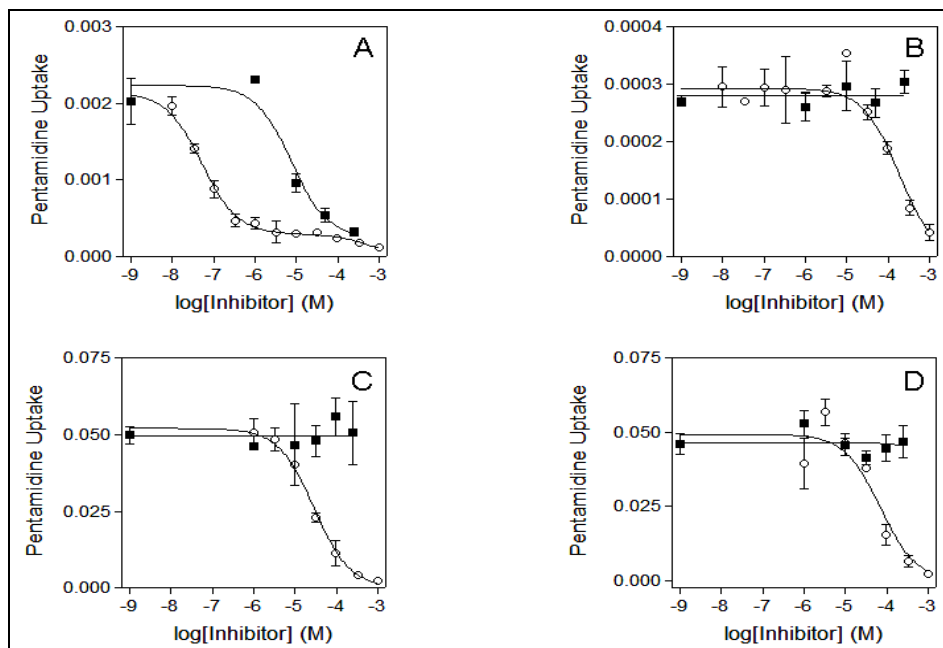


**Figure 3.7. Transport of [<sup>3</sup>H]-pentamidine in wild-type and ABR cell lines.**

Transport of 30 nM (panels A and B) or 1 μM [<sup>3</sup>H]-pentamidine (panels C and D) was assessed in bloodstream forms of the s427WT (panels A, C) and ABR (panels B, D) cell lines over 60 seconds in the presence or absence of various concentrations of propamidine (■) or unlabelled pentamidine (○). The experiments were performed in triplicate; error bars represent SE of internal replicates. Data shown are representative of at least three identical and independent experiments.

The K<sub>m</sub> value for [<sup>3</sup>H]-pentamidine uptake in the ABR strain was  $59 \pm 11 \mu\text{M}$  (n=3), identical to the published value for LAPT1 of  $56 \pm 8 \mu\text{M}$ ; the V<sub>max</sub> value of  $1.2 \pm 0.4 \text{ pmol}/(10^7 \text{ cells})^{-1}\text{s}^{-1}$  (n=3) was also highly similar to the published value of  $0.85 \pm 0.15 \text{ pmol}/(10^7 \text{ cells})^{-1}\text{s}^{-1}$  for LAPT1 (De Koning, 2001). The above results strongly suggest that the pentamidine cross-resistance in ABR strain adapted to high diminazene concentration was due to loss of HAPT1 transport. Yet, the differences in resistance pattern between the pentamidine-adapted B48 and diminazene-adapted ABR lines suggest that additional adaptations may be responsible for the further increase in diminazene resistance in the latter cells. Using 1 μM [<sup>3</sup>H]-diminazene we investigated whether this is attributable to differences in diminazene uptake rates. As the uptake rates in the resistant lines were very low we used timecourses with 7 points over 10 minutes in an effort to measure transport as accurately as possible (see Figure 3.8) and in this way measured the rate in each cell line 3-4 times. Identical experiments were then performed with 1 μM [<sup>3</sup>H]-pentamidine for comparison. The results are summarised in (Figure 3.9).

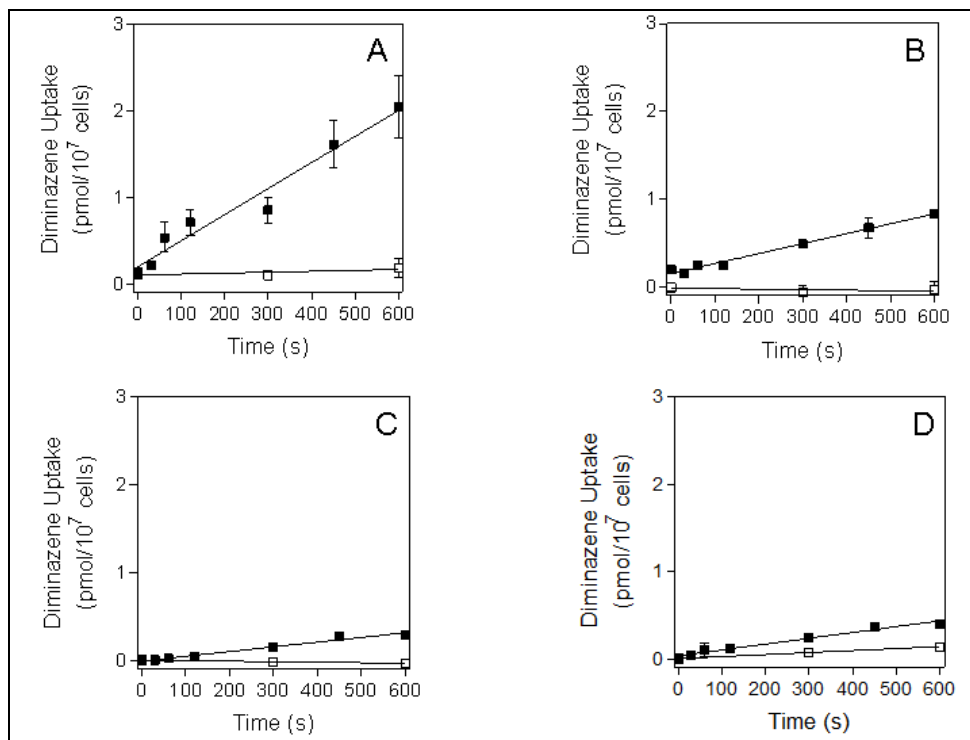


Figure 3.8. Transport of 1 μM [<sup>3</sup>H]-diminazene in the s427WT (A), *tbat1*<sup>-/-</sup> (B), B48 (C) and ABR (D) cell lines.

Representative experiments in triplicate are shown (average ± SE). Transport rates were calculated by linear regression. Y-axis scales were kept the same for all panels to highlight differences between the cell lines. ■, 1 μM [<sup>3</sup>H]-diminazene; □, with the addition of 1 mM unlabelled diminazene

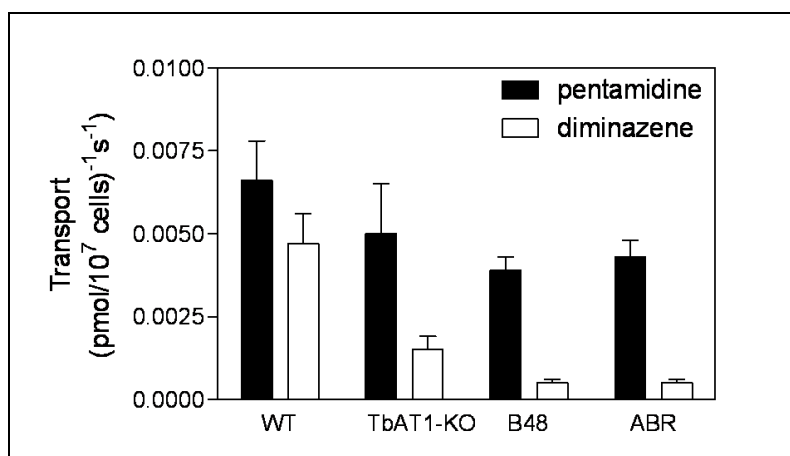


Figure 3.9. Transport of 1 μM [<sup>3</sup>H]-pentamidine (filled bars) or 1 μM [<sup>3</sup>H]-diminazene (open bars) in four different cell lines.

Transport rates were derived by linear regression from timecourses with points (in triplicate) at 0, 30, 60, 120, 300, 450 and 600 s. Zero uptake levels and saturability were verified in the presence of 1 mM unlabelled permeant. Bars show the average transport of 3 – 4 experiments and SE. Representative experiments are shown in Figure 3.8.

As expected from previous work (De Koning *et al*, 2004) transport of 1 μM [<sup>3</sup>H]-diminazene was significantly reduced in the *tbat1*<sup>-/-</sup> line compared to s427WT (P<0.05). The rate of [<sup>3</sup>H]-diminazene transport was further reduced in the B48

line ( $P < 0.05$ ), which additionally lacks HAPT1 (Bridges *et al.*, 2007), and similarly in the ABR ( $P < 0.05$ ) which also lacks HAPT1 activity (this paper). In contrast, reductions in  $1 \mu\text{M}$  [ $^3\text{H}$ ]-pentamidine transport rates were much less dramatic in the resistant lines (Figure 3.9), as, at this relatively high concentration of pentamidine, much of the flux is through LAPT1, with HAPT1 and P2 saturating at a lower concentration (Bray *et al.*, 2003). Transport of  $1 \mu\text{M}$  [ $^3\text{H}$ ]-diminazene, measured over 5 minutes in *tbat1*<sup>-/-</sup> cells, was still saturable and displayed an average  $K_m$  value of  $67 \pm 13 \mu\text{M}$  ( $n=3$ ) (Figure 3.10), fully consistent with uptake through HAPT1 (diminazene  $K_i$  for [ $^3\text{H}$ ]-pentamidine through HAPT1 is  $63 \pm 3 \mu\text{M}$  (Table 3.1)). These results are consistent with the presence of LAPT1 in all four cell lines and show a very minor role for LAPT1 in diminazene uptake.

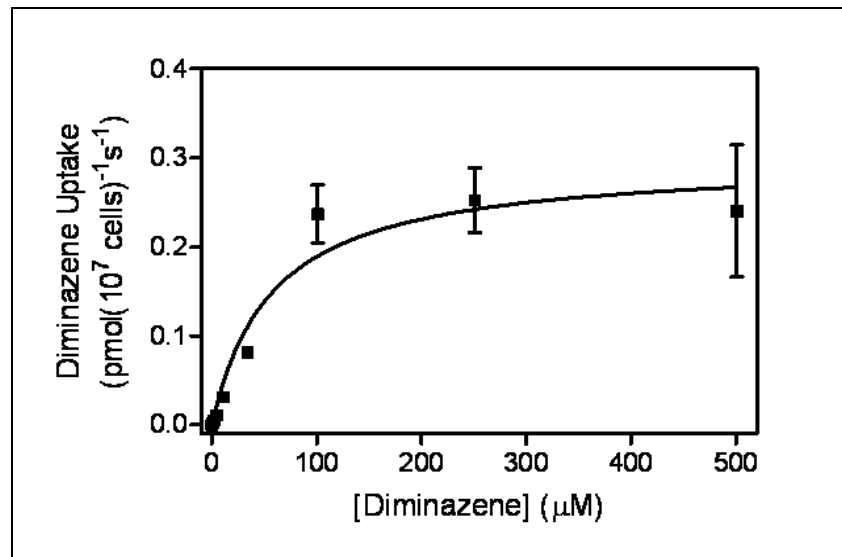


Figure 3.10. Saturation plot of [ $^3\text{H}$ ]-diminazene transport in bloodstream forms of the *tbat1*<sup>-/-</sup> cell line.

Transport of  $1 \mu\text{M}$  label was determined in triplicate at 5 minutes of incubation; error bars represent SE. The experiment shown is representative of three identical experiments

### 3.6 Conclusion

Development of trypanocidal resistance in *T. brucei* and loss of drug uptake is strongly linked to the loss of membrane transporters (Mäser *et al*, 2003). A cell line lacking the function of the P2 transporter was created by deletion of the encoding gene, *TbAT1*, and led to 2-3 fold resistance to melarsoprol and pentamidine but a significantly higher level of resistance to diminazene (18-fold) (Matovu *et al*, 2003) and DB75 (11-fold) compare to the parental cell line 427-WT (Lanteri *et al*, 2006). However, deletion of *TbAT1* left the cells with a level of sensitivity at sub-micromolar concentrations to diminazene and DB75, suggesting that the drugs get into the trypanosomes through other routes, possibly including endocytosis. HAPT1 and LAPT1 have been confirmed to be additional routes for the uptake of pentamidine and possibly other diamidines (de Koning, 2001d; de Koning & Jarvis, 2001). Procyclic trypanosomes do not express *TbAT1*/P2 aminopurine transporter (De Koning *et al.*, 1998), but they do express HAPT1 and LAPT1 (this study). Therefore, the procyclic forms make a convenient model to study diamidine transport. This study aimed to identify the transporter for diminazene aceturate in procyclics and verify the finding in bloodstream forms.

The kinetics of uptake of [<sup>3</sup>H]-diminazene in procyclic trypanosomes was entirely consistent with transport by HAPT1. In particular, the inhibition of diminazene transport by propamidine with a  $K_i$  value identical to HAPT1, and the reciprocal inhibition of diminazene and pentamidine provide compelling pharmacological evidence that HAPT1 is the main transporter of diminazene in procyclics.

The transport data in bloodstream forms appears to confirm the prediction of the procyclic model. Loss of HAPT1 activity appears generally to correlate with high levels of diamidine resistance: B48 and ABR both appear to have lost HAPT1 activity and have similarly-reduced diminazene transport rates. Moreover, the  $K_m$  value for [<sup>3</sup>H]-diminazene in *tbat1*<sup>-/-</sup> bloodstream forms was identical to the  $K_i$  value of diminazene on HAPT1-mediated [<sup>3</sup>H]-pentamidine transport. We conclude that adaptation of trypanosomes without a functional P2/*TbAT1* transporter may result in the loss the HAPT1 transporter under drug pressure with, pentamidine (B48), cymelarsan (Bridges *et al.*, 2007) or diminazene (ABR, this study) and become cross-resistant to new classes of drugs such as the

furamidines (ABR/DB75). Nevertheless it is equally clear that high-level drug resistance as achieved by prolonged drug exposure in a laboratory is indeed multifactorial. The sequential loss of the P2 and HAPT1 transporters still does not fully explain the observed resistance patterns: B48 and ABR display identical rates of diminazene transport (Figure 3.9) and LAPT1-mediated pentamidine transport but they differ in their level of diminazene resistance. Several possibilities for this paradox come to mind but if the initial rates of drug transport are identical in both strains, as we established, differential drug sensitivity can be explained by (1) introduction of an efflux pump in one strain or (2) additional non-transport-related adaptations that alter drug sensitivity of the parasite. This is the subject of ongoing investigations in our laboratories.

**4 Structure / Activity relationships of the *T. b. brucei* High Affinity Pentamidine transporter**

## 4.1 Introduction

Pentamidine belongs to the diamidine group of drugs, and it has a long and successful history in Human African Trypanosomosis chemotherapy. Diamidine compounds are highly charged at physiological pH and they require specific carriers for translocation across the plasma membrane of the cell. To ensure successful treatment these transporters should only be present in the pathogenic cell and not in the host cells (Delespaux & de Koning, 2007). The loss of these carriers enables the development of drug resistance due to the specificity of the compounds. The understanding of the nature of these transporters means that future drugs can potentially be designed to target only trypanosome and not human cells by modifying compounds for uptake by trypanosome transporters only.

In *Trypanosoma brucei*, pentamidine and other vital diamidines used against human sleeping sickness and the veterinary equivalent of the disease have been shown to be transported by the TbAT1/P2 transporter which has affinity only for aminopurines but not oxopurines (Barrett *et al*, 1995; de Koning & Jarvis, 1999; de Koning, 2001; de Koning *et al*, 2005). Moreover, this nucleoside transporter has been shown to facilitate transportation of other compounds that share the P2 recognition motif with adenosine such as arsenical compounds (e.g. melarsoprol) and diamidine compounds, for example pentamidine (Figure 4.1). In addition to TbAT1/P2 transporter, pentamidine is concentrated in *T. b. brucei* by at least other two transporters, the high affinity pentamidine transporter (HAPT1) which has been shown to mediate about 50% of pentamidine uptake together with the Low Affinity Pentamidine Transporter (LAPT1) (Carter & Fairlamb, 1993; de Koning & Jarvis, 1999; de Koning, 2001; Matovu *et al*, 2003; Bray *et al*, 2003; Collar *et al*, 2009). These classes of antiprotozoal compounds are only recognised as a substrate by the parasite transporters and not by human nucleoside transporters, ensuring the specificity of these classes of drugs (Luscher *et al*, 2007).

Protozoan purine and pyrimidine transporters have been well studied (de Koning *et al*, 2005; Al Salabi & de Koning, 2005; Papageorgiou *et al*, 2005) using several approaches to study membrane transporters including homology threading models for their structure (Papageorgiou *et al* 2005) as well as determining the

recognition motif of the transporter using structure activity relationship studies. The later approach is based on manipulation of chemical structure of some compounds and how small structural differences could affect the affinity of the potential substrate to the transporter.

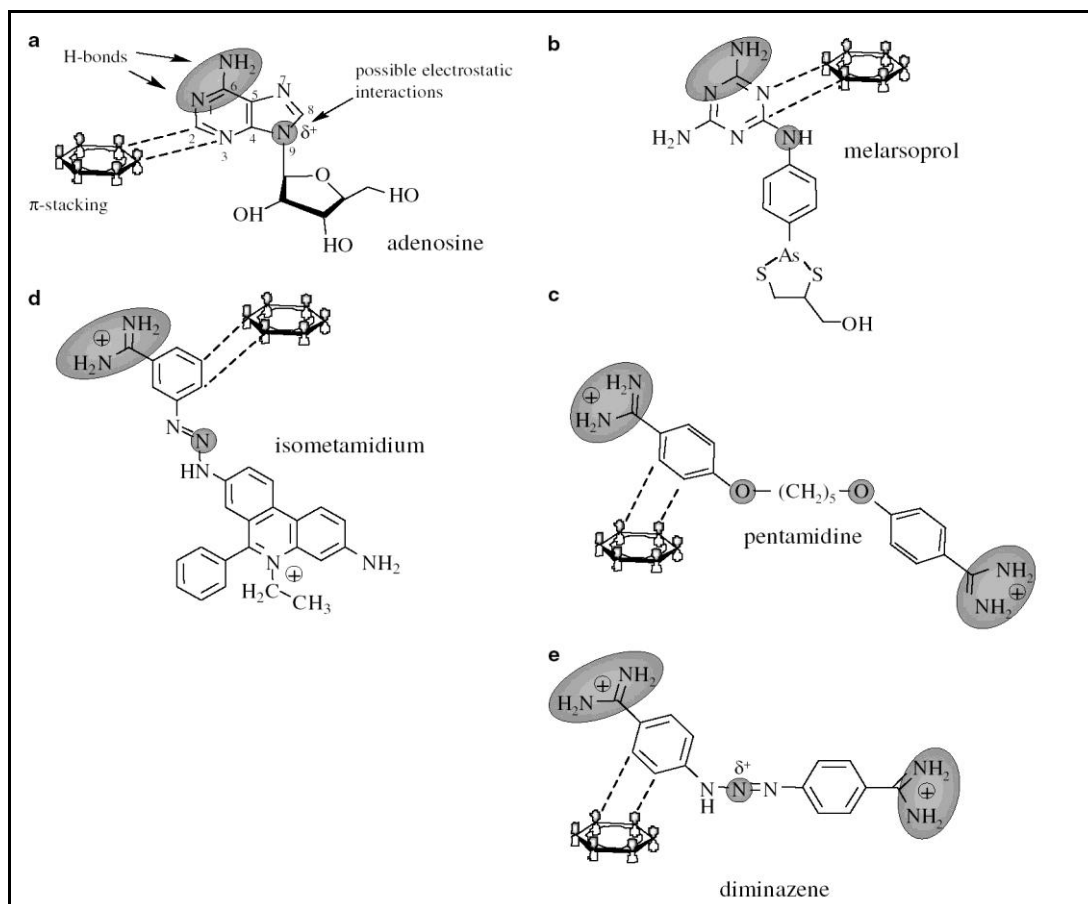


**Figure 4.1. The natural substrate for P2 transporter and some trypanocides.**

The natural substrate (adenosine) for P2 transporter and some trypanocides that share the recognition motif of the transporter. Shaded areas are the functional groups that interact with transporter binding pocket (Reproduced from De Koning et al., 2005).

The recognition motif of the TbAT1/P2 transporter (Figure 4.1) has been well characterized previously by structure activity relationship studies thus explaining its high affinity for adenosine. The mode of action is that the TbAT1/P2 transporter moves adenosine through hydrogen bond interactions, between the 6-amino group and the Nitrogen at position 1 of the purine ring (de Koning & Jarvis, 1999). However, the recognition motifs for HAPT1 and LAPT1 are still under investigation. Despite the fact that recognition of the substrate by the transporter is the key role for the uptake, any potential compound including drugs must share essential structural elements that will allow it to bind and enter through the transporter. Pentamidine is transported by the three

transporters and for that reason it should be possible to design molecules that meet the recognition requirements and possibly identify a unified motif for the three transporters. This of course would assist new drug design using these transporters as a target to deliver drugs into the trypanosome.

## 4.2 Characterisation of HAPT1 recognition motif

The study of the HAPT1 recognition motif project has been ongoing for several years and during this period several compounds have been tested in our laboratory, and their HAPT inhibition constants ( $K_i$  values,  $\mu\text{M}$ ) determined. These studies have shown that the minimal distance between the amidine groups in diamidine molecules, the *para*-position of the amidine groups and finally the benzamidine parts of the molecule are important for binding to HAPT1. We now have made substantial progress by studying numerous pentamidine analogues, including bis-benzo furanamidines and bis-benzamidines, as competitive inhibitors of pentamidine uptake in *T. b. brucei* bloodstream forms and in determining the  $K_i$  value of each compound. Using molecular modelling and structure-activity relationship analysis we tried to determine the common properties and the motif needed for high-affinity binding of HAPT1. We found that small changes of the main chemical structure of the ligand by the addition of minor substitutions such as Cl or OH to the benzamidine moiety causes major loss of affinity for HAPT1. Other findings include the importance of the oxygen atom in the pentamidine linkage chain and of the flexibility of this chain - with rigid linkers less likely to bind strongly to HAPT1.

## 4.3 Results

### 4.3.1 Drug Sensitivity Assays

This work was carried out by myself and an MSc student (Claire Anderson) under my supervision; we tested a set of RT compounds (see chapter 2) that belong to the bis-benzo furanamidine and bis-benzamidine classes of compounds. Alamar blue assays (method described in chapter 2) were applied to determine the  $\text{EC}_{50}$  of each compound against *T. b. brucei* wild type-427, *tbat1*<sup>-/-</sup>, TbAT1-B48 and P1000 to study cross-resistance patterns. This may highlight which compounds are likely to be transported by which of the known diamidine transporters, if

any, based on our knowledge of pentamidine transport in each of these cell lines. The RT -compounds were obtained from the laboratory of Professor Richard Tidwell.

	Drugs	AVG ( $\mu\text{M}$ )	SE	n	RF	P>
WT-427	pentamidine	0.004	0.001	3		
	RT01	0.377	0.206	3		
	RT05	0.015	0.008	3		
	RT18	0.063	0.017	3		
<i>TbAT1</i> -KO	pentamidine	0.010	0.001	3	2.38	>0.05
	RT01	0.487	0.143	3	1.29	>0.05
	RT05	0.026	0.005	3	1.76	>0.05
	RT18	0.117	0.033	3	1.84	>0.05
<i>TbAT1</i> -B48	pentamidine	0.310	0.02	3	176.19	<0.01
	RT01	0.240	0.046	3	0.64	>0.05
	RT05	0.173	0.012	3	11.56	<0.001
	RT18	0.210	0.042	3	3.32	>0.05
P1000	pentamidine	0.599	0.05	3	371.43	<0.01
	RT01	0.447	0.127	3	1.18	>0.05
	RT05	0.277	0.055	3	18.44	>0.05
	RT18	0.527	0.093	3	8.32	>0.05

Table 4.1. Represents  $\text{EC}_{50}$  values and resistance factors for selected RT compounds (RT01, RT05 and RT18) in WT-427 and *TbAT1*-KO, *TbAT1*-B48 and P1000.

The averages are of 3 independent experiments repeats. Statistical significance for the presence of resistance was calculated using the two-tailed, paired Student's T-test relative to  $\text{EC}_{50}$  of WT-427. The structure of the RT01, RT05 and RT08 are presented in Table 4.3.

The dose response curves were compared for 25 of the RT compounds and pentamidine was included in every experiment as an internal control to allow easy comparisons to the general activity of the drug. The results highlighted three of the compounds (RT01, RT05 and RT18) as being of particular interest. Table 4.1 shows the  $\text{EC}_{50}$  values and resistance factors of these compounds.

In the wild type cell line RT05 compound is seen to follow an identical pattern of action to that of pentamidine and the loss of *TbAT1*/P2 transporter resulted in 2.4-fold resistance showing that it is at least partly dependent on the P2 transporter for uptake by the trypanosome. In strain *TbAT1*-B48 where the P2 and HAPT1 transporters are both absent there is a further increase in RT05 resistance, with an  $\text{EC}_{50}$  of  $173 \pm 0.012$  nM. In P1000 cell line displays 18.44 folds resistance compared to WT-427 showing that it is a HAPT1 dependent compound.

RT18 follows a similar resistance pattern to pentamidine and RT05, with an increase in resistance in *TbAT1*-B48 compare to Wild Type 427 (Figure 4.2).

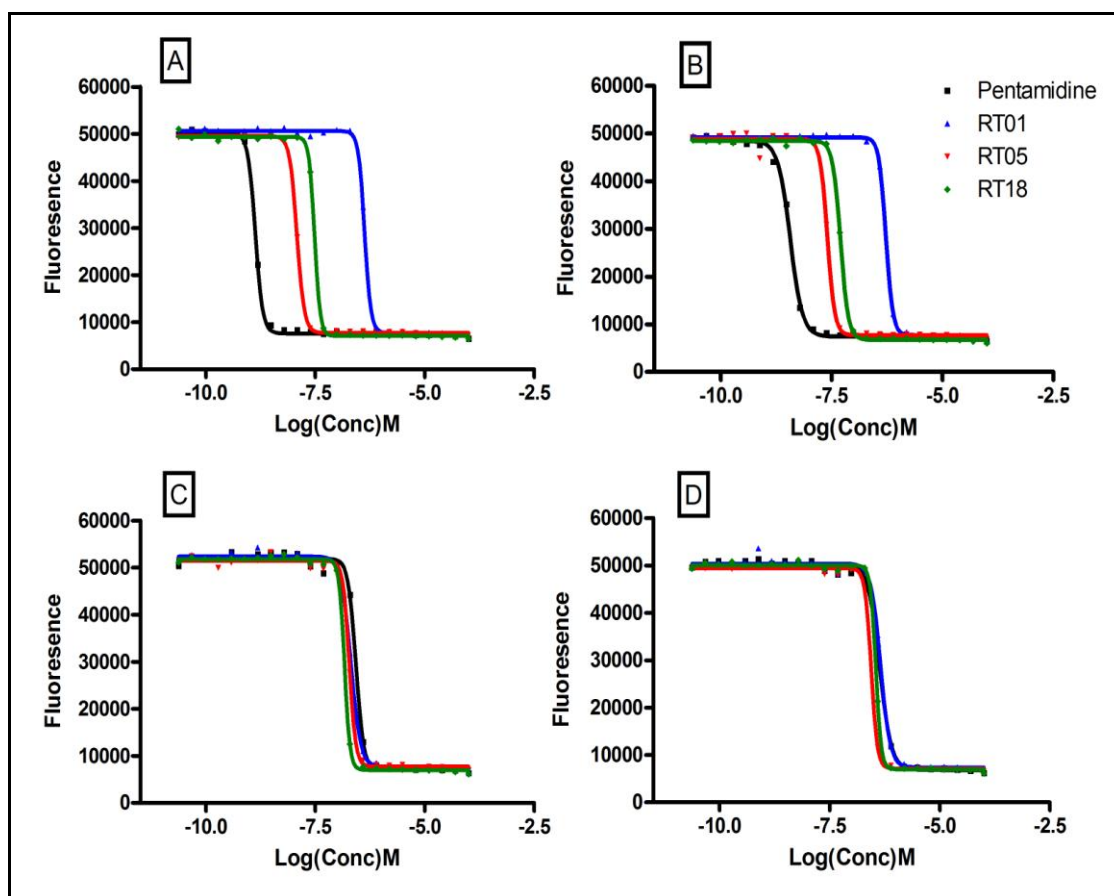


Figure 4.2.  $EC_{50}$  values of pentamidine and some RT compounds.

Diagrammatic representation of the differences in  $EC_{50}$  values between pentamidine, RT01 and RT05 in WT-427 (A), *TbAT1*-KO (B), *TbAT1*-B48 (C) and P1000 (D). Results are plotted as dose response curves, with concentration against fluorescence. A single experiment, representative of at least 3 independent experiments, is shown.

RT01 however does not show this pattern, and so its actions are not dependant on the P2 or HAPT transporters. It has a mechanism that sufficiently kills trypanosomes even when these transporters are absent. This drug is the only compound tested with the amidine groups in the *meta* position relative to the linker chain (Table 4.2), and is also the only one to clearly show no change in resistance with the loss of the transporters. One possibility therefore is that the drug is a very good substrate for the Low Affinity Pentamidine Transporter.

### 4.3.2 Drug Uptake Assays

Drug uptake assays were performed to determine the effects of changes in chemical structure on drug uptake. Drugs that displayed high affinity were

selected, as well as those with low affinity, so that comparisons in the structure and relative activity of the drugs could be easily distinguished. Uptake of [<sup>3</sup>H]-pentamidine at a concentration of 0.3 μM were carried out using a rapid-stop/oil-spin protocol in the presence of 1 mM adenosine, which competitively inhibits the *TbAT1/P2* transporter. The  $K_i$  values for the different analogues were determined from dose-response curves subject to the assumptions outlined in Chapter 2. A variety of compounds synthesised by a number of different collaborators has been used in this analysis.

The DB- compounds were received from Prof. David W. Boykin, Georgia State University / Chemistry Department, Atlanta, USA and other diamidine compounds (CHI-compounds) were obtained from Dr Paul O'Neil, University of Liverpool, UK. Some of the latter two groups of compounds have been tested earlier by previous students in our laboratory and the data and structure together with the compounds that we tested will be included in this chapter so that the affinity of those in question can be easily compared.

### **4.3.3 Structure-activity relationships**

Since pentamidine is the only confirmed permeant for HAPT1, a variety of pentamidine analogues and other related compounds were assayed for their ability to inhibit HAPT1 pentamidine transport activity in the *T. b. brucei* 427. The aim of this study was to correlate activity and structure to identify functional groups and other features of the test compounds that enhance or diminish trypanocidal activity and thus identify any structural motifs responsible for high-affinity binding on HAPT1 transporters. The  $K_i$  values were determined from dose-response curves subject to the assumptions outlined in Chapter 2. The  $K_i$  values then were used to calculate Gibbs free energy ( $\Delta G^\circ$ ), involved in the interaction between the transporter and the different molecules using the following equation:

$$\Delta G^\circ = -RT \ln(K_i)$$

Where R is the gas constant and T is the absolute temperature. The  $\Delta G^\circ$  value gives a measure of the binding energies existing between the transporter and its

substrate. The  $K_i$  and the  $\Delta G^\circ$  values for the different analogues are listed in (Table 4.2 - Table 4.7 ).

#### **4.3.4 HAPT1 recognition motif**

Most of the compounds used to characterise recognition of permeants by the HAPT1 transporter were selected to test the effects of various modifications on the skeleton of pentamidine. The uptake experiments involved testing these compounds in order to determine their ability to compete with  $^3\text{H}$  pentamidine uptake, and hence their affinity for the HAPT1 transporter. The  $K_i$  for each tested compound was obtained from three independent experiments and unlabelled pentamidine was included as a control in each experiment. To facilitate a clear understanding I will divide the observations based on the chemical features of the analogues relative to the pentamidine structure: (i) the importance of the two terminal amidine groups (ii) the position of the amidine groups on the benzene and benzofuran rings (relative to the linker), (iii) the roles of the two benzene rings (iv) the length of the linker and flexibility of the compound (v) the importance of the oxygen atom in the pentamidine linkage chain.

##### **4.3.4.1 The affect of the two amidine groups on binding**

The most relevant features of the amidine group are its H-bond donating ability and being positively charged at physiological pH (Wilson *et al*, 2008). At this stage we have investigated the role of the two terminal amidine groups in binding to the HAPT1 transporter. The replacement of the second amidine group with methyl group in CHI/72/1 reduced affinity to HAPT1 with  $K_i$  of  $2.6 \pm 0.7 \mu\text{M}$  (compare 35 nM for pentamidine), and the removal of one amidine group in CHI/1/69/1 similarly reduced affinity to HAPT1 with  $K_i$  of  $2.3 \pm 0.5 \mu\text{M}$ . Both RT32 and RT36 where the second amidine group was replaced with an imidazoline ring or amine group have resulted in relatively poor inhibition of pentamidine uptake with identical  $K_i$  for both compounds and identical  $\Delta G^\circ$  ( $\text{kJ mol}^{-1}$ ) of -36.52 and -36.36 respectively. Interestingly, the simple benzamidine compound 4-hydroxybenzamidine has virtually no affinity for HAPT1  $K_i = 2.8 \pm 1 \text{ mM}$  compared with  $35 \pm 5 \text{ nM}$  for pentamidine. This confirms that both terminal

benzamidinium parts of pentamidine (two terminal amidine groups) contribute strongly to binding with HAPT1 transporter (Table 4.2).

Chemical structure	Compound	$K_i$ ( $\mu\text{M}$ )	$\Delta G^\circ$ ( $\text{kJ mol}^{-1}$ )
	Pentamidine (PMD)	0.035 $\pm$ 0.005	-42.6
	CHI/72/1	2.62 $\pm$ 0.68	-31.9
	CHI/1/69/1	2.3 $\pm$ 0.5	-32.2
	RT32	0.40 $\pm$ 0.08	-36.52
	RT36	0.43 $\pm$ 0.07	-36.36
	** 4-hydroxy- benzamidinium	2888 $\pm$ 1048	-14.49

**Table 4.2.** The effect of the symmetrical amidine groups on affinity to HAPT1 transporter.

$K_i$  values are shown  $\pm$  standard error.  $\Delta G^\circ$  is the required energy for interaction. All  $K_i$  values are the average of at least three independent experiments. \*\*, data obtained from previous studies (Dr. Harry De Koning, University of Glasgow, with permission).

#### 4.3.4.2 The affect of the position of amidine groups on binding

This section demonstrates how the specific orientation of the amidine groups could affect affinity to HAPT1 transporter. For understandable argument; carbon atoms were initially numbered relative to the linker in benzene ring and to the oxygen atom in benzofuran ring. The reposition of amidine group to carbon 3 and 3' (*meta*-position) in *Meta*-pentamidine reduced affinity to HAPT1 with  $K_i$  of  $64.3 \pm 17.9 \mu\text{M}$ , the only difference with pentamidine being that its amidine groups

are located at carbon 4 and 4' (*para*-position). RT01 have shown to follow a similar pattern with a similar  $\Delta G^\circ$  of -23.93 kJ/mol and -24.48 kJ/mol respectively. The disagreement of both  $K_i$  values could be due to the short linker between the two benzofuranamidinium groups (Table 4.6).

Compounds RT05 and RT08 were tested as the only structural difference between the two drugs are the positioning of the amidine groups on the benzofuran rings. The RT05 compound has amidine groups at carbon 5 and 5' (*para*-position) similar to pentamidine and displayed a submicromolar  $K_i$  of  $0.57 \pm 18 \mu\text{M}$ . However the RT08 preference for interaction with the HAPT1 was greatly reduced following the relocation of the amidine groups to carbon 6 and 6' (*meta*-position). As can be seen in Figure 4.3, the position conferred by RT05 provides a significantly higher affinity than that of RT08. This confirms that position of amidine group relative to the linker is important and should be in *para*-position (Table 4.3).

Chemical structure	Compound	$K_i$ ( $\mu\text{M}$ )	$\Delta G^\circ$ ( $\text{kJ mol}^{-1}$ )
	** Meta-pentamidine	64.26 $\pm$ 17.86	-23.93
	RT01	49.39 $\pm$ 10.95	-24.58
	RT05	0.57 $\pm$ 0.18	-35.64
	RT08	75.24 $\pm$ 14.34	-23.54

**Table 4.3.** The importance of amidine group position in interaction with HAPT1 transporter.  $K_i$  values are shown  $\pm$  standard error.  $\Delta G^\circ$  is the Gibbs free energy of interaction. All  $K_i$  values are the average of at least three independent experiments. \*\*, data obtained from previous studies (Dr.Harry De Koning, University of Glasgow, with permission).

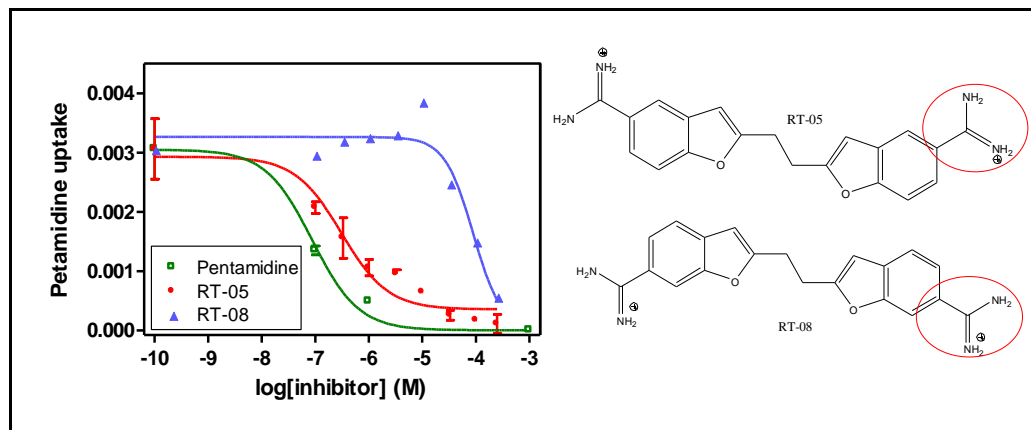


Figure 4.3. High Affinity Pentamidine Transporter-mediated uptake of  $^3\text{H}$ -pentamidine (RT05/RT08).

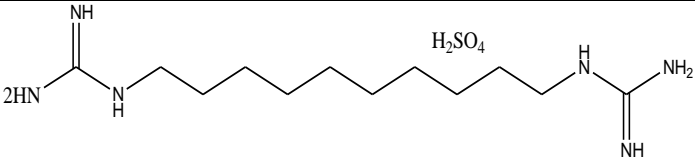
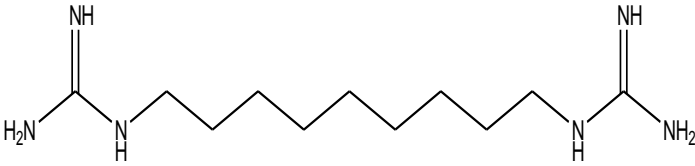
Results plotted as sigmoid inhibition plots, with concentration of drug against [ $^3\text{H}$ ]-Pentamidine uptake.

#### 4.3.4.3 The effect of the benzene rings on binding

As explained in section 4.3.4.1, the simple benzamidine compound (4-hydroxybenzamidine) has almost no affinity for HAPT1 with a  $K_i$  value of  $2.9 \pm 1$  mM, confirming that both benzamidine parts of pentamidine take part in binding. This was followed by demonstrating that a specific position of the amidine group and the orientation of both benzamidine or benzofuranamidinium groups, are required for optimal interaction with HAPT1.

The roles of the two benzene rings in binding to HAPT1 have been previously studied in our group using compounds that share similar terminal groups of those present in the diamidines but missing the benzene ring. Table 4.4 shows that replacement of the benzamidine groups with guanidine groups in the Synthalin Sulphate (Tocris Bioscience), with 10 carbons long linker; dramatically reduces affinity by >7700-fold compared to pentamidine. Similarly, the absence of the benzene rings in compound CD3 (supplied by Dr Christophe Dardonville / Instituto de Química Médica, Madrid, Spain), with 9 carbons long linker reduced affinity by almost 1300-fold. The loss of Gibbs free energy for synthalin and CD3, which have a similar total distance between the end groups as in pentamidine, is 22 and 18 kJ/mol, respectively, consistent with the loss of two strong bonds relative to pentamidine. While this is by no means an ideal comparison, it is certainly suggestive of involvement of the aromatic rings in binding to the HAPT active site, presumably through  $\pi$ - $\pi$  stacking. However, guanidines are less

charged than amidines and this makes a true comparison based on the available compounds difficult.

Chemical structure	Compound	$K_i$ ( $\mu\text{M}$ )	$\Delta G^\circ$ ( $\text{kJ mol}^{-1}$ )
	** Synthalin sulphate	270 $\pm$ 62	-20.37
	** CD3	45.2 $\pm$ 7.6	-24.80

**Table 4.4.** The roles of the two benzene rings in binding to HAPT1 transporter.

$K_i$  values are shown  $\pm$  standard error.  $\Delta G^\circ$  is the Gibbs free energy of interaction. All  $K_i$  values are the average of at least three independent experiments. \*\*, data obtained from previous studies (Dr. Harry De Koning, University of Glasgow, with permission).

#### 4.3.4.4 The effect of linker on binding

##### 4.3.4.4.1 Flexibility of the compound

The linker plays an important role in flexibility of the substrate which is required for optimal interaction with HAPT1. The replacement of the carbon chain between both benzene rings in pentamidine by a azide group in diminazene and a furan ring in DB-75 led to a significant decrease of affinity for HAPT1 with  $K_i$  values of  $62.5 \pm 3.2 \mu\text{M}$  and  $38.2 \pm 10.2 \mu\text{M}$  respectively. These replacements may have affected binding in two ways: (i) by decreasing the distance between the amidine groups and (ii) by reducing the flexibility of the molecule.

Three-dimensional analysis and basic energy minimisation were performed for the tested compounds stated in (Table 4.5) in parallel with pentamidine using the CS Chemdraw/ Chem3D Ultra software version 10 computer package (CambridgeSoft). For each molecule several minimisations were done with manual conformation changes between each minimisation in order to obtain the lowest energy conformation.

Chemical structure	Compound	$K_i$ ( $\mu\text{M}$ )	$\Delta G^\circ$ ( $\text{kJ mol}^{-1}$ )
	** Diminazene	62.48 $\pm$ 3.27	-24.00
	** DB75	38.2 $\pm$ 10.25	-25.21
	RT43	0.51 $\pm$ 0.15	-35.92
	RT46	NE	
	RT47	0.58 $\pm$ 0.04	-35.58

**Table 4.5.** The effect of rigid structure and flexibility of the molecule on affinity to HAPT1 transporter.

$K_i$  values are shown  $\pm$  standard error.  $\Delta G^\circ$  is the Gibbs free energy of interaction. All  $K_i$  values are the average of at least three independent experiments. NE, no inhibitory effect on [ $^3\text{H}$ ]-pentamidine uptake with  $K_i > 100$ . \*\*, data obtained from previous studies (Dr. Harry De Koning, University of Glasgow, with permission).

According to the 3-D models presented in Figure 4.4, pentamidine displays a significant level of flexibility (panel A) and must owe its high affinity ( $K_m = 0.035 \pm 0.005 \mu\text{M}$ ) for HAPT1 to its ability to engage in multiple hydrogen-bond and/or  $\pi$ -stacking interactions with the transporter. In contrast, the rigid (but otherwise very similar) structures of diminazene ( $K_m = 62 \pm 3 \mu\text{M}$ ) and DB75 ( $K_m = 38 \pm 10 \mu\text{M}$ ) allow the formation of fewer bonds (panel C and D), reflected in the much lower binding energy (Table 4.5).

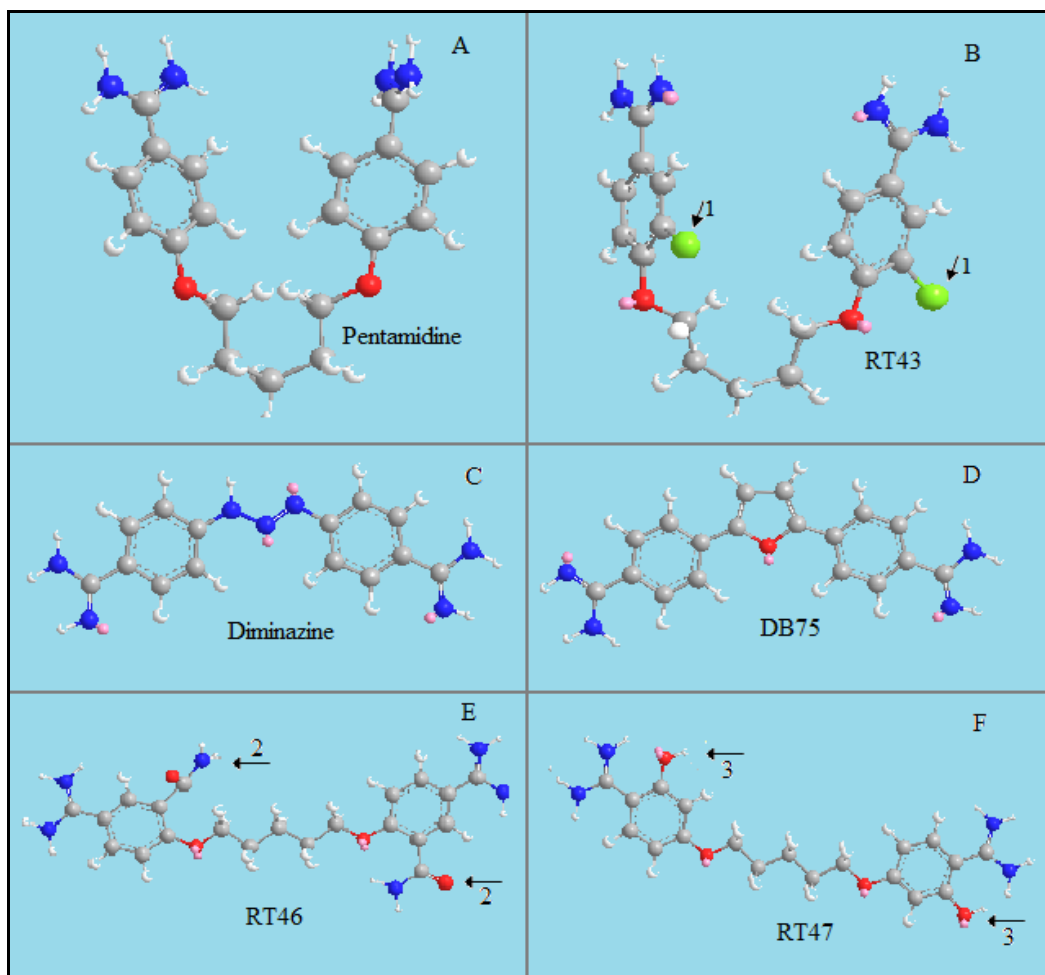


Figure 4.4. Images produced with Chem3D Ultra software version 10 (CambridgeSoft) after minimization of energy.

Rigid structures of diminazine (panel C) and DB75 (panel D) and flexible structure of pentamidine (panel A). Addition of the chloride on the benzene moiety in RT43 did not affect flexibility but reduced affinity (panel B, arrow 1). RT46 has a modified charge distribution and shape due to addition of amide groups on the benzene moieties (panel E, arrow 2); The introduction of hydroxyl groups in RT47 (panel E, arrowed 3) also changed charge distribution and shape, and additionally introduce internal H-bonds between hydroxyl and amidine groups, restricting rotation of the amidine groups.

In the same way, pentamidine with various substitutions on benzene rings were investigated for their function and we found that addition of even a small group on the benzene moiety reduced affinity. After basic energy minimisation, RT43 displayed almost the same flexibility to that of pentamidine, but the addition of chloride (Cl) in positions 2 and 2' caused a reduction in affinity to HAPT1 by over 14.5-fold, The electronegative chlorine atom will serve to make the aromatic ring slightly more positive, but its main effect will surely be steric hindrance, clearly indicating size restrictions in the benzamide binding site of HAPT1 (Figure 4.4, B).

The energy minimisation showed that presence of hydroxyl groups at position 3 and 3' in RT47 have made it less favourable to assume a U-shaped conformation; in addition, the rotational restriction of the amidines and the possible steric hindrance all contribute to a reduction in affinity by 16.7 fold (Figure 4.4, F). The same for the tested analogues RT46, addition of amide group at position 2 and 2' makes the bend conformation less favourable and introduced a bulky group in a critical position, reducing its affinity to HAPT1 (Figure 4.4, E).

#### **4.3.4.4.2 Length of the linker (number of carbon atom)**

The importance of the distance between the two terminal active groups has been studied based on the length of the linker. RT compounds used in this part of the study were selected with the only variation in structure is the length of their methylene linkers keeping the position of the amidine group on the benzofuran ring at carbon number 5 and 5' for better comparison.

Compounds RT02 and RT18 were tested compounds with big variations in the length of their methylene linkers, with 5 carbons in RT18 and only one carbon in RT02. As can be seen in (Figure 4.5), compound RT18 shows a similar affinity to that of pentamidine, inhibiting [<sup>3</sup>H]-pentamidine uptake at very low concentrations, while RT02 has a very low affinity. RT10, characterised by a 3-carbon linker displays a low affinity to HAPT1 but yet higher than RT02. This is in agreement with the loss of flexibility of the molecules with shorter linker.

Intriguingly, RT14 with 4 carbons on its methylene linker displays the highest affinity yet reported amongst the tested RT compounds with a  $K_i$  of  $0.06 \pm 0.015$   $\mu\text{M}$  and ( $\Delta G^\circ$ ) of 41.19 kJ/mol. This value is very similar to the  $K_m$  of pentamidine. Compounds RT24 ( $C_4$  linker) and RT26 ( $C_5$ ) display only slightly lower affinity but longer chains seems to be unfavourable, probably because the increasing length of the carbon chain actually makes the assumption of the binding conformation less favourable.

Table 4.6 shows the  $K_i$  values for this series of bis-benzofuranamidines. A similar trend is observed with the benzamidines that include pentamidine ( $C_5$ ). Whereas ethamidine ( $C_2$ ) has very low affinity for HAPT1, binding is optimal for pentamidine and hexamidine ( $C_6$ ) before becoming again less good inhibitors (Table 4.6). These observations strongly suggest that the optimal linker length is

5 to 7 carbons, as the 2 and 2' carbons of the benzofuran moieties also contribute to the atomic distance between the amidines.

Chemical structure	Compound	$K_i$ ( $\mu\text{M}$ )	$\Delta G^\circ$ ( $\text{kJ mol}^{-1}$ )
	RT02	66.06 ± 13.03	-23.9
	RT10	35.59 ± 13.39	-25.4
	RT14	0.061 ± 0.015	-41.2
	RT18	0.26 ± 0.09	-37.6
	RT24	0.12 ± 0.03	-39.6
	** Heptamidine	0.12 ± 0.01	-39.5
	RT26	0.34 ± 0.07	-37.0
	Hexamidine	0.058 ± 0.010	-41.30
	Ethamidine	> 100	NA

Table 4.6. The effect of length of the linker on affinity to *T. b. brucei* HAPT1 transporter.

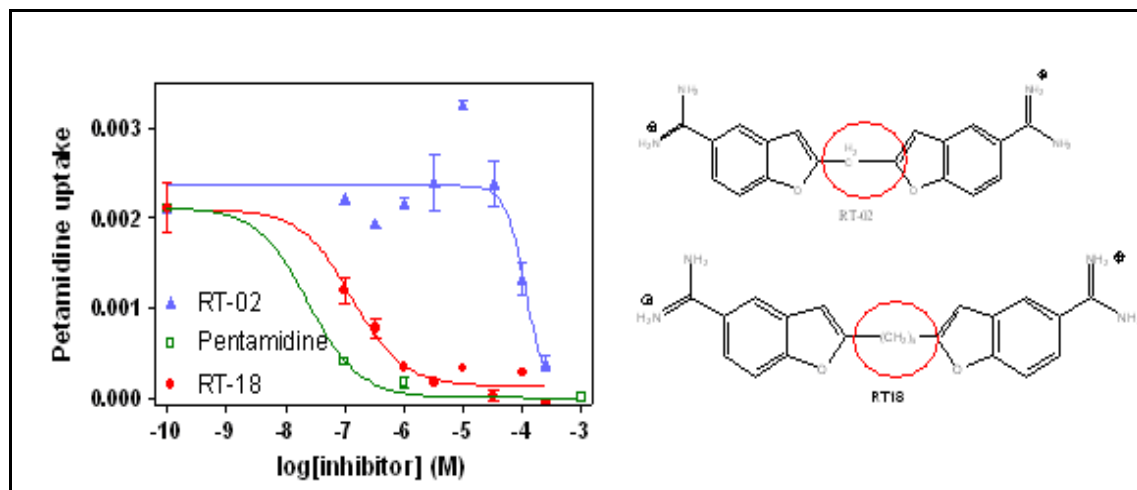


Figure 4.5. High Affinity Pentamidine Transporter Mediated Uptake of  $^3\text{H}$ -pentamidine (RT02/RT18).

Results plotted as sigmoid inhibition plots of inhibitor concentration against  $^3\text{H}$  Pentamidine uptake expressed as  $\text{pmol}(10^7 \text{ cells})^{-1} \text{ s}^{-1}$ .

#### 4.3.4.4.3 The role of oxygen on the linker

As it is seen in Table 4.7 replacing the third carbon atom on the linker chain of pentamidine with an oxygen atom in DB1699 reduced affinity by about 470 folds, as this constricts its folding and the C-O-C bond angle is smaller than the C-C-C bond angle (Figure 4.6, A). In the case of compound RT48 the oxygen atom of the linker in pentamidine is replaced by a sulphur atom (Figure 4.6, B); this replacement resulted in reduction of affinity to HAPT1 with  $K_i$  value of  $2.0 \pm 0.9 \mu\text{M}$ ).

Sulphur is a bigger and more polarisable and hydrophobic atom than oxygen. It is unlikely that the increase in size at that position in the chain is the cause of the relatively low affinity for HAPT, but again the carbon-sulphur bond angle is slightly different from carbon-oxygen. However, the 10 kJ/mol lower binding energy is more likely the result of a partial loss of a hydrogen bond for which oxygen is a much better acceptor than sulphur.

The even greater loss of binding energy seen in RT50 ( $K_i = 6.27 \pm 1.3 \mu\text{M}$ ; Table 4.7 & Figure 4.6, C), where the chain oxygen residues have been replaced by HN is fully consistent with this interpretation as the presence of a hydrogen bond donor facing another H-bond donor in the binding site would be even more unfavourable than the simple loss of the bond.

Another indication comes from comparing substituted benzamidines: whereas 4-hydroxybenzamide has a very low but measurable affinity of approx. 2.8 mM, benzamide did not inhibit pentamidine uptake at all at 1 mM (highest achievable concentration) and 2-hydroxybenzamide and 3-aminobenzamide had no effect on transport at 2.5 mM.

These findings show that the linker oxygen of pentamidine is likely to be directly involved in binding to HAPT1, probably as H-bond acceptor. Furthermore, both oxygen of the linker are strongly involved in binding as shown by the extremely low affinity of 4-hydroxybenzamide (Table 4.2)

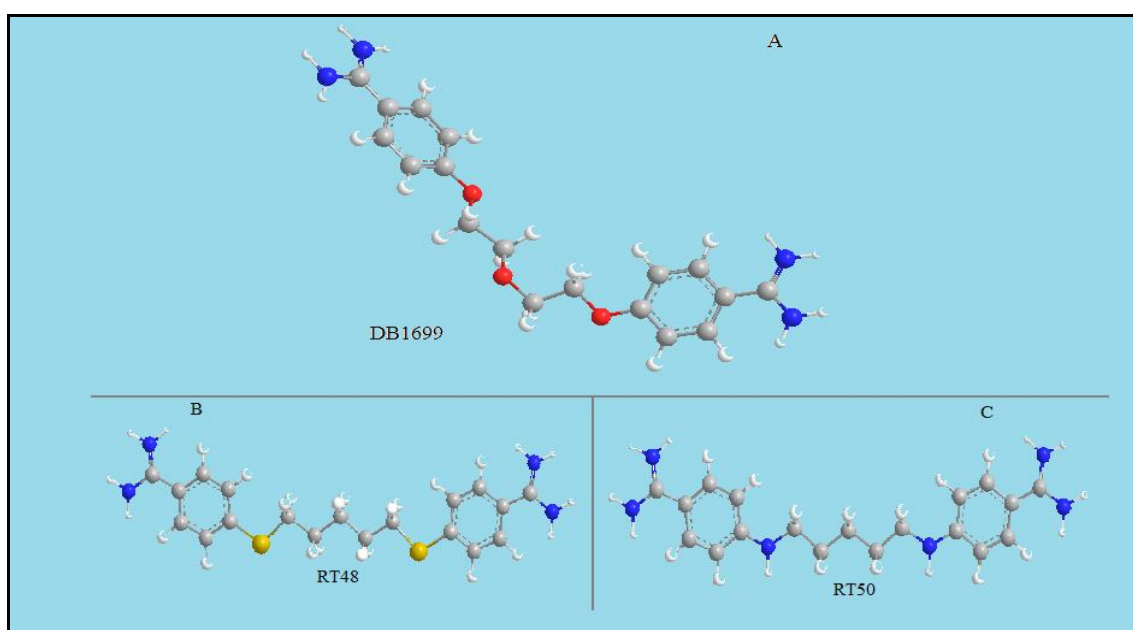


**Figure 4.6.** 3-D images after minimization of energy shows that presence of a third oxygen atom on the linker obviously reduces affinity to HAPT1 (panel A).

Replacement of oxygen linker with sulphur (yellow) resulted in the loss of two hydrogen bond acceptors, as Sulphur is a poor acceptor of such bonds (panel B). Replacement of the oxygen linker with nitrogen (blue) resulted in the exchange of two hydrogen bond acceptors for two hydrogen bond donors, which resulted in loss of affinity compared to pentamidine (panel C).

Chemical structure	Compound	$K_i$ ( $\mu\text{M}$ )	$\Delta G^\circ$ ( $\text{kJ mol}^{-1}$ )
	DB1699	$16 \pm 2$	-27.3
	RT48	$2.0 \pm 0.9$	-32.5
	RT50	$6.3 \pm 1.3$	-29.7

**Table 4.7. The role of the two oxygen residues on the linker in binding to the HAPT1 transporter.**

$K_i$  values are shown  $\pm$  standard error.  $\Delta G^\circ$  is the Gibbs free energy of interaction. All  $K_i$  values are the average of at least three independent experiments.

## 4.4 Discussion

Pentamidine resistance has been shown to result from the loss of the P2 transporter and HAPT1 (Bridges *et al*, 2007). For that reason the characterisation of the transporters and understanding their mode of binding the substrate is the key to the rational design of trypanocides that are efficiently accumulated by the parasitic cell membrane transporters. The recognition motif for the P2 transporter has been well characterized previously by structure activity relationship study (De Koning & Jarvis 1999). The ability of a compound to inhibit this adenosine uptake indicates that it has a high affinity for the P2 transporter, which is the case for diamidine drugs, including pentamidine. The identification of the HAPT1 transport systems, and understanding its mode of action will help in the design of drugs that carry the HAPT1 motif and hence can be used for successful treatment (Denise & Barrett, 2001; Hasne & Barrett, 2000; Barrett & Gilbert, 2006).

The structure activity relationship study was performed to test a number of compounds that were synthesized based on regular changes of the chemical properties of pentamidine, as this can be used to predict the means and the effectiveness of drug uptake by the HAPT1 transporter. Since pentamidine was used as a reference as it is the only known substrate with high affinity for HAPT1, uptake assay was employed to test the ability of unlabelled pentamidine analogues to inhibit the uptake of [<sup>3</sup>H]-pentamidine by this transporter. Conversion of the inhibition activity ( $K_i$ ) to  $\Delta G^\circ$  values helped in prediction of how strongly a drug can bind to the transporter binding pocket and how energy is won or lost upon a given modification of the molecule.

The first element we focused on was the importance of the amidine groups and their position on the benzene and benzofuran rings. CHI/72/1 and CHI/1/69/1 are analogue of pentamidine, where the second amidine group replaced by methyl group in the former and the amidine group being removed in the latter have displayed low affinity to HAPT1 with  $K_i$  values of  $2.6 \pm 0.7 \mu\text{M}$  and  $2.3 \pm 0.5 \mu\text{M}$ , respectively. Replacement of the amidine group was replaced with imidazoline ring or amine group resulted in very poor affinity for HAPT1. The simple benzamidine compound 4-hydroxybenzamidine displayed virtually no affinity for HAPT1 ( $K_i = 2.8 \pm 1 \text{ mM}$  compared with  $35 \pm 5 \text{ nM}$  for pentamidine).

This confirms that the two terminal amidine groups are required for high affinity binding to the HAPT1 binding pocket.

Comparison of Meta-pentamidine, RT01, RT05 and RT08, where the only structural difference is the positioning of the amidine group, provides a vast difference in terms of affinity of the drug. It would therefore seem that having the amidine group on the carbon 4 and 4' (*para*-position) relative to the linker (Figure 4.7) provides a higher affinity for HAPT1.

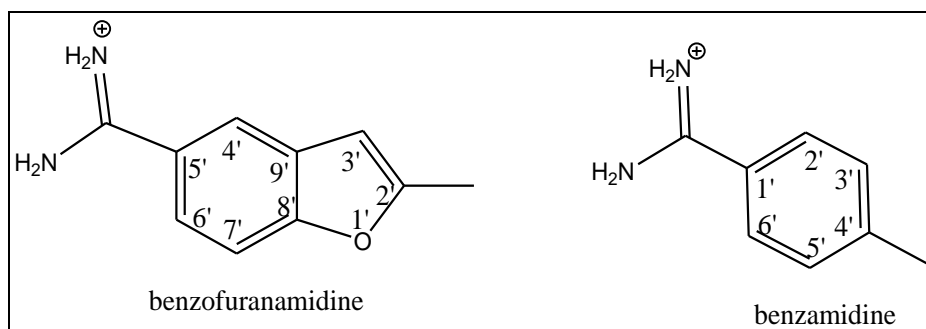


**Figure 4.7. Positioning of Amidine group that confers highest affinity for the High Affinity Pentamidine Transporter**

Although there is no conclusive evidence for  $\pi$ -stacking interactions between the two benzene rings and amino acid residues on the transporter, the fact that high affinity for HAPT1 demands a specific orientation between the two benzene rings and the presence of these two aromatic moieties, indicates clearly the importance of  $\pi$ -stacking in the interaction with the transporter.

The role of the linker on binding has also been investigated; the linker plays an important role in the flexibility of the substrate, which is required for optimal interaction with HAPT1, apparently using both amidines in a bent configuration. The benzamidinium groups in pentamidine are linked by a 1,5-dihydropentane chain. This linking chain is long, enabling an increase in flexibility and ability to bind to the P2, HAPT1 and LAPT1 transporters (de Koning, 2008). The experimental results and three dimensional analysis via basic energy minimisation showed that the replacement of the linker between both benzene rings in pentamidine by an azide group in diminazene or a furan ring in DB-75 affected the flexibility of the molecule and therefore resulted in significant loss of affinity for HAPT1, consistent with the interpretation that in these molecules only one amidinium group can interact with the binding site, as they lack the flexibility to assume a configuration in which both ends can interact.

As expected from this model, the length of the linker proved to play an important role in affinity for HAPT1. The most obvious observation was that the optimal linker length is between 4 to 7 carbons on the methylene linker. Compound RT14 is characterized by 4 carbons in its linker displayed the closest affinity to that of pentamidine. Compound RT18 acts in much the same way as pentamidine due to the 5 methylene linker chain. The 3-carbon linker displays a low affinity to HAPT1 but still higher than RT02 which is characterised by presence of a single-carbon linker. These observations are in agreement with low flexibility of the molecules with shorter linkers. Increasing the linker length beyond 7 carbons noticeably reduced affinity to the transporter as was shown in compound RT26. It therefore would seem that that the optimal length of linker chain in diamidines is between 4 to 7 carbons (Figure 4.8, A). This will enhance the flexibility, and therefore ability to fit the binding pocket of the transporter by changing the shape of the molecule. These observations strongly support the previous study data using the benzamidine compounds in which the optimal length of the linker was between 5 and 7 carbons (Figure 4.8, B).

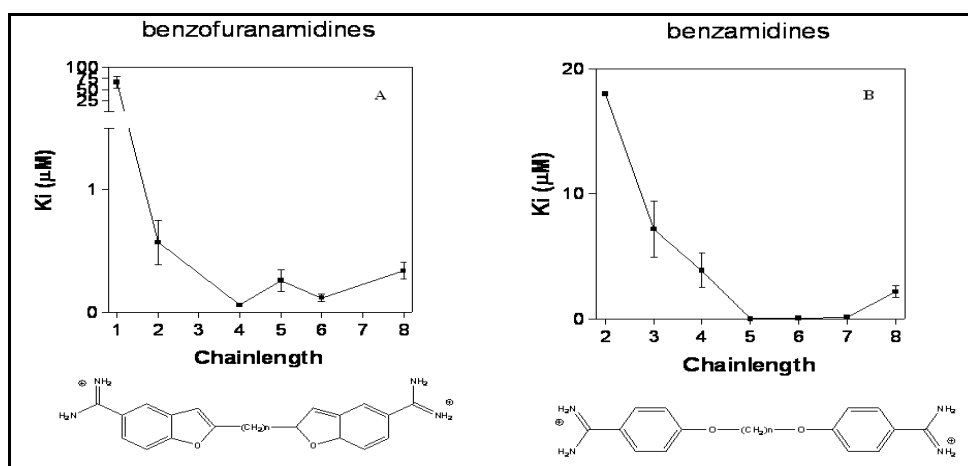
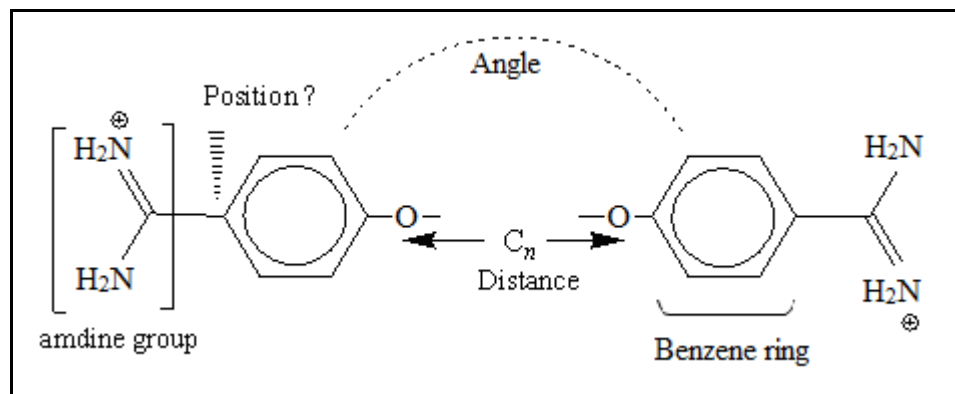


**Figure 4.8.** Graph represents the relationship between the length of the linker and affinity to the HAPT1 transporter. The study involved the benzofuranamidine compounds (panel A) and benzamidine compounds (panel B).

Other factors were noticed to have a great affect on flexibility of the compounds and as a result reduce their affinity to HAPT1 is the addition of even a small substitution on the benzene moiety, this again confirms that flexibility is an important part in the recognition process.

Finally, capacity of binding was also linked to the oxygen atoms as an important element in the interaction, possibly as hydrogen bond acceptor.



Property	Requirement
Amidine group	<ul style="list-style-type: none"> <li>▪ 2 amidines (positive)</li> <li>▪ Position: <i>para</i> position</li> </ul>
Benzene rings	<ul style="list-style-type: none"> <li>▪ Both rings: required</li> </ul>
Linker	<ul style="list-style-type: none"> <li>▪ <math>C_n</math>: C4 – C7</li> <li>▪ Linker oxygen: 2 atoms</li> </ul>
Shape (angle)	<ul style="list-style-type: none"> <li>▪ Flexibility: required</li> </ul>

Figure 4.9. Recognition motif model for HAPT1

The final conclusion is presented in (Figure 4.9) and could be addressed as both benzene rings together with the two terminal amidine groups of pentamidine keeping their position at *para* position relative to the linker are essential for the binding process. In addition, the presence of the two oxygen atoms, and the linker length and flexibility are key determinants in diamidine binding to HAPT1, and pentamidine has its high affinity due to its flexible shape, which it owes to the 1,5-dihydroxypentane linker.

## **5 Development and characterisation of a clonal line resistant to 1 $\mu$ M pentamidine**

## 5.1 Introduction

Since 1937 pentamidine has been the only aromatic diamidine used in HAT treatment, its mode of action against the parasite is still unknown although a number of targets have been suggested, including ability to bind to DNA minor groove leading to inhibition of protein synthesis (Wilson *et al*, 2005).

In order for it to act as a therapeutic agent pentamidine should enter the parasite, and it was found to be transported by at least three distinct transporters (De Koning, 2001). The P2 nucleoside transporter is responsible for transporting the vast majority of pentamidine (Bray *et al*, 2003). The other two transporters are the High (HAPT1) and low (LAPT1) affinity pentamidine transporters (De Koning, 2001). If any of the three transporters is lost the parasite will develop a degree of resistance to the drug and the loss of the three transporters should result in a very high level of resistance as well as cross-resistance with other drugs that share the route of entry.

Due to the multiple routes of entry, unlike many of the other trypanocides such as melarsoprol (Brun *et al*, 2001) no pentamidine resistance has been officially reported in the field (Matovu *et al*, 2003). Even though there can be little doubt that resistance will eventually arise with the continued use of pentamidine and recent anecdotal reports from OCEAC in West Africa indicate an alarming increase in pentamidine treatment failures in some foci. For that reason there is an urgent need to understand the mechanism by which resistance occurs and thus prevent treatment failure. Various mechanisms have been proposed to be involved in pentamidine resistance (Berger *et al*, 1995). Deletion of the two copies of the TbAT1 gene that encodes the P2 transporter leads to a 2.5-fold loss of pentamidine sensitivity, though the cells remain sensitive to nanomolar concentrations of the drug (Matovu *et al.*, 2003).

This suggests that several factors are involved in resistance. Other ways to develop resistant cells is by exposure to ever-increasing concentrations of drug (Berger *et al*, 1995). This method was successfully used when the TbAT1/P2 knockout cell line was adapted to high pentamidine concentrations, resulting in the B48 cell line that has lost the HAPT1 transporter activity. This selection has

been shown to lead to 130-fold increase in resistance in a *T. brucei* B48 line compare to the wild type cell line (Bridges *et al*, 2007).

By using the same method we hoped to increase the likelihood of success in generating drug resistant by adapting the B48 to even higher concentrations of pentamidine and create a null pentamidine sensitive cell line by losing the LAPT1 transporter (Figure 5.1). This could also provide essential insights into the likelihood mechanisms of pentamidine resistance.

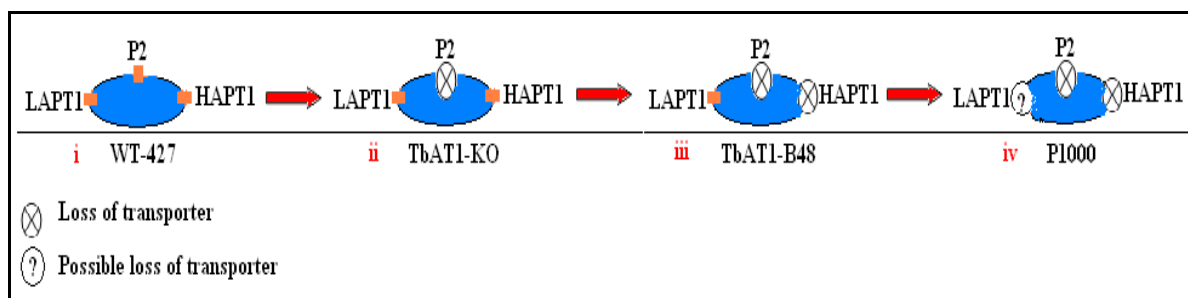


Figure 5.1. A diagram representing the steps involved in creating the pentamidine resistant cell line.

(i) 427-WT(*TbAT1*/P2, HAPT1 and LAPT1) are present. (ii) *TbAT1*-KO (HAPT1 and LAPT1) are present (iii) LAPT1 is present (vi) possible loss of LAPT1 (P1000 cell line)

## 5.2 Results

### 5.2.1 Induction of resistance

The cell line *T. brucei*-B48 was derived from the isogenic cell line *TbAT1*-KO in which the *TbAT1* gene was deleted (Matovu *et al.*, 2003), by selection to high concentrations of pentamidine, leading to the loss of the HAPT1 transporter (Bridges *et al.*, 2007).

Further *in vitro* selection for higher level resistance against the diamidine drug pentamidine was often difficult to maintain, especially at concentration under 400nM. The process involved culturing *T. brucei*-B48 cells in a stepwise manner with gradual increment of pentamidine. Initially, selection started at 75 nM which was almost a quarter of the IC<sub>50</sub> of *TbAT1*-B48 for pentamidine (270 nM ± 17). The concentration was gradually increased by 25 to 50 nM per step. As described in section 2.5, the induction process took about 12 months of selection

until cells went on to develop a stable resistance phenotype in increasing concentrations of drug (Figure 5.2).

The selection of *TbAT1*-B48 cell cultures with very high levels of pentamidine resistance (normal growth in 1  $\mu\text{M}$ ) was achieved after a minimum of 95 passages in the presence of pentamidine. After reaching 1000 nM level of tolerance, cells were passaged for several weeks at this concentration. This was followed by passage in drug free medium prior to the cloning process (section 2.5). A new cell line was generated by cloning using the limiting dilution technique, and was designated P1000.

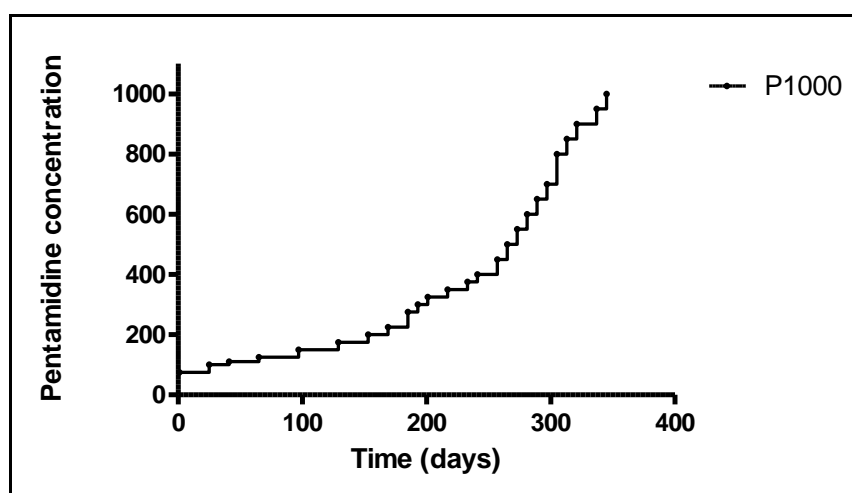


Figure 5.2. Creation of P1000 cell line.

Selection for resistance to pentamidine in the *TbAT1*-B48 cell line cultured in increasing drug concentrations for about 12 month period. As seen it took about 4 months to reach toleration of 200 nM pentamidine in the growth medium, followed by a period of two months to reach 400nM levels. This was followed by accelerated adaptation to 1000 nM of pentamidine.

### 5.2.2 Cloning out

Once cells were stable thus capable of surviving in the presence of 1  $\mu\text{M}$  pentamidine, clonal populations were generated by limiting dilution on 96 well plates using HMI-9 supplemented with 10% FCS and 1  $\mu\text{M}$  pentamidine (section 2.9.7). After seven days of incubation at 37  $^{\circ}\text{C}$  + 5%  $\text{CO}_2$ ; only 5 unique clones were initially established. Having acquired a stable drug resistance phenotype, it was important to test the extent of resistance for each clone at 1  $\mu\text{M}$  pentamidine. This was achieved by cell counts, using an improved Neubauer

haemocytometer. Even after several passages under drug pressure, no growth phenotype difference was observed between the 4 clones.

One clone of the newly-adapted strain was chosen to be used during this project and a drug profile for this clone was created. Alamar blue was used to create an  $EC_{50}$  for pentamidine as well as other compounds including diminazene (Sigma) and cymelarsan to check for any changes of their  $EC_{50}$  values compared to B48 and wild type strain 427, which were included in the experiments as a reference (Figure 5.5).

### 5.2.3 *In-vitro* monitoring cell growth

Direct microscopy cell count was applied to check for any growth changes between the 4 clones and then between the selected clone and the reference cell lines (WT427 and *TbAT1*-B48). No phenotypic changes have been observed when cell growth levels in of the 4 clones obtained were monitored (data not shown). The monitoring process was repeated on clone 9 of the P1000 strain after removing the drug pressure for 3 months and the growth level was compared with the growth of the parental cell line (*TbAT1*-B48) and the wild type 427 (Figure 5.3), with counts taken every 12 hours for 168 hours; this involved 3 passages to fresh medium.

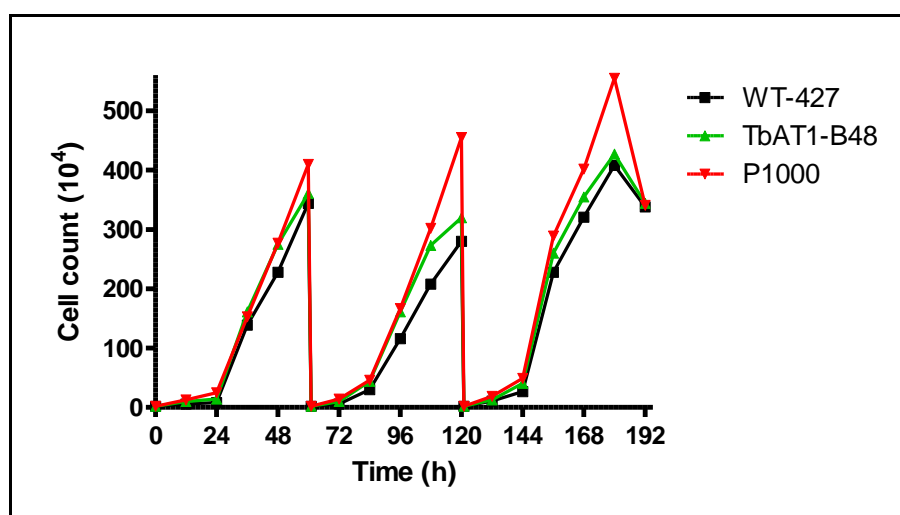


Figure 5.3. The Effect of pentamidine adaptation on growth of P1000 cell line *T. b. brucei* S427 and *TbAT1*-B48.

Trypanosomes were seeded at  $2 \times 10^4$  cells/ml in fresh HMI-9 (427-WTblack line, *TbAT1*-B48 green line and P1000 red line). Data represents the growth for 181 hours involving 3 passages at  $2 \times 10^4$  cells/ml.

The results showed that P1000 cells displayed a slight increase in growth rates, particularly at high density, compared to the reference lines. The growth level of the TbAT1-B48 was also noticeably growing faster than 427-WT strain; the later observation was also confirmed by professor Pascal Mäser's group (personal communication through my supervisor). Clearly, the P2 and HAPT1 transporters are not essential for bloodstream forms under standard in vitro conditions in rich HMI-9 medium. It is worth recalling that B48 displayed considerable loss of infectivity in mice, compared to s427 (Bridges *et al.*, 2007).

#### **5.2.4 Alamar Blue assay and in vitro drug profile**

A drug sensitivity profile for P1000 for pentamidine and a selection of other trypanocides was obtained using the standard Alamar Blue protocol (section 2.4.1). The drugs included diamidines (pentamidine, diminazene and DB75) and a melaminophenyl arsenical (cymelarsan). The adenosine analogue (tubercidin) was also included as a control for P2 activity.

Non-P2 dependent trypanocides including Eflornithine (DFMO) and suramin; other controls included in the experiments are isometamidium and ethidium bromide, which were previously found to be associated with cross-resistance as they are structurally similar and might share the same uptake mechanism (Peregrine *et al.*, 1997), to check whether adaptation to pentamidine interfered with their parameters.  $IC_{50}$  values were obtained by non-linear regression to a sigmoidal curve with variable slope and defined as the value that reduced the maximum fluorescence by 50% of the difference with the minimum fluorescence.

The results of the first application showed that the  $EC_{50}$  of pentamidine was very similar in all clones (Figure 5.4). Clone9 was chosen over the other clones, as it appeared to display the highest resistance phenotype (Table 5.1), for further biochemical and molecular studies.

$EC_{50}$  values for all the test drugs were generated and are summarised in Table 5.2. These results were obtained directly after the selection and cloning process was completed without allowing the cells to proliferate without drug.

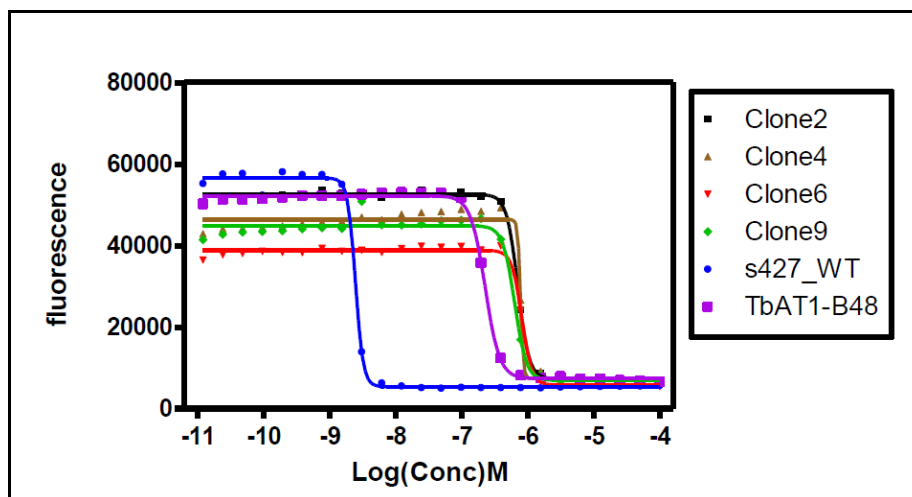


Figure 5.4. Pentamidine sensitivity in four clones of P1000.

Alamar blue assay result demonstrating the difference in sensitivity to pentamidine between the four obtained clones in contrast to 427-WT and TbAT1-B48.

Drug	Cell line	IC <sub>50</sub> (nM) (1x10 <sup>5</sup> cells/ml)	n
pentamidine	WT s427	2.4	1
	TbAT1-B48	227	1
	IT-P1000		
	Clone 2	709	1
	Clone 4	708	1
	Clone 6	630	1
	Clone 9	810	1

Table 5.1. Resistance phenotypes of the P1000 clones.

*In vitro* Alamar Blue results of the 4 obtained clones of the 1000 nM pentamidine resistant cell line.

From this table, a number of observations can be made. Firstly, TbAT1-B48 displayed an average 143-fold pentamidine resistance compared to WT, which is remarkably similar to the previously published resistant factor of 139 folds (Bridges *et al.*, 2007). However, the P1000 cell line displayed much higher resistance, reaching an average of 438-fold. Yet, P1000 developed resistance of only 3.1-fold relative to its parental cell line TbAT1-B48. We had expected to see a higher level of adaptation, considering that induction started at a pentamidine concentration of only 75 nM in the growth medium and the cells adapted to a final concentration of 1000 nM - a 13.3-fold increase.

The alamar blue analysis also highlighted further interesting results. The further adaptation to pentamidine also led to increased resistance to other compounds, especially those that share the same main route of entry with pentamidine;

namely the P2 and HAPT1 transporter-dependent drugs (diminazene and cymelarsan). One explanation is that the previous adaptation to pentamidine (*TbAT1*-B48) left the cells with a much-reduced activity of HAPT1 and that further adaptation to pentamidine completely abolished HAPT1 activity.

The profile for isometamidium included in these experiments failed to give completely reproducible results, especially in the case of *TbAT1*-B48. This strain became much more sensitive to isometamidium compared to 427-WT and even P1000 (Table 5.2 and Figure 5.5).

DB75 was also tested but the data was excluded as they showed big variations between the experimental repeats. The control drugs suramin and DFMO did not show any significant difference in their profile in the three strains.

Compounds	427-WT		TbAT1-B48			>P	P1000			>P
	AVG	SE	AVG	SE	RF		AVG	SE	RF	
pentamidine	0.002	0.0001	0.37	0.04	158.14	p<0.05	0.87	0.07	374.96	p<0.01
diminazene	0.08	0.01	0.78	0.06	10.08	p<0.01	0.95	0.25	12.24	p<0.01
Cymelarsan	0.03	0.00	0.60	0.04	21.16	p<0.01	0.94	0.30	33.38	p<0.01
Tubercidin	0.19	0.03	3.42	0.10	18.09	p<0.001	13.89	3.21	73.43	p<0.01
Isometamidium	0.12	0.04	0.01	0.00	0.05	p<0.05	0.04	0.01	0.31	NS
Ethidium Bromide	1.36	0.06	1.50	0.07	1.10	NS	2.06	0.29	1.52	NS
Suramin	0.007	0.003	0.012	0.001	1.75	NS	0.006	0.0004	0.94	NS
DFMO	14.88	3.35	20.12	2.49	1.35	NS	20.00	2.04	1.34	NS

**Table 5.2.** The averages of EC<sub>50</sub> values of various trypanocides determined by using alamar blue assays.

Induction of resistance to 1000 nM of pentamidine resulted in a clear resistance to the drug compared to the parental cell line (*TbAT1*-B48) and much higher resistance compare to pentamidine sensitive cell line wild-type 427 with resistance factor of 423 folds. All assays were performed in triplicate. Average of 3 independent experiments to calculate IC<sub>50</sub> values are shown in sub-micromolar with standard errors. Values were calculated from sigmoidal dose-response curves, with variable slopes, using GraphPad Prism software. Statistical significance for the presence of resistance was calculated using a one-way ANOVA test (GraphPad Prism 5.0) in which the strains were grouped (a,b,c) according to significant difference (p<0.05) or not (p>0.05); see Appendix E.

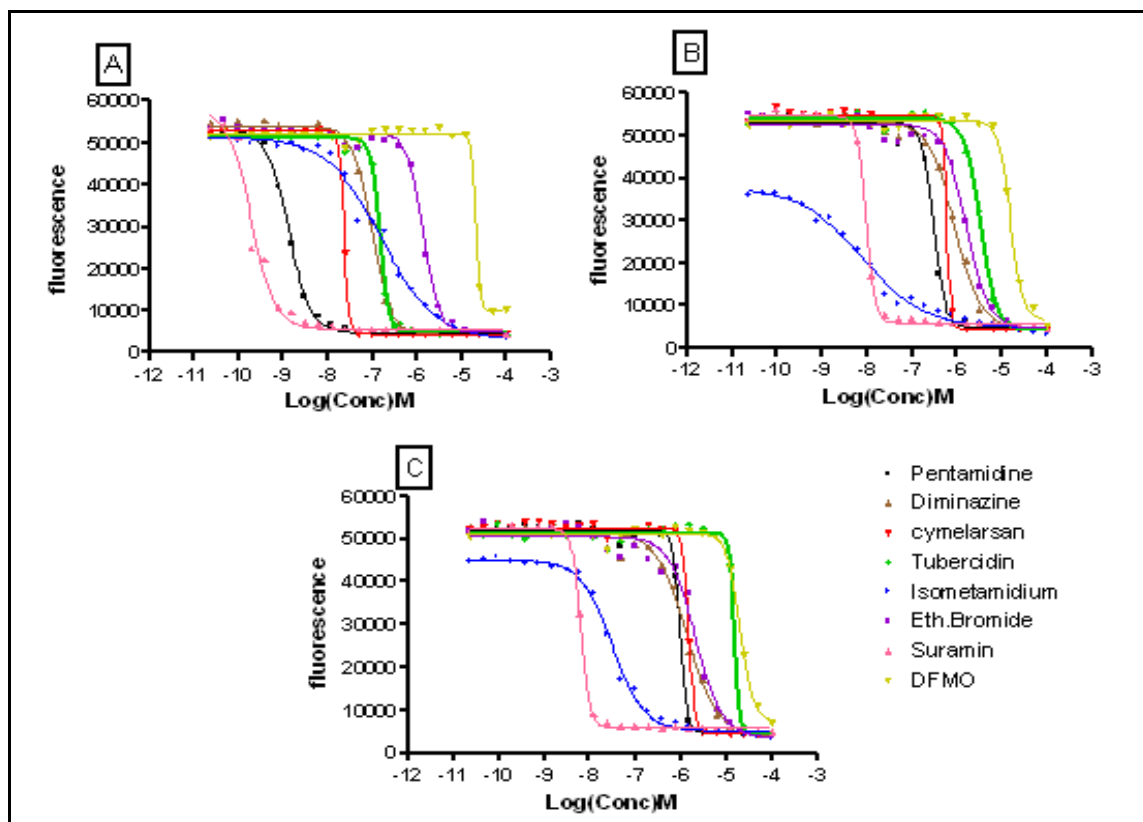


Figure 5.5. Drug profile of P1000 compare to 427 wild type and TbAT1-B48.

Graphs showing the *in vitro* alamar blue assay results for a number of drugs against bloodstream form trypanosomes of (A): 427 wild type, (B): TbAT1-B48 and (C): P1000. Cell growth was assessed as the amount of fluorescence produced from an excitation wavelength of 530 nm and emission wavelength of 590 nm from the metabolism of resazurin by living trypanosomes. This graph represents data of 1 representative experiment from several repeats.

### 5.3 Stability of resistance phenotype

To assess the relative stability of the resistance phenotype the P1000 cells were withdrawn from drug and passaged in drug-free medium for a minimum of 30 passages. Alamar blue assay were then used in order to verify the stability of resistance phenotype to 1000 nM pentamidine. The results indicated the drug resistance phenotype of the P1000 cell line was stable after removing the drug pressure for a period of 3 months with an  $IC_{50}$  of  $981 \pm 35$  nM (Table 5.3).

This suggests that the adaptation to pentamidine is most likely to be defined at the genetic levels rather than protein level.

Cell line	Pentamidine				
	IC <sub>50</sub> AVG (nM)	SE	(n)	RF to WT	RF to B48
WT -427	2.6	0.3	3		
<i>TbAT1-B48</i>	248	23	3	95	
P1000	981	35	3	377	3.9

**Table 5.3.** *In vitro* susceptibility, comparing resistance phenotypes of the pentamidine resistance cell line P1000 to WT s427 and *TbAT1-B48*.

(n), number of experiments performed. RF, resistance factor. IC<sub>50</sub> values are the average of three independent experiments.

## 5.4 Pentamidine transport in P1000 cell line

[<sup>3</sup>H]-pentamidine transport assays were carried out to look for any changes in the relative rates of pentamidine uptake between the parental (*TbAT1-B48*) and drug adapted (P1000) line and to determine whether further adaptation to pentamidine resulted in loss of LAPT1 activity.

The rapid oil-stop method described in section (2.4.3) was used and in each experiment a control reaction to measure the radiolabel associated with the cell pellet at zero-uptake conditions ( $T_0$ ) was determined by adding ice cold cells to a mix of ice cold of [<sup>3</sup>H]-pentamidine label and unlabelled pentamidine. Mediated uptake, after subtraction of the  $T_0$  values, was expressed as  $\text{pmol}(10^7 \text{ cells})^{-1}\text{s}^{-1}$ .

## 5.5 Kinetic characterisation

The adapted cell line P1000 is derived from *T. b. brucei* line *TbAT1-B48* which has previously been shown to lack HAPT1 activity, and therefore pentamidine enters *TbAT1-B48* cells only through LAPT1 (Bridges *et al.*, 2007). To determine the transport phenotype of P1000, a series of experiments were performed to determine  $K_m$  and  $V_{max}$  values. This involved testing high concentrations (1  $\mu\text{M}$ ) of radiolabeled pentamidine to assess the status of the low affinity pentamidine transporter LAPT1 (de Koning & Jarvis, 2001; de Koning 2001).

The report by Bridges *et al* (2007) showed that in *TbAT1*-B48 the  $K_m$  value and  $V_{max}$  for LAPT1 are  $55.6 \pm 6.6 \mu\text{M}$  and  $0.82 \pm 0.20 \text{ pmol} (10^7 \text{ cells}^{-1})\text{s}^{-1}$ , respectively, almost identical to those previously reported for LAPT1 in wild type 427 bloodstream forms (De Koning, 2001).

Even though P1000 cells were resistant to 1000 nM pentamidine, the uptake of  $1 \mu\text{M}$  [ $^3\text{H}$ ]-pentamidine experiments illustrated that LAPT1 activity was not affected (Figure 5.6); the apparent  $K_m$  value was  $99 \pm 24 \mu\text{M}$  and the apparent  $V_{max}$  was  $1.26 \pm 0.27 \text{ pmol}(10^7 \text{ cells}^{-1})\text{s}^{-1}$  ( $n=4$ ). This finding confirmed our tentative hypothesis that the cells did not lose the LAPT1 transporter but instead the adapted cell line developed a new mechanism of resistance.

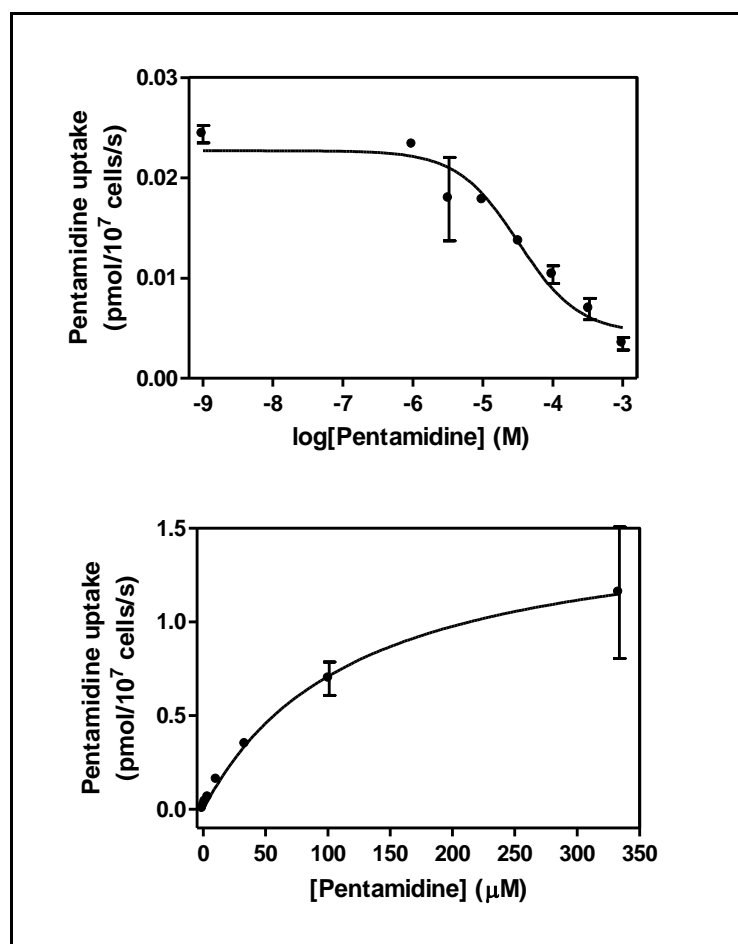


Figure 5.6. Inhibition of  $1 \mu\text{M}$  [ $^3\text{H}$ ]-pentamidine uptake by P1000 bloodstream forms. This Diagram represents one of four independent repeats.

## 5.6 Study of Mitochondrial Membrane Potential (MMP)

Adaptation to 1000 nM of pentamidine did not cause any change in LAPT1 transport activity, therefore we addressed four questions (i) is the increase of

resistance to pentamidine related to mitochondrial transportation; (ii) is there a difference in MMP in response to drug caused by pentamidine resistance; (iii) is there difference in MMP in response to drug caused by deletion of TbAT1/P2; (iv) if MMP proven to be affected (1<sup>st</sup> question), is it possible to restore sensitivity phenotype?

The first two questions will involve comparisons between P1000 and parental cell line *TbAT1*-B48 with 427-WT. The third question requires comparison between TbAT1-KO and 427-WT. The fourth question will include comparison of MMP between 427-WT, *TbAT1*-B48 and two cell lines which has been recently created in our laboratory. Briefly, these cell lines are derived from TbAT-B48 by transfection with either of the two AT-E alleles (chapter 6 describes the differences between the two alleles).

The two alleles were simply named AT-E1 and AT-E2, thus transfected *TbAT1*-B48 was named B48+AT-E1 or B48+AT-E2. Initial kinetic data showed that AT-E1 strongly interacts with pentamidine but AT-E2 displayed much less activity (Transfection and kinetic studies were carried out by other members of the group, Jane Munday and Anthonius Eze).

The process involved cultivating the cells for up to 12 h in the presence and absence of 0.5  $\mu$ M pentamidine. Two chemical controls were included in each experiment for each strain; Valinomycin for mitochondrial membrane depolarisation and Troglitazone as a control for mitochondrial membrane hyperpolarisation as described previously for *T. b. brucei* by (Denninger *et al.*, 2007).

Results are presented in histograms of TMRE fluorescence (Appendix A) after incubating the cells with and without tested compounds, with readings taken at zero time, 6 hours and 12 hours. The first time point involves exposure to the compounds for a minimum time, approximately 15 minutes, during harvesting and washing steps, and will therefore be labelled 15 minutes. A drug-free group was included as a further no-exposure control. Values are given as the percentage of cells with fluorescence above 100 arbitrary units (AU), which was around (50%) for the controls (427-WT/ Drug free). A shift to higher fluorescence signifies an increased MMP, whereas a shift to lower fluorescence signifies a depolarization of the mitochondrial membrane (Denninger *et al.*, 2007).

A summary of the average values of the MMP obtained from a minimum of three repeats in the six strains is shown in Table 5.4; the statistical analysis, performed using one-way ANOVA test (GraphPad Prism 5.0), see appendix E.

In drug free control (427-WT) the MMP at 15 minutes was (50.16%) and at 6 hours (49.97%) and (49.84 %) at 12 hours. The results also showed that in the absence of drug, the MMP was reduced in *TbAT1-KO* (Figure 5.7) and *TbAT1-B48*, to 41.6% and (31.3%), respectively, at the 15 minute point. P1000 showed a much stronger reduction in mitochondrial membrane potential at 9.75%, which remained almost unchanged during the period of 12 hours incubation. This could be explained by the loss of the mitochondrial function as a result of the long-term exposure to high concentrations of pentamidine.

Exposure to 500 nM pentamidine resulted in clear depolarisation of MMP in 427-WT cell with fluorescence >100 AU constituting 27.8% at 15 minutes, to only 5.8% at 12 hours - indicating a very strong depolarisation of the mitochondrial membrane. *TbAT1-KO* followed a similar pattern with a reduction from (28.27%) at 15 minutes to (8.61%) at 12 hours. *TbAT1-B48* pentamidine caused less aggressive reduction in MMP from (27.64%) at 15 minutes to (16.12%) at 12 hours, perhaps reflecting somewhat slower accumulation of the drug as a result of HAPT1 loss. In contrast, P1000 showed an almost identical percentage to the drug-free culture and did not show any significant change in the MMP as the percentage was ( $8.4 \pm 0.9\%$ ) at 15 minutes and ( $6.9 \pm 0.6\%$ ) at 12 hours (Figure 5.7), confirming that the adaptation to higher concentrations of pentamidine had resulted in loss of mitochondrial function.

Sequence analysis (which will be presented in chapter 6) defined that the AT-E gene is present as at least two different alleles with several single nucleotide polymorphisms (SNPs) causing amino acid differences, which we named AT-E1 and AT-E2. The AT-E1 and AT-E2 were found identical in 427-WT, B48 and P1000 cell lines. To study the roles of the AT-E1 and AT-E2 gene products in pentamidine uptake, the transfected *TbAT1-B48* cell lines B48+AT-E1 and B48+AT-E2 were included in this study to determine whether any or both of them will reinstall wild type mitochondrial membrane potential and pentamidine response.

Interestingly, reintroducing AT-E1 almost restored the WT phenotype, as it brought back MMP to 56.3% at 15 minutes and 54.0% at 12 hours. The cells followed the exact 427-WT pattern and exposure to pentamidine caused a reduction of MMP from 25.9% at 15 minutes to 10.9% at 12 hours. Reintroducing the AT-E2 also restored the wild type MMP to similar levels in the absence of drug (52.1% at 15 minutes and 45.8% at 12 hours). However, transformation with AT-E2 appeared not to enhance the pentamidine effects on MMP, as exposure to drug resulted in an only partially depolarised mitochondrial membrane (MMP was 39.5% at 15 minutes and 28.7% at 12 hours). This observation strongly agrees with the recent findings in our group that AT-E1 is the form of the gene responsible for HAPT activity whereas AT-E2 appears to be involved in other uptake activities. Currently, both alleles are being introduced in P1000 to assess pentamidine sensitivity and MMP.

In some cases the histograms displayed two fluorescence peaks, the one at approximately 150 AU representing cells with a highly depolarised mitochondrial membrane and those displaying fluorescence below 100 AU possibly represented dead cells. The included controls valinomycin and troglitazone displayed similar effects on all strains as the former resulted in mitochondrial membrane depolarisation and the later caused mitochondrial membrane hyperpolarisation (Denninger *et al*, 2007)

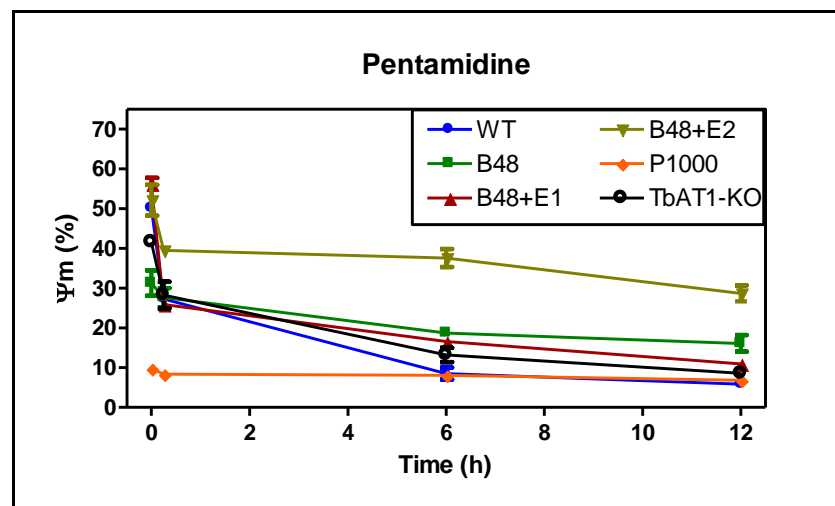


Figure 5.7. The Effect of 500 nM pentamidine on the mitochondrial membrane potential in drug sensitive and resistant *T. brucei* bloodstream forms as measured by fluorescence of TMRE.

Strains / Averages & number of repeats		WT-427			TbAT1-KO			TbAT1-B48		
Time	Tested Compounds	AVG	SE	>P	AVG	SE	>P	AVG	SE	>P
15 min	Drug free	50.16	0.7		41.57	1.4		31.31	3.2	
	Valinomycin	3.17	0.4		2.99	0.3		1.95	0.5	
	Troglitazone	61.32	1.8		57.12	2.8		40.90	2.1	
	Pentamidine 500nM	27.28	0.8	P<0.001	28.27	3.4	P=0.051	27.63	2.4	P>0.05
6 hours	Drug free	49.97	0.4		38.03	2.0		26.44	5.6	
	Valinomycin	4.65	1.2		2.50	0.4		2.18	0.5	
	Troglitazone	61.62	2.8		53.79	2.1		44.93	2.0	
	Pentamidine 500nM	8.52	1.5	P<0.001	13.22	1.8	P<0.001	18.70	1.3	P<0.05
12 hours	Drug free	49.84	0.4		36.68	2.5		28.644	4.3	
	Valinomycin	4.57	1.1		3.08	0.3		1.89	0.2	
	Troglitazone	62.61	2.4		59.97	4.1		43.49	1.5	
	Pentamidine 500nM	5.82	0.8	P<0.001	8.61	1.3	P<0.001	16.12	2.1	P<0.01

Strains / Averages & number of repeats		P1000			B48+AT-E1			B48+AT-E2		
Time	Tested Compounds	AVG	SE	>P	AVG	SE	>P	AVG	SE	>P
15 min	Drug free	9.75	0.7		56.3	1.5		52.2	3.9	
	Valinomycin	3.12	0.8		2.6	0.5		2.7	0.3	
	Troglitazone	22.81	4.4		59.2	2.6		59.5	1.8	
	Pentamidine 500nM	8.39	0.9	P>0.05	25.9	1.4	P<0.01	39.5	1.2	P>0.05
6 hours	Drug free	10.68	0.8		55.4	1.0		46.7	0.8	
	Valinomycin	3.59	0.9		2.8	0.5		2.5	0.4	
	Troglitazone	21.18	5.2		60.2	2.4		59.7	0.8	
	Pentamidine 500nM	8.09	1.0	P>0.05	16.6	1.4	P<0.001	37.6	2.2	P<0.05
12 hours	Drug free	10.48	1.6		54.0	0.9		45.8	2.2	
	Valinomycin	3.48	0.5		3.3	0.2		1.9	0.3	
	Troglitazone	24.33	6.0		59.9	0.7		60.1	2.3	
	Pentamidine 500nM	6.86	0.6	P>0.05	10.9	1.1	P<0.001	28.7	2.0	P<0.05

**Table 5.4. Summary of the MMP results.**

The effect of 500 nM pentamidine on mitochondrial membrane potential in various *T. brucei* strains, 427-WT, TbAT1-KO, TbAT1-B48, P1000, TbAT1-B48+AT-E1 and TbAT1-B48+AT-E2. Samples were collected for reading at 15 minutes, 6 hours and 12 hours of incubation with or without tested compounds. The values are the averages of a minimum of 3 independent experiments with (SE). Drug free samples were included in each experiments as a reference to enable clear comparison of the mitochondrial membrane potential at each time point for each strain, and between the all strains in relative to 427-WT. Positive controls include (100 nM) valinomycin and (10  $\mu$ M) troglitazone to monitor the decrease and increase the mitochondrial membrane potential, respectively. Statistical significance for the presence of resistance was calculated using a one-way ANOVA test (GraphPad Prism 5.0) in which the strains were grouped (a,b,c) according to significant difference ( $p<0.05$ ) or not ( $p>0.05$ ); see Appendix E.

## 5.7 Effect of pentamidine adaptation on expression of AT-E gene and sequencing analysis

Analysis of transporter transcription has been successfully investigated using reverse transcriptase PCR (RT-PCR) in P1000 and *TbAT1*-B48 and 427-WT bloodstream forms. The process involved using of cDNA, generated in the same quantity from the three strains. This was used to investigate the expression levels for AT-E, AT-A and *TbAT1*/P2 genes (see section 2.9.9).

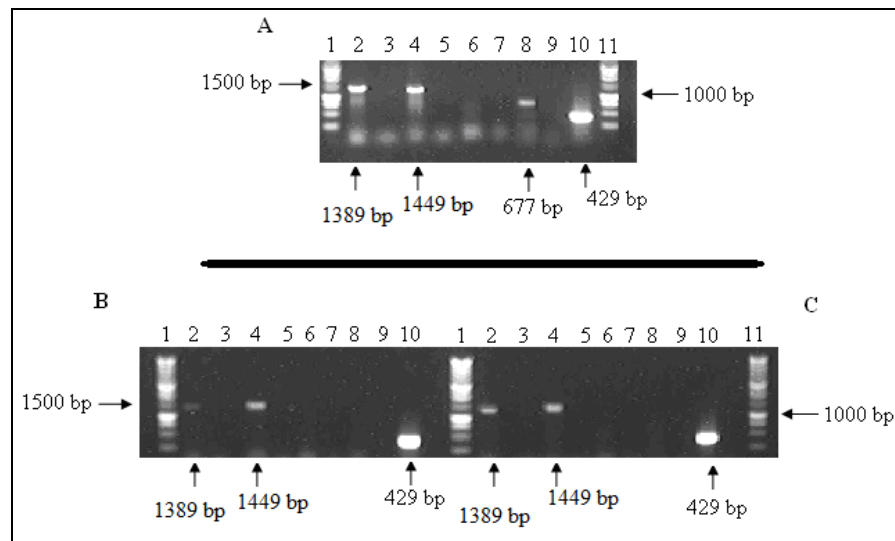


**Figure 5.8. Reverse transcriptase PCR (RT-PCR) result.**

Reverse transcriptase PCR (RT-PCR) gel result represents the expression levels of AT-E, AT-A and *TbAT1*/P2 genes in and (A) wild type 427, (B) P1000 and (C) *TbAT1*-B48

cDNA from 427-WT strain, Lane 1: 1KB ladder. Lane 2 AT-E + RT. Lane 3: AT-E – RT. Lane 4 AT-A + RT. Lane 5: AT-E gene – RT. Lane 6, lane 7 Negative control (+ RT and –RT). Lane 8: *TbAT1*/P2 + RT. Lane 9: *TbAT1*/P2 – RT. Lane 10: Actin (positive control). Lane 11: 1KB ladder.

cDNA from P1000 strain, Lane 1: 1KB ladder. Lane 2 AT-E + RT. Lane 3: AT-E – RT. Lane 4 AT-A + RT. Lane 5: AT-E gene – RT. Lane 6, lane 7 Negative control (+ RT and –RT). Lane 8: *TbAT1*/P2 + RT. Lane 9: *TbAT1*/P2 – RT. Lane 10: Actin (positive control).

cDNA from *TbAT1*-B48 strain, Lane 1: 1KB ladder. Lane 2 AT-E + RT. Lane 3: AT-E – RT. Lane 4 AT-A + RT. Lane 5: AT-E gene – RT. Lane 6, lane 7 Negative control (+ RT and –RT). Lane 8: *TbAT1*/P2 + RT. Lane 9: *TbAT1*/P2 – RT. Lane 10: Actin (positive control). Lane 11: 1KB ladder.

+RT: cDNA treated with Reverse transcriptase

– RT: No reverse transcriptase was added when making cDNA.

Negative control: samples of PCR reaction lacking gene primers.

The result showed that AT-A transcription was perhaps slightly reduced in both pentamidine resistant cell lines when compared to the 427-WT. However, adaptation to high concentrations of pentamidine resulted in a clear decrease of the AT-E transcription in *TbAT1*-B48 and further reduction to 1000 nM of pentamidine resulted in substantial decrease of AT-E transcription. The bands in Figure 5.8 correspond to the right size of AT-E and AT-A genes and *TbAT1/P2* (1389 bp, 1449 bp and 677 bp, respectively, for the fragments amplified). As expected, all three genes are present in 427-WT whereas *TbAT1/P2* is missing in P1000 and B48. The density of the bands in (panels A, B and C- lane 4) appears to show a slight reduction of the AT-A gene expression in P1000 and *TbAT1*-B48 compare to the wild type. However, AT-E expression was reduced in the *TbAT1*-B48 (panel C- lane 2) cell line and almost vanished in the P1000 cell line (panel B- lane 2). This strongly suggests that adaptation to a higher concentration of pentamidine somehow disrupted the (expression of the) AT-E gene and downregulated the mRNA transcription, presumably leading to reduced protein synthesis.

## 5.8 Discussion

Alterations in drug targets or loss of drug uptake by membrane transporters is associated with development of trypanocidal resistance in *T. brucei* (Mäser *et al*, 2003). Loss of TbAT1/P2 led to 2-3-fold resistance to melarsoprol and pentamidine but a significantly higher level of resistance to diminazene (18-fold) (Matovu *et al*, 2003; Lanteri *et al*, 2006). However, the *tbat1*<sup>-/-</sup> mutant was still sensitive pentamidine and diminazene due to the presence of HAPT1 and LAPT1 which are used as other routes for the uptake of pentamidine and possibly other diamidines (de Koning, 2001; de Koning & Jarvis, 2001). Adaptation of this strain to high concentration of pentamidine resulted in loss of HAPT1 activity in pentamidine transportation leaving LAPT1 activity untouched (Bridges *et al*, 2007).

Thus *in vitro* adaptation successfully selected for loss of the HAPT1 transport activity and it was anticipated that further adaptation might cause the loss of LAPT as well, yielding a null-pemntamidine transport line. Uptake of radiolabelled pentamidine in P1000 have shown that LAPT1 phenotype activity remained unchanged with  $K_m$  value of  $99 \pm 24 \mu\text{M}$  and  $V_{\text{max}}$  of  $1.3 \pm 0.3 \text{ pmol}(10^7 \text{ cells}^{-1})\text{s}^{-1}$ . These values are very similar to the published values for *TbAT1*-B48 cell line in which the  $K_m$  value and a  $V_{\text{max}}$  for LAPT1 were  $56 \pm 7 \mu\text{M}$  and  $0.82 \pm 0.20 \text{ pmol}(10^7 \text{ cells}^{-1})\text{s}^{-1}$  respectively. This finding strongly suggests that P1000 cells have developed a new resistance mechanism unrelated to transport of the drug across the plasma membrane.

The resistance induction process was initially started with culturing *TbAT1*-B48 cells at a concentration as low as 75 nM of pentamidine; that equals a 13 fold resistance when considering the final concentration of 1000 nM in the growth medium. However, the alamar blue results show resistance factor of only 3 fold, this could be explained either by: induction of pentamidine resistance somehow led to a new mutation that interrupted the reduction pathway of resazurin dye, thus resulted in less fluorescence to be measured. This case was also observed when AT-E gene was knocked down using RNAi in bloodstream forms. Pentamidine adaptation also resulted in increased resistance to other P2 and HAPT1 dependent trypanocides, including diminazene and cymelarsan.

The most fundamental need was to obtain a better understanding of the mechanism of resistance. The molecular investigation of the levels of transcription of both AT-A and AT-E genes, which are thought to encode LAPT1 and HAPT1, respectively, showed that adaptation to high concentrations of pentamidine resulted in a small decrease in mRNA levels of AT-E, and possibly of AT-A, in *TbAT1*-B48. This experiment further showed that AT-E expression is downregulated after further adaptation to 1000 nM of pentamidine without affecting AT-A transcription. The sequence analysis presented afterwards identified no alterations to the AT-E and AT-A genes, compared to the wild type 427 and the parental cell line *TbAT1*-B48.

The study of the mitochondrial membrane potential has shown that adaptation to 1000 nM pentamidine has resulted in apparently dysfunctional mitochondria, but it is important to note that troglitazone was able to modestly increase fluorescence in this cell line, apparently restoring some membrane potential to the mitochondrion, by an unknown mechanism. This study was performed in presence and absence of drug. In a drug-free environment the mitochondrial membrane potential was significantly reduced to (9.75%) in P1000 compare to (50.2%) in 427-WT and (31.3%) in *TbAT1*-B48 to cell line. Cultivation with pentamidine showed that the drug caused a clear reduction of the mitochondrial membrane potential in both 427-WT and *TbAT1*-B48, whereas in P1000 was shown to be very similar to the drug free samples. This strongly suggests that pentamidine targets the mitochondrial and additional resistance to pentamidine is related to the loss of the mitochondrial function and cells are able to overcome the absence of this function.

The wild type AT-E1 and AT-E2 open reading frame is present unchanged in the three strains. From the MMP results AT-E2 was shown to be less active than AT-E1 in mediating a response to pentamidine after expression in a drug resistant cell line.

This lead us to conclude that AT-E1 is important for pentamidine transport and the findings are consistent with the gene encoding HAPT1. *TbAT*-E2 does not appear to mediate pentamidine uptake, at least not to the same extent as AT-E1, but its expression in B48 restored the mitochondrial membrane potential, showing it to be a physiologically important protein. It is possible that it is

located on the mitochondrial membrane and tagging experiments will have to determine this. Further investigations including biochemical and molecular methods have also been carried out to confirm the relationship between the two AT-like genes and the three pentamidine transporters (P2, HAPT1 and LAPT1); these investigations are detailed in chapter 7.

**6 Cloning, sequencing, and analysis of the AT-like transporter genes from multiple *T. b. brucei* lines**

## 6.1 Introduction

The interaction of drugs that are used in treating many tropical parasitic diseases and the study of the way in which the drugs cross cell membrane has always been through comparative biochemistry, leaving a lack of information about the drug entry. Sometimes the way of entry is rather complicated; especially if the drug has to cross more than one plasma membrane in order to reach its target. A good example of this are *Leishmania*, which reside intracellularly and drugs have to cross both the mammalian plasma membrane and the parasitophorous vacuole membrane, as well as the parasites membrane (Johnston *et al.*; 1999).

The various protozoan genome projects, in combination with comparative biochemical approaches, have resulted in new insights into how parasites develop, survive and reproduce within the host, as well as the response of the immune system. The identification of factors such as pathogenicity, drug resistance and antigenic variation has allowed more rapid identification of drug targets (Johnston *et al.*; 1999).

The understanding of the molecular biology of trypanosomes has become of great interest in the de Koning laboratory, specifically to study transporters and define the mechanism of the drug delivery and bridge the gap between research and clinical necessities. Many tools have been developed in order to facilitate the understanding of molecular biology and the biochemical physiology of the protozoa in contrast to their mammalian hosts. These tools include on-line databases, functional genomics, proteomics, gene knockout protocols, and transgenic strategies (Christensen, 2004).

In this thesis we report on the roles of some transporters involved in the uptake and delivery of the diamidine and melaminophenyl arsenical drugs to *Trypanosoma spp* cells, using pentamidine resistance and uptake as a convenient probe. Pentamidine is concentrated in *T. b. brucei* by at least three transporters designated P2, HAPT1 and LAPT1 transporters; this may explain why little or no resistance to pentamidine occurs in the field. In 1999 Mäser and coworkers identified the *TbAT1* gene as encoding the P2 transporter. To study the function of this transporter, *TbAT1* was knocked out in the parental strain *T. brucei* s427-

WT (Matovu *et al.*, 2003). Besides being an adenosine transporter it was found to be responsible for most of the pentamidine delivery (Bray *et al.*, 2003). The *TbAT1*- KO strain was adapted to higher concentrations of pentamidine *in vitro* in our laboratory. This strain is named TbAT1-B48 and has been used to study the uptake of various concentrations of pentamidine (Bridges *et al.*, 2007).

The purine and pyrimidine transporters that have been cloned so far in trypanosomatids are members of the Equilibrative Nucleoside Transporter (ENT) family. This family of transporters takes up a number of nucleosides and nucleobases; some of them specifically recognise purines, whereas others recognize both purines and pyrimidines (De Koning *et al.*, 2005).

The genome of *T. brucei* revealed 12 different nucleoside transporters of the ENT family (Ortiz *et al.*; 2009). Some of these transporters and the genes coding for them have been well characterised, others are still under investigation. *TbAT1* encoding the P2 transporter was the first ENT gene to be identified and was cloned in *T. b. brucei* and found to mediate adenosine and adenine (Carter *et al.*; 1993; Sanchez *et al.*; 1999).

The P2 transporter is only expressed in the bloodstream form of *T. brucei*. It displays a high-affinity for adenosine and adenine (aminopurines) with a low affinity for guanosine, inosine, hypoxanthine, guanine and allopurinol (oxopurines) (de Koning & Jarvis, 1997; de Koning, 2001; Lanteri *et al.*; 2006).

A cell line lacking P2 transporter activity was produced by targeted deletion of the *TbAT1* gene and confirmed that P2 is greatly involved in the uptake of several drugs including diamidine and melaminophenyl arsenical classes of trypanocides, which are considered as first line drugs against HAT and in veterinary medicine (Carter *et al.* 1995, Matovu *et al.* 2003).

In addition to the P2 transporter, two other pentamidine transport activities have been characterised. The High Affinity Pentamidine Transporter (HAPT1) and the Low Affinity Pentamidine Transporter (LAPT1). High concentrations of purines and pyrimidines do not affect either of these proteins, and the genes responsible for encoding them still need to be investigated (de Koning 2001; de Koning *et al.*, 2005).

The second nucleoside transporter, P1, is expressed in both the procyclic form (PF) and the bloodstream form (BSF). The encoding gene is designated *Trypanosoma brucei* Nucleoside Transporter 2 (TbNT2). This gene was cloned and expressed in *Xenopus* oocytes (Sanchez *et al.*; 1999) and was found to mediate the uptake of adenosine, inosine and guanosine (Landfear, 2001; Mäser *et al.*; 1999).

Several genes belonging to the ENT family were lately characterised and named TbNT2 to TbNT12. The study of their functional expression in *Xenopus oocytes* found that some high affinity purine transporter genes are ~85% identical to TbNT2 (Ortiz *et al.*; 2009; Landfear, 2010). In 2004 Sanchez and colleagues identified TbNT10 within the short stumpy form of the life cycle, which is pre-adapted for infection of the tsetse fly. In the yeast *Saccharomyces cerevisiae* the TbNT10 gene conferred a capability to mediate the uptake of adenosine, guanosine and inosine (Sanchez *et al.*; 2004).

## 6.2 Identification of AT-like genes

The cloning of TbNT2 - TbNT10 was followed by the identification of three adenosine-insensitive ENT transporter genes from the same phylogenetic subgroup as the *TbAT1* gene; these were designated AT-A, AT-G and AT-E (Figure 1.8) (de Koning *et al.* 2005). Other authors have named those genes differently using *TbNT* numbers by linking the genes to their nucleoside transport function (Ortiz *et al.*, 2009), see Table 6.1.

As mentioned in Chapter 2 the identification of the AT-like genes was used the genome sequence for *Trypanosoma brucei* strain TREU927 from GeneDB as a reference sequence. The GeneDB *Trypanosoma brucei* database was screened using BLAST searches with known ENT transporter genes (TbAT1, TbNT2, TbNBT1) to identify these genes: Tb09.244.2020 for the AT- A, Tb09.V4.0106 for AT- G and Tb927.3.590 for AT- E. The old systematic number Tb03.6N20.7000 for AT-E was also used in the search using the GeneDB database.

Systematic Name	Name used by de Koning	Name used by Landfear	substrate	Location of gene
Tb09.244.2020	AT- A	TbNT11.1	Hyp. Ade, Xan, Pentamidine	Chromosome 9
Tb09.V4.0106	AT- G	TbNT11.2	Not studied	Chromosome 9
Tb927.3.590	AT- E1	TbNT12.1	Ade, pentamidine	Chromosome 3
Tb927.3.590	AT- E2	TbNT12.2	Ade	Chromosome 3

**Table 6.1. Alternative nomenclature for the AT like genes.**

The amino acid sequences on the genome database shows that the three putative genes share 58%, 58% and 66% identity with the *TbAT1* gene, respectively. They are also the most closely related genes to the *TbAT1* gene on the phylogenetic tree and they cluster together to form one group (see Figure 1.8). Due to the close position of the AT-like genes to *TbAT1*, the only known pentamidine transporter, it was hypothesised that these novel three genes may encode the High Affinity Pentamidine Transporter (HAPT1) and/or Low Affinity Pentamidine Transporter (LAPT1). AT-A has been previously confirmed to be capable of diamidine uptake when expressed in yeast (De Koning, unpublished). It has also been shown that high concentrations of purines or pyrimidines failed to inhibit HAPT or LAPT, but the function of the transporters is as yet unknown (de Koning *et al.*, 2005).

In this project, the complete open reading frame of the AT-A and AT-E putative genes were amplified by PCR from genomic DNA using specific primers. Subsequently, they were cloned into the pGEM-T Easy vector and sequenced in order to verify nucleotide sequence and amino acid translation compositions.

### **6.2.1 Polymerase chain reactions and cloning of AT-like sequences**

PCR was used to amplify segments of DNA between two known regions from total *T. b. brucei* genomic DNA. Forward and reverse PCR primers were designed for the AT-like sequences (AT-A, AT-G and AT-E) (Figure 6.1) (See chapter 2).

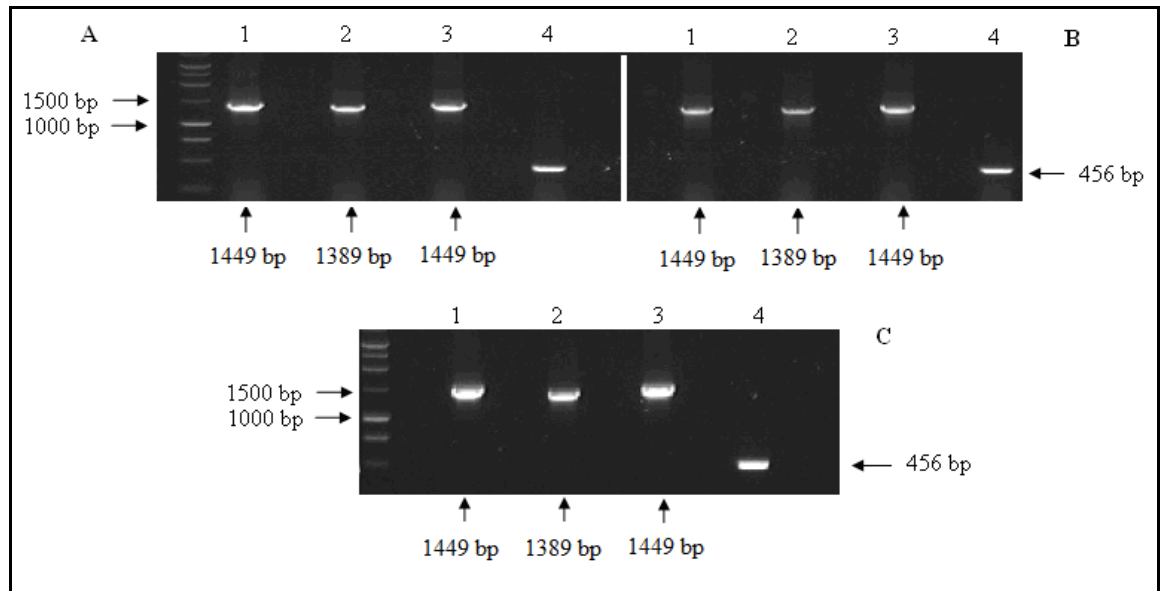


**Figure 6.1.** PCR amplification of AT-A (lane1), AT- E (lane2) and AT-G (lane 3) from the three strains of blood stream form *T. b. brucei*.

(A) s427-WT (B) TbAT1-B48 and (C) P1000. Primers used are detailed above. Actin (at 456 bp) was included as a positive control (lane 4). 1 molecular markers show the amplified fragments at the expected size.

Products of the expected sizes were obtained for all three putative genes from three different cell lines, using *KOD* hot start DNA polymerase following PCR conditions described in chapter 2. Temperature and incubation times were optimized for each reaction. As a control PCR, the actin gene of 456 bp was amplified using forward and reverse primers.

PCR products were A-tailed by incubation with *Taq* as described in Section 2.7.4 and ligated into the pGEM-T easy vector. After ligation, the resulting constructs were amplified in *E. coli* JM109 or XL1 blue cells and a series of restriction enzyme digests, as described below, confirmed that all inserts were of the correct predicted size and possessed the restriction enzyme sites predicted from the genome database sequences.

*Eco*RI digestion of the AT-A+pGEM-T Easy yields the 1449 bp insert and the approximately 3.0 kb backbone of the pGEM-T Easy vector (Figure 6.2, A). When the AT-like A+ pGEM-T Easy construct is digested with *Sal*I two fragments are produced, one of 965 bp and the other of ~3.5 kb. This step was carried out to confirm correct cloning of the insert since this enzyme has two restriction sites one within the AT-A sequence and the second is within the sequence of the vector (Figure 6.2, B).

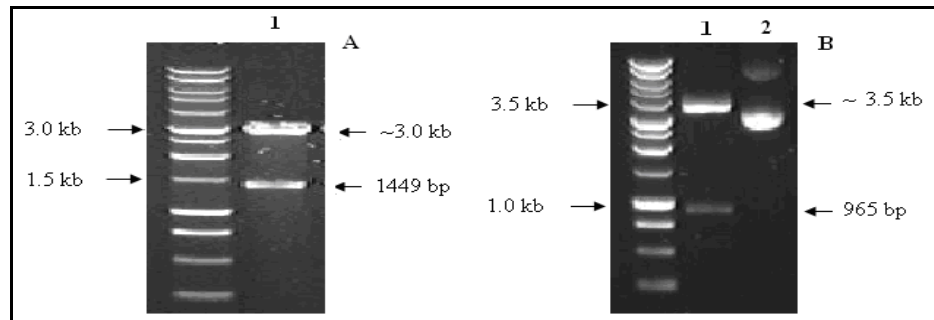


**Figure 6.2.** *EcoRI* digestion releases AT-A insert (1449 bp) from the pGEM-T Easy. pGEM-T Easy backbone at about 3.0 kb (A, Lane 1). (B) Digestion with *SalI* resulted in 965 bp confirming correct ligation of the insert into the pGEM-T Easy (Lane1). Lane 2: undigested construct (AT-A + vector). The molecular weight marker is a 1.0 kb ladder.

*EcoRI* digestion of the AT-E + pGEM-T Easy construct gave bands of 1389 bp for the AT-E insert fragments and about 3.0 kb represents backbone of the pGEM-T Easy vector (Figure 6.3, A). There are two sites for the *A/wNI* enzyme within the AT- E sequence and within the sequence of the vector; digestion with this enzyme resulted in release of 982 bp fragment from the construct (about 3.4 kb) confirming correct cloning of the insert (Figure 6.3, B).

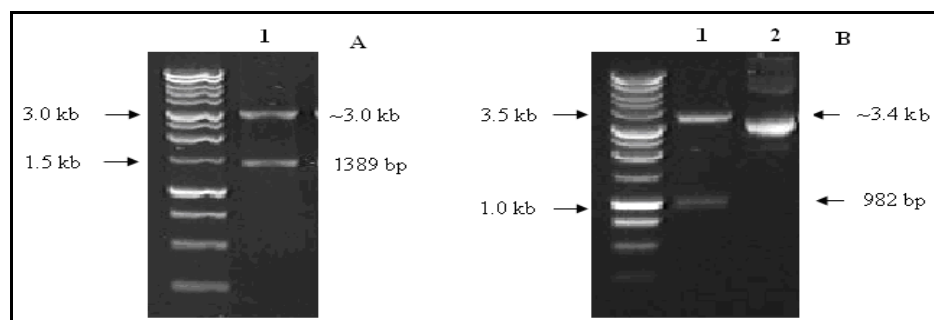


**Figure 6.3.** *EcoRI* digestion releases AT-E insert (1389 bp) from the pGEM-T Easy. pGEM-T Easy backbone at about 3.0 kb (A, lane 1). (B) Digestion with *A/wNI* resulted in 982 bp confirming correct ligation of the insert into the pGEM-T Easy (lane 1). Lane 2: undigested construct (AT-E + vector).

Digestion of the AT-G + pGEM-T Easy construct with *EcoRI* released the 1449bp insert from the vector (about 3.0 kb) as shown in (Figure 6.4, A). Another digest of the construct to confirm correct cloning was completed using *A/wNI*. This led to a linearisation of the construct and produced a single fragment of about 4.5 kb corresponding to the size of the AT-G insert plus the vector backbone (Figure 6.4, B).

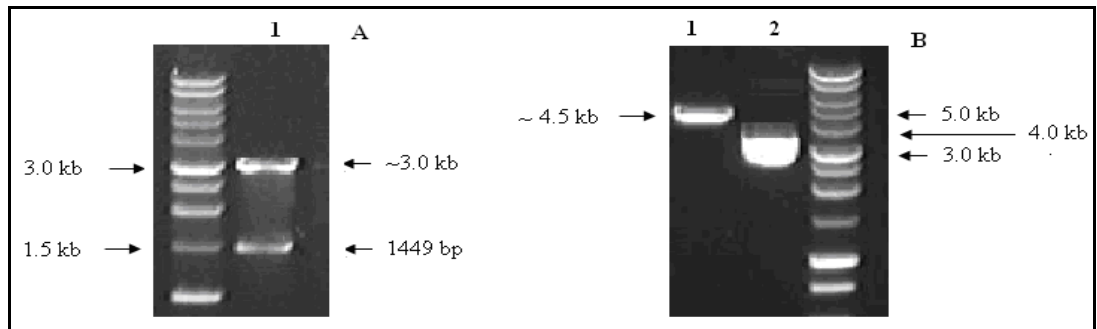


**Figure 6.4.** *EcoRI* digestion releases AT-G insert (1449bp) from the pGEM-T Easy. pGEM-T Easy backbone at about 3.0 kb (a, lane 1). (B) Digestion with *A/wM* led to a linearisation of the construct and produced a single fragment of about 4.5 kb. Lane 2: undigested construct (AT-G + vector).

### 6.2.2 Sequence analysis

The AT-like clones in pGEM-T Easy were generated from two or three independent polymerase chain reactions per gene. Each gene was amplified from genomic DNA isolated from bloodstream forms of three different cell lines of *T. brucei*: 427-WT, *TbAT1*-B48 and P1000. Sequences were checked for any mutations that could explain the increase in resistance to pentamidine.

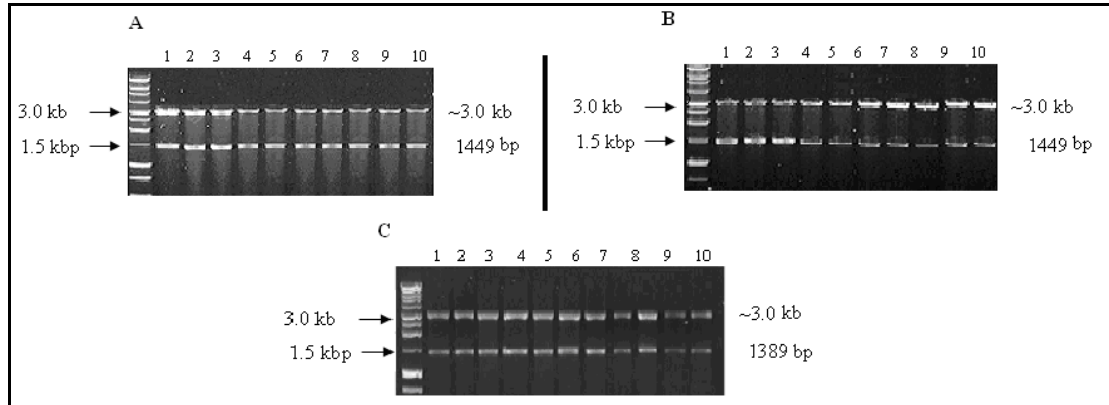


**Figure 6.5.** Electrophoresis gels representing some of the *EcoRI* digest of the purified plasmid DNA containing the AT-like inserts.

(A) AT-A (B) AT-G and (C) AT-E genes appropriate enzymes. Each lane corresponds to a purified sample generated from a single colony.

After confirmative digests with *EcoRI* (Figure 6.5), a minimum of 12 separate clones per gene (from three strains) were sequenced. A number of the AT-like constructs and sequences, from *T. brucei* WT and *TbAT1*-B48 were made by a different member in the De Koning group, Dr. Jane Munday, but are included in this chapter to allow for a fuller comparison.

Full-length sequencing was completed by two reads from either end of the insert in pGEM-T Easy using primer pairs T7 and SP6 or M13F and M13R. The sequence alignments for the AT-E gene from the three strains showed that there are two different sequences of the gene which from now on will be named AT-E1 and AT-E2. The sequences of 427-WT, TbAT1-B48 and P1000 displayed 21 single nucleotide differences from the AT-E reference in GeneDB. Only 10 of these point mutations were of importance at the amino acid level (Table 6.2 & Appendix D). However, in the three strains utilised in this study (s427, B48 and P1000) the AT-E1 and AT-E2 sequences were identical. Table 6.2 shows in detail the similarities and point mutations in AT-E1 and AT-E2 relative to the AT-E reference (strain 927, GeneDB). For example, C146A results in the amino acid change proline-49 to histidine in AT-E2 whereas the DNA sequence of AT-E1 at this position is identical to the reference. An overview is presented in Table 6.2.

Potentially the most important single mutation, which is currently believed to have contributed to the loss of pentamidine uptake by AT-E2 is G728A, leading to a change of the small aliphatic amino acid glycine-243 to aspartate, a negatively charged amino acid. The defectiveness of AT-E2 for pentamidine transport was concluded after re-expressing the AT-E1 and AT-E2 genes in the TbAT1-B48 cell line and assessing pentamidine sensitivity with alamar blue, as well as pentamidine transport analysis (De Koning, unpublished), together with the study of the MMP described in chapter 5 showed the reduced activity of pentamidine uptake in the B48 + AT-E2 compare to the B48 transfected with the active copy of AT-E1. Both alleles were also expressed in yeast and, whereas AT-E1 clearly sensitised these cells to pentamidine during growth on glycerol, AT-E2 had hardly any effect on this (De Koning, unpublished).

In two of the sequences, AT-A5 and AT-A6, there is a 44 bp deletion from the 1187<sup>th</sup> base onwards; this deletion results in a frameshift and an early stop codon, resulting in the translated protein only having 10 transmembrane domains, instead of 11. Further investigation is underway in the De Koning group as to whether sequence AT-A5 is indeed a real sequence. Sequence AT-A3 has a deletion at base 89, resulting in a frameshift and a very early stop codon. These three sequences are unlikely to code for functional transporters.

In contrast, the three remaining sequences, AT-A1, A2 and A4 are all predicted to code for proteins with 11 transmembrane domains (using "DAS" - Transmembrane Prediction - M. Cserzo *et al.* 1997), suggesting they are functional transporter proteins. Sequences AT-A1 and A2 have four SNPs different from one another, but they both code for the same amino acid sequence. Sequence AT-A4 has a slightly different amino acid sequence, not having the change E54G.

An alignment of the predicted amino acid sequences of AT-E1, AT-E2 and the six different sequences of AT-A (1-6) from the 427 wild type are presented in (Appendix D). However, while these sequences indicate the number of different alleles present in s427WT, the copy number for each gene cannot be derived from this information.

AT-like/cell line	bp	SNP	AA	AA <sub>s</sub>	bp	SNP	AA	AA <sub>s</sub>	bp	SNP	AA	AA <sub>s</sub>	bp	SNP	AA	AA <sub>s</sub>
927-WT.AT-Eref	84	A	Thr	ACA	111	T	Phe	TTT	126	C	Tyr	TAC	132	T	Tyr	TAT
427-WT.AT-E1	.	G	.	ACG	.	C	.	TTC	.	C	.	TAC	.	C	.	TAC
427-WT.AT-E2	.	G	.	ACG	.	C	.	TTC	.	T	.	TAT	.	C	.	TAC
B48.AT-E1	.	G	.	ACG	.	C	.	TTC	.	C	.	TAC	.	C	.	TAC
B48.AT-E2	.	G	.	ACG	.	C	.	TTC	.	T	.	TAT	.	C	.	TAC
P1000.A T-E1	.	G	.	ACG	.	C	.	TTC	.	C	.	TAC	.	C	.	TAC
P1000.A T-E2	.	G	.	ACG	.	C	.	TTC	.	T	.	TAT	.	C	.	TAC
	bp	SNP	AA	AA <sub>s</sub>	bp	SNP	AA	AA <sub>s</sub>	bp	SNP	AA	AA <sub>s</sub>	bp	SNP	AA	AA <sub>s</sub>
927-WT.AT-Eref	135	G	Ala	GCG	146	C	Pro	CCC	186	C	Val	GTC	236	T	Leu	TTA
427-WT.AT-E1	.	A	.	GCA	.	C	Pro	CCC	.	C	.	GTC	.	T	.	TTA
427-WT.AT-E2	.	A	.	GCA	.	A	His	C4 C	.	T	.	GTT	.	C	Ser	TCA
B48.AT-E1	.	A	.	GCA	.	C	Pro	CCC	.	C	.	GTC	.	T	Leu	TTA
B48.AT-E2	.	A	.	GCA	.	A	His	C4 C	.	T	.	GTT	.	C	Ser	TCA
P1000.A T-E1	.	A	.	GCA	.	C	Pro	CCC	.	C	.	GTC	.	T	Leu	TTA
P1000.A T-E2	.	A	.	GCA	.	A	His	C4 C	.	T	.	GTT	.	C	Ser	TCA
	bp	SNP	AA	AA <sub>s</sub>	bp	SNP	AA	AA <sub>s</sub>	bp	SNP	AA	AA <sub>s</sub>	bp	SNP	AA	AA <sub>s</sub>
927-WT.AT-Eref	322	G	Val	GTC	502	A	Ile	ATC	649	C	Pro	CCA	687	C	Ala	GCC
427-WT.AT-E1	.	G	Val	GTC	.	G	Val	TGT	.	T	Ser	TCA	.	C	.	GCC
427-WT.AT-E2	.	A	Ile	A TC	.	A	Ile	ATC	.	C	Pro	CCA	.	T	.	GCT
B48.AT-E1	.	G	Val	GTC	.	G	Val	TGT	.	T	Ser	TCA	.	C	.	GCC
B48.AT-E2	.	A	Ile	A TC	.	A	Ile	ATC	.	C	Pro	CCA	.	T	.	GCT
P1000.A T-E1	.	G	Val	GTC	.	G	Val	TGT	.	T	Ser	TCA	.	C	.	GCC
P1000.A T-E2	.	A	Ile	A TC	.	A	Ile	ATC	.	C	Pro	CCA	.	T	.	GCT
	bp	SNP	AA	AA <sub>s</sub>	bp	SNP	AA	AA <sub>s</sub>	bp	SNP	AA	AA <sub>s</sub>	bp	SNP	AA	AA <sub>s</sub>
927-WT.AT-Eref	728	G	Gly	GGC	730	G	Ala	GCA	741	C	Gly	GGC	763	T	Ser	TCC
427-WT.AT-E1	.	G	Gly	GGC	.	A	Thr	A CA	.	T	.	GGT	.	C	Pro	CCC
427-WT.AT-E2	.	A	Asp	G4 C	.	A	.	A CA	.	C	.	GGC	.	C	.	CCC
B48.AT-E1	.	G	Gly	GGC	.	A	.	A CA	.	T	.	GGT	.	C	.	CCC
B48.AT-E2	.	A	Asp	G4 C	.	A	.	A CA	.	C	.	GGC	.	C	.	CCC
P1000.A T-E1	.	G	Gly	GGC	.	A	.	A CA	.	T	.	GGT	.	C	.	CCC
P1000.A T-E2	.	A	Asp	G4 C	.	A	.	A CA	.	C	.	GGC	.	C	.	CCC
	bp	SNP	AA	AA <sub>s</sub>	bp	SNP	AA	AA <sub>s</sub>	bp	SNP	AA	AA <sub>s</sub>	bp	SNP	AA	AA <sub>s</sub>
927-WT.AT-Eref	828	C	Thr	ACC	853	G	Asp	GAC	1050	C	Asp	GAC	1243	G	Ala	GCG
427-WT.AT-E1	.	G	.	ACG	.	A	Asn	A AC	.	T	.	GAT	.	A	Thr	A CG
427-WT.AT-E2	.	G	.	ACG	.	G	Asp	GAC	.	C	.	GAC	.	G	Ala	GCG
B48.AT-E1	.	G	.	ACG	.	A	Asn	A AC	.	T	.	GAT	.	A	Thr	A CG
B48.AT-E2	.	G	.	ACG	.	G	Asp	GAC	.	C	.	GAC	.	G	Ala	GCG
P1000.A T-E1	.	G	.	ACG	.	A	Asn	A AC	.	T	.	GAT	.	A	Thr	A CG
P1000.A T-E2	.	G	.	ACG	.	G	Asp	GAC	.	C	.	GAC	.	G	Ala	GCG
	bp	SNP	AA	AA <sub>s</sub>	bp	SNP	AA	AA <sub>s</sub>								
927-WT.AT-Eref	1248	A	Leu	CTA	1356	C	Leu	CTC								
427-WT.AT-E1	.	G	.	CTG	.	T	.	CTT								
427-WT.AT-E2	.	A	.	CTA	.	T	.	CTT								
B48.AT-E1	.	G	.	CTG	.	T	.	CTT								
B48.AT-E2	.	A	.	CTA	.	T	.	CTT								
P1000.A T-E1	.	G	.	CTG	.	T	.	CTT								
P1000.A T-E2	.	A	.	CTA	.	T	.	CTT								

**Table 6.2. Summary of the polymorphic nucleotides in AT-E genes.**

**Polymorphic nucleotides in AT-E genes.** in the drug sensitive 427-WT strain of *T.b. brucei* and the two pentamidine resistance strains after pentamidine induction (B48 and P1000).

Nucleotide positions are numbered vertically (conserved sites are not shown) from the start codon of the reference sequences. Dots indicate identity with the above data. Uppercase and bold italic letters indicate single nucleotide polymorphism caused the change of amino acid. (bp) position of polymorphic nucleotide. (AAs) Amino acid coding sequence. Highlighted cells indicate changes with the reference amino acid. Sequencing data was created using CLC 4.0.1 software using a minimum of 10 sequences per strain and the table indicating the polymorphic sites was created manually.

### **6.2.3 Southern blot analysis**

In order to determine the number of copies for the AT-E gene southern blotting was performed using AT-E gene probes from *T. b. brucei* genomic DNA. Restriction endonuclease digestions were performed with 10 µg genomic DNA from s427-WT (BSF), incubated with restriction enzymes for 24 hours. Restriction endonucleases were chosen to provide a diagnostic pattern of bands detectable on a Southern blot, as some of them cut at least once inside the gene and others cut once or several times in the region flanking the gene or cut once within upstream or downstream sequence (see restriction maps in Appendix C).

The restriction map was designed using GeneDB genome sequence for *Trypanosoma brucei* strain TREU927 as a reference. AT-E sequences ligated into pGEM-T Easy (pIT.03 and pIT.05 (chapter 2)) were also used to check for digestion sites in order to draw a restriction map for the enzymes. Vector NTI software was used to design the map and pick the restriction enzymes using a fragment of 412,389 bp in size, where 20 kb were added to each side of the AT-E gene (5' and 3' UTR) to provide a good cover of the sequences surrounding the putative gene (Appendix C).

As is shown in Figure 6.6 the fragments resulting from digestion with *Bgl*III, *Cl*I, *Eco*RI, *Mlu*I, *Nco*I, *Sal*I, *Xba*I and *Sna*BI hybridized to a single band suggesting that the gene could be present as a single copy inside the genome. However, digestion with *Bcl*I, *Eco*RV, *Kpn*I, *Pst*I and *Sac*I disagree with the digestion pattern of the other enzymes, and could be explained by differences in the sequences between homologous chromosomes confirming the presence of two copies AT-E gene or at least two different alleles (Figure 6.6 & Figure 6.7).

Combining the later observations with the data obtained from the sequences it is almost certain that there are two, and only two, different alleles of AT-E.

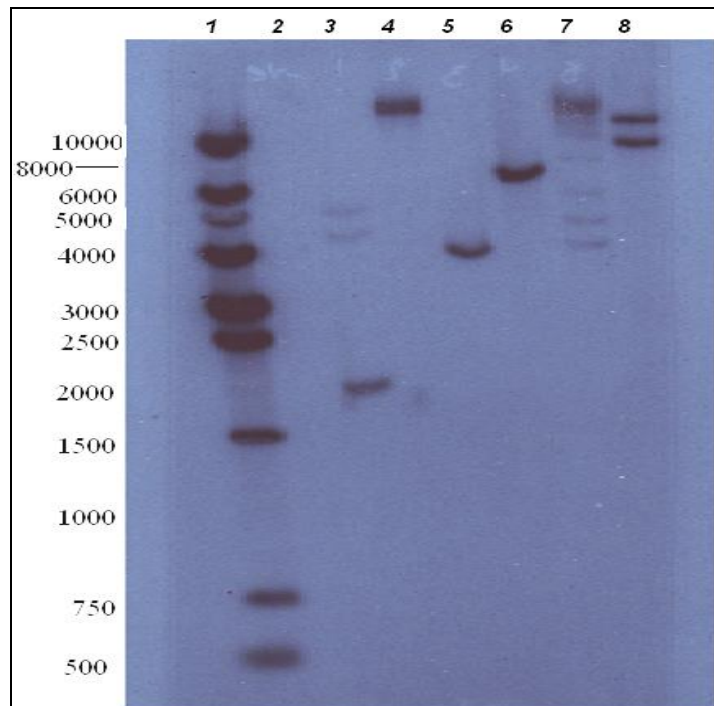


**Figure 6.6. Southern blot 1.**

Lane1: 1.0 kb ladder, 2: Blank well, 3: BclII digest, 4: BglIII digest, 5: ClaI digest, 6: EcoRI, 7: EcoRV, 8: KpnI digest.

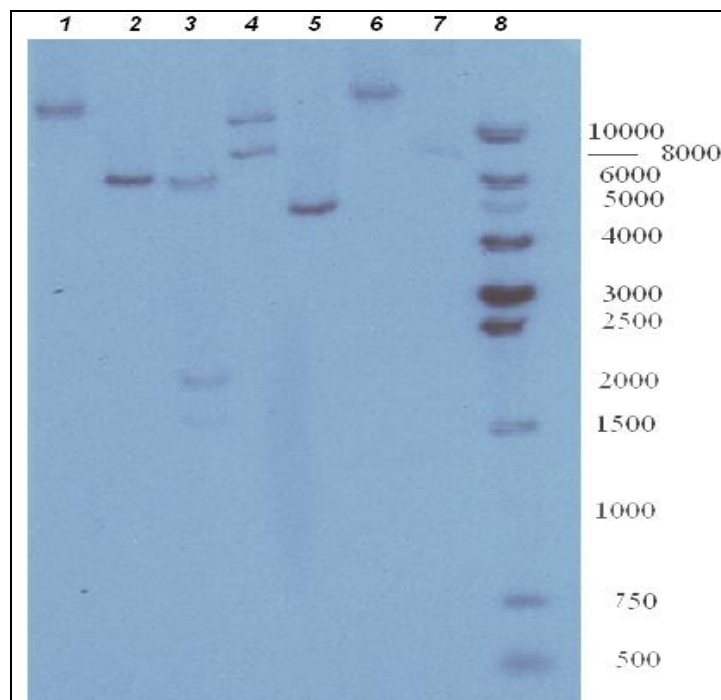


**Figure 6.7. Southern blot 2.**

Lane1: MluI digest, 2: NcoI digest, 3: PstI digest, 4: SacI digest, 5: Sall digest, 6: XbaI digest, 7: SnaBI digest, 8: 1.0 kb ladder.

Enzyme	Expected Fragment (bp)	Produced fragment (bp)	Comments
<i>BclI</i>	2022 + 6543	2022 + ~ 4500 + ~ 5500	The difference in the two bands could be explained as follows: There could be two alleles of a single gene. The 2022 bp band is as expected, with the two extra bands representing one allele each with a different site for the <i>BclI</i> enzyme in their
<i>BglII</i>	21022	> 10 kb	Band seems to be of the expected size
<i>ClaI</i>	4105	4105	Band of the expected size
<i>EcoRI</i>	7481	7481	Band of the expected size
<i>EcoRV</i>	4385	up to 8 distinct bands	Several bands in array pattern, this could be due to an incomplete digest.
<i>KpnI</i>	11461	11461 + ~ 13000	The additional band could be due to the presence of the restriction site at different position in the UTR of one of the alleles.
<i>MluI</i>	28351	> 10 kb	Band seems to be of the expected size
<i>NcoI</i>	11318	~ 6000	Could be an additional restriction site in one of the UTRs that is not anticipated on the reference genome, but present in the 427-WT strain.
<i>PstI</i>	1672 + 2091	1672 + ~ 2091 + ~ 6000	Using <i>PstI</i> expected to result in two bands as it cuts within the sequence of the gene 21089 bp. In addition it cuts at 18998 bp upstream of the gene and at 22761 bp downstream of the gene. The third unexpected band could be the absence of cutting site at 18998 bp upstream of the gene. on one of the alleles resulting in hybridization of the probe to an extra band between 21089 bp and 15160 bp.
<i>SacI</i>	9042	9042 + ~ 12000	Again different position of cutting site on the one of the alleles and absent on the other.
<i>SalI</i>	5158	5158	Band of the expected size
<i>XbaI</i>	~ 36000	> 10 kb	Band higher than 10 kb.
<i>SnaBI</i>	19871	~ 8000	Could be an additional restriction site in one of the UTRs that is not anticipated on the reference genome, but present in the 427-WT strain

Table 6.3. Southern blot analysis

#### 6.2.4 Expression of AT-like genes in P1000 in comparison to 427-WT and TbAT1-B48

As discussed in chapter 5, transcription levels of the relevant transporters were investigated using RT-PCR for s427WT, B48 and P1000. It was shown that mRNA levels of AT-E, but not AT-A, were progressively reduced in lines with increasing pentamidine resistance (B48, P1000) (Figure 5.8).

## 6.3 Discussion

There are several putative ENT family members in the *T. b. brucei* genome database for which activities have yet to be assigned. In addition to the three AT-like sequences described here, there are several transporters of unknown function, including several of the NT genes described by Sanchez and colleagues (Sanchez *et al.* 2002). In relation to pentamidine uptake and resistance TbAT1 is the only gene has been shown to be involved in pentamidine uptake. An additional three AT-like genes share the same phylogenetic group and based on this relationship AT-like A, E and G might code for the additional pentamidine transporters HAPT1 and LAPT1 (De Koning *et al.* 2005).

As pentamidine resistance in the B48 line and others has been clearly shown to be related to reduced pentamidine transport, it was thought that an analysis of the AT-like sequences in s427WT, B48 and P1000 could provide valuable insights in whether these genes code for pentamidine transporters.

The three AT-like genes have better sequence homology to TbAT1 than to the TbNT genes (Appendix D). Thus sequencing was essential for two reasons. Firstly, to check for any new point mutation in the pentamidine resistant cell lines compared to wild type. Secondly, to identify any sequence similarities between the three genes, which is essential to target any single gene using RNA interference. The latter technique, if sufficiently specific, would directly inform the investigator as to the involvement of the gene product in pentamidine transport (see chapter 7).

The cloning and sequencing were also important in determining the gene copy number using southern blot analysis. The sequence analysis showed that AT-A and AT-G were each 100% identical in all three strains and most likely to be a copies of one gene that is present as six different sequences, accordingly designated AT-A1 to AT-A6. This variability in the sequence shows that there are at least three copies of the AT-A gene (each heterozygote), each with two different alleles, or may be as many as six different genes (each being homozygote). This is still under investigation by other members of the group, as is its relation with the HAPT1 and LAPT1 pentamidine transporters.

The AT-E sequences in the three cell lines have clearly shown that the gene is present as two different sequences with a number of single nucleotide polymorphisms between them. One polymorphism that occurs in AT-E2, G728A, causes a change of glycine-243 to aspartate and is believed to be at least partly responsible for the loss of pentamidine uptake function. The loss of activity has been confirmed on many occasions including uptake assays and alamar blue pentamidine sensitivity assays (studied by other group members); it was also confirmed during the study of the mitochondrial membrane potential (see chapter 5).

Southern blotting was undertaken to study the copy number of the AT-E gene and from the data described above AT-E gene is highly likely to be present in one locus with two different alleles unless there is a duplication of the whole region. Final proof of this model was provided very recently by the construction of a AT-E knockout strain using only 2 rounds of transfection with homologous recombination cassettes (Munday and De Koning, unpublished). This latter observation also confirmed that AT-E is not an essential gene, at least not *in vitro*.

The large amount of sequence data obtained for this thesis has provided a clear picture for the study of HAPT1 at the molecular level. Among other things it allowed the identification of the sequences of the AT-like genes and enabled the design of RNAi constructs to specifically target the AT-E gene. AT-E RNAi cells could then be used to explore and clarify the role of AT-E in pentamidine transport in *T. b. brucei* (see chapter 7).

## **7 Validation of AT-E as a candidate diamidine transporter**

## 7.1 Introduction

The previous chapter described how the AT-like genes were identified, cloned and sequenced. This chapter will focus on AT-E and its role in diamidine uptake by *T. brucei*. The RNA interference (RNAi) technique was applied to test whether knockdown of AT-E gene activity will alter diamidine transportation in *T. brucei*. RNA interference is a technique in which a short homologous double stranded RNA is introduced to a cell, targeting expression of a specific gene at the level of mRNA stability, resulting in a reduced synthesis of the gene product. RNAi was first discovered by Fire and Mello and collaborators in the roundworm *C. elegans* (Fire *et al.*, 1998), in response to which defined gene functions were silenced (Hannon, 2002).

Gene expression involves two main processes, which are transcription and translation. These steps include the synthesis, maturation, and degradation of protein-coding messenger RNA (mRNA).

Transcription occurs when precursor-mRNA (pre-mRNA) molecules are produced due to the action of RNA polymerase II in the nucleus. This process involves some steps including removal of non-coding intron sequences in a process known as splicing. Then the cap is added to the 5' end and the poly-A tail to the 3' end of the fragment, after which it is transported to the cytoplasm and subsequently to the ribosome where translation takes place. Gene expression can be controlled by hybridizing an anti-sense agent to mRNA, which results in (1) blocking the translation process, and (2) degradation of part of the mRNA-anti-sense duplex through RNase H (Kent & MacMillan, 2004).

Many recent studies have now confirmed the ability of double-stranded RNA (dsRNA) to strongly decrease the production of a specific gene product. To monitor the effect of RNAi on the function of a single cell or whole organism is a powerful strategy for rapid analysis of gene function. This tool is widely used to silence specific genes coding for an endogenous protein. The mechanism of RNAi is simple and it proceeds through a number of sequential steps: starting with the cleavage of dsRNA by the RNase III enzyme DICER into shorter 21- 23 nucleotide dsRNA pieces that are also called short interfering RNAs or small interfering anti-sense strand of the RNAs (siRNAs). The siRNA guides its cognate mRNA into an

RNA-induced silencing complex, which rapidly cleaves the target mRNA, leading to an observable phenotype from which the function of the gene of interest can be derived (Rangasamy *et al*, 2008).

In the study of *Trypanosoma* species, the RNAi technique has been applied on many occasions as a method to study specific gene knockdown phenotypes. Rusconi and coworkers showed that an RNAi-induced phenotype can be verified by re-introduction of an RNAi-insensitive copy of the target gene. This functional complementation then proves that the observed phenotype really is attributable to the gene under study (Rusconi *et al*, 2005).

In order to improve the understanding of the roles of AT-E gene in the uptake of diamidines, the RNA Interference (RNAi) technique was applied to reduce expression of the gene. Diamidine transport was compared in trypanosomes with and without active expression of a dsRNA fragment of AT-E.

## 7.2 Results

### 7.2.1 RNAi in bloodstream forms

Bloodstream forms of *T. brucei* type 2T1 (Alsford & Horn, 2008) were used as expression model in the RNAi studies during this project. To generate a transgenic cell line, the 2T1 cells were transfected with an RNAi cassette containing a segment of the AT-E gene (designated RNAi/AT-E in chapter 2) via electroporation (Figure 2.7). This cassette is integrated into *T. brucei* genomic DNA after which the dsRNA expression, which is produced in a stem-loop formation, is controlled by tetracycline and driven by an RNA polymerase I promoter (Alsford & Horn, 2008).

A set of forward and reverse primers were designed (using RNAit software) (Redmond *et al.*, 2003) that incorporated four selected restriction sites noticing that the sites are present in the selected RNA fragment (Figure 7.1). These sites are included in order to create cohesive sites that are compatible with vector cloning sites.

Primers for sense and antisense fragment of RNAi/AT-E	<b>Forward:</b>
	5' AC <b>GGGCC</b> <b>GGTACC</b> AAGCTTGATCCCTCTGGCTGTTC GAC3'
	<b>Key to restriction sites:</b> <b>GGGCC</b> = <i>Apa</i> I, <b>GGTACC</b> = <i>Kpn</i> I
	<b>Reverse:</b>
	5' ACT <b>TCTAGA</b> <b>GGATCC</b> TCTGCTGCATACTTCATGGC 3'
	<b>Key to restriction sites:</b> <b>TCTAGA</b> = <i>Xba</i> I <b>GGATCC</b> = <i>Bam</i> HI

Table 7.1. Forward and reverse primers for RNAi/AT-E amplification.

Primers include restriction sites of the enzymes which were used afterwards to digest both the amplified fragment and the pRPa<sup>ISL</sup> vector for compatible ligation.

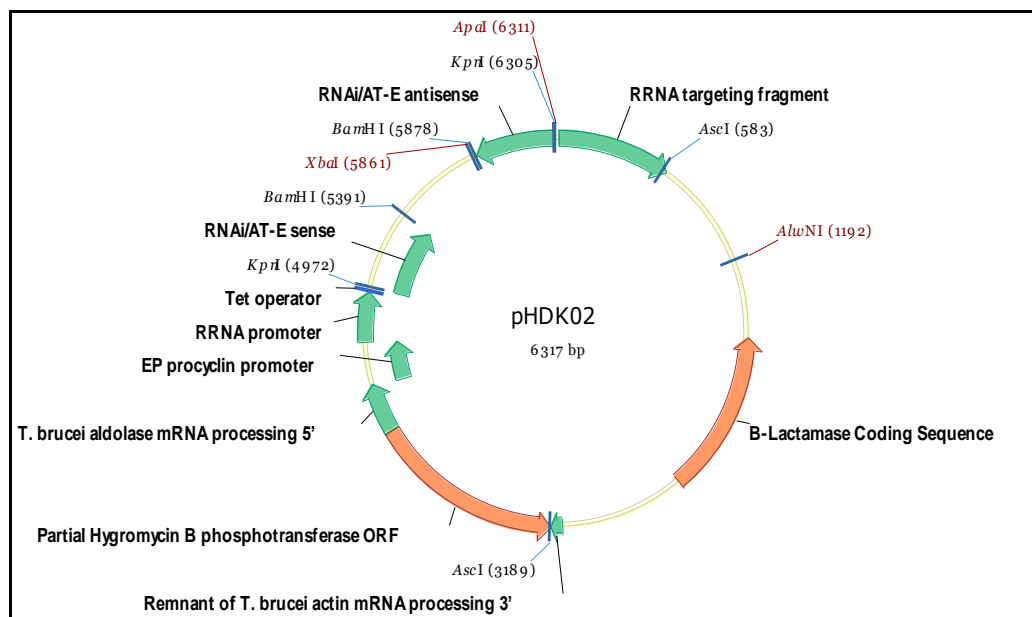


Figure 7.1. Map of pHDK02.

The sense fragment ligated into *Xba*I and *Apa*I sites and the antisense RNAi/AT-E fragment ligated into with *Kpn*I and *Bam*HI. The map also shows the restriction site of *Alw*NI and *Asc*I used in the screening for the correct ligation and in the release of the RNAi cassette from the vector backbone.

A segment of 411bp from position 263bp to position 674bp from the *T. brucei* AT-E gene was amplified from *T. brucei* strain 427 genomic DNA using the primers described below (Table 7.1) and cloned into pGEM-T- easy vector as described in section 2.8.1.

The stem-loop pRPa<sup>iSL</sup> vector (Alsford & Horn, 2008) was used as an RNAi vector in bloodstream forms of *T. brucei*, where the RNAi construct was created by cloning the RNAi/AT-E fragments twice in sense and antisense manner. The sense was ligated into pRPa<sup>iSL</sup> after restriction digestion with *KpnI* and *BamHI*, whereas the antisense was subsequently created after digestion with *XbaI* and *ApaI*.

### 7.2.1.1 Plasmid construction and cloning selection

A construct for AT-E RNAi using stem-loop pRPa<sup>iSL</sup> vector was generated by first inserting the sense fragment, followed by the insertion of the antisense fragment. The two steps are described below in details:

### 7.2.1.2 Ligation of the sense fragment

The RNAi/AT-E segment corresponding to 411bp of AT-E gene (Figure 7.2) was amplified from the bloodstream form 427-WT genomic DNA using the forward and reverse primers described above and *KOD* hot start polymerase (Novagen).

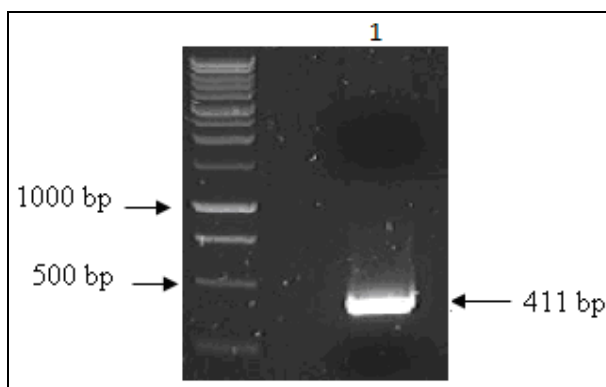
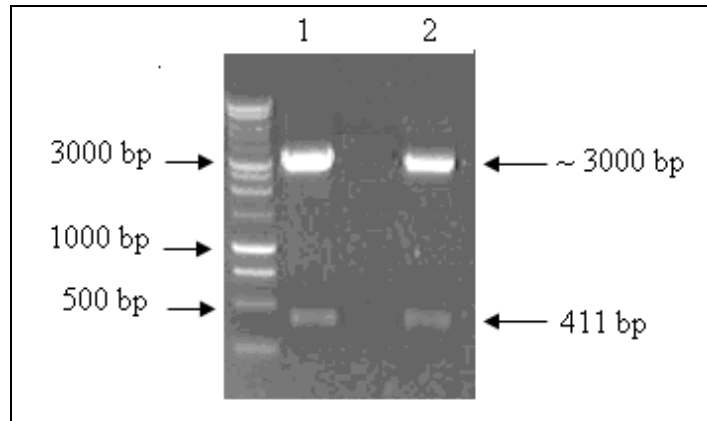


Figure 7.2. Amplification of the RNAi/AT-E fragment corresponding to 411 bp of AT-E gene of *T. brucei* (lane1).

The PCR product was incubated with 0.5  $\mu$ l *Taq* at 72 °C (as described in chapter 2) to create an A-overhang. After running on a 1% agarose gel the product was extracted using Qiagen gel extraction kit (Qiagen) then cloned into pGEM-T-Easy (Promega). The resulting construct was amplified in *E. coli* type XL1 (Stratagen), and then the plasmid was purified using the Qiagene miniprep kit. The presence of the RNAi/AT-E fragment was confirmed by enzymatic digestion (Figure 7.3).



**Figure 7.3.** Confirmation of correct restriction sites in the RNAi/AT-E fragment after transformation.

Restriction digest using *XbaI* and *ApaI* (Lane 1) and using *KpnI* and *BamHI* (lane 2) resulted in the release of the correct size of the RNAi/AT-E fragment from the pGEM-T-easy vector confirming the presence of the restriction sites required for subcloning into the RNAi vector. The molecular DNA size marker was included in every gel to identify the size of each band.

The cloning process involved a digestion of the sense segment of the RNAi/AT-E in pGEM-T-Easy along with the pRPa<sup>iSL</sup> vector with *KpnI* and *BamHI* in order to create compatible ligation sites (Figure 7.4).

Ligation into pRPa<sup>iSL</sup> vector was performed with 5  $\mu$ L of the restriction digested plasmid, 10  $\mu$ L of the restriction digested insert, 2  $\mu$ L ligation buffer, 1  $\mu$ L T4 DNA ligase and 2  $\mu$ L ddH<sub>2</sub>O followed by overnight incubation at 4 °C. The resulting construct carries the sense fragment of the RNAi/AT-E was amplified in XL1 competent cells then the plasmid DNA was purified using Qiagene miniprep kit and used thereafter in the second step of cloning.

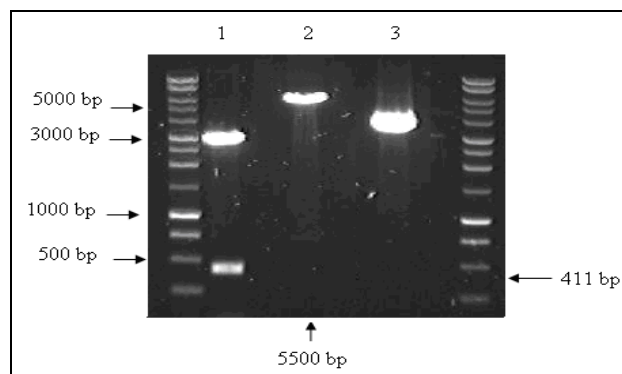


**Figure 7.4.** Digestion of pGEM-T-Easy + RNAi/AT-E construct with *KpnI* and *BamHI*. (Lane 1) digestion resulted in the release of the 411 bp RNAi/AT-E fragment. The 5500 bp band in lane 2) corresponds to the linearised pRPa<sup>iSL</sup> vector using *KpnI* and *BamHI*. Control, Non-digested pRPa<sup>iSL</sup> vector (lane5),

### 7.2.1.3 Second step of cloning (insertion of antisense fragment)

The previous paragraph describes the insertion of the sense of the RNAi/AT-E fragment into the RNAi stem-loop vector. In order to complete the RNAi/AT-E construct a second fragment of the same size of 411bp was cloned into the construct that resulted from the first step of cloning (pRPa<sup>iSL</sup> vector + sense RNAi/AT-E segment) after digestion with *Xba*I and *Apa*I enzymes (Figure 7.5).

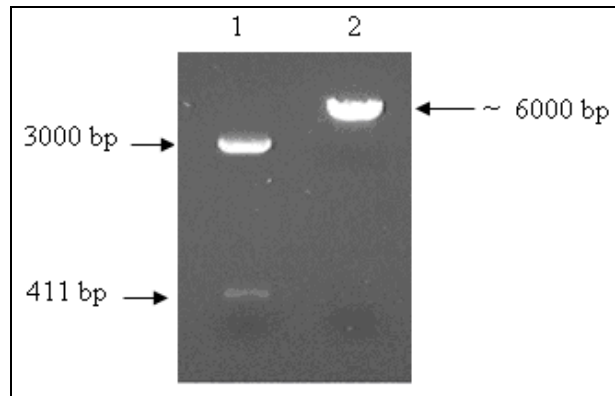
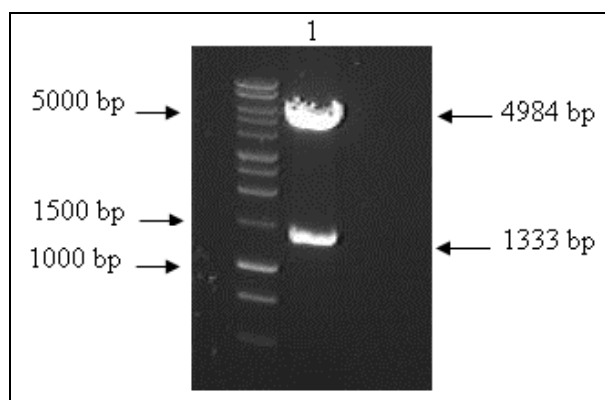


Figure 7.5. Required digestion for second step ligation.

Digestion of the antisense RNAi/AT-E segment out of the pGEM-T-Easy vector, using *Xba*I and *Apa*I enzymes (lane1). The construct from the first step of cloning (pRPa<sup>iSL</sup> vector + sense RNAi/AT-E segment) was digested using the same restriction enzymes (lane 2).

The antisense RNAi/AT-E segment was digested out of the pGEM-T-Easy vector using *Xba*I and *Apa*I enzymes and subsequently ligated into the pre-digested construct from step one of cloning (section 7.2.1.2).

This new construct was designated pHDK02 (Figure 7.1) and amplified in XL1 competent cells. The presence of the two RNAi fragments and the correct orientation were confirmed by sequencing using Eurofins MWG Operon service using forward primer (5'ACGGGCCCGGTACCAAGCTTGATCCCTCTGGCTGTTCGAC-3') and reverse primer (5'-ACTCTAGAGGATCCTCTGCTGCATACTTCATGGC-3') and *Kpn*I restriction digest (Figure 7.6).



**Figure 7.6. Confirmation of complete ligation and correct orientation of the RNAi-AT-E cassette.**

**Digestion of pHDK02 with *KpnI* resulted in a release of the RNAi cassette with size of 1333 bp (lane 1)**

Correct insertion and orientation was validated by several restriction digests, where the final RNAi construct (pHDK02) was digested with *KpnI* resulting in two separate bands, one at 1333 bp corresponds to a portion of the vector including the sense and antisense inserts, and a band at 4984bp corresponds to the rest of the vector backbone (Figure 7.6). Moreover, a digestion with *Ascl* and *AlwNI* resulted in release of three distinct bands at 3711bp for the RNAi cassette and two other bands corresponding to the rest of the vector back bone; at 1997bp and 609bp (Figure 7.7, lane1).

#### **7.2.1.4 Plasmid DNA preparation**

To prepare a large amount of plasmid DNA (pHDK02), a 100 ml culture of a positive transformed colony was grown overnight in luria broth with ampicillin at 37°C under shaking condition. The culture was spun and the plasmid DNA was purified using Qiagen Plasmid Miniprep Kit. The pHDK02 vector was linearised using *Ascl* in order to release the 3711bp of the RNAi cassette (Alsford & Horn, 2008).The digestion of plasmid DNA was carried out in a volume of 40 µl using 1 unit of the enzyme, 4 µl of 10X buffer and 10 µg of plasmid DNA and incubated in a water bath at 37°C overnight. This was followed by addition of 1 additional unit of the enzyme and the reaction was incubated for one more hour. Complete digestion of the plasmid DNA was checked by loading 1 µl of the reaction on agarose gel electrophoresis.

The linearised DNA plasmid was run on 1% agarose gel by electrophoresis at low voltage, resulting in two distinct bands as described above. The band at 3711 bp, corresponding to the RNAi cassette (Figure 7.7), was extracted from the gel using the Qiagene gel extraction kit and 10 µg of the cassette was sterilized by ethanol precipitation, resuspended in sterile water and used in transfection of the 2T1 cells. Stable transfectants were selected by culturing the cells in the presence of Hygromycin B (Roche) at 2.5 µg/ml as described in chapter 2.

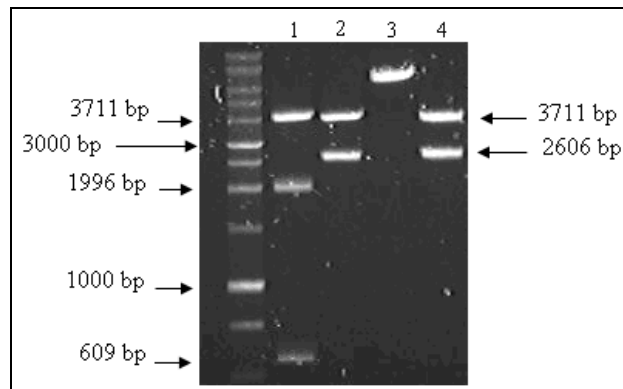


**Figure 7.7. Digestion of pHDK02 prior to transfection into bloodstream form cell line (2T1). Digestion of pHDK02 with *Ascl* and *AlwNI* (lane 1). Lane 2 and 4 digestion with *Ascl*, the bands at 3711bp (RNAi cassette) was extracted from the gel and subsequently transfected into 2T1 cells. Lane 1 non-digested pHDK02 as control.**

Growth of trypanosomes was observed in some wells after 5 days of Hygromycin B selection; these wells were selected and the trypanosomes cloned by limiting dilution (see section 2.9.7). After 7 to 10 day, several clonal lines had been obtained and maintained in the presence of drugs. These clones were studied further to check for correct integration of the RNAi construct within the 2T1 genome using PCR. The growth phenotype in the presence of tetracycline was also studied.

The genome of 2T1 parasites contains a construct with a puromycin resistance gene. The pRP<sup>aSLi</sup> is targeted to this region, and contains a partial hygromycin resistance gene. Upon correct integration, the puromycin gene is disturbed while the hygromycin gene is complemented this will result in loss of resistance to puromycin resistance but the gain of hygromycin resistance.

### 7.2.1.5 Growth Curve after Tetracycline induction

One stable clone, herein designated IT.BERi, was chosen to be used in the RNAi studies during this project. To examine the effect of tetracycline on the growth levels, the growth of the IT.BERi clonal cells (carrying the RNAi construct) upon tetracycline induction was compared to non-induced. A culture was initiated in 24-well microtitre plates at  $5 \times 10^4$ /ml in HMI-9/FCS medium in the presence or absence of tetracycline. Growth curves were generated by cell count using an improved Neubauer hemocytometer (Weber Scientific), every 12 hours after induction for 5 days. Cells were passed twice during the induction to fresh medium in the presence and absence of tetracycline to avoid overgrowth. RNAi induction with tetracycline causes no significant growth phenotype compared to the non-induced cell line (Figure 7.8).

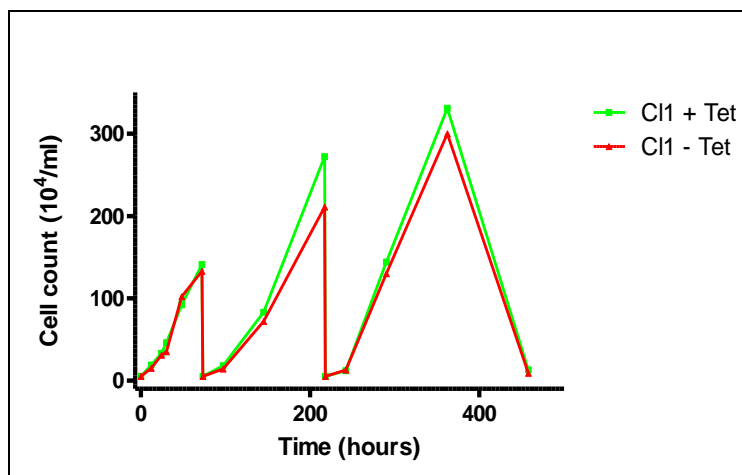


Figure 7.8. Growth curve of bloodstream form RNAi/AT-E cell line (IT.BERi).

Growth curve of RNAi/AT-E clone (IT.BERi) in the presence and absence of 1  $\mu$ g/ml tetracycline. The graph shows no significant difference in the growth phenotype in the presence and absence of tetracycline. This result represents data from 3 similar repeats.

Moreover, microscopic inspection of the cells showed no major changes in cell morphology upon RNAi induction. RNA was extracted at four time points (every 24 hours) and was used to make up cDNA for Reverse Transcriptase RNA in order to check whether AT-E mRNA levels were indeed reduced after RNAi induction.

### 7.2.1.6 Reverse Transcriptase -PCR showing knockdown of AT-E

The knockdown of the AT-E mRNA levels was investigated by reverse transcriptase PCR using cDNA as a template. cDNA was generated from extracted

RNA from four samples taken at 24 hour intervals during the growth of the transfectants in the presence and absence of tetracycline. The time points for RNA extraction were so chosen to determine when AT-E transcripts are depleted. This later assisted the uptake experiments and as AT-E mRNA was found to be maximally depleted at about 48 hours of induction.

The RT-PCR reaction used a 1µl volume of each template at identical concentrations (from cultures in the presence or absence of Tetracycline) and *Taq* polymerase (Promega), along with gene-specific primers (see section 2.9.10). The effect of expressing the AT-E RNAi cassette on the mRNA levels of the most closely related *T. b. brucei* genes AT-A and TbAT1/P2 was also investigated. The results showed that AT-E mRNA levels were substantially reduced after 48 h of tetracycline induction (Figure 7.9, panel A. lane 1), but neither the AT-A nor the TbAT1/P2 transcripts appeared to be affected (Figure 7.9, panels B and C).

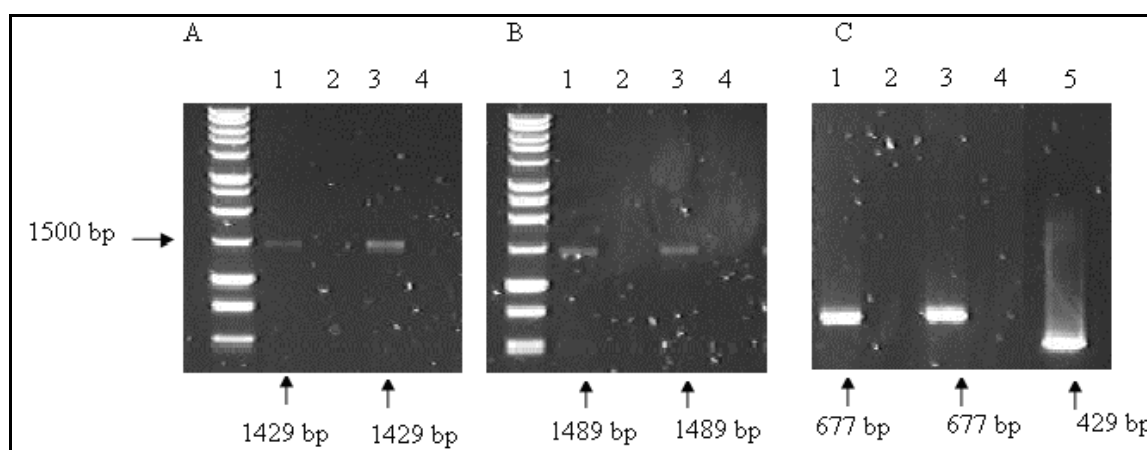


**Figure 7.9. Reverse Transcriptase -PCR analysis in the RNAi/AT-E in blood stream form cell line (IT.BERi).**

Tetracycline induction for 48 hours resulted in AT-E RNAi knockdown in bloodstream form (IT.BERi). Only AT-E mRNA levels were reduced (panel A, lane 1) compared to the non-induced (panel A, lane 3). RNAi knockdown of AT-E did not affect AT-A (panel B) or TbAT1/P2 (panel C) mRNA levels.

Lane 1 + Tet + RT. Lane 2 + Tet – RT. Lane 3 – Tet + RT lane 4 –Tet + RT

Lane 1 + Tet + RT. Lane 2 + Tet – RT. Lane 3 – Tet + RT lane 4 –Tet + RT

Lane 1 + Tet + RT. Lane 2 + Tet – RT. Lane 3 – Tet + RT lane 4 –Tet + RT. Lane 5 Actin as control

+ Tet: Tetracycline induced, - Tet: Non-induced, +RT cDNA treated with Reverse transcriptase and – RT: No reverse transcriptase was added when making cDNA.

Controls included in this experiment were: tetracycline non-induced samples as a control to measure reduction of mRNA levels against; samples of mRNA that were not treated with reverse transcriptase enzyme (superScript III RT) during the cDNA generating process were included as a control for DNA contamination; actin was included as a positive control for the PCR reaction.

#### 7.2.1.7 [<sup>3</sup>H]-Pentamidine uptake in bloodstream forms

The rate of uptake of [<sup>3</sup>H]-pentamidine in the RNAi/AT-E cell line (IT.BERi) was investigated in the presence and absence of Tetracycline using a time course over 600 s. Each experiment was performed in triplicate using rapid oil stop protocol (Carter & Fairlamb, 1993; de Koning & Jarvis, 1997) in which a suspension of  $1 \times 10^7$  cells in 100  $\mu$ l assay buffer (AB) was mixed with the same volume of radiolabeled [<sup>3</sup>H]-pentamidine at twice the final concentration. Uptake rates were measured over a range of time points up to 10 minutes (see section 2.4.3). Uptake was linear over the entire duration of the experiment, as determined by linear regression. Linearity was defined as displaying a correlation coefficient  $\geq 0.95$  and a significant difference from zero uptake (F-test; GraphPad Prism versions 4 and 5).

Two different concentrations of [<sup>3</sup>H]-pentamidine, 50 nM and 1  $\mu$ M, were used to assess pentamidine uptake rates through HAPT and LAPT, respectively. The well-documented ability of TbAT1/P2 to transport pentamidine (Carter *et al.*, 1995; De Koning, 2001; Collar *et al.*, 2009) required the inclusion of 1mM adenosine as a competitive inhibitor of P2 but not of HAPT or LAPT (De Koning, 2001; Matovu *et al.*, 20003). The P2 transporter is only expressed in long-slender bloodstream forms (De Koning *et al.*, 1998).

No significant difference was observed between the results of the three repeats of this experiment. In all cases the transport of 50 nM [<sup>3</sup>H]-pentamidine was linear for up to 10 minutes in both the induced and non-induced RNAi cell lines. However, the uptake rate upon tetracycline induction was significantly reduced compare to the non-induced cell line (Figure 7.10). A paired Student's t-test confirmed that [<sup>3</sup>H]-pentamidine transport was reduced, by  $60.61 \pm 8 \%$ , after tetracycline induction ( $P < 0.05$ ) (Table 7.2).

The LAPT1 activity was studied by measuring the uptake of  $1\mu\text{M}$  [ $^3\text{H}$ ]-pentamidine and found not to be affected in both induced and non-induced cell line (Figure 7.10, panel C & D). These observations show that knockdown of the AT-E gene via RNAi resulted in the loss of the HAPT1 function, and suggest that AT-E could be the gene coding for HAPT1.

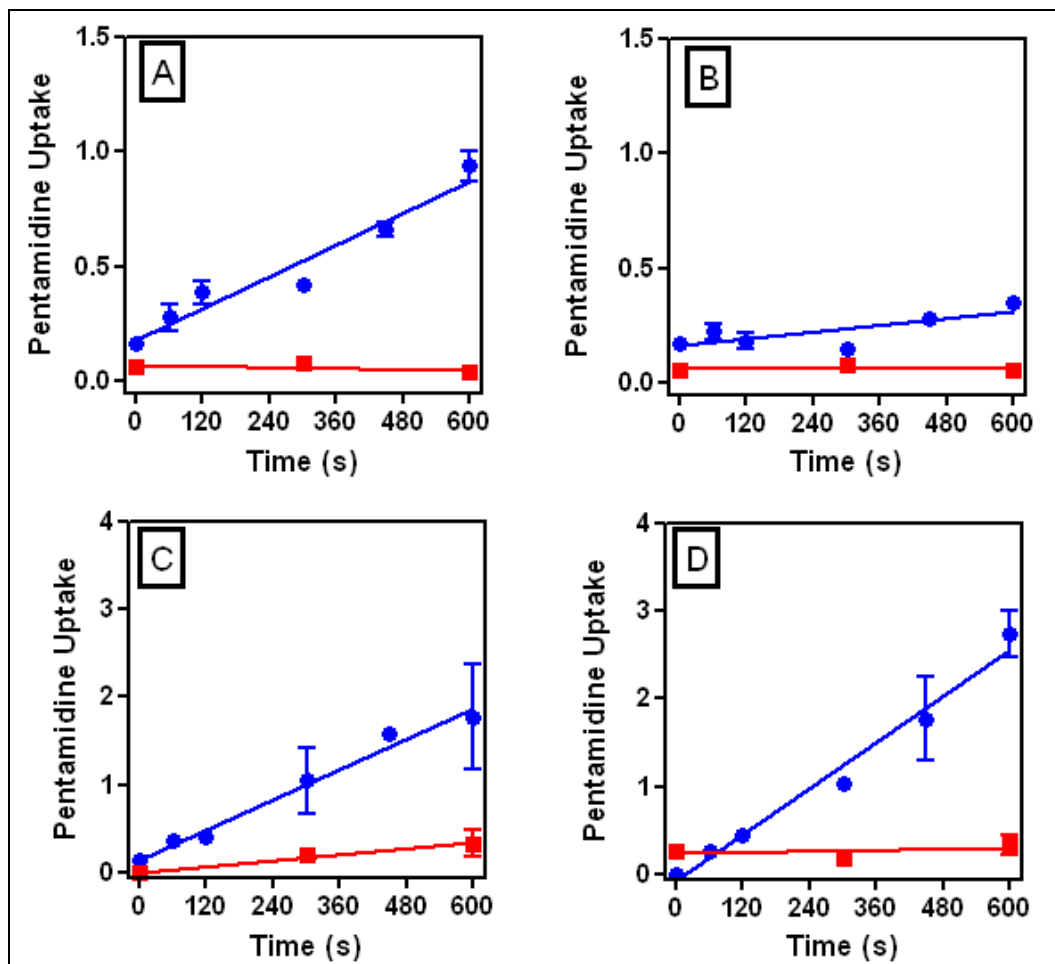


Figure 7.10. Time course for the uptake of low and high concentrations of [ $^3\text{H}$ ]-pentamidine in IT.BERi cell line.

Uptake of 50 nM [ $^3\text{H}$ ]-pentamidine in bloodstream forms of RNAi cell line IT.BERi with and without tetracycline RNAi induction. Panel A: Uptake of 50 nM [ $^3\text{H}$ ]-pentamidine (●) was linear up to 10 minutes. Panel B: The rate of [ $^3\text{H}$ ]-pentamidine uptake in the Tetracycline-induced cell line is dramatically reduced compared to the non-induced cell line. Panel C: The uptake of 1  $\mu\text{M}$  [ $^3\text{H}$ ]-pentamidine was linear up to 10 minutes in the absence of Tetracycline and almost completely inhibited by 1 mM unlabeled pentamidine. Panel D: The rate of 1  $\mu\text{M}$  [ $^3\text{H}$ ]-pentamidine uptake was not affected upon Tetracycline compared to the non-induced cell line. Uptake in the presence of 1 mM [ $^3\text{H}$ ]-pentamidine (■) was not significantly different from zero. Error bars show the standard error of the mean (SEM). The graphs represent one of three similar experiments.

	Uptake rate ( $\mu\text{mol}/10^7\text{cells}/\text{s}$ )		% Knockdown	Paired t-test
	Non-induced	Induced		
HAPT1	$0.0012 \pm 0.0001$	$0.00046 \pm 0.00009$	$60.61 \pm 8$	$P < 0.05$
LAPT1	$0.0046 \pm 0.0005$	$0.00047 \pm 0.0003$	$-4.1 \pm 4.5$	NS

**Table 7.2. RNAi knockdown of pentamidine transport activities in *T. b. brucei* bloodstream forms (IT.BERi).**

All data are the average of three independent experiments, with induced and non-induced controls performed in parallel from cultures grown in identical densities. NS = Not significant. Statistical analysis was performed using paired Student's t-test.

### 7.2.1.8 Drug profile and in vitro drug sensitivity

Sensitivity of the IT.BERi cell line to pentamidine was investigated with and without tetracycline induction of RNAi. This was performed by using propidium iodide endpoint assay in which  $1 \times 10^6/\text{ml}$  was tested against several concentration of drug starting at  $100 \mu\text{M}$  in order to determine  $\text{EC}_{50}$  values and check whether RNAi knockdown of the AT-E gene increases resistance to pentamidine (Figure 7.11).

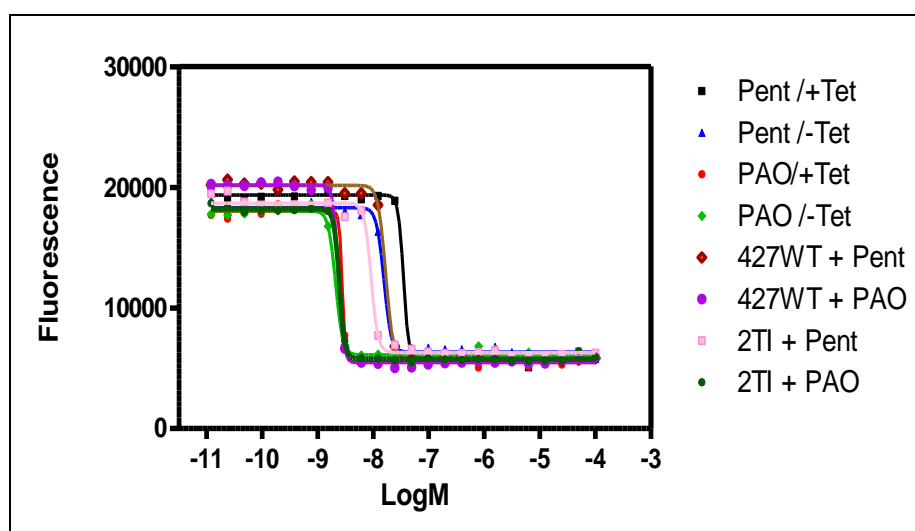


**Figure 7.11. Pentamidine profile in RNAi/AT-E bloodstream form cell line (IT.BERi).**

Propidium iodide (PI) assay testing the sensitivity of tetracycline-induced and non-induced IT.BERi cells to pentamidine and PAO (phenylarsine oxide) as control. 427WT and untransfected

The test was carried out in three independent repeats as described in chapter 2, but due to the presence of the TbAT1/P2 transporter activity the assay showed an increase of resistance to pentamidine by 2.3 folds only ( $P < 0.05$ ; Table 7.3).

		AVG	SE	RF	Paired-T-test	n
<b>IT.BERi / Tetracycline induced</b>						
	pentamidine	0.04	0.004	2.3	P<0.05	3
	PAO	0.003	0.0002	1.2	NS	3
<b>IT.BERi / Tetracycline Non- induced</b>						
	pentamidine	0.02	0.0005			3
	PAO	0.002	0.0002			3
<b>Non-transfected 2T1</b>						
	pentamidine	0.034	0.03			3
	PAO	0.002	0.0001			3
<b>427-WT</b>						
	pentamidine	0.02	0.002			3
	PAO	0.003	0.0002			3

**Table 7.3. The EC<sub>50</sub> of pentamidine and PAO in (IT.BERi).**

The average and standard error of three independent experiments (n) showing the EC<sub>50</sub> in  $\mu\text{M}$  for pentamidine and PAO determined by propidium iodide (PI) after and without tetracycline induction. The induced and non-induced controls were performed in parallel from cultures grown to identical densities. NS = Not significant. Statistical analysis was performed using paired Student's t-tests. The non-transfected 2T1 cell line was included as control. NS = Not significant

## 7.2.2 RNAi in procyclic forms

The TbAT1/P2 transporter is responsible for mediating the uptake of 50-70% of pentamidine in bloodstream form *T. brucei* (Bray *et al.*, 2003). This transporter was also present in the RNAi cell line (IT.BERi) described above, and to study the role of AT-E in pentamidine uptake requires blocking the activity of the P2 transport by adding adenosine at mill molar concentrations. This practise was achievable in the uptake assay, but it was not possible when studying the resistance profile to pentamidine *in vitro* this is due to toxicity of 1mM adenosine to the Trypanosoma cells (De Koning / personal communication)

Procyclic cell line lacks the P2 transporter activity (De Koning *et al.*, 1998) and thus could be used as an excellent test system in the RNAi studies. Procyclic cell line 29-13 derived from *Trypanosoma brucei brucei* strain 427 was successfully used in RNAi studies This cell line was engineered to express T7 RNA polymerase and the tetracycline repressor from bacteriophage  $\lambda$  (Wirtz *et al.*, 1999). In this

project we attempted to knockdown the *T. brucei* AT-E gene using 29-13 cell line.

### 7.2.2.1 Cloning of RNAi/AT-E Constructs

The RNAi vector used in this study (p2T7Ti) is based on the strategy of placing the sequence of interest between opposing T7 promoters (La Count *et al.*, 2000). The vectors contain an rRNA spacer for integration into the rRNA locus of the parasite's genome, a tetracycline inducible operator, as well as a drug resistance gene for selection (phleomycin).

The vector must be used in specially derived *T. brucei* cell lines (29-13), which express bacteriophage T7 RNA polymerase and the tet repressor from bacteriophage  $\lambda$ .

A 411 bp fragment from the AT-E open reading frame was inserted between the two opposing T7 promoters of the p2T7Ti vector that are both regulated by tetracycline repressors. The T7 polymerase and the tetracycline repressor constructs were maintained in the 29-13 cell line (La Count *et al.*, 2000) by the addition of 15  $\mu\text{g/ml}$  G418 and 25  $\mu\text{g/ml}$  Hygromycin B to the medium.

To induce the RNAi effect, tetracycline was added at a concentration of 100 ng/ml. Without tetracycline, the tet repressor expressed in the cells binds to the tet operator to inhibit transcription from the integrated construct. With the addition of tetracycline, the repressor is bound and this prevents binding to the operator, thus allowing transcription to occur. The 411 bp segment of the *T. brucei* AT-E was amplified from *T. brucei* strain 427 genomic DNA using the following primers (Eurofins MWG Operon):

5'-ATATGGATCCGATCCCTCTGGCTGTTTCGAC-3', forward primer including a *Bam*HI site (underlined), and 5'- TACGAAAGCTTAGACGACGTATGAAGTACCG -3', reverse primer (complementary) including a *Hind*III site (underlined).

PCR reactions were performed using *KOD* hot start DNA polymerase (Novagen) followed by extraction of the amplicon from the gel and its cloning into pGEM-T-Easy. The 411bp segment was released from pGEM-T-easy by digestion with *Bam*HI and *Hind*III (Figure 7.12), and cloned to the identically digested RNAi

vector p2T7Ti between the two head-to-head T7 promoters (LaCount *et al*, 2000), this digestion released the 760 bp fragment of the green fluorescent protein (GFP) from the vector (Figure 7.13).

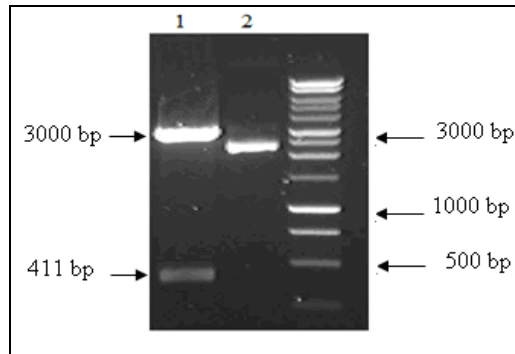


Figure 7.12. Digestion with *Bam*HI and *Hind*III release the RNAi/AT-E fragment of 411 bp from the pGEM-T-easy (lane1). Lane 2. Uncut p2T7Ti plasmid.

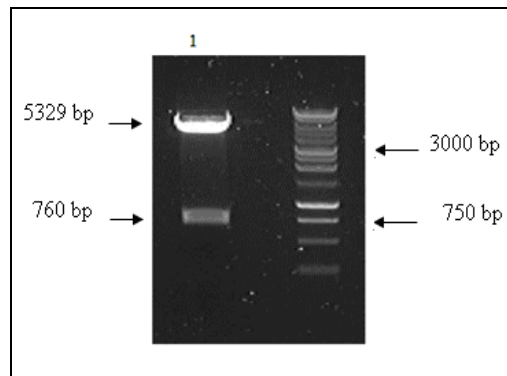


Figure 7.13. Digestion of p2T7Ti vector with *Bam*HI and *Hind*III releases the GFP gene at 760 bp (lane 1).

The resulting RNAi construct, designated pHDK07 (Figure 7.14), was then transformed into *E. coli* competent cells strain XL1 and positive clones for the RNAi/AT-E construct were confirmed by sequencing.

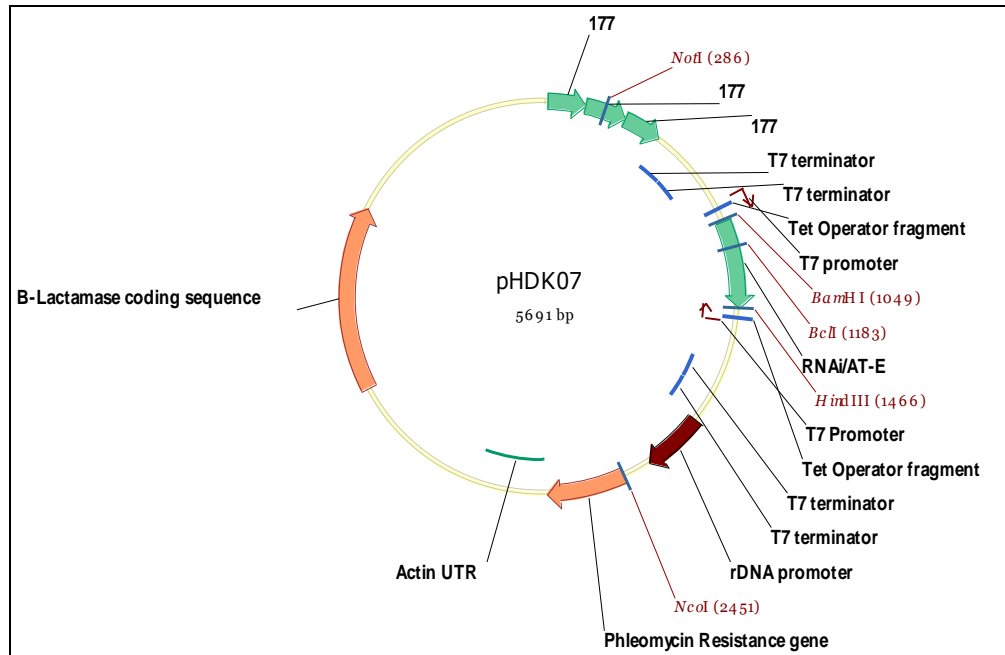


Figure 7.14. Map of pHDK07, derived from the p2T7Ti vector.

The RNAi/AT-E fragment was ligated at the *Bam*HI and *Hind*III sites located between two head to head T7 promoters. The map also shows the restriction sites for *Nco*I and *Not*I used in screening for the RNAi fragment and *Not*I used in the linearization process.

The vector was recovered from a positive clone grown in the presence of ampicillin, and used to transfect the 29-13 *T. brucei* cell line after being linearized by *Not*I restriction enzyme. Correct transformation was confirmed by restriction digest and by sequencing using forward primer mentioned above. Digestion with *Nco*I and *Not*I restriction enzymes resulted in two distinct bands, one at 2165 bp that includes the RNAi/AT-E insert, and a band at 3526 bp for the rest of the vector (Figure 7.15).

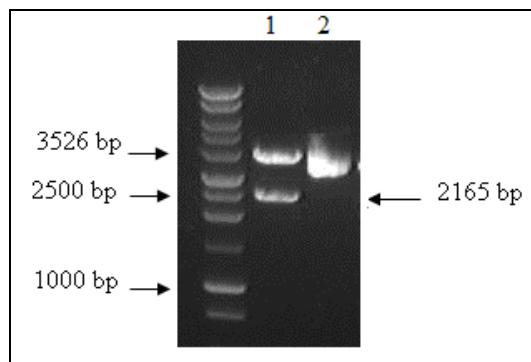


Figure 7.15. Confirmation of correct ligation of the RNAi/AT-E in p2T7Ti vector.

This step is taken prior to transfection to 29-13 procyclic cell line. Digestion of pHDK07 with *Nco*I and *Not*I enzymes resulted in two distinct bands confirms correct ligation (lane 1). Lane 2, uncut plasmid.

After a selection of stable transfectants using 10µg/ml phleomycin the transgenic parasites were grown at 27°C in SDM-79 supplemented with 10% heat inactivated fetal calf serum and 15 µg/ml G418 and 25 µg/ml hygromycin B to maintain the T7 RNA polymerase and the tetracycline repressor constructs. To induce the RNAi effect, tetracycline was added at a concentration of 100ng/ml (LaCount *et al*, 2000).

### 7.2.2.2 Tetracycline induction and Analysis of growth curve

After successful transfection and selection of unique clones (see section 2.9.7) a single clone, herein designated IT.CERi, was used to assess the growth rate of RNAi cell lines upon tetracycline induction. Cultures were initiated at a starting density of  $5 \times 10^5$  cells/ml in the presence and absence of tetracycline. Cells were grown in 24 well plates; using a total volume of 1 ml of SDM-79 medium with 10% FCS supplemented with 15 µg/ml G418 and 25 µg/ml Hygromycin B. Growth curves of the parasite were generated by cell count using a Neubauer haemocytometer (Weber Scientific) every 24 hours for 13 days; cells were passage to new fresh medium with antibiotics and in the presence and absence of tetracycline every three days.

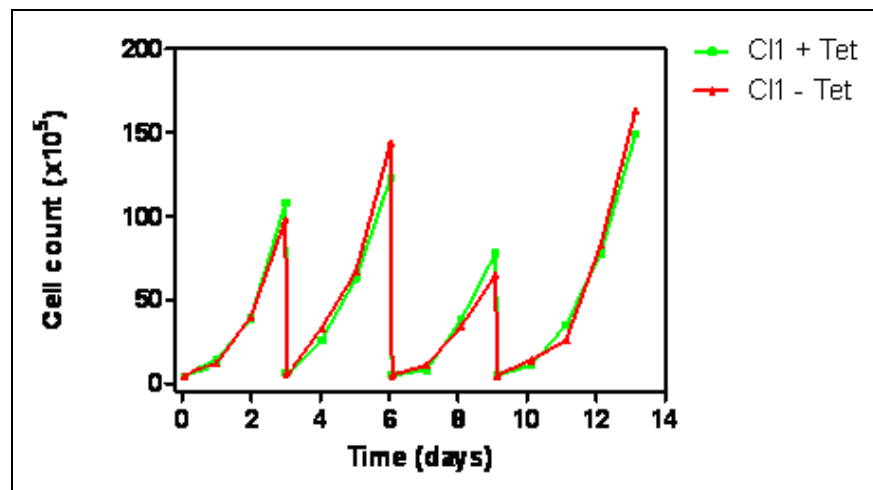


Figure 7.16. Growth curve of procyclic form RNAi/AT-E cell line (IT.CERi).

Growth curve of procyclic IT-CERi upon tetracycline induction (green line) and non-induced cell line (red line). The graph shows no significant difference in the growth phenotype in the presence and absence of tetracycline. The experiment was carried out over 13 days with passage every 3 days under the same condition with fresh tetracycline added every passage.

RNAi induction with tetracycline did not result in any significant changes in the growth rate compared to the non-induced cell line (Figure 7.16) and microscopic examination showed no major changes in cell morphology upon tetracycline induction. From the same culture, RNA was extracted at four time points 24 hours apart, which was used for reverse transcriptase PCR in order to determine the level and timing of any down-regulation of the AT-E gene.

### 7.2.2.3 Reverse Transcriptase -PCR showing knockdown of AT-E

Addition of tetracycline allows transcription of the RNAi fragment to take place, whereas without adding tetracycline, the *Tet* repressor, expressed in the 29-13 cell line, binds to the *Tet* operator to prevent transcription from the integrated construct; tetracycline therefore results in down regulation of the AT-E transcription.

Reverse transcriptase PCR (RT-PCR) was used to investigate the extent and timing of RNAi knockdown of the AT-E gene. The template used in RT-PCR reaction was cDNA that was generated from extracted RNA over four time points alongside the growth analysis of the transfectants in the presence and absence of tetracycline (see previous section). It was found that RNAi knockdown of the AT-E gene was maximal at about 72 hours of tetracycline induction (Figure 7.17, panel A. lane1). This induction time was subsequently used for assessment of uptake and drug sensitivity with and without tetracycline induction. For the RT-PCR reaction a 1µl volume of each template (+/- Tetracycline and +/- RT) at equal concentrations and *Taq* polymerase (Promega) along with gene-specific primers was used (see section 2.9.10).

The result showed that RNAi knockdown of the AT-E gene resulted in a reduction in the mRNA levels. This was evident from the less dense band of the tetracycline induced band compared to the band of the non-induced sample (Figure 7.17, panel A. lane1). It also showed that that expression of the AT-E RNAi fragment did not affect the transcription levels of the AT-A gene (Figure 7.17, panel B. lane 1).

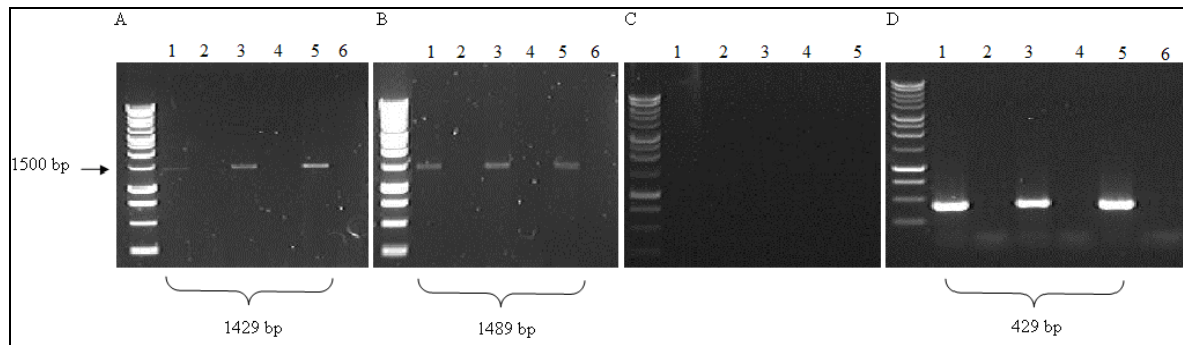


**Figure 7.17. Reverse transcriptase –PCR analysis of the RNAi/AT-E knockdown in procyclic form (IT.CERi).**

AT-E RNAi knockdown upon 72 hours of tetracycline induction in procyclic form IT.CERi cells. Only AT-E mRNA was reduced (Panel A, lane 1) compared to the non-induced control (Panel A, lane 3). RNAi knockdown of the AT-E did not affect AT-A (Panel, B lane 1 ,3). TbAT1/P2 was not expressed in the procyclic form (Panel C). Actin was used as a control + RT, -RT (Panel D). Lanes 5 and 6 in panels A,B,C and D are samples from 427-WT genomic DNA (used as positive control)

Lane 1: +Tet, +RT; Lane 2: +Tet, –RT; Lane 3: –Tet, +RT; Lane 4: –Tet, -RT.

+Tet, Tetracycline induced; -Tet, Non-induced; +RT, mRNA treated with Reverse transcriptase; –RT, No reverse transcriptase was added when making cDNA.

Controls included in this experiment were tetracycline non-induced samples as a control for reduction of mRNA levels, and samples of cDNA without reverse transcriptase (superScript III RT) treatment to check for any DNA contamination; DNA from 427-WT procyclic form was included in the PCR to amplify AT-A and AT-E as markers; actin primers were included as a positive control (Figure 7.17, panel. D). TbAT1/P2 was not expressed in PCF, as expected (Figure 7.17, panel. C).

#### 7.2.2.4 Uptake Assays

The procyclic form of *T. brucei* lacks the TbAT1/P2 transporter activity, thus the study of the [<sup>3</sup>H]-pentamidine uptake will be limited to HAPT1 and LAPT1 (see chapter 2), without the need to block P2 with a competitive inhibitor. [3H]-pentamidine transport rates in the IT.CERi clonal cell line were determined in the presence and absence of Tetracycline.

HAPT1 and LAPT1 mediated uptake was studied at 50 nM and 1 μM [3H]-pentamidine, respectively. Each experiment was repeated three times, and the three repeats displayed very similar results at 72 hours of induction with tetracycline. The uptake of 50 nM [3H]-pentamidine was linear for up to 10

minutes in induced and non-induced RNAi cells, with a clear and reproducible reduction in the uptake rate in the later cells line (Figure 7.18).

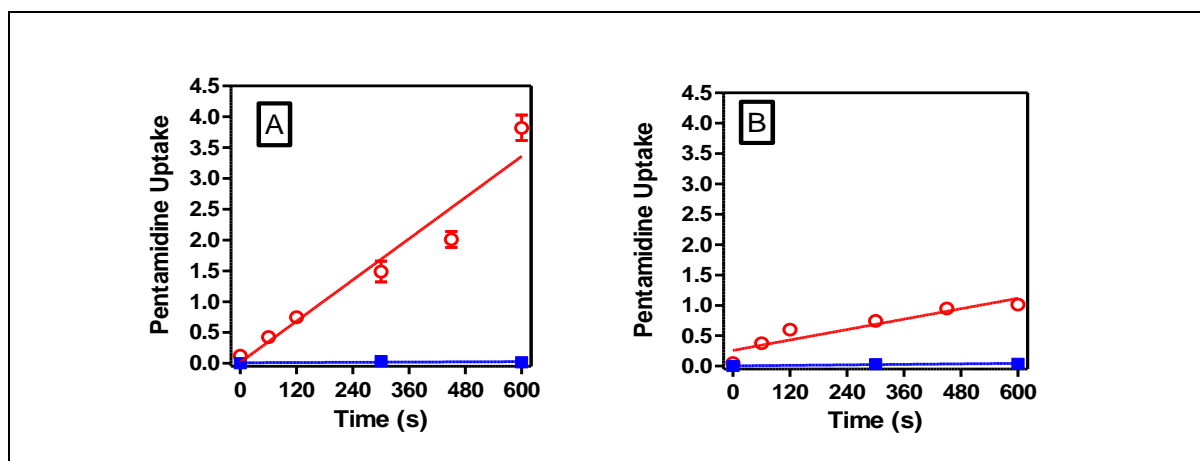


Figure 7.18. Time course for the uptake of low concentration of [<sup>3</sup>H]- pentamidine in procyclic forms of RNAi cell line (IT.CERi).

Uptake of 50nM [<sup>3</sup>H]- pentamidine in (IT.CERi) cell line with and without Tetracycline RNAi induction. Uptake of 50nM [3H]-pentamidine (○) was linear up to 10 minutes. Uptake in the presence of 1mM [3H]-pentamidine (■) was not significantly different from zero. Uptake rate upon tetracycline induction (B) is significantly reduced compare to the non-induced cell line (A). Error bars show the standard error of the mean (SEM). The graphs representative of 3 similar experiments one of three similar experiments.

The result, shown in Table 7.4 as the average of three independent experiments, shows a reduction of  $70 \pm 3\%$  ( $P < 0.05$ , Paired Student's t-test).

	Uptake rate (pmol/10 <sup>7</sup> cells/s)		% Knockdown	Paired t-test
	Induced	Non-induced		
HAPT1	0.0013 ± 0.0002	0.00042 ± 0.0006	69.6 ± 2.6	P<0.05
LAPT1	0.0172 ± 0.0022	0.0172 ± 0.0019	- 0.3± 6.4	NS

Table 7.4. RNAi knockdown of pentamidine transportations in *T. b. brucei* procyclic form (IT.CERi).

All data are the average of three independent experiments, with induced and non-induced controls performed in parallel from cultures grown in identical densities. NS = Not significant. Statistical analysis was performed using paired Student's t-tests.

Expression of the AT-E RNAi fragment did not affect the uptake of 1 μM [3H]-pentamidine in both induced and non-induced cells (Figure 7.19). These observations strongly agree with the results found in the bloodstream form (IT.BERi) and are entirely consistent with the results from the reverse transcriptase PCR and strongly suggest that AT-E knockdown is specific and limited to the target gene, and that AT-E is the coding gene for HAPT1.

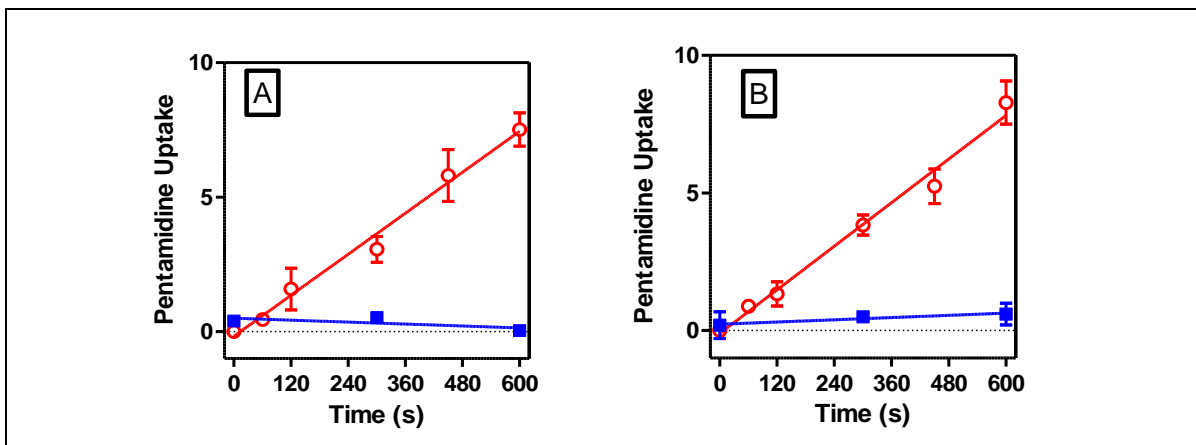


Figure 7.19. Time course for the uptake of high concentration [3H]- pentamidine in procyclic forms of RNAi cell line with and without tetracycline RNAi induction.

Uptake of 1 μM [3H]-pentamidine (○) was linear up to 10 minutes. Uptake in the presence of 1 mM [3H]-pentamidine (■) was not significantly different from zero. Uptake rate in the tetracycline induced cell line (B) was not significantly different compare to the non-induced cell line (A). Error bars show the standard error of the mean (SEM). The graphs representative of 3 similar experiments one of three similar experiments.

#### 7.2.2.5 Propidium iodide and pentamidine resistance

Sensitivity of the IT.CERi cell line to pentamidine was investigated with and without tetracycline induction, using the propidium iodide endpoint assay. Trypanosome cultures ( $1 \times 10^6$ /ml) were exposed to doubling dilutions of drug starting at 100 μM in order to determine  $EC_{50}$  values (Figure 7.20). Each experiment was repeated at least three times.

Tetracycline-induced cells were more than 11-fold resistant to pentamidine ( $P < 0.01$ ; Student's t-test), but were similarly sensitive to the control drug PAO (Table 7.5). This difference is much more pronounced than in bloodstream forms. Thus, the absence of pentamidine transport through the P2 transporter, which masked the effect of AT-E knockdown in bloodstream forms, did indeed make the procyclic system more predictive for this study.

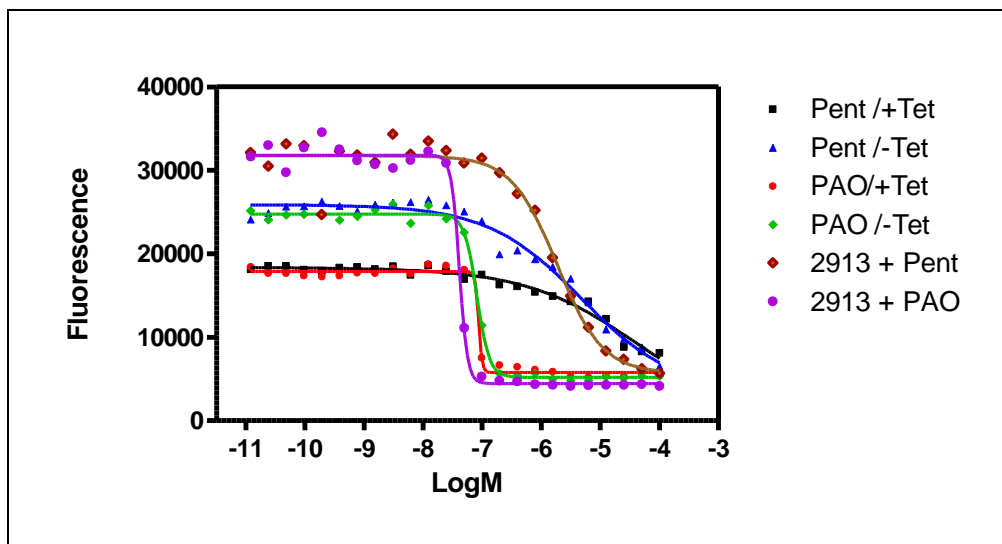


Figure 7.20. Pentamidine profile in RNAi/AT-E procyclic form cell line (IT.CERi). Propidium iodide (PI) assay testing the sensitivity of the tetracycline-induced and non-induced IT.CERi cell line to pentamidine and PAO. The untransfected 29-13 cell line was also included in the experiment as control.

		AVG	SE	RF	Paired-T-test	n
<b>IT. CERi / Tetracycline induced</b>						
	pentamidine	38	4	11.2	P<0.01	3
	PAO	0.09	0.009	1.1	NS	3
<b>IT. CERi / Tetracycline Non- induced</b>						
	pentamidine	3.4	0.8			3
	PAO	0.08	0.003			3
<b>Non-transfected 29-13</b>						
	pentamidine	1.6	0.3			3
	PAO	0.04	0.002			3

Table 7.5. The EC50 of pentamidine and PAO in IT-CERi cell line.

The average and standard error of three experiments (n) showing the EC50 in  $\mu\text{M}$  for the pentamidine and PAO determined by (PI) upon Tetracycline induction resulted in 11.2 folds resistant to pentamidine. The induced and non-induced controls were performed in parallel from cultures grown in identical densities. Non-transfected 29-13 cell line was included as control. Statistical analysis was performed using paired Student's t-tests between induced and Non-induced cell line. NS = Not significant.

## 7.3 Discussion

It has long been established that uptake of diamidine compounds including pentamidine in trypanosomes relies mainly on the P2 transporter (Carter *et al.*, 1995; De Koning, 2001; Bray *et al.*, 2003), which was first identified as a main route of entry for aminopurines (Carter and Fairlamb, 1993; De Koning and Jarvis, 1999). Two additional transporters, the High Affinity Pentamidine Transporter (HAPT1) and Low Affinity Pentamidine Transporter (LAPT1) are believed to be responsible for the remaining uptake of pentamidine (De Koning, 2001; Matovu *et al.*, 2003; Bridges *et al.*, 2007).

The coding gene for the P2 transporter was identified and a *T. b. brucei* strain lacking function of P2 transporter was created through TbAT1 gene knockout and used to study P2 transporter at the molecular level (Mäser *et al.*, 1999; Matovu *et al.*, 2003). In contrast, the existence of HAPT1 and LAPT1 has only been inferred from transport kinetic studies and thus far no the genes encoding the transporters have not been identified. However, a clear link with pentamidine resistance was established when the P2 knockout strain was adapted to higher concentrations of pentamidine and it was shown that this had led to loss of HAPT1 transporter activity (Bridges *et al.*, 2005).

The identification of the pentamidine transporters was attempted starting from the hypothesis that these transporters might be related to TbAT1/P2, the only pentamidine transporter gene identified to date. Three candidate genes were readily identified from the genomic database, clustering with TbAT1 in a phylogenetic analysis. Like TbAT1, these were members of the Equilibrative Nucleoside Transporter (ENT) gene family and TbAT-E (Tb927.3.590) displayed the highest level of homology with TbAT1 (de Koning *et al.* 2005).

After the commencement of the current project, AT-E (TbNT12) was functionally expressed in a mutant cell line of *Leishmania* deficient in nucleobase uptake and was found to be involved in purine nucleobase transportation. It was also shown to be capable of pentamidine uptake after being expressed in *Xenopus leavis* oocytes (Ortiz *et al.*, 2008). Yet, this report left much uncertainty as to whether this transporter does contribute significantly to pentamidine transport in *T. b. brucei*. Our analysis of HAPT1- and LAPT1-mediated uptake [<sup>3</sup>H]-pentamidine in

this parasite showed that these transporters were not inhibited by purine nucleobases or nucleosides (De Koning, 2001), which is incompatible with the possibility of AT-E encoding a high affinity nucleobase transporter as well as one of the pentamidine carriers. Bizarrely, the pentamidine uptake activity reported by Ortiz *et al* (2008) was not inhibited by up to 20-fold excess of adenine. Moreover, the Ortiz paper estimates the pentamidine  $K_m$  of this transporter, when expressed in *X. laevis* oocytes, at over 400  $\mu\text{M}$ , much higher than previously reported for either HAPT1 or LAPT1 (36 nM and 56  $\mu\text{M}$ , respectively; De Koning, 2001). To determine any role for AT-E in pentamidine uptake in *T. b. brucei* this process had thus to be studied in the parasite itself.

To study the possible role of the AT-E gene in *T. b. brucei* pentamidine uptake, the RNA interference technique was employed to disrupt the function of the candidate gene. This loss of function is achieved by introducing a double stranded RNA molecule into a cell, leading to the degradation of the corresponding endogenous messenger RNA by creating 24 to 26 nucleotides RNAs fragments called small interfering RNAs (siRNAs) which will then interact with the targeted RNA (Tschdi *et al.*, 2003; Clayton *et al.*, 2005)

RNAi is an attractive method and was used to good effect during this study, as a small fragment of the AT-E gene managed to reduce the level of mRNA from this gene, allowing the investigation of its role in pentamidine uptake in relation to HAPT1 and LAPT1 transporters. Two *T. b. brucei* cell lines that are capable of expressing and processing RNAi were used, the 2T1 bloodstream form cell line and 2913 procyclic cell line. The AT-E RNAi fragment was ligated into two different constructs, the stem-loop pRP<sup>aiSL</sup> vector described previously by Alsford and Horn in the 2T1 bloodstream form cell line (Alsford & Horn, 2008), whereas p2T7Ti were used in RNAi construct in the procyclic form 29-13 cell line (LaCount *et al*, 2000).

The correct creation of the constructs was verified by restriction digests and sequencing, and correct integration was confirmed by PCR amplification of the resistance markers. Stable clones RNAi cell line were obtained and the AT-E constructs were functionally validated using reverse transcriptase PCR (RT-PCR).

The p2T7Ti vector produced a highly active RNAi construct, with the AT-E fragment inserted once between two opposing T7 promoters and transcription

controlled by the *Tet* repressor/ *Tet* operator system. The construction of the pRP<sup>aiSL</sup>-based vector involved the insertion of two fragments of opposite strands in a stem-loop conformation. Its expression was controlled by tetracycline and driven by an RNA polymerase I promoter (Alsford & Horn, 2008). The growth phenotype of stable clones was studied upon tetracycline induction, in parallel with the identical but non-induced cell lines. AT-E gene was apparently not essential for the parasite survival at the level of knockdown achieved (~60% at mRNA level after 72 h as determined with RT-PCR), which assisted further experimental work without growth complications.

The RNAi-expressing bloodstream and procyclic cell lines were used to investigate the effect of AT-E knockdown on HAPT1- and LAPT1-mediated [<sup>3</sup>H]-pentamidine uptake, at 50 nM and 1 μM of radiolabel, respectively. In bloodstream forms, TbAT1/P2 was blocked by the inclusion of saturating concentrations of adenosine and under those conditions HAPT1 and LAPT1 can be studied in virtual isolation (De Koning, 2001; Bray *et al.*, 2003; Matovu *et al.*, 2003; Bridges *et al.*, 2007). The same results were obtained in bloodstream forms and procyclics: in both cases, LAPT1-mediated uptake was statistically identical in cells grown in the presence of tetracycline and in non-induced control cells, whereas HAPT1 activity was approximately 60% reduced upon tetracycline induction - mirroring the reduction in AT-E mRNA.

Consistent with the observations in pentamidine transport, AT-E RNAi induction produced only a modest loss of pentamidine sensitivity in BSF, due to the presence of the other high affinity pentamidine transporter, TbAT1/P2 ( $K_m = 0.26 \mu\text{M}$  compared to  $0.035 \mu\text{M}$  for HAPT1 (De Koning, 2001). As discussed by Bray *et al* (2003) at low nM concentrations the contribution of the highest affinity transporter have the highest impact and the partial AT-E knockdown will thus shift the pentamidine  $IC_{50}$  value to higher concentrations, where the P2-mediated flux becomes sufficient to compensate for the loss of HAPT1. The quite limited shift in  $IC_{50}$  value is further explained by the much higher capacity of the P2 transporter relatively to HAPT1 ( $V_{max}$  values are  $0.068$  and  $0.0044 \text{ pmol}(10^7 \text{ cells})^{-1}\text{s}^{-1}$ ) (De Koning, 2001; Bray *et al.*, 2003; De Koning, 2008).

In procyclic cells, AT-E knockdown caused a much larger shift in  $EC_{50}$  values, due to the absence of P2 activity in this life-cycle form (De Koning *et al.*, 1998; De

Koning *et al.*, 2005). It is remarkable that the  $IC_{50}$  value ( $38 \pm 4 \mu\text{M}$ ) after tetracycline-induction was almost identical to the LAPT1  $K_m$  value in procyclic s427 ( $33 \pm 10$ ).

All the results are thus entirely as would be predicted if AT-E encodes for the HAPT transport activity. More definitive confirmation might be obtained by assessing the AT-E protein rather than the mRNA levels after knockdown, by Western blot or immunocytochemistry. Such assessments are notoriously difficult with complex membrane proteins with many trans-membrane helices and few exposed epitopes. The very low abundance of the proteins, the presence of other, closely related membrane proteins and the very considerable challenges of gel-based separation of such proteins (Bridges *et al.*, 2008) render this technique an almost impossible tool for knockdown quantification in this particular study.

To summarise, RNAi has proven to be a powerful tool to study drug resistance phenotypes in both procyclic and bloodstream form trypanosomes. The knockdown appeared to be specific, as judged by the unaltered expression levels of the most closely related genes, and by the unaltered function of the other pentamidine transport activities in cellular assays. The levels of knockdown achieved correlated well with the observed reduction in HAPT1 activity in both life cycle stages and the resulting resistance levels were entirely consistent with loss of most of the HAPT1 activity. We conclude that it is highly probable that AT-E encodes this high affinity pentamidine carrier.

## **8 General discussion**

The increasing burden of parasitic diseases including human African trypanosomiasis (HAT) is a major concern in the world and management and control of the disease is fraught with numerous problems. These include extreme toxicity of the treatments, for example treatment of the late-stage of sleeping sickness with melarsoprol is reported to cause a fatal reactive encephalopathy in 10% of patients (Fairlamb, 2003). The other issue is the high cost of the treatment and the difficulty of administration as most of these therapies require hospital admission. An even more pressing problem is the increase in drug resistance to the few available antiparasitic agents. For example, resistance to melarsoprol (Bacchi, 1993; Brun *et al*, 2001; Legros *et al*, 1999; Balasegaram *et al*, 2006; Delespaux & De Koning, 2007) and diminazene (Geerts *et al*, 2001; Anene *et al*, 2006) have been widely reported. The emergence and spread of parasites resistant to the commonly used anti-trypanosomiasis drugs means that current treatments are losing their efficacy in certain regions, rendering the diseases nearly untreatable as no new drugs have been approved. Thus, the limitations of registered drugs used against the disease and the problems associated with these drugs necessitate the urgent development of new therapies to combat HAT and an understanding of the causes of resistance.

The mechanism of resistance is not completely understood, but one way by which the parasite could develop resistance is the loss of route of drug entry as a result of loss cell membrane transporters. Recently, Vincent *et al*, 2010, found that Eflornithine resistance can be easily induced in the laboratory, resulting in loss of a putative amino acid transporter, *TbAAT6*. The loss of this gene was confirmed by PCR, and knockdown of the wild type gene using RNA interference led to acquisition of resistance while expression of an ectopic copy of the gene introduced into the resistant deletion lines restored sensitivity, confirming the role of *TbAAT6* in eflornithine uptake and resistance (Vincent *et al.*; 2010).

The importance of these transporters in the uptake of nutrients into the cells and their possible use as drug targets has recently received much of interest. Purine nucleosides and nucleobases are essential to the trypanosomes as they form the basic constituents of nucleic acid and other important biomolecules. Since the parasite is unable to synthesise these purines *de novo*, it has to rely solely on the host's purine for survival and proliferation (de Koning *et al*, 2005). The availability of accurate and reliable information on the functional properties

of purine transporters in *Trypanosoma* should facilitate the development of a rational purine-based chemotherapy of African trypanosomiasis and similar strategies could be envisaged for other uptake systems of parasites (Lüscher *et al.*, 2007). The main aim of this project, therefore, was to provide further detailed information on the kinetic characteristics of the transporters of the parasitic protozoan *Trypanosoma brucei* involved in uptake of diamidine drugs including pentamidine and diminazene. It has been confirmed that diamidines including pentamidine and diminazene acetate rapidly accumulate to very high levels in trypanosomes due to the presence of specific transporters in the plasma membrane that enables entry into the cell (Damper *et al.*, 1976; Carter *et al.*, 1995; De Koning, 2001). Pentamidine is actively taken up and concentrated by at least three distinct transporters (De Koning, 2001). Kinetic studies using [<sup>3</sup>H]-pentamidine uptake inhibitors showed that in *T. b. brucei* 50% of pentamidine uptake is mediated by the P2 aminopurine transporter (Bray *et al.*, 2003). The P2 transporter has been characterised at biochemical and molecular level and its natural substrates have been identified as adenosine and adenine, and the coding gene is the *Trypanosoma brucei* Adenosine Transporter 1 (TbAT1). The TbAT1 gene was expressed in the yeast *Saccharomyces cerevisiae* lacking a normal purine synthesis and was found to encode the P2 adenosine/adenine transporter. The deletion or the alteration of this gene resulted in melaminophenyl arsenical resistance *in vitro* and *in vivo* with cross-resistance to diminazene acetate and increase of resistance to pentamidine (Mäser *et al.*, 1999; Matovu *et al.*, 2001). In some strains resistance was linked to the deletion of the TbAT1 gene, whereas in other strains point mutations or a lack of transcription of the TbAT1 open reading frame was associated with resistance (Stewart *et al.*; 2010).

The other two transporters involved in the uptake of pentamidine are the high affinity pentamidine transporter (HAPT1) and the low affinity pentamidine transporter (LAPT1). They have been identified only by kinetic methods of pentamidine uptake and no natural substrate is known for them and, at the start of this study, had not been studied at molecular levels (de Koning, 2001, de Koning *et al.*, 2005).

For some time it was thought that the P2 transporter is the only route of entry for diminazene acetate. The idea was based on the occurrence of resistance to

diminazene but not to pentamidine in the field because the loss of the single nonessential gene *TbAT1* would prevent almost all diminazene entry into trypanosomes (De Koning, 2004). The emerging model was confirmed by the phenotype of *TbAT1*-KO cell line: bloodstream forms of this strain were highly resistant to diminazene (18-fold) but only two-fold to three-fold less sensitive to pentamidine than the parental wild-type strain (Matovu *et al.*, 2003). However, deletion of *TbAT1* still left the cells with a level of sensitivity to diminazene at near-micromolar concentrations, suggesting the drugs either get into the trypanosomes through other routes, possibly including diffusion or endocytosis. HAPT1 and LAPT1 transporters had been confirmed to be additional routes for the uptake of pentamidine and possibly other diamidines (de Koning, 2001; de Koning & Jarvis, 2001). The hypothesis that the high level of diminazene resistance is associated with the concomitant loss of P2 and possibly HAPT1 transporter activity has been tested during this project in a cell line that lacked both transporters. This was achieved by exposure of *TbAT1*-KO cell line to gradually increased concentrations of pentamidine or diminazene, which resulted in the *TbAT1*-B48 (Bridges *et al.*, 2007) and ABR (Teka *et al.*, 2011) cell lines. Time-course uptake assays showed that the uptake of [<sup>3</sup>H]-diminazene in these lines was greatly reduced compared to the wild type and *TbAT1*-KO cell lines but still detectable and linear for up to 10 minutes, confirming that diminazene uptake is mainly mediated by the P2 transporter but HAPT1 was identified as an additional, minor route for the uptake of diminazene.

Further evidence came from the observation that the ABR line had lost the HAPT1 transporter, whereas the LAPT1 activity was unchanged. Hypothetically, the sequential loss of the P2 and HAPT1 should result in no diminazene uptake in the ABR strain if diminazene resistance correlates to loss of both *TbAT1*/P2 and HAPT1. The ABR cell line was subjected to a diminazene time-course transport assay using 1  $\mu\text{M}$  [<sup>3</sup>H]-diminazene. The obtained results revealed that diminazene transport was not completely abolished in the ABR cell line at 1  $\mu\text{M}$  [<sup>3</sup>H]-diminazene suggesting that at least a third transporter is involved in the transport of high concentrations of diminazene (chapter 3), although it is highly questionable whether the very low rate of uptake through this third transporter is of any therapeutic significance. Curiously, the results also showed that B48 and ABR display identical rates of diminazene transport and LAPT1-mediated pentamidine transport but they differ in their level of diminazene resistance.

The similarity of the initial transport rates in both strains but with differential drug sensitivity can be explained by one of the following possibilities: (1) the ABR expresses an efflux pump that recognises diminazene as a substrate or (2) ABR has developed an additional non-transport-related adaptation that increases resistance to diminazene. Finally, this study has shown that loss of HAPT1 via adaptation to diminazene (ABR) potentially increases resistance to the melaminophenyl arsenicals as a result. This is an important finding in the light of the very liberal usage of diminazene for sick cattle in sub-Saharan Africa - usually without confirmation of trypanosomiasis. It has long been speculated that this practise, inevitably inducing diminazene resistance, may have contributed to the emergence of melarsoprol resistance (De Koning, 2001; Barrett, 2001).

The pentamidine adapted B48 clonal line was found to be 139-fold more resistant to pentamidine in the Alamar blue assay, relative to the wild-type strain. The resistance phenotype was apparently the result of the loss of the HAPT1 transport activity but LAPT1 remained unchanged (Bridges *et al.*, 2007). No cell line lacking LAPT1 activity has been constructed or identified to date; therefore this project also aimed for the disruption of LAPT1 transporter activity, which would create a cell line with null pentamidine uptake background. Such a model would help to investigate the mechanism of resistance and study the uncharacterised pentamidine transporters at the molecular level. The adaptation of the TbAT1-B48 to gradual increase of pentamidine concentration, over approximately 12 months, which aimed to create a trypanosome line without pentamidine transporters, resulted in the P1000 strain.

Transport studies using [<sup>3</sup>H]-pentamidine showed that LAPT1 remained intact in this cell line, arguing that this activity cannot be easily deleted or switched off - either because it is essential or because there are too many copies of the gene (or both). This is consistent with the hypothesis that AT-A genes encode the LAPT1 activity, as at least 6 different alleles were identified in WT427 trypanosomes (this thesis, chapter 6), and an attempt to knockdown expression of these genes with RNAi consisting of AT-A fragments was unsuccessful (Munday and De Koning, unpublished).

However, the alamar blue study revealed that this cell was 350-fold more resistant to pentamidine than the wild type. These results, together with the data from the mitochondrial membrane potential (MMP) that show that B48 and, in particular P1000, have lost most of their MMP, strongly suggest that the cells have developed a transport-independent mechanism of resistance in addition to the loss of plasma membrane transporters. The study of the P1000 strain thus confirmed that the mitochondrion is a target for the drug as adaptation resulted in loss of the mitochondrial potential. This would reduce accumulation of the dicationic diamidines inside the mitochondrion with its inside-negative membrane potential.

The molecular studies showed that the sequences of the AT-like genes that are believed to be involved in the pentamidine uptake were identical in the B48, P1000 and 427-WT strains. This suggested that there must be another technique by which the cells have developed resistance by genetic modification; for example by downregulation of mRNA translation or reduced mRNA stability, which can come about through alterations in flanking regions or even different gene transcription regulatory genes, rather than in the open reading frame of the transporter gene. Reverse transcriptase PCR analysis confirmed that AT-E mRNA levels were reduced in B48 and even more in P1000, and we tentatively conclude that adaptation to 1000 nM of pentamidine caused down regulation of the AT-E gene expression only; the mRNA levels of the other related genes were not affected.

Sequence analysis of the 427-WT, *TbAT1*-B48 and P1000 AT-A and AT-E genes did not reveal any changes in the open reading frames, although B48 and P1000 are clearly deficient in HAPT1-mediated pentamidine transport. As we show that AT-E1 encodes the HAPT1 transporter (RNAi study, Chapter 7, and re-expression of AT-E1 in *TbAT1*-B48, leading to restoration of pentamidine sensitivity and mitochondrial membrane potential (Chapter 5) and [<sup>3</sup>H]-pentamidine uptake (Eze, Munday and De Koning, unpublished)), this seems to confirm that changes in expression and/or translation, rather than mutations in the ORF, may be responsible for the permanent disappearance of the HAPT1 activity. Even though AT-E2 is not believed to be directly involved in pentamidine transport; reintroduction of WT AT-E2 into *TbAT1*-B48 restored mitochondrial membrane potential, showing that defects in this transporter may contribute to reduced

mitochondrial function, which appears to be an adaptation to increase pentamidine resistance.

All this is consistent with the existing evidence that diamidines including pentamidine target and disrupt mitochondria as their main target.

The identification of the gene encoding HAPT1 finally allows us to study its presence in drug sensitive and resistant isolates from the field - from both veterinary and human samples. The characterisation of the highly similar AT-E1 and E2 as displaying high affinity and efficient pentamidine transport or no detectable pentamidine transport, may make the interpretation of sequence data with various SNPs from clinical samples difficult, however, as translation of primary sequence into functional characteristics is extremely challenging given the current state of knowledge of the transporter's secondary and tertiary structure. Functional studies, as well as structural ones, remain therefore important and in Chapter 4 we attempt to construct a model of substrate recognition for HAPT1.

The identification of a substrate recognition motif may lead to the identification of the natural substrate of the transporter, and is of obvious pharmacological relevance given the importance of drug uptake in chemotherapy of trypanosomiasis. Our analysis did not identify the natural substrate for HAPT1 yet, but still reported very important elements required for substrate recognition. Pentamidine remains the substance of highest affinity to HAPT1 and both amidine groups of pentamidine contribute strongly to binding and their position at *para* position relative to the linker is essential for the binding process. Linker length and flexibility are key determinants in diamidine binding to HAPT1 and the optimal linker length is between 5 and 7 carbons between the benzamidines, not counting the chain oxygen residues. For fixed-angle diamidines, affinity increases with the bond angle between the two benzamidine groups and finally the oxygen atom in the linker of pentamidine is directly involved in binding to HAPT1, probably as H-bond acceptor. It is hoped that computer-aided 3D analysis of the dataset, using Comparative Molecular Field Analysis (CoMFA) and Comparative Molecular Similarity Indices Analysis (CoMSIA), will yield a clearer, 3D model of substrate recognition. This approach was highly successful in modelling substrate binding of the P2/TbAT1 transporter (Collar *et al.*, 2009).

At the start of this project the P2 transporter was the only *Trypanosoma* transporter involved in pentamidine uptake that had been characterised at the molecular level and its coding gene was confirmed to be *TbAT1*. The fact that *TbAT1* shares the same phylogenetic group with three AT-like genes could implicate them in pentamidine uptake and it was hypothesised that they might code for LAPT1 and/or HAPT1. This was the major part of the project and the focus was on the AT-E gene, using RNAi-based approaches and analysis of resistant lines. The RNAi-expressing bloodstream cell lines were used to investigate the effect of AT-E knockdown on HAPT1- and LAPT1-mediated [<sup>3</sup>H]-pentamidine uptake, using low and high concentrations of [<sup>3</sup>H]-pentamidine, respectively. During these experiments P2-mediated transport was blocked by the inclusion of saturating concentrations of adenosine and under those conditions HAPT1 and LAPT1 can be studied independently (De Koning, 2001; Bray *et al.*, 2003; Matovu *et al.*, 2003; Bridges *et al.*, 2007).

The same approach was used in procyclic cells, which naturally lack the P2 transporter activity. In both bloodstream and procyclic forms, LAPT1-mediated uptake was statistically identical in cells grown in the presence of tetracycline (RNAi-induced) and in non-induced control cells, whereas HAPT1 activity was approximately 60% reduced upon tetracycline induction - mirroring the reduction in AT-E mRNA. The results prove that RNAi is a powerful tool to study drug resistance phenotypes in both procyclic and bloodstream form trypanosomes. The knockdown appeared to be specific, as judged by the unaltered expression levels of the most closely related genes, and by the unaltered function of the other pentamidine transport activities in cellular assays. The levels of knockdown caused identical reduction in HAPT1 activity in both life cycle stages and the resulting resistance levels were entirely consistent with loss of most of the HAPT1 activity. Therefore, it can be concluded that it is highly probable that AT-E is the gene encoding for the high affinity pentamidine transporter (HAPT1).

Leaving the investigation of the pentamidine transporting mechanism in trypanosome cells at this stage makes the next priority the characterisation of LAPT1 at the molecular level, and the identification of its natural substrate, as the basis for future work.

## Appendices

### Appendix A: general buffers, solutions and mediums

#### Assay buffer (pH 7.3)

D-Glucose	2.53 g
HEPES	8 g
MOPS	5 g
NaHCO <sub>3</sub>	2 g
KCl	347.5 mg
MgCl <sub>2</sub> ·6H <sub>2</sub> O	62.5 mg
NaH <sub>2</sub> PO <sub>4</sub> ·2H <sub>2</sub> O	913.5 mg
CaCl <sub>2</sub> ·2H <sub>2</sub> O	40.7 mg
MgSO <sub>4</sub> ·7H <sub>2</sub> O	19.9 mg
NaCl	5.7 g
Store at 4 °C.	

#### CBSS buffer (pH 7.4)

Hepes	25 mM
NaCl	120 mM
KCl	5.4 mM
CaCl <sub>2</sub>	0.6 mM
MgSO <sub>4</sub> ·7 H <sub>2</sub> O	0.4 mM
Na <sub>2</sub> HPO <sub>4</sub>	5.6 mM
D-glucose	11.1 mM

Store at -20 °C

#### 6× DNA loading dye

Bromophenol blue	25 mg
Xylene cyanol FF	25 mg
Sucrose	4 g
Made with double distilled water	10 ml

#### LB medium -Luria Bertani broth- (pH 7)

LB powder (Sigma-Aldrich)	25 g
dH <sub>2</sub> O	1 L

#### LB agar

Luria Agar (Sigma-Aldrich)	35 g
dH <sub>2</sub> O	1 L

Autoclaved and agar is liquefied before making agar plates.

**Lysis buffer**

Tris-HCl, pH 8.0	10 mM
EDTA, pH 8.0	100 mM
Sarkosyl	1 %

**Oil Mixture**

Mineral oil (Sigma)	50 ml
di-n-butyl phthalate	350 ml

**PBS**

NaCl	137 mM
KCl	2.7 mM
Na <sub>2</sub> HPO <sub>4</sub>	10 mM
KH <sub>2</sub> PO <sub>4</sub>	2 mM

**PSG buffer (pH 8)**

Na <sub>2</sub> HPO <sub>4</sub>	56.9 mM
NaH <sub>2</sub> PO <sub>4</sub>	3.9 mM
NaCl	43.5 mM
Glucose	60 mM

Dissolve the above component in litre with dH<sub>2</sub>O (PS buffer). Dissolve 10 g of glucose in approximately 200 ml of dH<sub>2</sub>O (Glucose solution). Add six volumes of PS to four volume of glucose solution (PSG buffer). Adjust to pH 8.0 exactly and store at 4°C.

**TAE buffer (1×) (pH 8.5)**

Tris-acetate	40 mM
EDTA (pH 8.0)	1 mM

**TE buffer**

Tris-HCl (pH 8)	10 mM
EDTA (pH 8)	1 mM
dd H <sub>2</sub> O	1 litre

**1× TE**

1 M Tris.HCl	10 ml
0.5 M EDTA at pH 8.0	2 ml
dd H <sub>2</sub> O	1 litre

**2% SDS**

Sodium Dodecyl Sulfate	10 g
ddH <sub>2</sub> O	500 ml

**SOC medium**

Tryptone	20 g
Yeast extract	5 g
NaCl	0.5 g
250 mM KCl	10 ml
2 M MgCl <sub>2</sub>	5 ml
dd H <sub>2</sub> O	1 litre

Adjust pH at 7.0 with 5 M NaOH. Autoclave and when cooled down 1 M of sterile glucose 20 ml was added.

**Denaturation solution**

NaCl	1.5 M
NaOH	0.5 M

**Denhardt's reagent (50×)**

Ficoll 400 (w/v)	1%
Polyvinylpyrrolidone (w/v)	1%
Bovine serum albumin (w/v)	1%

**Lysis buffer for gDNA extraction**

Tris-HCl (pH 8)	10 mM
EDTA	100 mM
<i>N</i> -Lauroylsarcosine (w/v)	1%
Proteinase K (added fresh)	100 µg

**Neutralising solution**

Tris-HCl (pH 7.4)	1 M
NaCl	1.5 M

**Prehybridisation/hybridisation solution**

Formamide (v/v)	50%
SSC	5×
Denhardt's reagent	10×
SDS (w/v)	0.1%
NaH <sub>2</sub> PO <sub>4</sub> (pH 6.5)	20 mM
EDTA (pH 8)	5 mM
Herring sperm DNA (Promega)	200 µg/ml

**SSC (20×) (pH 7)**

NaCl	3 M
Tri-sodium citrate	0.3 M

**Washing solution for membrane stripping**

SSC	0.1×
SDS (w/v)	0.1%
Tris-HCl (pH 7.6)	0.2 M

**Depurination solution**

HCl 0.25 M

**ZPFM Media**

NaCl 132mM

KCl 8mM

 $\text{Na}_2\text{H}_2\text{PO}_3^{2+}$  8Mm $\text{KH}_2\text{PO}_3$  1.5 mM $\text{Mg}(\text{C}_2\text{H}_3\text{O}_2)$  1.5 mM $\text{C}_4\text{H}_6\text{CaO}_2$  90  $\mu\text{M}$ **SDM-79 medium (pH 7.3)**

Components	(per L)
$\text{NaH}_2\text{PO}_4$	157 mg
NaCl	6.8 g
$\text{MgSO}_4$	100 mg
KCl	400 mg
$\text{CaCl}_2$	200 mg
L-Arginine	100 mg
L-Methionine	70 mg
L-Phenylalanine	80 mg
L-Threonine	350 mg
L-Tyrosine	100 mg
Taurine	160 mg
L-Alanine	200 mg
L-Asparagine	13.2 mg
L-Aspartate	13.3 mg
L-Glutamate	14.7 mg
L-Glutamine	200 mg
Glycine	7.5 mg
L-Serine	60 mg
HEPES	8 g
MOPS	5 g
$\text{NaHCO}_3$	2.2 g
Pyruvate	220 mg
Mercaptoethanol (0.1 M)	2 ml
Hypoxanthine	14 mg
Thymidine	4 mg
Vitamins (100 X)	10 ml
Essential amino acids (50 X)	20 ml
Phenol Red	4 ml
Hemin (2.5 mg/ml)	2 ml
Dialysed Foetal Calf Serum	10%

pH 7.3, filter sterilise. Store at 4°C.

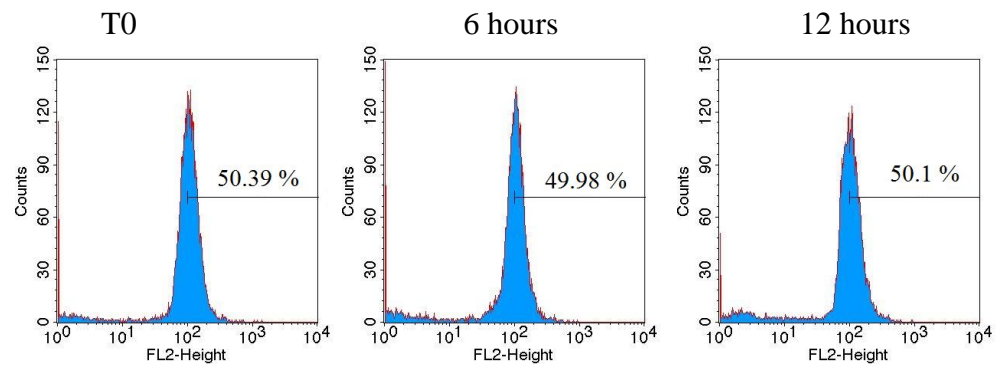
**HMI-9 medium (pH 7.4)**

Components	(mg/L)
CaCl <sub>2</sub>	165
KCl	330
KNO <sub>3</sub>	0.076
MgSO <sub>4</sub>	98
NaCl	4,500
NaHCO <sub>3</sub>	3,020
NaH <sub>2</sub> PO <sub>4</sub> ·H <sub>2</sub> O	125
Na <sub>2</sub> SeO <sub>3</sub> ·5 H <sub>2</sub> O	0.017
Glucose	4,500
Phenol Red	15
HEPES	5,960
Bathocuproine sulfonate	28
Mercaptoethanol	15
Alanine	25
Arginine·HCl	84
Asparagine	25
Aspartic acid	30
Cysteine	182
Cystine	91
Glutamic acid	75
Glutamine	584
Glycine	30
Histidine·HCl·H <sub>2</sub> O	42
Isoleucine	105
Leucine	105
Lysine·HCl	146
Methionine	30
Phenylalanine	66
Proline	40
Serine	42
Threonine	95
Tryptophan	16
Tyrosine	104
Valine	94
B12	0.013
Biotin	0.013
D-Ca pantothenate	4
Choline chloride	4
Folic Acid	4
i-Inositol	7.2
Nicotinamide	4
Pyridoxal·HCl	4
Riboflavin	0.4
Thiamine·HCl	4
Pyruvate·Na	114
Hypoxanthine	136
Thymidine (deoxy)	39
Serum	10%

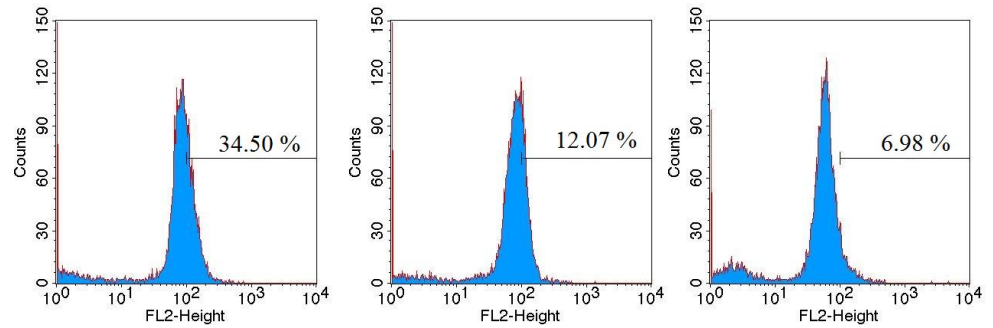
pH at 7.4, filter sterilise. Store at 4°C.

**Appendix B: Mitochondrial membrane potential determinations**

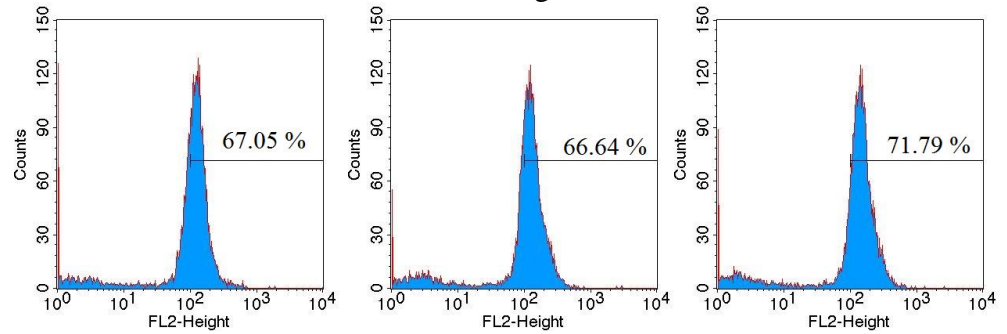
## 427-WT. Drug Free



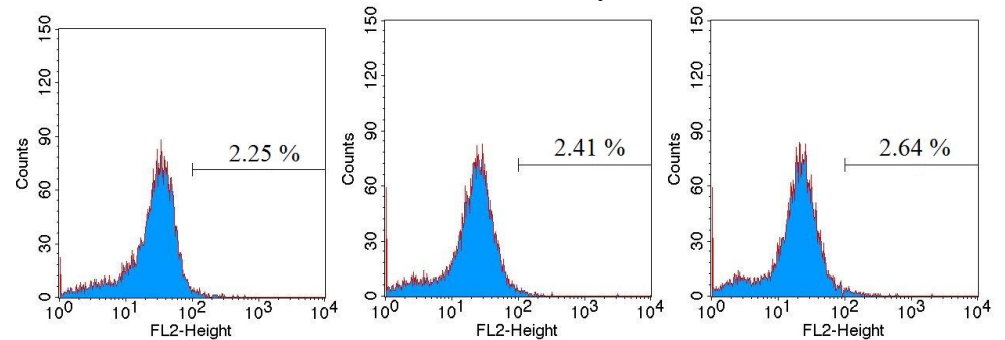
## 427-WT. Pentamidine 500nM



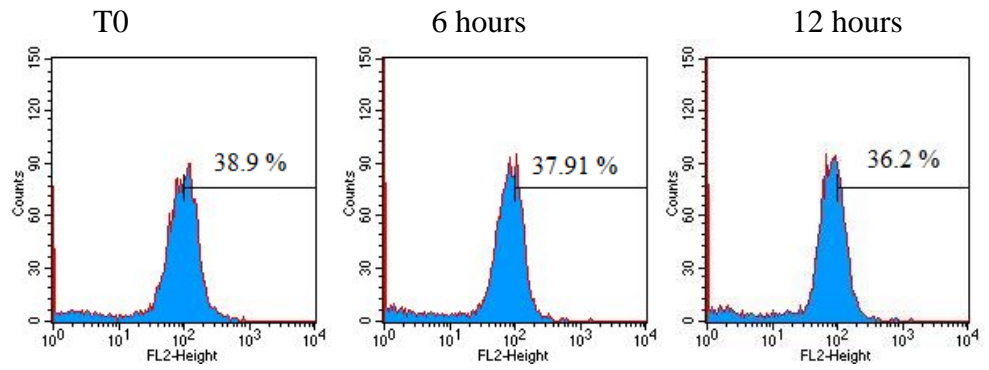
## 427-WT. Troglitazone



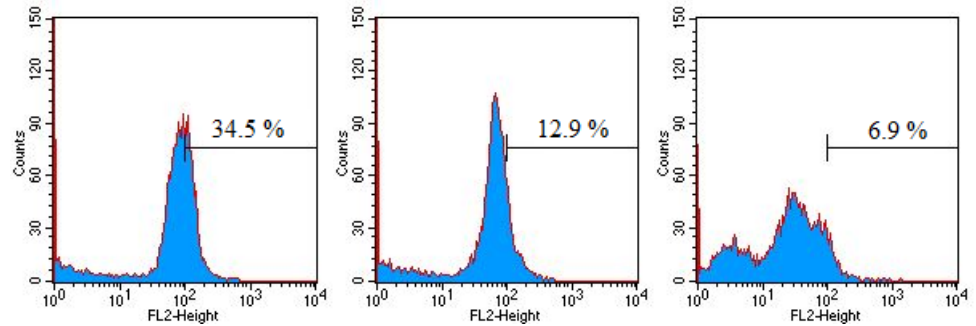
## 427-WT. Valinomycin



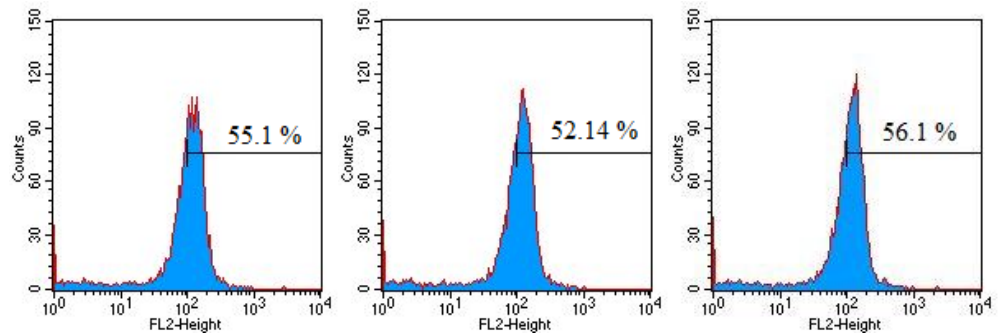
TbAT1-KO. Drug Free



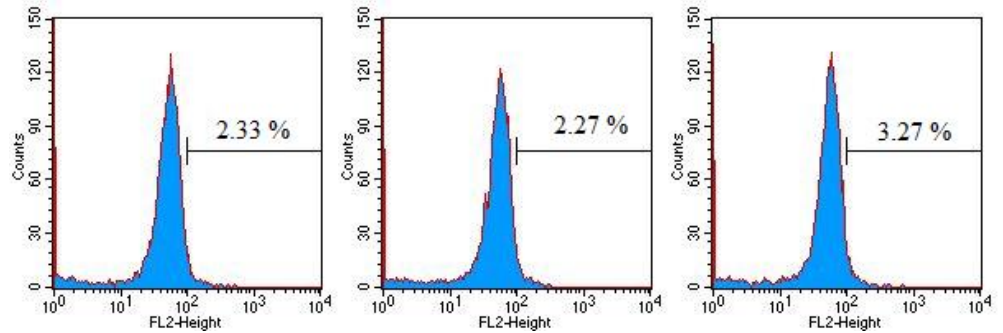
TbAT1-KO. Pentamidine 500nM



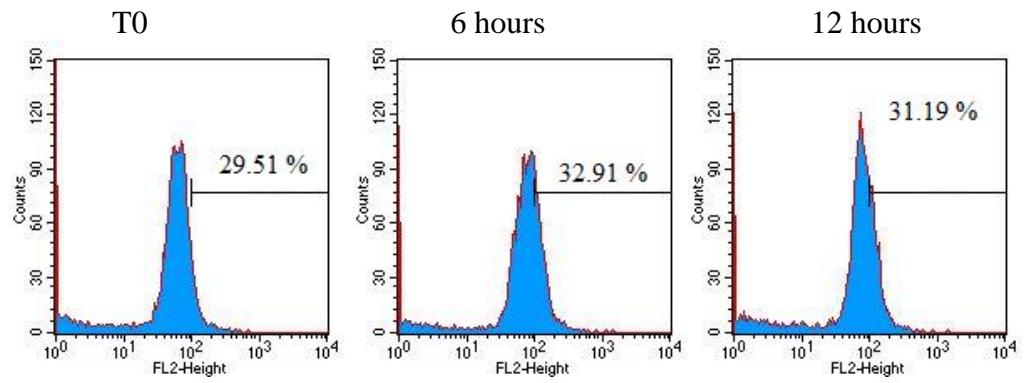
TbAT1-KO. Troglitazone



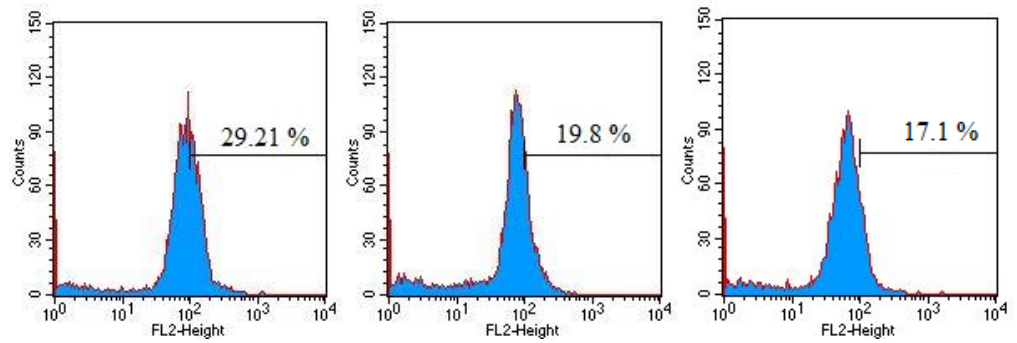
TbAT1-KO. Valinomycin



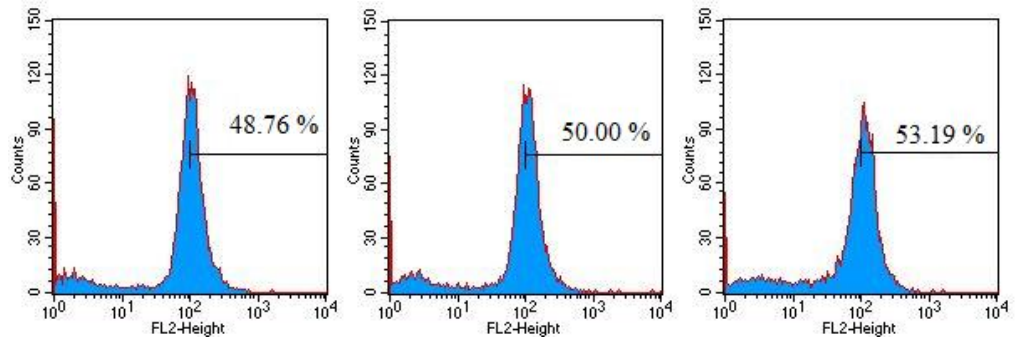
TbAT1-B48. Drug Free



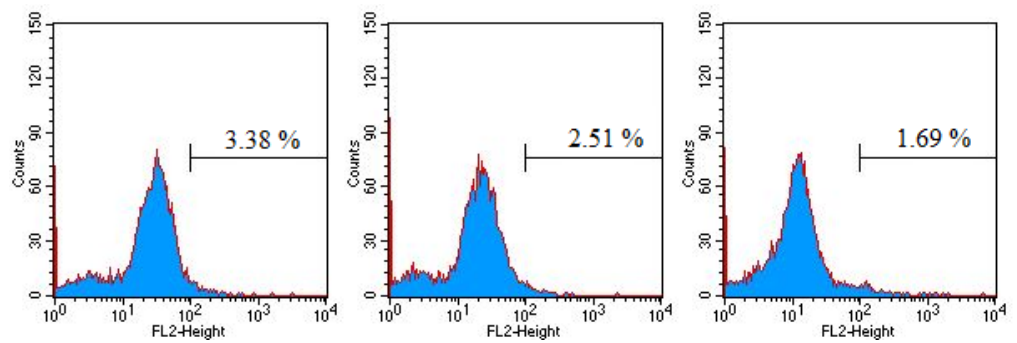
TbAT1-B48. Pentamidine 500nM



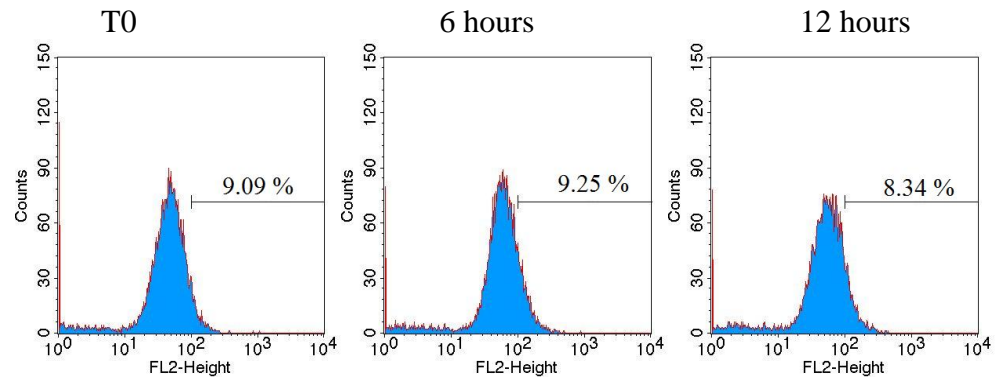
TbAT1-B48. Troglitazone



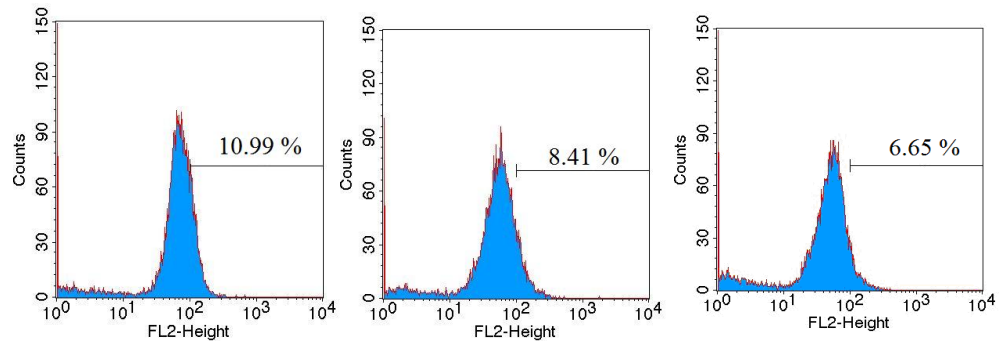
TbAT1-B48. Valinomycin



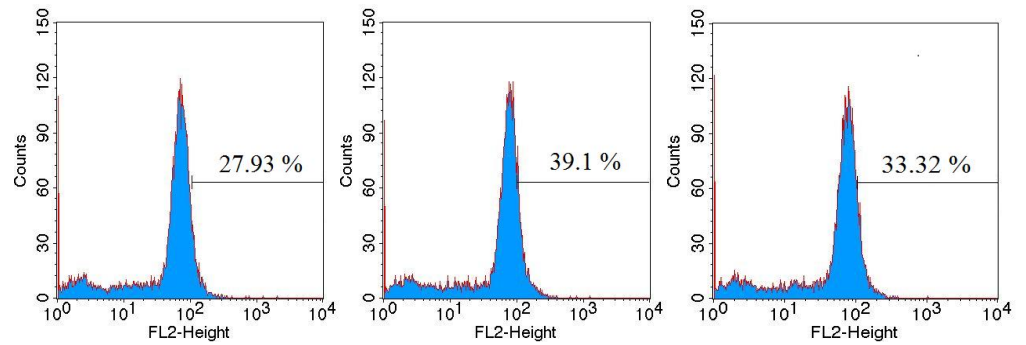
## P1000. Drug Free



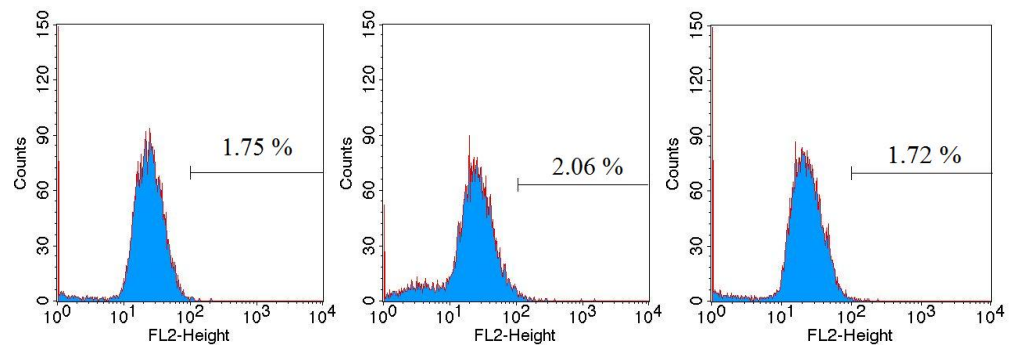
## P1000. Pentamidine 500 nM



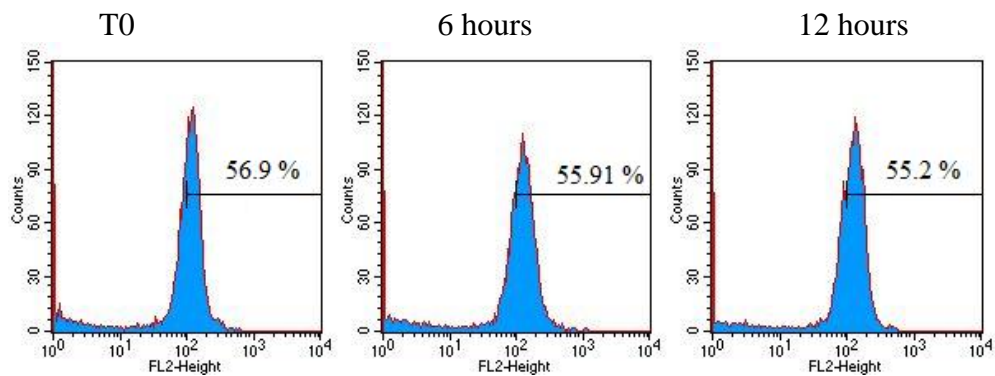
## P1000. Troglitazone



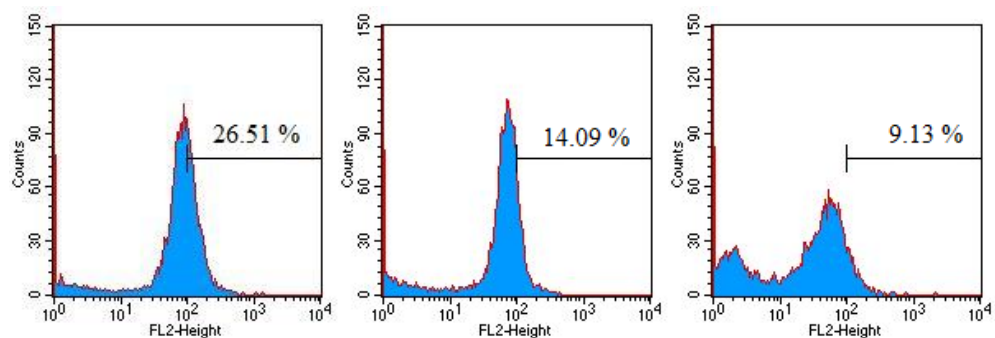
## P1000. Valinomycin



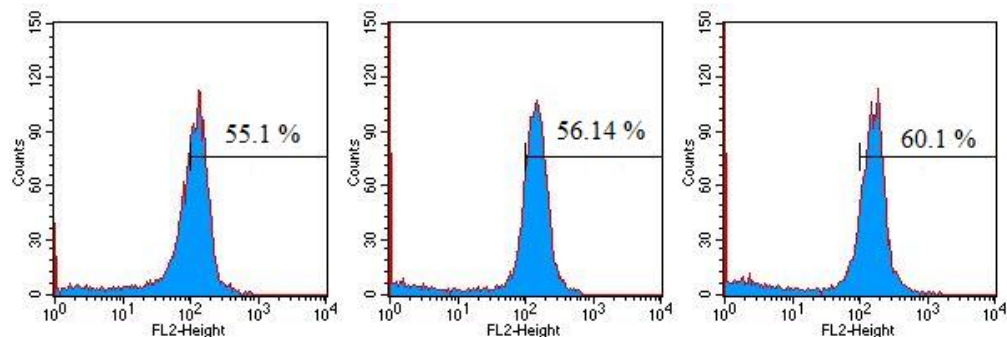
TbAT1-B48 + AT-E1. Drug Free



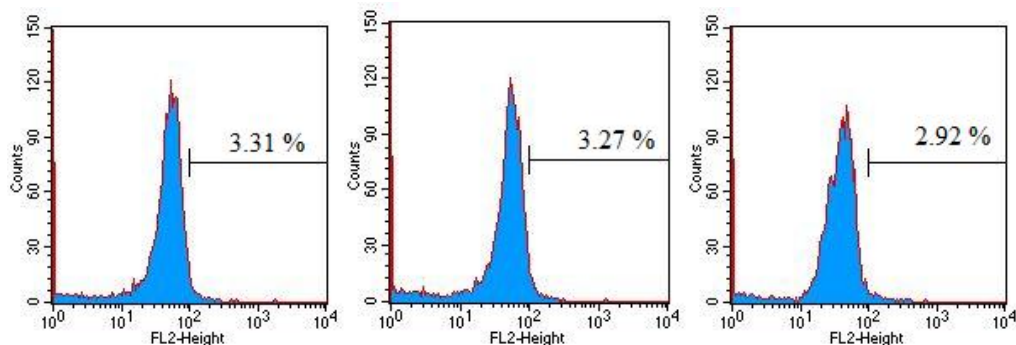
TbAT1-B48 + AT-E1. Pentamidine 500nM



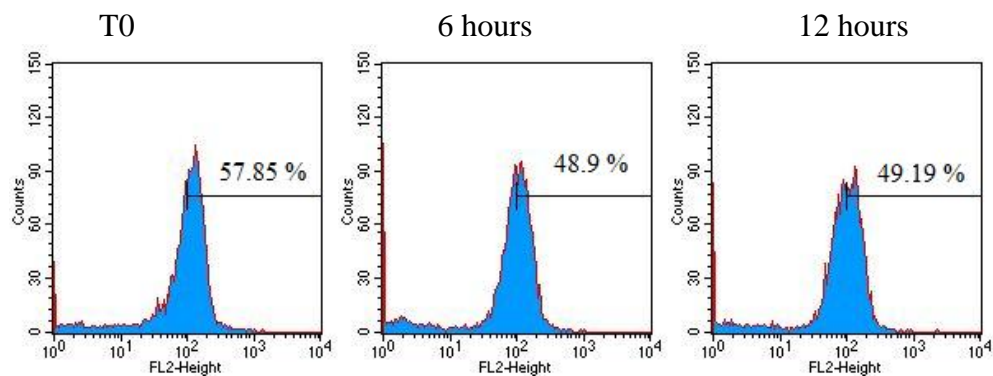
TbAT1-B48 + AT-E1. Troglitazone



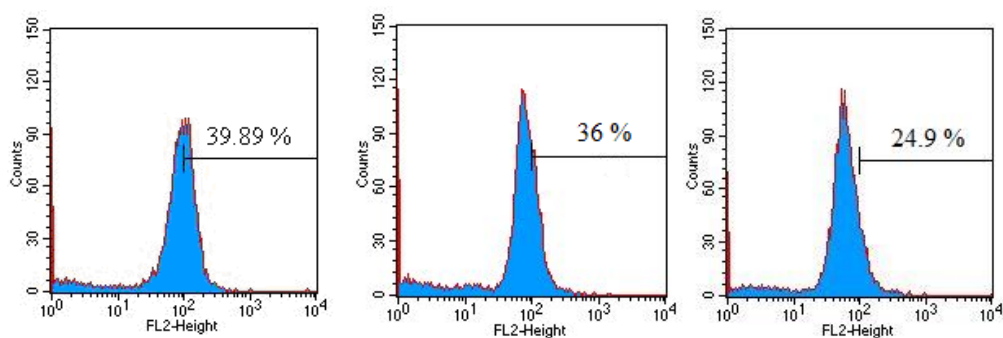
TbAT1-B48 + AT-E1. Valinomycin



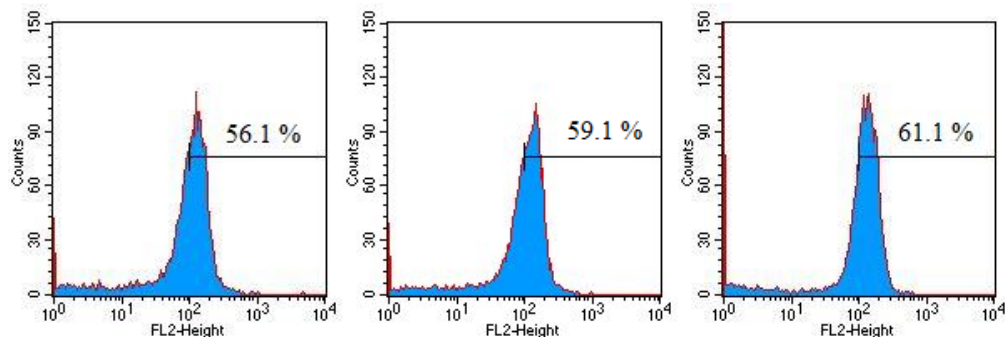
TbAT1-B48 + AT-E2. Drug Free



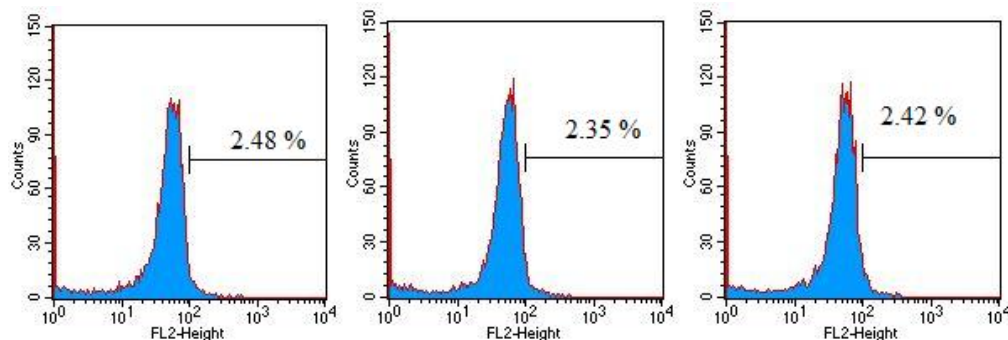
TbAT1-B48 + AT-E2. Pentamidine 500nM



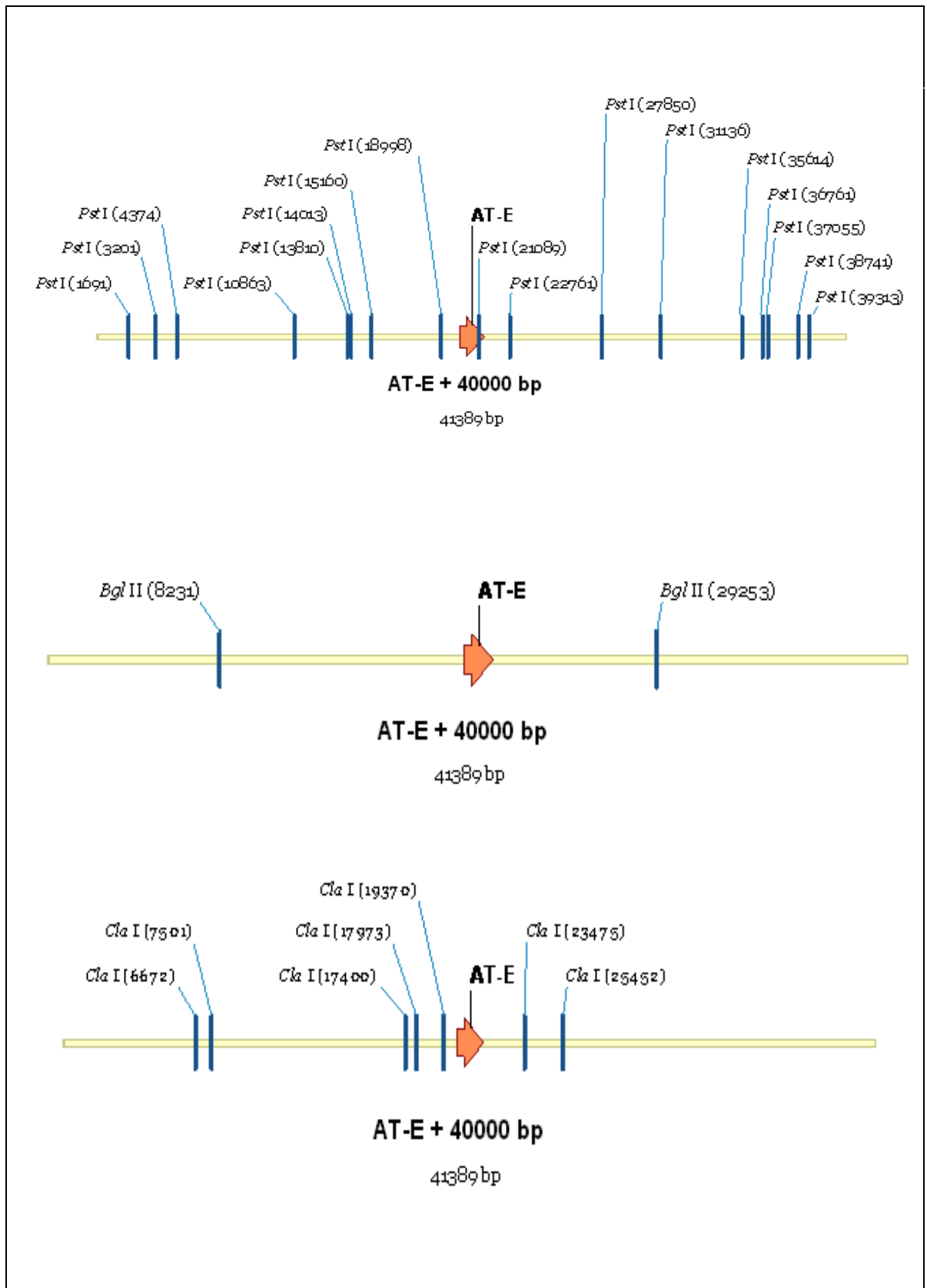
TbAT1-B48 + AT-E2. Troglitazone

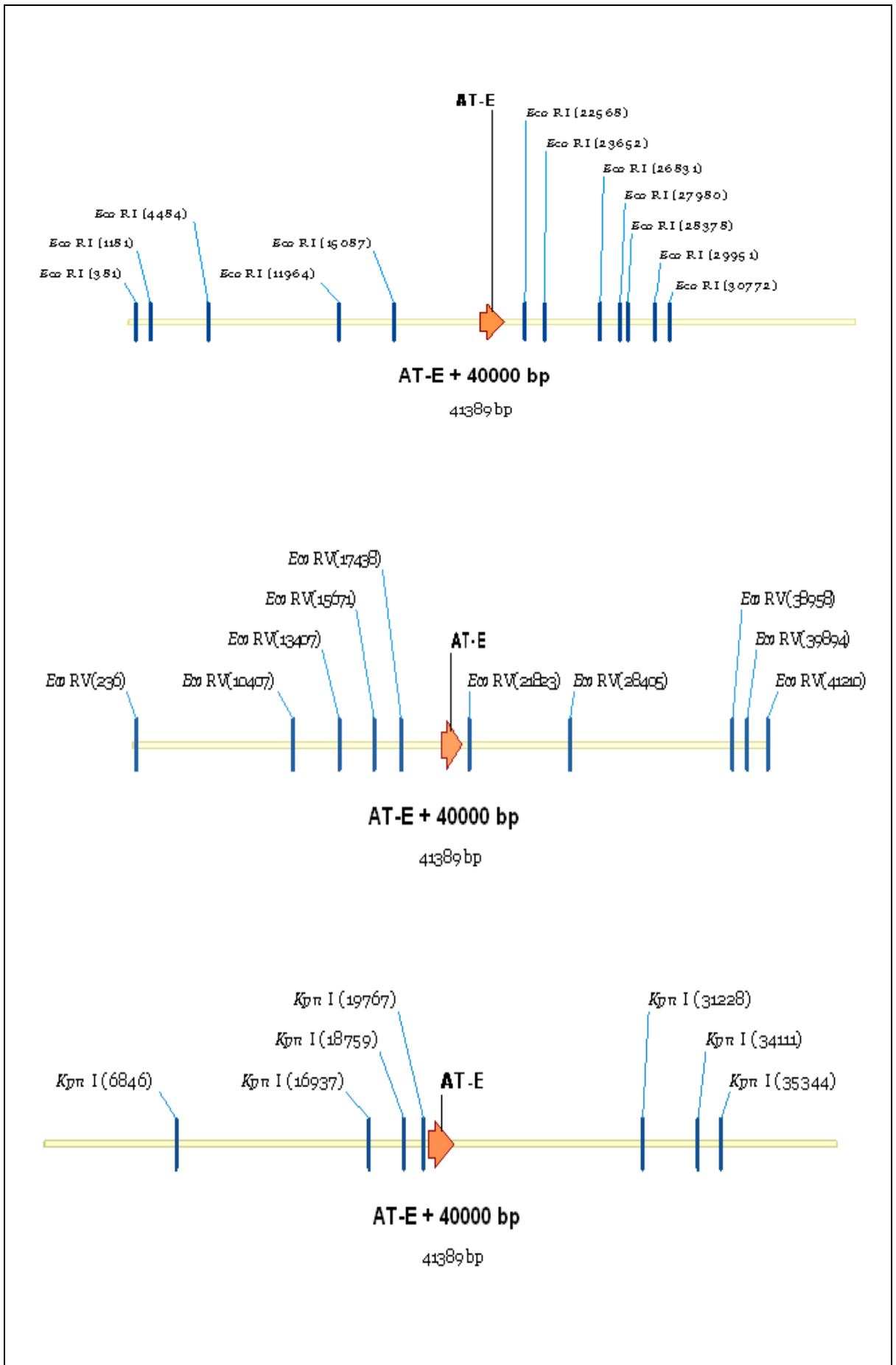


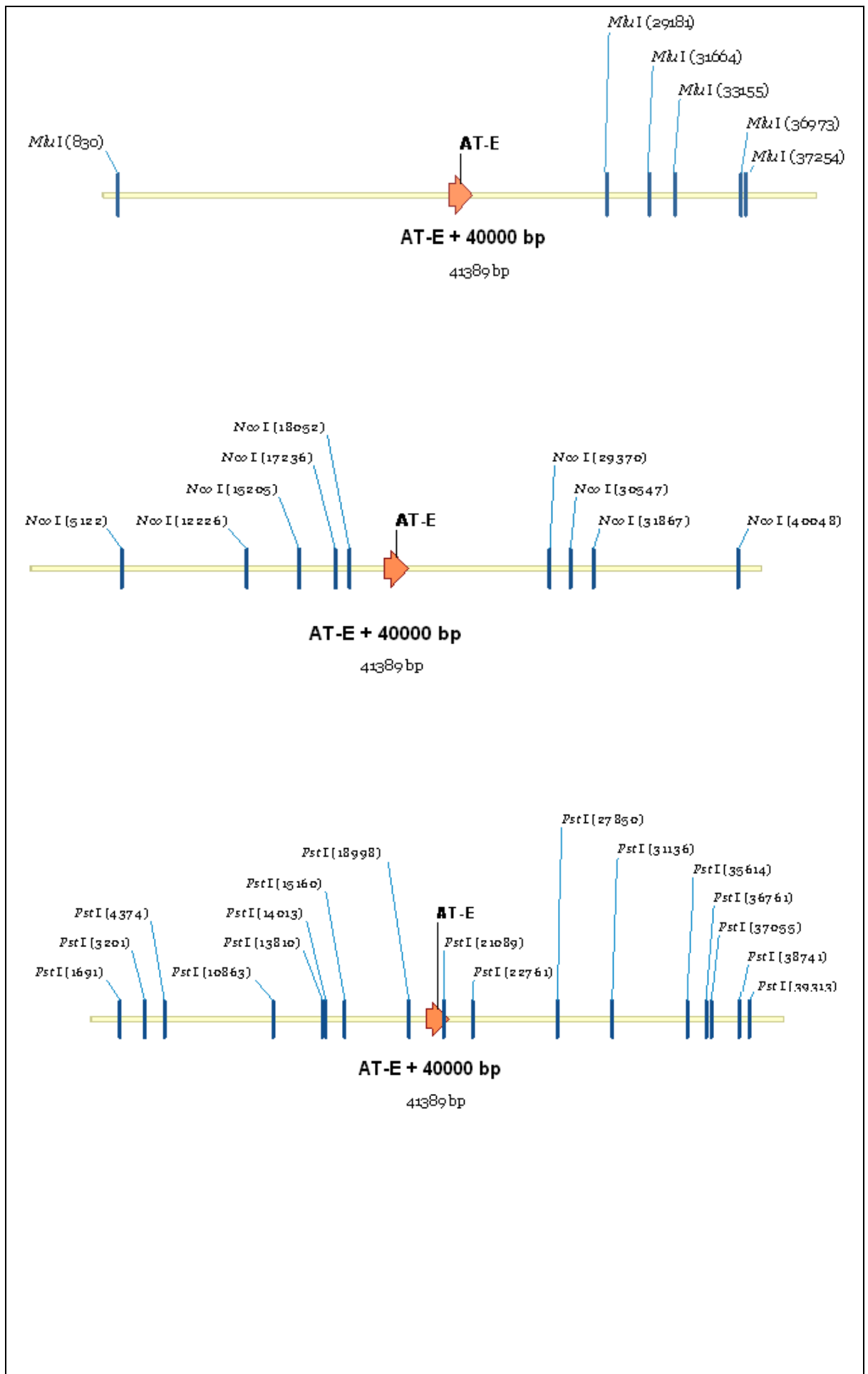
TbAT1-B48 + AT-E2. Valinomycin

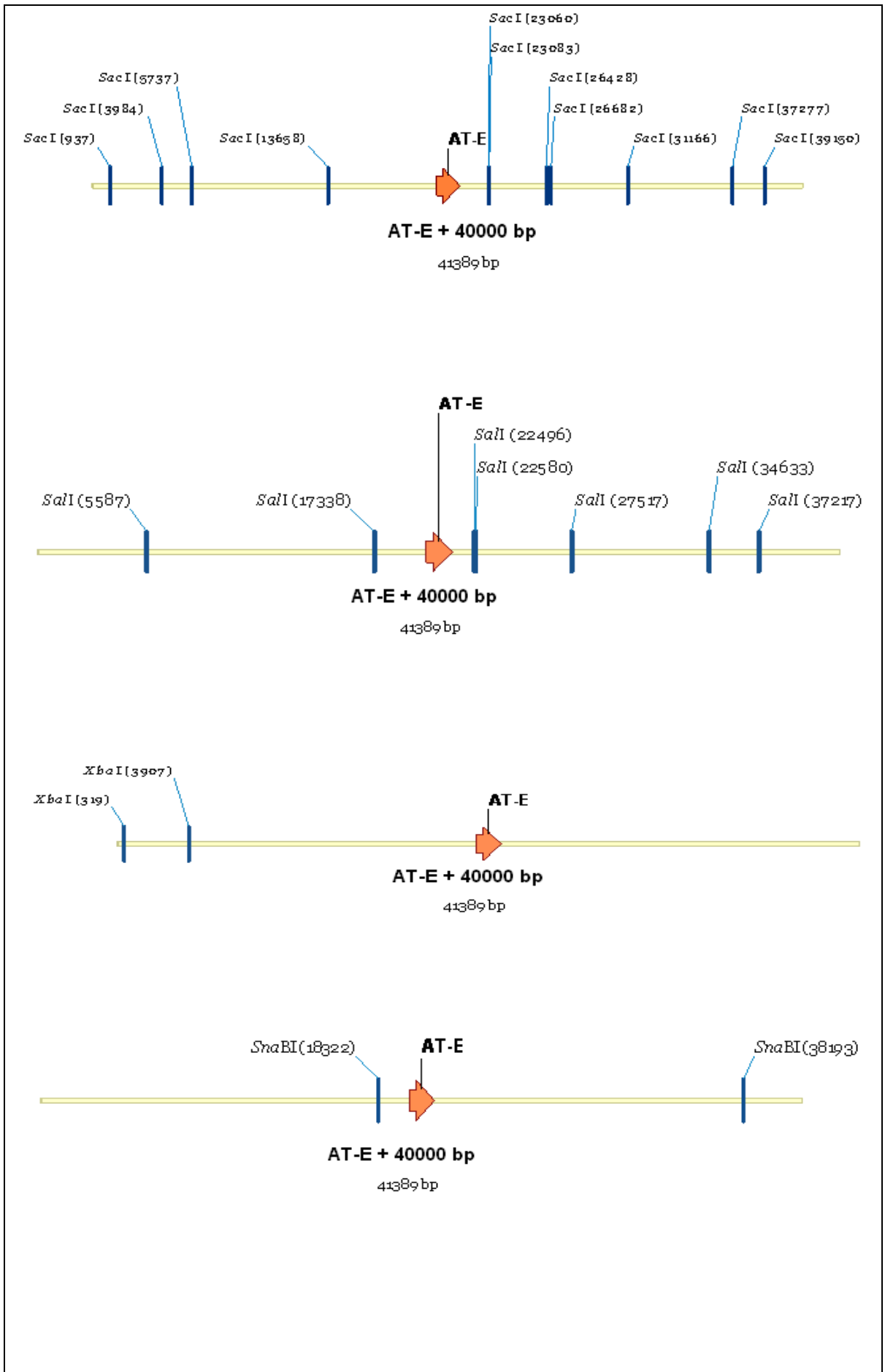


**Appendix C:** Restriction map of 41389 bp fragment from *T. b. brucei* including AT-E gene used for Southern blot

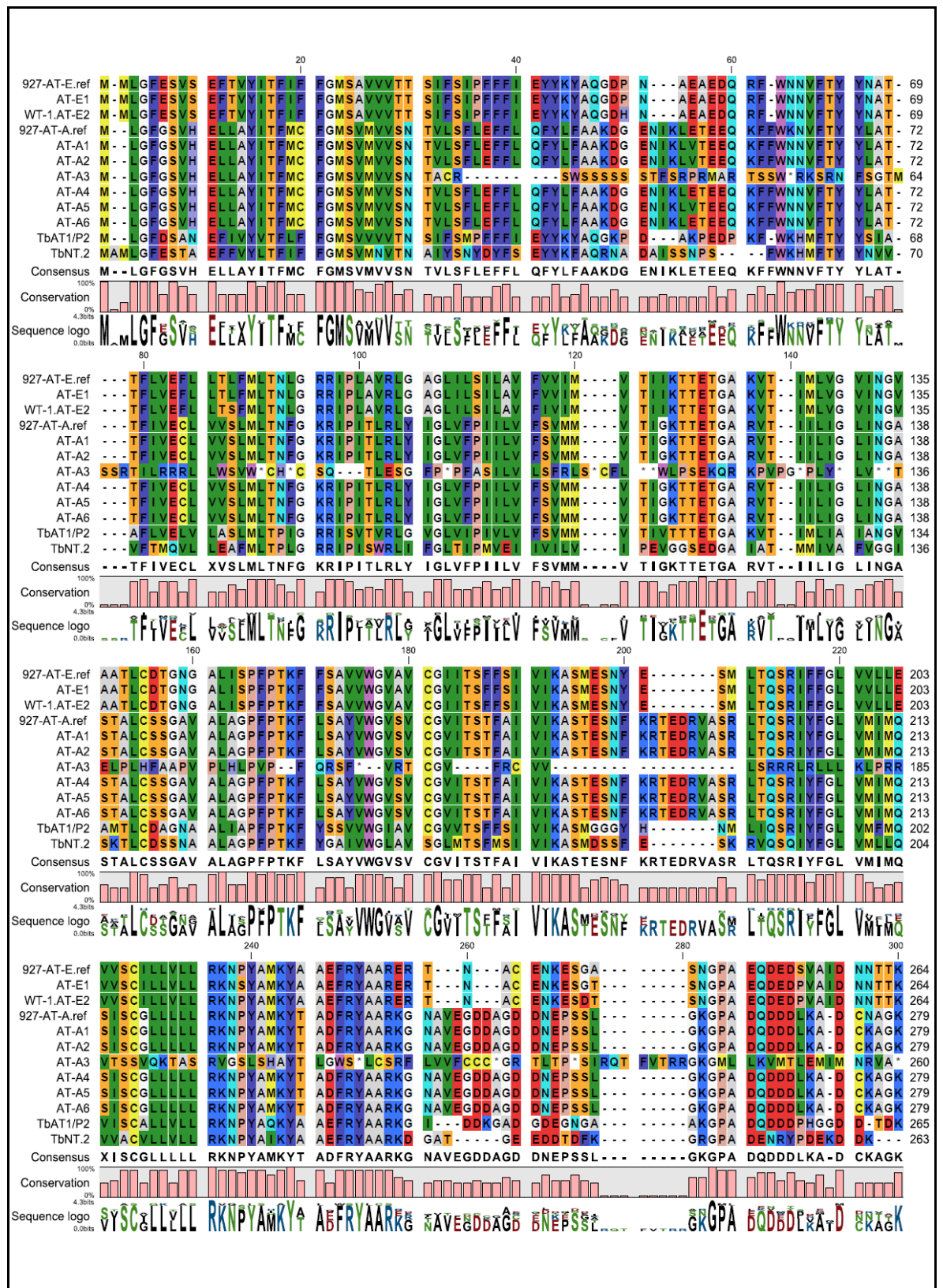


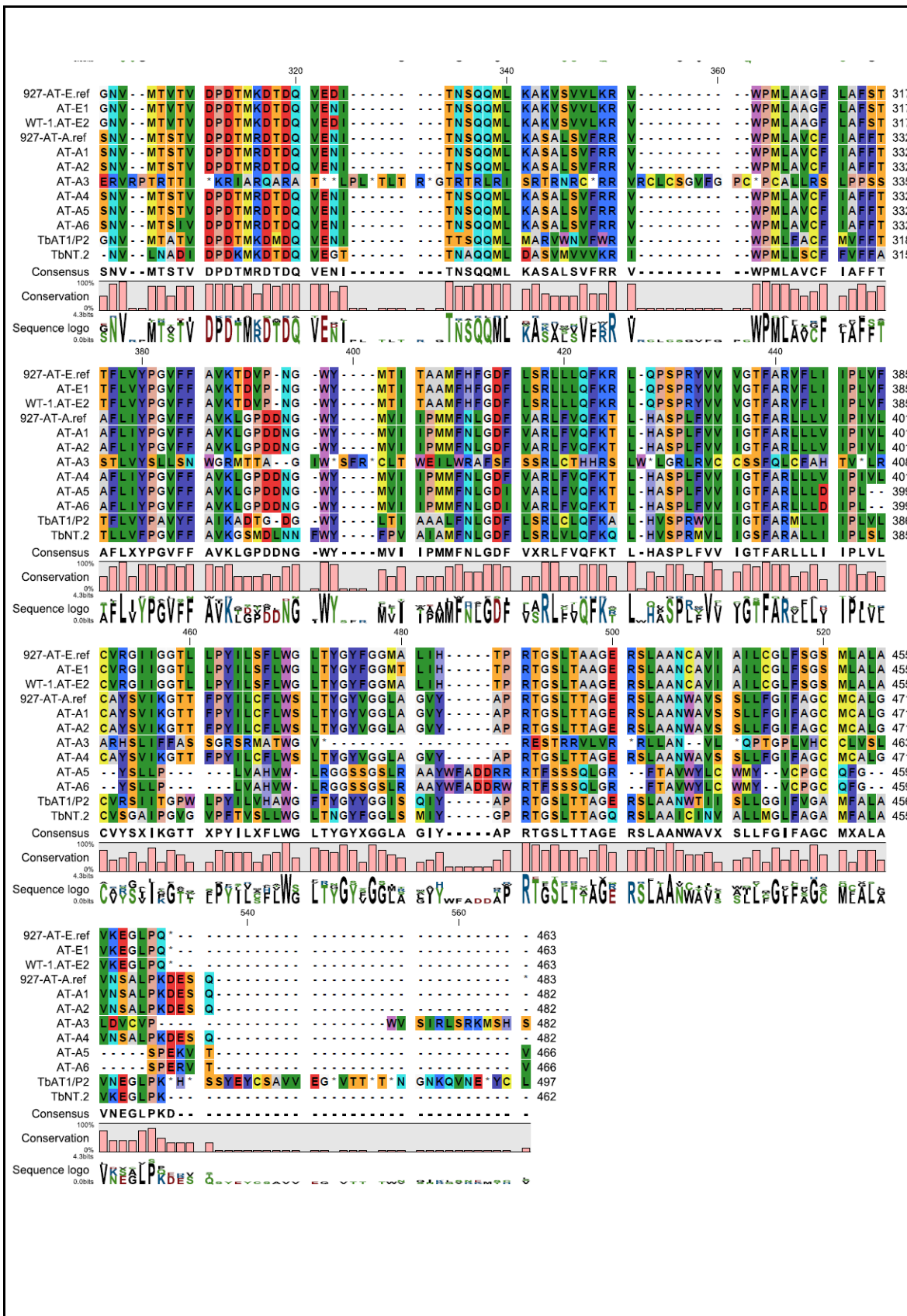






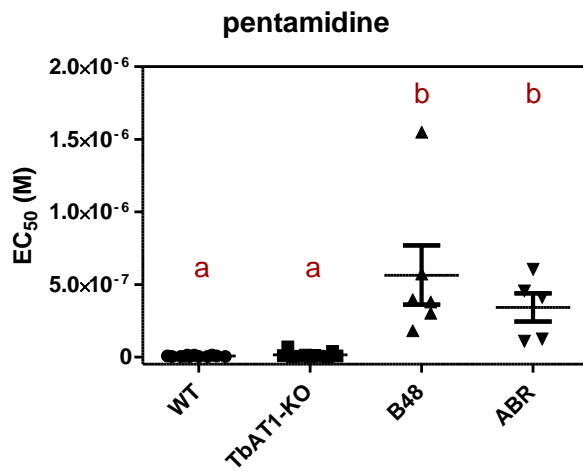
# Appendix D: Protein sequence alignment of AT-A 1-6, ATE1 and AT-E2 in comparison with TbAT1/P2 and TbNT.2



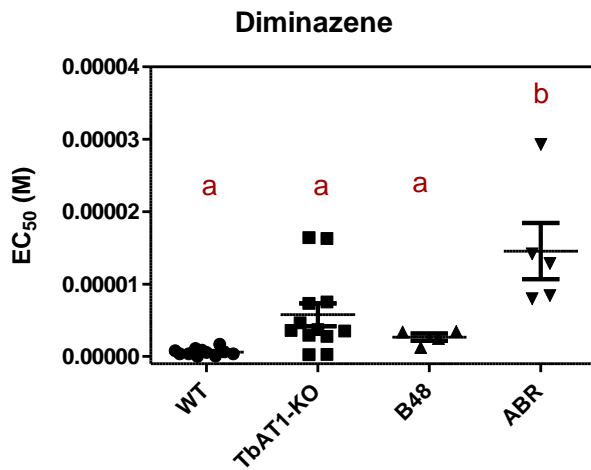


## Appendix E: Stastical analysis

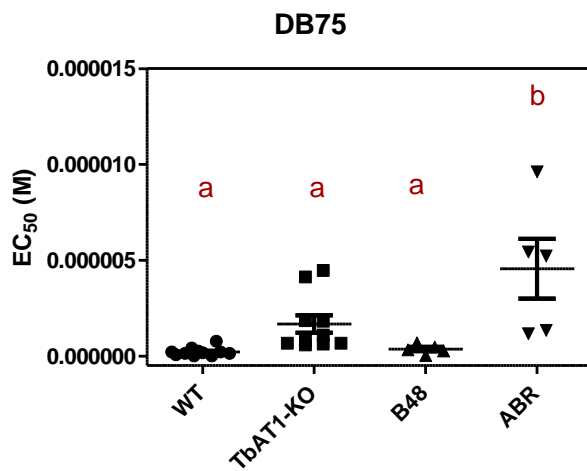
AN OVA test ABR cell lline and controls



Tukey's Multiple Comparison Test	
WT vs TbAT1-KO	ns
WT vs B48	***
WT vs ABR	*
TbAT1-KO vs B48	***
TbAT1-KO vs ABR	*
B48 vs ABR	ns

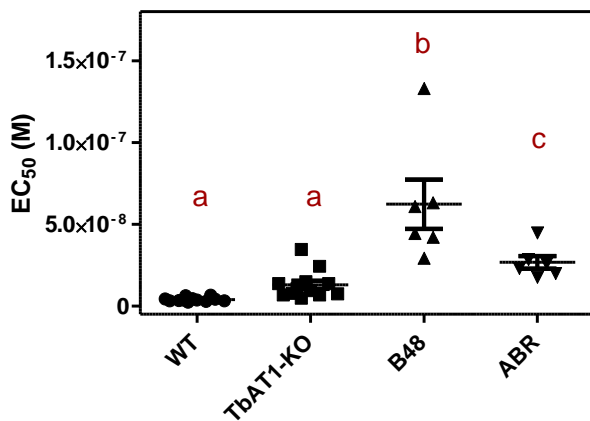


Tukey's Multiple Comparison Test	
WT vs TbAT1-KO	ns
WT vs B48	ns
WT vs ABR	***
TbAT1-KO vs B48	ns
TbAT1-KO vs ABR	**
B48 vs ABR	**



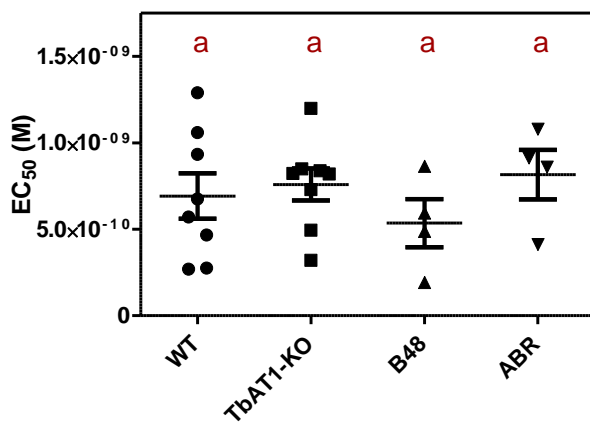
Tukey's Multiple Comparison Test	
WT vs TbAT1-KO	ns
WT vs B48	ns
WT vs ABR	***
TbAT1-KO vs B48	ns
TbAT1-KO vs ABR	*
B48 vs ABR	**

**Cymelarsan**



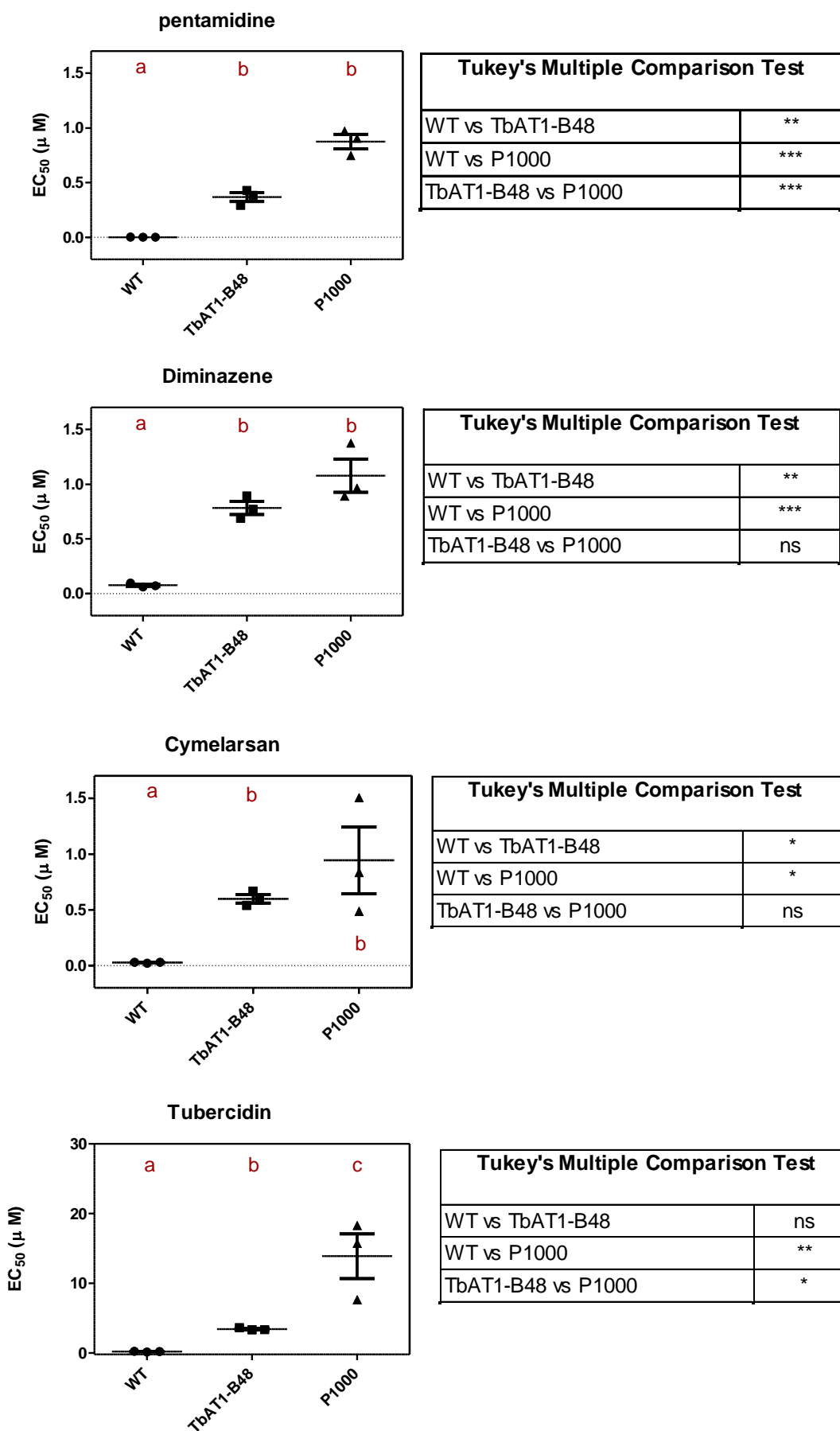
Tukey's Multiple Comparison Test	
WT vs TbAT1-KO	ns
WT vs B48	***
WT vs ABR	*
TbAT1-KO vs B48	***
TbAT1-KO vs ABR	ns
B48 vs ABR	**

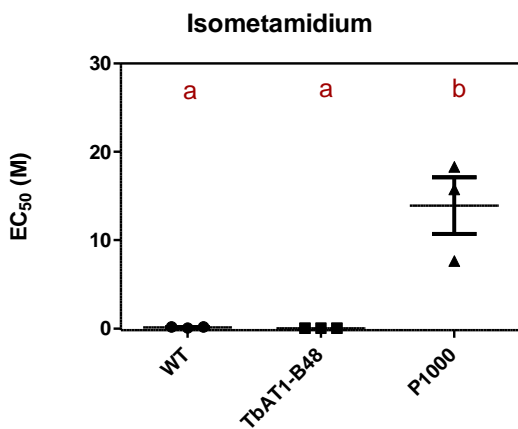
**PAO**



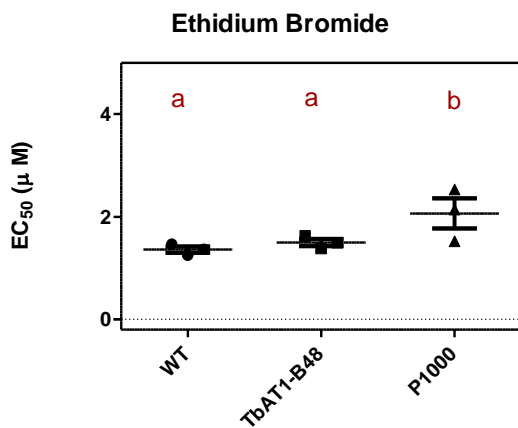
Tukey's Multiple Comparison Test	
WT vs TbAT1-KO	ns
WT vs B48	ns
WT vs ABR	ns
TbAT1-KO vs B48	ns
TbAT1-KO vs ABR	ns
B48 vs ABR	ns

AN OVA test P1000 cell line and controls drug profile (Alamar Blue)

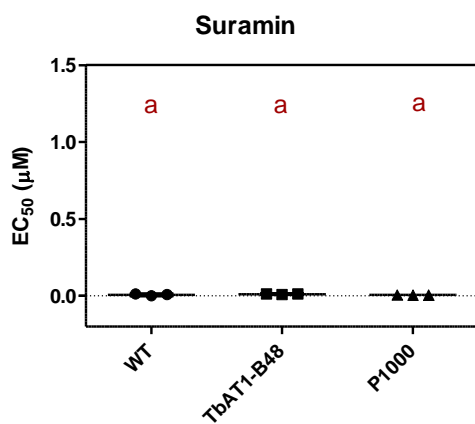




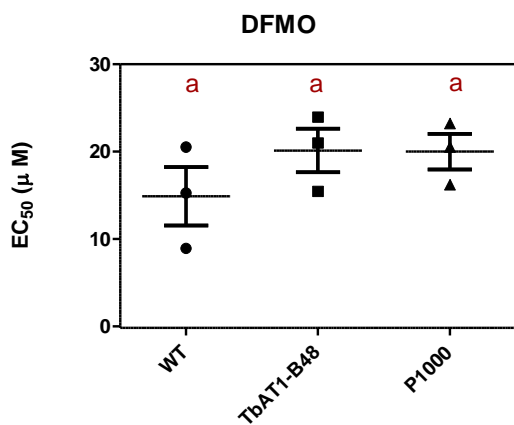
Tukey's Multiple Comparison Test	
WT vs TbAT1-B48	ns
WT vs P1000	**
TbAT1-B48 vs P1000	**



Tukey's Multiple Comparison Test	
WT vs TbAT1-B48	ns
WT vs P1000	ns
TbAT1-B48 vs P1000	ns

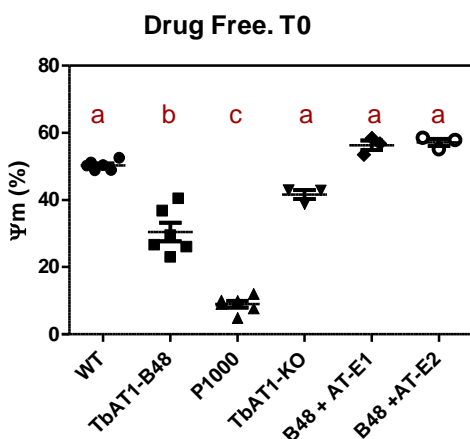


Tukey's Multiple Comparison Test	
WT vs TbAT1-B48	ns
WT vs P1000	ns
TbAT1-B48 vs P1000	ns

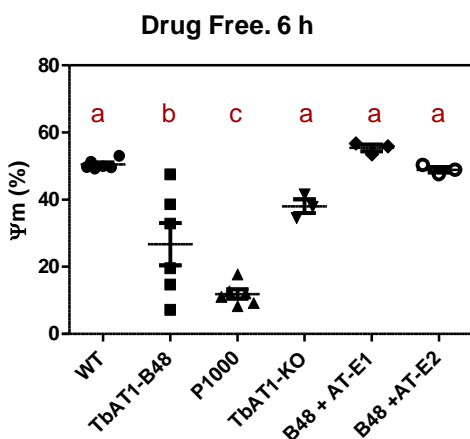


Tukey's Multiple Comparison Test	
WT vs TbAT1-B48	ns
WT vs P1000	ns
TbAT1-B48 vs P1000	ns

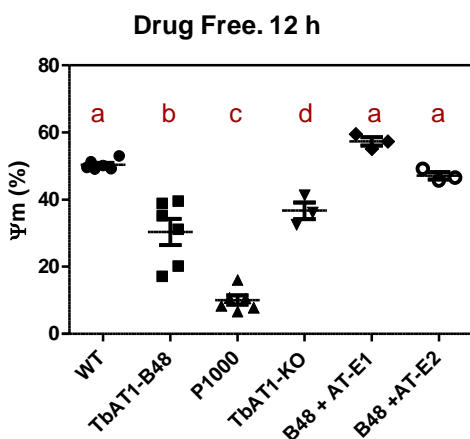
AN OVA test P1000 cell line and controls mitochondrial membrane potential



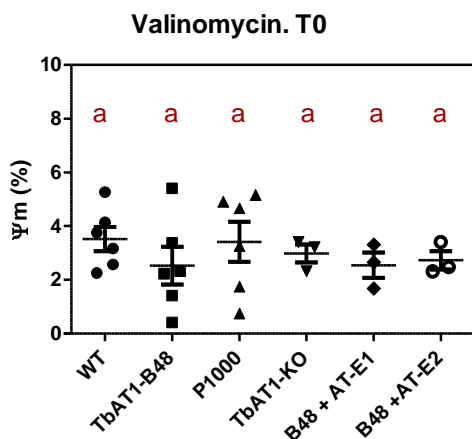
Drug free Time Zero	
Tukey's Multiple Comparison Test	
WT vs TbAT1-B48	***
WT vs P1000	***
WT vs TbAT1-KO	*
WT vs B48 + AT-E1	ns
WT vs B48 + AT-E2	ns
TbAT1-B48 vs P1000	***
TbAT1-B48 vs TbAT1-KO	**
TbAT1-B48 vs B48 + AT-E1	***
TbAT1-B48 vs B48 + AT-E2	***
P1000 vs TbAT1-KO	***
P1000 vs B48 + AT-E1	***
P1000 vs B48 + AT-E2	***
TbAT1-KO vs B48 + AT-E1	**
TbAT1-KO vs B48 + AT-E2	***
B48 + AT-E1 vs B48 + AT-E2	ns



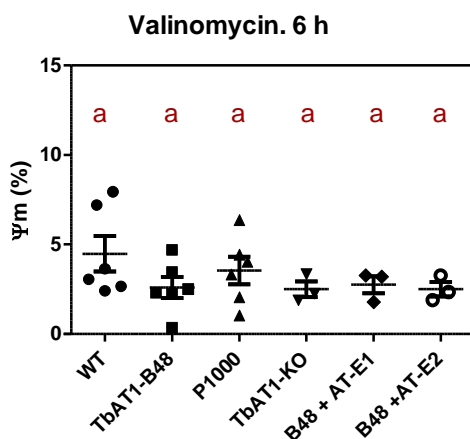
Drug free 6 h	
Tukey's Multiple Comparison Test	
WT vs TbAT1-B48	***
WT vs P1000	***
WT vs TbAT1-KO	ns
WT vs B48 + AT-E1	ns
WT vs B48 + AT-E2	ns
TbAT1-B48 vs P1000	*
TbAT1-B48 vs TbAT1-KO	ns
TbAT1-B48 vs B48 + AT-E1	***
TbAT1-B48 vs B48 + AT-E2	**
P1000 vs TbAT1-KO	**
P1000 vs B48 + AT-E1	***
P1000 vs B48 + AT-E2	***
TbAT1-KO vs B48 + AT-E1	ns
TbAT1-KO vs B48 + AT-E2	ns
B48 + AT-E1 vs B48 + AT-E2	ns



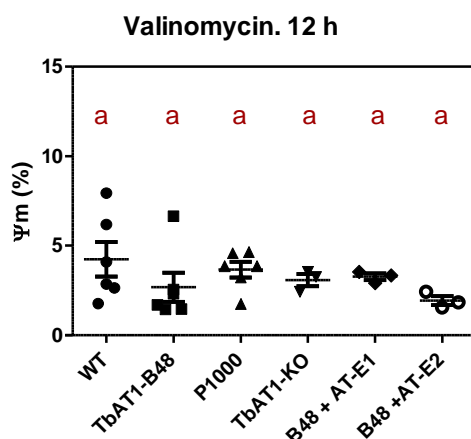
Drug free 12 h	
Tukey's Multiple Comparison Test	
WT vs TbAT1-B48	***
WT vs P1000	***
WT vs TbAT1-KO	*
WT vs B48 + AT-E1	ns
WT vs B48 + AT-E2	ns
TbAT1-B48 vs P1000	***
TbAT1-B48 vs TbAT1-KO	ns
TbAT1-B48 vs B48 + AT-E1	***
TbAT1-B48 vs B48 + AT-E2	**
P1000 vs TbAT1-KO	***
P1000 vs B48 + AT-E1	***
P1000 vs B48 + AT-E2	***
TbAT1-KO vs B48 + AT-E1	**
TbAT1-KO vs B48 + AT-E2	ns
B48 + AT-E1 vs B48 + AT-E2	ns



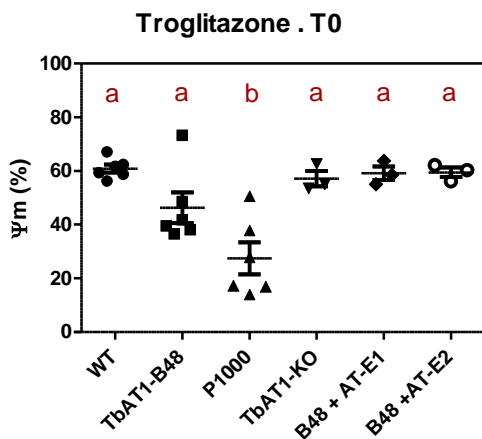
Valinomycin Time Zero	
Tukey's Multiple Comparison Test	
WT vs TbAT1-B48	ns
WT vs P1000	ns
WT vs TbAT1-KO	ns
WT vs B48 + AT-E1	ns
WT vs B48 +AT-E2	ns
TbAT1-B48 vs P1000	ns
TbAT1-B48 vs TbAT1-KO	ns
TbAT1-B48 vs B48 + AT-E1	ns
TbAT1-B48 vs B48 +AT-E2	ns
P1000 vs TbAT1-KO	ns
P1000 vs B48 + AT-E1	ns
P1000 vs B48 +AT-E2	ns
TbAT1-KO vs B48 + AT-E1	ns
TbAT1-KO vs B48 +AT-E2	ns
B48 + AT-E1 vs B48 +AT-E2	ns



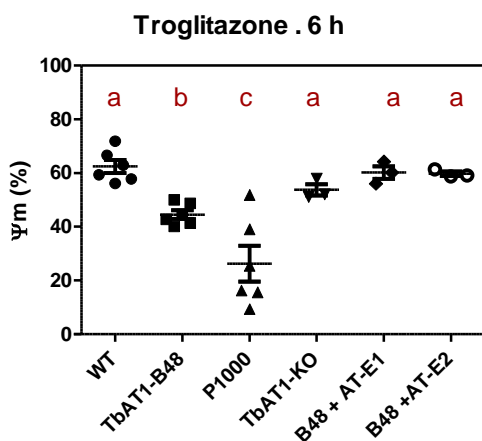
Valinomycin 6 h	
Tukey's Multiple Comparison Test	
WT vs TbAT1-B48	ns
WT vs P1000	ns
WT vs TbAT1-KO	ns
WT vs B48 + AT-E1	ns
WT vs B48 +AT-E2	ns
TbAT1-B48 vs P1000	ns
TbAT1-B48 vs TbAT1-KO	ns
TbAT1-B48 vs B48 + AT-E1	ns
TbAT1-B48 vs B48 +AT-E2	ns
P1000 vs TbAT1-KO	ns
P1000 vs B48 + AT-E1	ns
P1000 vs B48 +AT-E2	ns
TbAT1-KO vs B48 + AT-E1	ns
TbAT1-KO vs B48 +AT-E2	ns
B48 + AT-E1 vs B48 +AT-E2	ns



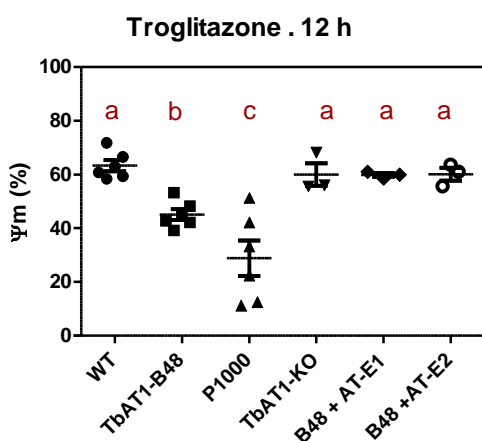
Valinomycin 12 h	
Tukey's Multiple Comparison Test	
WT vs TbAT1-B48	ns
WT vs P1000	ns
WT vs TbAT1-KO	ns
WT vs B48 + AT-E1	ns
WT vs B48 +AT-E2	ns
TbAT1-B48 vs P1000	ns
TbAT1-B48 vs TbAT1-KO	ns
TbAT1-B48 vs B48 + AT-E1	ns
TbAT1-B48 vs B48 +AT-E2	ns
P1000 vs TbAT1-KO	ns
P1000 vs B48 + AT-E1	ns
P1000 vs B48 +AT-E2	ns
TbAT1-KO vs B48 + AT-E1	ns
TbAT1-KO vs B48 +AT-E2	ns
B48 + AT-E1 vs B48 +AT-E2	ns



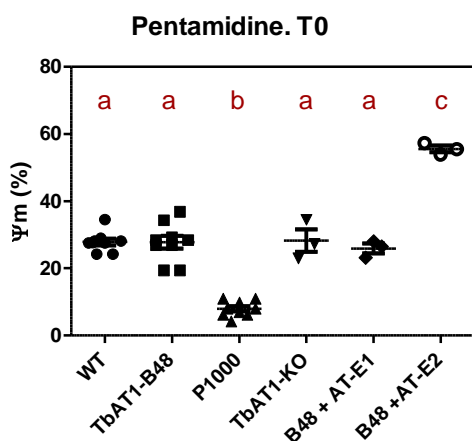
Troglitazone Time Zero	
Tukey's Multiple Comparison Test	
WT vs TbAT1-B48	ns
WT vs P1000	***
WT vs TbAT1-KO	ns
WT vs B48 + AT-E1	ns
WT vs B48 + AT-E2	ns
TbAT1-B48 vs P1000	*
TbAT1-B48 vs TbAT1-KO	ns
TbAT1-B48 vs B48 + AT-E1	ns
TbAT1-B48 vs B48 + AT-E2	ns
P1000 vs TbAT1-KO	**
P1000 vs B48 + AT-E1	**
P1000 vs B48 + AT-E2	**
TbAT1-KO vs B48 + AT-E1	ns
TbAT1-KO vs B48 + AT-E2	ns
B48 + AT-E1 vs B48 + AT-E2	ns



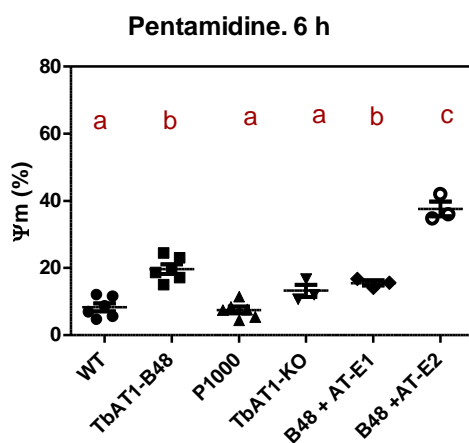
Troglitazone 6 h	
Tukey's Multiple Comparison Test	
WT vs TbAT1-B48	*
WT vs P1000	***
WT vs TbAT1-KO	ns
WT vs B48 + AT-E1	ns
WT vs B48 + AT-E2	ns
TbAT1-B48 vs P1000	*
TbAT1-B48 vs TbAT1-KO	ns
TbAT1-B48 vs B48 + AT-E1	ns
TbAT1-B48 vs B48 + AT-E2	ns
P1000 vs TbAT1-KO	**
P1000 vs B48 + AT-E1	***
P1000 vs B48 + AT-E2	***
TbAT1-KO vs B48 + AT-E1	ns
TbAT1-KO vs B48 + AT-E2	ns
B48 + AT-E1 vs B48 + AT-E2	ns



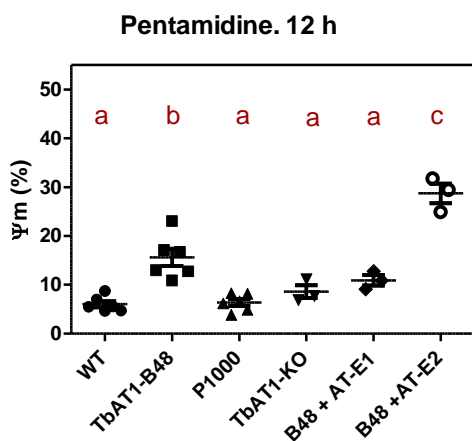
Troglitazone 12 h	
Tukey's Multiple Comparison Test	
WT vs TbAT1-B48	*
WT vs P1000	***
WT vs TbAT1-KO	ns
WT vs B48 + AT-E1	ns
WT vs B48 + AT-E2	ns
TbAT1-B48 vs P1000	ns
TbAT1-B48 vs TbAT1-KO	ns
TbAT1-B48 vs B48 + AT-E1	ns
TbAT1-B48 vs B48 + AT-E2	ns
P1000 vs TbAT1-KO	**
P1000 vs B48 + AT-E1	**
P1000 vs B48 + AT-E2	***
TbAT1-KO vs B48 + AT-E1	ns
TbAT1-KO vs B48 + AT-E2	ns
B48 + AT-E1 vs B48 + AT-E2	ns



Pentamidine Time Zero	
Tukey's Multiple Comparison Test	
WT vs TbAT1-B48	ns
WT vs P1000	***
WT vs TbAT1-KO	ns
WT vs B48 + AT-E1	ns
WT vs B48 +AT-E2	***
TbAT1-B48 vs P1000	***
TbAT1-B48 vs TbAT1-KO	ns
TbAT1-B48 vs B48 + AT-E1	ns
TbAT1-B48 vs B48 +AT-E2	***
P1000 vs TbAT1-KO	***
P1000 vs B48 + AT-E1	***
P1000 vs B48 +AT-E2	***
TbAT1-KO vs B48 + AT-E1	ns
TbAT1-KO vs B48 +AT-E2	***
B48 + AT-E1 vs B48 +AT-E2	***



Pentamidine 6 h	
Tukey's Multiple Comparison Test	
WT vs TbAT1-B48	***
WT vs P1000	ns
WT vs TbAT1-KO	ns
WT vs B48 + AT-E1	*
WT vs B48 +AT-E2	***
TbAT1-B48 vs P1000	***
TbAT1-B48 vs TbAT1-KO	ns
TbAT1-B48 vs B48 + AT-E1	ns
TbAT1-B48 vs B48 +AT-E2	***
P1000 vs TbAT1-KO	ns
P1000 vs B48 + AT-E1	*
P1000 vs B48 +AT-E2	***
TbAT1-KO vs B48 + AT-E1	ns
TbAT1-KO vs B48 +AT-E2	***
B48 + AT-E1 vs B48 +AT-E2	***



Pentamidine 12 h	
Tukey's Multiple Comparison Test	
WT vs TbAT1-B48	***
WT vs P1000	ns
WT vs TbAT1-KO	ns
WT vs B48 + AT-E1	ns
WT vs B48 +AT-E2	***
TbAT1-B48 vs P1000	***
TbAT1-B48 vs TbAT1-KO	*
TbAT1-B48 vs B48 + AT-E1	ns
TbAT1-B48 vs B48 +AT-E2	***
P1000 vs TbAT1-KO	ns
P1000 vs B48 + AT-E1	ns
P1000 vs B48 +AT-E2	***
TbAT1-KO vs B48 + AT-E1	ns
TbAT1-KO vs B48 +AT-E2	***
B48 + AT-E1 vs B48 +AT-E2	***

## References

- Acimovic, Y. & Coe, I.R. (2002) Molecular evolution of the equilibrative nucleoside transporter family: identification of novel family members in prokaryotes and eukaryotes. *Mol. Biol. Evol.*, **19**, 2199-2210.
- Allsopp, R. (2001) Options for vector control against trypanosomiasis in Africa. *Trends Parasitol.*, **17**, 15-19.
- Al Salabi, M.I. & de Koning, H.P. (2005) Purine nucleobase transport in amastigotes of *Leishmania mexicana*: involvement in allopurinol uptake. *Antimicrob. Agents Chemother.*, **49**, 3682-3689.
- Alsford, S. & Horn, D. (2008) Single-locus targeting constructs for reliable regulated RNAi and transgene expression in *Trypanosoma brucei*. *Mol. Biochem. Parasitol.*, **161**, 76-79.
- Anene, B.M., Ezeokonkwo, R.C., Mmesirionye, T.I., Tettey, J.N., Brock, J.M., Barrett, M.P., & De Koning, H.P. (2006) A diminazene-resistant strain of *Trypanosoma brucei brucei* isolated from a dog is cross-resistant to pentamidine in experimentally infected albino rats. *Parasitology*, **132**, 127-133.
- Aymerich, I., Duflot, S., Fernandez-Veledo, S., Guillen-Gomez, E., Huber-Ruano, I., Casado, F.J., & Pastor-Anglada, M. (2005) The concentrative nucleoside transporter family (SLC28): new roles beyond salvage?. *Biochem. Soc. Trans.*, **33**, 216-219.
- Bacchi, C.J. (1993) Resistance to clinical drugs in African trypanosomes. *Parasitol. Today*, **9**, 190-193.
- Bacchi, C.J. (2009) Chemotherapy of human african trypanosomiasis. *Interdiscip. Perspect. Infect. Dis.*, **2009**, 195040.
- Balana-Fouce, R. & Reguera, R.M. (2007) RNA interference in *Trypanosoma brucei*: a high-throughput engine for functional genomics in trypanosomatids?. *Trends Parasitol.*, **23**, 348-351.
- Baldwin, S.A., Beal, P.R., Yao, S.Y., King, A.E., Cass, C.E., & Young, J.D. (2004) The equilibrative nucleoside transporter family, SLC29. *Pflugers Arch.*, **447**, 735-743.

- Balasegaram, M., Harris, S., Checchi, F., Ghorashian, S., Hamel, C., & Karunakara, U. (2006) Melarsoprol versus eflornithine for treating late-stage Gambian trypanosomiasis in the Republic of the Congo. *Bull. World Health Organ*, **84**, 783-791.
- Barrett, M.P. (2006) The rise and fall of sleeping sickness. *Lancet*, **367**, 1377-1378.
- Barrett, M.P., Boykin, D.W., Brun, R., & Tidwell, R.R. (2007) Human African trypanosomiasis: pharmacological re-engagement with a neglected disease. *Br. J. Pharmacol.*, **152**, 1155-1171.
- Barrett, M.P., Burchmore, R.J., Stich, A., Lazzari, J.O., Frasch, A.C., Cazzulo, J.J., & Krishna, S. (2003) The trypanosomiasis. *Lancet*, **362**, 1469-1480.
- Barrett, M.P. & Fairlamb, A.H. (1999) The Biochemical Basis of Arsenical-Diamidine Crossresistance in African Trypanosomes. *Parasitology Today*, **15**, 136-140.
- Barrett, M.P. & Gilbert, I.H. (2006) Targeting of toxic compounds to the trypanosome's interior. *Adv. Parasitol.*, **63**, 125-183.
- Barrett, M.P., Zhang, Z.Q., Denise, H., Giroud, C., & Baltz, T. (1995) A diamidine-resistant *Trypanosoma equiperdum* clone contains a P2 purine transporter with reduced substrate affinity. *Molecular and Biochemical Parasitology*, **73**, 223-229.
- Barry, J.D., Marcello, L., Morrison, L.J., Read, A.F., Lythgoe, K., Jones, N., Carrington, M., Blandin, G., Bohme, U., Caler, E., Hertz-Fowler, C., Renauld, H., El Sayed, N., & Berriman, M. (2005) What the genome sequence is revealing about trypanosome antigenic variation. *Biochem. Soc. Trans.*, **33**, 986-989.
- Barry, J.D. & McCulloch, R. (2001) Antigenic variation in trypanosomes: enhanced phenotypic variation in a eukaryotic parasite. *Adv. Parasitol.*, **49**, 1-70.
- Bellofatto, V. (2007) Pyrimidine transport activities in trypanosomes. *Trends Parasitol.*, **23**, 187-189.
- Bentivoglio, M. & Kristensson, K. (2007) Neural-immune interactions in disorders of sleep-wakefulness organization. *Trends Neurosci.*, **30**, 645-652.

- Berger, B.J., Carter, N.S., & Fairlamb, A.H. (1995) Characterisation of pentamidine-resistant *Trypanosoma brucei brucei*. *Mol.Biochem. Parasitol.*, **69**, 289-298
- Borst, P. & Sabatini, R. (2008) Base J: discovery, biosynthesis, and possible functions. *Annu.Rev.Microbiol.*, **62**, 235-251.
- Bray, P.G., Barrett, M.P., Ward, S.A., & de Koning, H.P. (2003) Pentamidine uptake and resistance in pathogenic protozoa: past, present and future. *Trends Parasitol.*, **19**, 232-239.
- Brecht, M. & Parsons, M. (1998) Changes in polysome profiles accompany trypanosome development. *Mol.Biochem. Parasitol.*, **97**, 189-198..
- Bridges, D.J., Gould, M.K., Nerima, B., Mäser, P., Burchmore, R.J., & de Koning, H.P. (2007) Loss of the high-affinity pentamidine transporter is responsible for high levels of cross-resistance between arsenical and diamidine drugs in African trypanosomes. *Mol. Pharmacol.*, **71**, 1098-1108.
- Brun, R. & Schonenberger (1979) Cultivation and in vitro cloning or procyclic culture forms of *Trypanosoma brucei* in a semi-defined medium. Short communication. *Acta Trop.*, **36**, 289-292.
- Brun, R., Schumacher, R., Schmid, C., Kunz, C., & Burri, C. (2001) The phenomenon of treatment failures in Human African Trypanosomiasis. *Trop.Med.Int.Health*, **6**, 906-914.
- Brun, R., Blum, J., Chappuis, F., & Burri, C. (2010) Human African trypanosomiasis. *Lancet*, **375**, 148-159.
- Burchmore, R.J., Wallace, L.J., Candlish, D., Al Salabi, M.I., Beal, P.R., Barrett, M.P., Baldwin, S.A., & de Koning, H.P. (2003) Cloning, heterologous expression, and in situ characterization of the first high affinity nucleobase transporter from a protozoan. *J.Biol. Chem.*, **278**, 23502-23507.
- Burkard, G., Fragoso, C.M., & Roditi, I. (2007) Highly efficient stable transformation of bloodstream forms of *Trypanosoma brucei*. *Mol.Biochem. Parasitol.*, **153**, 220-223.
- Burton, P., McBride, D.J., Wilkes, J.M., Barry, J.D., & McCulloch, R. (2007) Ku heterodimer-independent end joining in *Trypanosoma brucei* cell extracts relies upon sequence microhomology. *Eukaryot.Cell*, **6**, 1773-1781.

- Carmichael, G.G. (2002) Medicine: silencing viruses with RNA. *Nature*, **418**, 379-380.
- Carrillo, C., Cejas, S., Cortes, M., Ceriani, C., Huber, A., Gonzalez, N.S., & Algranati, I.D. (2000) Sensitivity of trypanosomatid protozoa to DFMO and metabolic turnover of ornithine decarboxylase. *Biochem.Biophys.Res. Commun.*, **279**, 663-668.
- Carrillo, C., Gonzalez, N.S., & Algranati, I.D. (2007) Trypanosoma cruzi as a model system to study the expression of exogenous genes coding for polyamine biosynthetic enzymes. Induction of DFMO resistance in transgenic parasites. *Biochim.Biophys.Acta*, **1770**, 1605-1611.
- Carter, N.S., Berger, B.J., & Fairlamb, A.H. (1995) Uptake of diamidine drugs by the P2 nucleoside transporter in melarsen-sensitive and -resistant Trypanosoma brucei brucei. *J.Biol. Chem.*, **270**, 28153-28157.
- Carter, N.S. & Fairlamb, A.H. (1993) Arsenical-resistant trypanosomes lack an unusual adenosine transporter. *Nature*, **361**, 173-176.
- Cheng, Y. & Prusoff, W.H. (1973) Relationship between the inhibition constant (K<sub>1</sub>) and the concentration of inhibitor which causes 50 per cent inhibition (I<sub>50</sub>) of an enzymatic reaction. *Biochem. Pharmacol.*, **22**, 3099-3108.
- Cherian, P., Junckerstorff, R.K., Rosen, D., Kumarasinghe, P., Morling, A., Tuch, P., Raven, S., Murray, R.J., & Heath, C.H. (2010) Late-stage human African trypanosomiasis in a Sudanese refugee. *Med.J.Aust.*, **192**, 417-419.
- Christensen, B.M. (2004) Presidential address. Classical is critical: alleviating the burden of parasitic diseases. *J. Parasitol.*, **90**, 1199-1203.
- Clayton, C.E., Ha, S., Rusche, L., Hartmann, C., & Beverley, S.M. (2000) Tests of heterologous promoters and intergenic regions in Leishmania major. *Mol.Biochem. Parasitol.*, **105**, 163-167.
- Cohn, C.S. & Gottlieb, M. (1997) The acquisition of purines by trypanosomatids. *Parasitol.Today*, **13**, 231-235.
- Conway, C., Proudfoot, C., Burton, P., Barry, J.D., & McCulloch, R. (2002) Two pathways of homologous recombination in Trypanosoma brucei. *Mol. Microbiol.*, **45**, 1687-1700.

- Collar, C.J., Al Salabi, M.I., Stewart, M.L., Barrett, M.P., Wilson, W.D., & de Koning, H.P. (2009) Predictive computational models of substrate binding by a nucleoside transporter. *J.Biol. Chem.*, **284**, 34028-34035.
- M. Cserzo, E. Wallin, I. Simon, G. von Heijne and A. Elofsson: Prediction of transmembrane alpha-helices in procariotic membrane proteins: the Dense Alignment Surface method; *Prot. Eng.* vol. 10, no. 6, 673-676, 1997
- de Koning, H. & Diallinas, G. (2000) Nucleobase transporters (review). *Mol.Membr. Biol.*, **17**, 75-94.
- de Koning, H.P. (2001) Transporters in African trypanosomes: role in drug action and resistance. *Int.J. Parasitol.*, **31**, 512-522.
- De Koning, H.P. (2001) Uptake of pentamidine in *Trypanosoma brucei brucei* is mediated by three distinct transporters: implications for cross-resistance with arsenicals. *Mol. Pharmacol.*, **59**, 586-592.
- de Koning, H.P. (2008) Ever-increasing complexities of diamidine and arsenical crossresistance in African trypanosomes. *Trends Parasitol.*, **24**, 345-349.
- de Koning, H.P., Al Salabi, M.I., Cohen, A.M., Coombs, G.H., & Wastling, J.M. (2003) Identification and characterisation of high affinity nucleoside and nucleobase transporters in *Toxoplasma gondii*. *Int.J.Parasitol.*, **33**, 821-831.
- de Koning, H.P., Anderson, L.F., Stewart, M., Burchmore, R.J., Wallace, L.J., & Barrett, M.P. (2004) The trypanocide diminazene aceturate is accumulated predominantly through the TbAT1 purine transporter: additional insights on diamidine resistance in african trypanosomes. *Antimicrob.Agents Chemother.*, **48**, 1515-1519.
- de Koning, H.P., Bridges, D.J., & Burchmore, R.J. (2005) Purine and pyrimidine transport in pathogenic protozoa: from biology to therapy. *FEMS Microbiol. Rev.*, **29**, 987-1020.
- de Koning, H.P. & Jarvis, S.M. (1997) Hypoxanthine uptake through a purine-selective nucleobase transporter in *Trypanosoma brucei brucei* procyclic cells is driven by protonmotive force. *Eur.J. Biochem.*, **247**, 1102-1110.
- de Koning, H.P. & Jarvis, S.M. (1999) Adenosine transporters in bloodstream forms of *Trypanosoma brucei brucei*: substrate recognition motifs and affinity for trypanocidal drugs. *Mol. Pharmacol.*, **56**, 1162-1170.

- de Koning, H.P., Anderson, L.F., Stewart, M., Burchmore, R.J.S., Wallace, L.J.M., & Barrett, M.P. (2004) The Trypanocide Diminazene Aceturate Is Accumulated Predominantly through the TbAT1 Purine Transporter: Additional Insights on Diamidine Resistance in African Trypanosomes. *Antimicrobial Agents and Chemotherapy*, **48**, 1515-1519.
- de Koning, H.P., Watson, C.J., & Jarvis, S.M. (1998) Characterization of a nucleoside/proton symporter in procyclic *Trypanosoma brucei brucei*. *J.Biol. Chem.*, **273**, 9486-9494.
- de Koning, H.P. & Jarvis, S.M. (2001) Uptake of pentamidine in *Trypanosoma brucei brucei* is mediated by the P2 adenosine transporter and at least one novel, unrelated transporter. *Acta Tropica*, **80**, 245-250.
- de Koning, H.P., MacLeod, A., Barrett, M.P., Cover, B., & Jarvis, S.M. (2000) Further evidence for a link between melarsoprol resistance and P2 transporter function in African trypanosomes. *Molecular and Biochemical Parasitology*, **106**, 181-185.
- Delespaux, V. & De Koning, H.P. (2007) Drugs and drug resistance in African trypanosomiasis. *Drug Resistance Updates*, **10**, 30-50.
- Denise, H. & Barrett, M.P. (2001) Uptake and mode of action of drugs used against sleeping sickness. *Biochem. Pharmacol.*, **61**, 1-5.
- Docampo, R., Ulrich, P., & Moreno, S.N. (2010) Evolution of acidocalcisomes and their role in polyphosphate storage and osmoregulation in eukaryotic microbes. *Philos.Trans.R.Soc.Lond B Biol. Sci.*, **365**, 775-784.
- Donelson, J.E. (2003) Antigenic variation and the African trypanosome genome. *Acta Trop.*, **85**, 391-404.
- Denninger, V., Figarella, K., Schonfeld, C., Brems, S., Busold, C., Lang, F., Hoheisel, J., & Duszenko, M. (2007) Troglitazone induces differentiation in *Trypanosoma brucei*. *Exp.Cell Res.*, **313**, 1805-1819.
- Downie, M.J., El Bissati, K., Bobenchik, A.M., Nic,L.L., Amerik, A., Zufferey, R., Kirk, K., & Ben Mamoun, C. (2010) PfNT2, a permease of the equilibrative nucleoside transporter family in the endoplasmic reticulum of *Plasmodium falciparum*. *J.Biol. Chem.*, **285**, 20827-20833.

- Ekwanzala, M., Pepin, J., Khonde, N., Molisho, S., Bruneel, H., & De Wals, P. (1996) In the heart of darkness: sleeping sickness in Zaire. *Lancet*, **348**, 1427-1430.
- El Sayed, N.M., Hegde, P., Quackenbush, J., Melville, S.E., & Donelson, J.E. (2000) The African trypanosome genome. *Int.J. Parasitol.*, **30**, 329-345.
- Fairlamb, A.H. (2003) Chemotherapy of human African trypanosomiasis: current and future prospects. *Trends Parasitol.*, **19**, 488-494.
- Fairlamb, A.H., Carter, N.S., Cunningham, M., & Smith, K. (1992) Characterisation of melarsen-resistant *Trypanosoma brucei brucei* with respect to cross-resistance to other drugs and trypanothione metabolism. *Mol.Biochem.Parasitol.*, **53**, 213-222.
- Figurella, K., Uzcategui, N.L., Beck, A., Schoenfeld, C., Kubata, B.K., Lang, F., & Duszenko, M. (2006) Prostaglandin-induced programmed cell death in *Trypanosoma brucei* involves oxidative stress. *Cell Death.Differ.*, **13**, 1802-1814.
- Fire, A., Xu, S., Montgomery, M.K., Kostas, S.A., Driver, S.E., & Mello, C.C. (1998) Potent and specific genetic interference by double-stranded RNA in *Caenorhabditis elegans*. *Nature*, **391**, 806-811.
- Geerts, S., Holmes, P.H., Eisler, M.C., & Diall, O. (2001) African bovine trypanosomiasis: the problem of drug resistance. *Trends Parasitol.*, **17**, 25-28.
- Gherardi, A. & Sarciron, M.E. (2007) Molecules targeting the purine salvage pathway in Apicomplexan parasites. *Trends Parasitol.*, **23**, 384-389.
- Gibson, W. (2002) Will the real *Trypanosoma brucei rhodesiense* please step forward?. *Trends Parasitol.*, **18**, 486-490.
- Gillingwater, K., Kumar, A., Ismail, M.A., Arafa, R.K., Stephens, C.E., Boykin, D.W., Tidwell, R.R., & Brun, R. (2010) In vitro activity and preliminary toxicity of various diamidine compounds against *Trypanosoma evansi*. *Vet. Parasitol.*, **169**, 264-272.
- Gray, J.H., Owen, R.P., & Giacomini, K.M. (2004) The concentrative nucleoside transporter family, SLC28. *Pflugers Arch.*, **447**, 728-734.
- Griffith, D. A & Jarvis, S. M. (1996) Nucleoside and nucleobase transport systems of mammalian cells. *Biochimica et Biophysica Acta* 1286: 153-181.

- Gudin, S., Quashie, N.B., Candlish, D., Al Salabi, M.I., Jarvis, S.M., Ranford-Cartwright, L.C., & de Koning, H.P. (2006) Trypanosoma brucei: a survey of pyrimidine transport activities. *Exp. Parasitol.*, **114**, 118-125.
- Hannaert, V. (2010) Sleeping Sickness Pathogen (Trypanosoma brucei) and Natural Products: Therapeutic Targets and Screening Systems. *Planta Med.*
- Hannon, G.J. (2002) RNA interference. *Nature*, **418**, 244-251.
- Hasne, M. & Barrett, M.P. (2000) Drug uptake via nutrient transporters in Trypanosoma brucei. *J.Appl. Microbiol.*, **89**, 697-701.
- Hertz-Fowler, C., Figueiredo, L.M., Quail, M.A., Becker, M., Jackson, A., Bason, N., Brooks, K., Churcher, C., Fakhro, S., Goodhead, I., Heath, P., Kartvelishvili, M., Mungall, K., Harris, D., Hauser, H., Sanders, M., Saunders, D., Seeger, K., Sharp, S., Taylor, J.E., Walker, D., White, B., Young, R., Cross, G.A., Rudenko, G., Barry, J.D., Louis, E.J., & Berriman, M. (2008) Telomeric expression sites are highly conserved in Trypanosoma brucei. *PLoS.One.*, **3**, e3527.
- Hide, G. (1999) History of sleeping sickness in East Africa. *Clin.Microbiol.Rev.*, **12**, 112-125.
- Hoare, C.A. The trypanosomes of mammals. A Zoological Monograph. 1972. Blackwell Scientific Publications, Oxford, U.K. Ref Type: Generic
- Hotez, P.J. & Kamath, A. (2009) Neglected tropical diseases in sub-saharan Africa: review of their prevalence, distribution, and disease burden. *PLoS.Negl. Trop.Dis.*, **3**, e412.
- Hyde, R.J., Cass, C.E., Young, J.D., & Baldwin, S.A. (2001) The ENT family of eukaryote nucleoside and nucleobase transporters: recent advances in the investigation of structure/function relationships and the identification of novel isoforms. *Mol.Membr. Biol.*, **18**, 53-63.
- Ibrahim, H.M., Al Salabi, M.I., El Sabbagh, N., Quashie, N.B., Alkhaldi, A.A., Escale, R., Smith, T.K., Vial, H.J., & de Koning, H.P. (2011) Symmetrical choline-derived dications display strong anti-kinetoplastid activity. *J.Antimicrob.Chemother.*, **66**, 111-125.
- Jannin, J. & Cattand, P. (2004) Treatment and control of human African trypanosomiasis. *Curr.Opin.Infect. Dis.*, **17**, 565-571.
- Johnston, D.A., Blaxter, M.L., Degraeve, W.M., Foster, J., Ivens, A.C., & Melville, S.E. (1999) Genomics and the biology of parasites. *Bioessays*, **21**, 131-147.

- Kennedy, P.G. (2004) Human African trypanosomiasis of the CNS: current issues and challenges. *J.Clin.Invest*, **113**, 496-504.
- Kennedy, P.G. (2006) Human African trypanosomiasis-neurological aspects. *J. Neurol.*, **253**, 411-416.
- Kennedy, P.G. (2008) The continuing problem of human African trypanosomiasis (sleeping sickness). *Ann. Neurol.*, **64**, 116-126.
- Kent, O.A. & MacMillan, A.M. (2004) RNAi: running interference for the cell. *Org.Biomol. Chem.*, **2**, 1957-1961.
- Kieft, R., Capewell, P., Turner, C.M., Veitch, N.J., MacLeod, A., & Hajduk, S. (2010) Mechanism of *Trypanosoma brucei gambiense* (group 1) resistance to human trypanosome lytic factor. *Proc.Natl.Acad.Sci.U.S.A*, **107**, 16137-16141.
- Kuzoe, F.A. (1993) Current situation of African trypanosomiasis. *Acta Trop.*, **54**, 153-162.
- LaCount, D.J., Bruse, S., Hill, K.L., & Donelson, J.E. (2000) Double-stranded RNA interference in *Trypanosoma brucei* using head-to-head promoters. *Mol.Biochem. Parasitol.*, **111**, 67-76.
- Landfear, S.M. (2001) Molecular genetics of nucleoside transporters in *Leishmania* and African trypanosomes. *Biochem. Pharmacol.*, **62**, 149-155.
- Landfear, S.M., Ullman, B., Carter, N.S., & Sanchez, M.A. (2004) Nucleoside and nucleobase transporters in parasitic protozoa. *Eukaryot.Cell*, **3**, 245-254.
- Landfear, S.M. (2010) Transporters for drug delivery and as drug targets in parasitic protozoa. *Clin.Pharmacol. Ther.*, **87**, 122-125.
- Lanteri, C.A., Trumpower, B.L., Tidwell, R.R., & Meshnick, S.R. (2004) DB75, a novel trypanocidal agent, disrupts mitochondrial function in *Saccharomyces cerevisiae*. *Antimicrob.Agents Chemother.*, **48**, 3968-3974.
- Lanteri, C.A., Stewart, M.L., Brock, J.M., Alibu, V.P., Meshnick, S.R., Tidwell, R.R., & Barrett, M.P. (2006) Roles for the *Trypanosoma brucei* P2 Transporter in DB75 Uptake and Resistance. *Molecular Pharmacology*, **70**, 1585-1592.
- Lee, M.G. & van der Ploeg, L.H. (1991) The hygromycin B-resistance-encoding gene as a selectable marker for stable transformation of *Trypanosoma brucei*. *Gene*, **105**, 255-257.

- Legros, D., Evans, S., Maiso, F., Enyaru, J.C., & Mbulamberi, D. (1999) Risk factors for treatment failure after melarsoprol for *Trypanosoma brucei gambiense* trypanosomiasis in Uganda. *Trans.R.Soc.Trop. Med.Hyg.*, **93**, 439-442.
- Legros, D., Ollivier, G., Gastellu-Etchegorry, M., Paquet, C., Burri, C., Jannin, J., & Buscher, P. (2002) Treatment of human African trypanosomiasis--present situation and needs for research and development. *Lancet Infect. Dis.*, **2**, 437-440.
- Luscher, A., de Koning, H.P., & Mäser, P. (2007) Chemotherapeutic strategies against *Trypanosoma brucei*: drug targets vs. drug targeting. *Curr.Pharm.Des*, **13**, 555-567.
- Lutje, V., Seixas, J., & Kennedy, A. (2010) Chemotherapy for second-stage Human African trypanosomiasis. *Cochrane.Database.Syst. Rev.*, CD006201.
- Mansfield, J.M. & Paulnock, D.M. (2008) Genetic manipulation of African trypanosomes as a tool to dissect the immunobiology of infection. *Parasite Immunol.*, **30**, 245-253.
- Mäser, P., Sütterlin, C., Kralli, A., & Kaminsky, R. (1999) A Nucleoside Transporter from *Trypanosoma brucei* Involved in Drug Resistance. *Science*, **285**, 242-244.
- Mäser, P., Luscher, A., & Kaminsky, R. (2003) Drug transport and drug resistance in African trypanosomes. *Drug Resistance Updates*, **6**, 281-290.
- Maslov, D.A., Podlipaev, S.A., & Lukes, J. (2001) Phylogeny of the kinetoplastida: taxonomic problems and insights into the evolution of parasitism. *Mem.Inst.Oswaldo Cruz*, **96**, 397-402.
- Matovu, E., Stewart, M.L., Geiser, F., Brun, R., Mäser, P., Wallace, L.J., Burchmore, R.J., Enyaru, J.C., Barrett, M.P., Kaminsky, R., Seebeck, T., & de Koning, H.P. (2003) Mechanisms of arsenical and diamidine uptake and resistance in *Trypanosoma brucei*. *Eukaryot.Cell*, **2**, 1003-1008.
- Matovu, E., Geiser, F., Schneider, V., Mäser, P., Enyaru, J.C.K., Kaminsky, R., Gallati, S., & Seebeck, T. (2001) Genetic variants of the TbAT1 adenosine

- transporter from African trypanosomes in relapse infections following melarsoprol therapy. *Molecular and Biochemical Parasitology*, **117**, 73-81.
- Matovu, E., Seebeck, T., Enyaru, J.C.K., & Kaminsky, R. (2001) Drug resistance in *Trypanosoma brucei* spp., the causative agents of sleeping sickness in man and nagana in cattle. *Microbes and Infection*, **3**, 763-770.
- Matovu, E., Stewart, M.L., Geiser, F., Brun, R., Mäser, P., Wallace, L.J.M., Burchmore, R.J., Enyaru, J.C.K., Barrett, M.P., Kaminsky, R., Seebeck, T., & de Koning, H.P. (2003) Mechanisms of Arsenical and Diamidine Uptake and Resistance in *Trypanosoma brucei*. *Eukaryotic Cell*, **2**, 1003-1008.
- Maudlin, I. (2006) African trypanosomiasis. *Ann.Trop.Med.Parasitol.*, **100**, 679-701.
- Michels, P.A., Hannaert, V., & Bringaud, F. (2000) Metabolic aspects of glycosomes in trypanosomatidae - new data and views. *Parasitol.Today*, **16**, 482-489.
- Modesti, M. & Kanaar, R. (2001) Homologous recombination: from model organisms to human disease. *Genome Biol.*, **2**, REVIEWS1014.
- Molina-Arcas, M., Moreno-Bueno, G., Cano-Soldado, P., Hernandez-Vargas, H., Casado, F.J., Palacios, J., & Pastor-Anglada, M. (2006) Human equilibrative nucleoside transporter-1 (hENT1) is required for the transcriptomic response of the nucleoside-derived drug 5'-DFUR in breast cancer MCF7 cells. *Biochem. Pharmacol.*, **72**, 1646-1656.
- Moore, D.A.J., Edwards, M., Escombe, R., Agranoff, D., Bailey, J.W., S.B, S, & Chiodini, P.L. (2002) African Trypanosomiasis in travellers returning to the United Kingdom. *Emerging Infectious Diseases*, **8**, 74-76.
- Moreno, S.N. & Docampo, R. (2003) Calcium regulation in protozoan parasites. *Curr.Opin. Microbiol.*, **6**, 359-364.
- Motyka, S.A. & Englund, P.T. (2004) RNA interference for analysis of gene function in trypanosomatids. *Curr.Opin. Microbiol.*, **7**, 362-368.
- Mukherjee, A., Padmanabhan, P.K., Sahani, M.H., Barrett, M.P., & Madhubala, R. (2006) Roles for mitochondria in pentamidine susceptibility and resistance in *Leishmania donovani*. *Mol.Biochem. Parasitol.*, **145**, 1-10.

- Ngo, H., Tschudi, C., Gull, K., & Ullu, E. (1998) Double-stranded RNA induces mRNA degradation in *Trypanosoma brucei*. *Proc.Natl.Acad.Sci.U.S.A*, **95**, 14687-14692.
- Njiru, Z.K., Ndung'u, K., Matete, G., Ndungu, J.M., & Gibson, W.C. (2004a) Detection of *Trypanosoma brucei rhodesiense* in animals from sleeping sickness foci in East Africa using the serum resistance associated (SRA) gene. *Acta Trop.*, **90**, 249-254.
- Nok, A.J. (2003) Arsenicals (melarsoprol), pentamidine and suramin in the treatment of human African trypanosomiasis. *Parasitol. Res.*, **90**, 71-79.
- Opperdoes, F.R., Baudhuin, P., Coppens, I., De Roe, C., Edwards, S.W., Weijers, P.J., & Misset, O. (1984) Purification, morphometric analysis, and characterization of the glycosomes (microbodies) of the protozoan hemoflagellate *Trypanosoma brucei*. *J.Cell Biol.*, **98**, 1178-1184.
- Ortiz, D., Sanchez, M.A., Quecke, P., & Landfear, S.M. (2009) Two novel nucleobase/pentamidine transporters from *Trypanosoma brucei*. *Mol.Biochem. Parasitol.*, **163**, 67-76.
- Overath, P., Czichos, J., & Haas, C. (1986) The effect of citrate/cis-aconitate on oxidative metabolism during transformation of *Trypanosoma brucei*. *Eur.J. Biochem.*, **160**, 175-182.
- Plagemann, P. G., Wohlhueter, R. M., & Woffendin, C. (1988) Nucleoside and nucleobase transport in animal cells. *Biochimica et Biophysica Acta* 947: 405-443.
- Papageorgiou, I.G., Yakob, L., Al Salabi, M.I., Diallinas, G., Soteriadou, K.P., & de Koning, H.P. (2005) Identification of the first pyrimidine nucleobase transporter in *Leishmania*: similarities with the *Trypanosoma brucei* U1 transporter and antileishmanial activity of uracil analogues. *Parasitology*, **130**, 275-283.
- Parrish, S., Fleenor, J., Xu, S., Mello, C., & Fire, A. (2000) Functional anatomy of a dsRNA trigger: differential requirement for the two trigger strands in RNA interference. *Mol.Cell*, **6**, 1077-1087.
- Pepin, J. & Khonde, N. (1996) Relapses following treatment of early-stage *Trypanosoma brucei gambiense* sleeping sickness with a combination of pentamidine and suramin. *Transactions of the Royal Society of Tropical Medicine and Hygiene*, **90**, 183-186.

- Pepin, J. & Milord, F. (1994) The treatment of human African trypanosomiasis. *Adv. Parasitol.*, **33**, 1-47.
- Podgorska, M., Kocbuch, K., & Pawelczyk, T. (2005) Recent advances in studies on biochemical and structural properties of equilibrative and concentrative nucleoside transporters. *Acta Biochim. Pol.*, **52**, 749-758.
- Rahn, C.A., Bombick, D.W., & Doolittle, D.J. (1991) Assessment of mitochondrial membrane potential as an indicator of cytotoxicity. *Fundam.Appl. Toxicol.*, **16**, 435-448.
- Rangasamy, D., Tremethick, D.J., & Greaves, I.K. (2008) Gene knockdown by ecdysone-based inducible RNAi in stable mammalian cell lines. *Nat. Protoc.*, **3**, 79-88.
- Raper, J., Portela, M.P., Lugli, E., Frevert, U., & Tomlinson, S. (2001) Trypanosome lytic factors: novel mediators of human innate immunity. *Curr. Opin. Microbiol.*, **4**, 402-408.
- Raz, B., Iten, M., Grether-Buhler, Y., Kaminsky, R., & Brun, R. (1997) The Alamar Blue assay to determine drug sensitivity of African trypanosomes (*T.b. rhodesiense* and *T.b. gambiense*) in vitro. *Acta Trop.*, **68**, 139-147.
- Rodgers, J. (2009) Human African trypanosomiasis, chemotherapy and CNS disease. *J. Neuroimmunol.*, **211**, 16-22.
- Roditi, I. & Clayton, C. (1999) An unambiguous nomenclature for the major surface glycoproteins of the procyclic form of *Trypanosoma brucei*. *Mol. Biochem. Parasitol.*, **103**, 99-100.
- Rusconi, F., Durand-Dubief, M., & Bastin, P. (2005) Functional complementation of RNA interference mutants in trypanosomes. *BMC Biotechnol.*, **5**, 6.
- Sambrook, J., Fritsch, E.F., & Maniatis, T. (1989) *Molecular Cloning: A Laboratory Manual.*, 99 edn, pp. 89-101. Cold Spring Harbor Laboratory Press, NY.
- Sanchez, M.A., Drutman, S., van Ampting, M., Matthews, K., & Landfear, S.M. (2004) A novel purine nucleoside transporter whose expression is up-regulated in the short stumpy form of the *Trypanosoma brucei* life cycle. *Mol. Biochem. Parasitol.*, **136**, 265-272.
- Sanchez, M.A., Ullman, B., Landfear, S.M., & Carter, N.S. (1999) Cloning and functional expression of a gene encoding a P1 type nucleoside transporter from *Trypanosoma brucei*. *J. Biol. Chem.*, **274**, 30244-30249.

- Sanderson, L., Khan, A., & Thomas, S. (2007) Distribution of suramin, an antitrypanosomal drug, across the blood-brain and blood-cerebrospinal fluid interfaces in wild-type and P-glycoprotein transporter-deficient mice. *Antimicrob. Agents Chemother.*, **51**, 3136-3146.
- Schofield, C.J. & Maudlin, I. (2001) Trypanosomiasis control. *Int.J. Parasitol.*, **31**, 614-619.
- Seed, J.R. (2001) African trypanosomiasis research: 100 years of progress, but questions and problems still remain. *Int.J. Parasitol.*, **31**, 434-442.
- Scott, A.G., Tait, A., & Turner, C.M. (1997) Trypanosoma brucei: lack of cross-resistance to melarsoprol in vitro by cymelarsan-resistant parasites. *Exp. Parasitol.*, **86**, 181-190.
- Shlomai, J. (2002) Specific recognition of the replication origins of the kinetoplast DNA. *Acta Microbiol. Immunol. Hung.*, **49**, 455-467.
- Simarro, P.P., Cecchi, G., Paone, M., Franco, J.R., Diarra, A., Ruiz, J.A., Fevre, E.M., Courtin, F., Mattioli, R.C., & Jannin, J.G. (2010) The Atlas of human African trypanosomiasis: a contribution to global mapping of neglected tropical diseases. *Int.J. Health Geogr.*, **9**, 57.
- Skarka, L. & Ostadal, B. (2002) Mitochondrial membrane potential in cardiac myocytes. *Physiol Res.*, **51**, 425-434.
- Smith, A.B., Esko, J.D., & Hajduk, S.L. (1995) Killing of trypanosomes by the human haptoglobin-related protein. *Science*, **268**, 284-286.
- Spoerri, I., Chadwick, R., Renggli, C.K., Matthews, K., Roditi, I., & Burkard, G. (2007) Role of the stage-regulated nucleoside transporter TbNT10 in differentiation and adenosine uptake in Trypanosoma brucei. *Mol. Biochem. Parasitol.*, **154**, 110-114.
- Stewart, M.L., Burchmore, R.J., Clucas, C., Hertz-Fowler, C., Brooks, K., Tait, A., MacLeod, A., Turner, C.M., de Koning, H.P., Wong, P.E., & Barrett, M.P. (2010) Multiple genetic mechanisms lead to loss of functional TbAT1 expression in drug-resistant trypanosomes. *Eukaryot. Cell*, **9**, 336-343.
- Stewart, M.L., Krishna, S., Burchmore, R.J., Brun, R., de Koning, H.P., Boykin, D.W., Tidwell, R.R., Hall, J.E., & Barrett, M.P. (2005) Detection of arsenical drug resistance in Trypanosoma brucei with a simple fluorescence test. *Lancet*, **366**, 486-487.

- Stein, A., Vaseduvan, G., Carter, N.S., Ullman, B., Landfear, S.M., & Kavanaugh, M.P. (2003) Equilibrative nucleoside transporter family members from *Leishmania donovani* are electrogenic proton symporters. *J.Biol. Chem.*, **278**, 35127-35134.
- Stich, A., Barrett, M.P., & Krishna, S. (2003) Waking up to sleeping sickness. *Trends Parasitol.*, **19**, 195-197.
- Tamarit, A., Gutierrez, C., Arroyo, R., Jimenez, V., Zagala, G., Bosch, I., Sirvent, J., Alberola, J., Alonso, I., & Caballero, C. (2010) Trypanosoma evansi infection in mainland Spain. *Vet. Parasitol.*, **167**, 74-76.
- Teka, I., Kazibwe, A., El-Sabbagh, N., Al Salabi, M.I., Ward, C.P., Eze, A.A., Munday, J.C., Mäser, P., Matovu, E., Barrett, M.P. and De Koning, H.P. (2011) The diamidine diminazene aceturate is a substrate for the High Affinity Pentamidine Transporter: implications for the development of high resistance levels. *Molecular Pharmacology*, submitted
- ten Asbroek, A.L., Ouellette, M., & Borst, P. (1990) Targeted insertion of the neomycin phosphotransferase gene into the tubulin gene cluster of *Trypanosoma brucei*. *Nature*, **348**, 174-175.
- Tevis, D.S., Kumar, A., Stephens, C.E., Boykin, D.W., & Wilson, W.D. (2009) Large, sequence-dependent effects on DNA conformation by minor groove binding compounds. *Nucleic Acids Res.*, **37**, 5550-5558.
- Turner, C.M. (1999) Antigenic variation in *Trypanosoma brucei* infections: an holistic view. *J.Cell Sci.*, **112 ( Pt 19)**, 3187-3192.
- Ulbert, S., Eide, L., Seeberg, E., & Borst, P. (2004) Base J, found in nuclear DNA of *Trypanosoma brucei*, is not a target for DNA glycosylases. *DNA Repair (Amst)*, **3**, 145-154.
- van Gent, D.C., Hoeijmakers, J.H., & Kanaar, R. (2001) Chromosomal stability and the DNA double-stranded break connection. *Nat.Rev. Genet.*, **2**, 196-206.
- van Weelden, S.W., Fast, B., Vogt, A., van der, M.P., Saas, J., van Hellemond, J.J., Tielens, A.G., & Boshart, M. (2003) Procyclic *Trypanosoma brucei* do not use Krebs cycle activity for energy generation. *J.Biol. Chem.*, **278**, 12854-12863.
- Vanhamme, L., Pays, E., McCulloch, R., & Barry, J.D. (2001) An update on antigenic variation in African trypanosomes. *Trends Parasitol.*, **17**, 338-343.

- Vara, J.A., Portela, A., Ortin, J., & Jimenez, A. (1986) Expression in mammalian cells of a gene from *Streptomyces alboniger* conferring puromycin resistance. *Nucleic Acids Res.*, **14**, 4617-4624.
- Vasudevan, G., Carter, N.S., Drew, M.E., Beverley, S.M., Sanchez, M.A., Seyfang, A., Ullman, B., & Landfear, S.M. (1998) Cloning of *Leishmania* nucleoside transporter genes by rescue of a transport-deficient mutant. *Proceedings of the National Academy of Sciences*, **95**, 9873-9878.
- Verner, Z., Paris, Z., & Lukes, J. (2010) Mitochondrial membrane potential-based genome-wide RNAi screen of *Trypanosoma brucei*. *Parasitol. Res.*, **106**, 1241-1244.
- Vickerman, K. (1969) On the surface coat and flagellar adhesion in trypanosomes. *J.Cell Sci.*, **5**, 163-193.
- Vickerman, K. (1985) Developmental cycles and biology of pathogenic trypanosomes. *Br. Med.Bull.*, **41**, 105-114.
- Vickerman, K., Tetley, L., Hendry, K.A., & Turner, C.M. (1988) Biology of African trypanosomes in the tsetse fly. *Biol.Cell*, **64**, 109-119.
- Vincent, I.M., Creek, D., Watson, D.G., Kamleh, M.A., Woods, D.J., Wong, P.E., Burchmore, R.J., & Barrett, M.P. (2010) A molecular mechanism for eflornithine resistance in African trypanosomes. *PLoS. Pathog.*, **6**, e1001204.
- Vreysen M.J. (2001). Principles of area-wide integrated tsetse fly control using the sterile insect technique. *Med. Trop.* **61** (4-5):397-411
- Wang, C.C. (1995) Molecular mechanisms and therapeutic approaches to the treatment of African trypanosomiasis. *Annu.Rev.Pharmacol. Toxicol.*, **35**, 93-127.
- Wang, Z., Morris, J.C., Drew, M.E., & Englund, P.T. (2000) Inhibition of *Trypanosoma brucei* gene expression by RNA interference using an integratable vector with opposing T7 promoters. *J.Biol. Chem.*, **275**, 40174-40179.
- Ward, C.P., Burgess, K.E., Burchmore, R.J., Barrett, M.P., & de Koning, H.P. (2010) A fluorescence-based assay for the uptake of CPD0801 (DB829) by African trypanosomes. *Mol.Biochem. Parasitol.*, **174**, 145-149.
- Welburn, S.C., Fevre, E.M., Coleman, P.G., Odiit, M., & Maudlin, I. (2001) Sleeping sickness: a tale of two diseases. *Trends Parasitol.*, **17**, 19-24.

- Wenzler T., Boykin D.W., Ismail M.A., Hall J.E., Tidwell R.R. and Brun R. (2009). New treatment option for second-stage African sleeping sickness: *in vitro* and *in vivo* efficacy of aza analogs of DB289. *Antimicrob. Agents Chemother.* **53** (10): 4185-4192
- Williamson, J; (1970) Review of chemotherapeutic and Chemoprophylactic agents. In: Mulligan, H. W. (Ed), *The African Trypanosomiases*. George Allen and Unwin, London, Pp. 125-221.
- Wilson, W.D., Nguyen, B., Tanious, F.A., Mathis, A., Hall, J.E., Stephens, C.E., & Boykin, D.W. (2005) Dications that target the DNA minor groove: compound design and preparation, DNA interactions, cellular distribution and biological activity. *Curr.Med.Chem.Anticancer Agents*, **5**, 389-408.
- Wilson, W.D., Tanious, F.A., Mathis, A., Tevis, D., Hall, J.E., & Boykin, D.W. (2008) Antiparasitic compounds that target DNA. *Biochimie*, **90**, 999-1014.
- Wirtz, E., Leal, S., Ochatt, C., & Cross, G.A. (1999) A tightly regulated inducible expression system for conditional gene knock-outs and dominant-negative genetics in *Trypanosoma brucei*. *Mol.Biochem. Parasitol.*, **99**, 89-101.
- Witola, W.H., Inoue, N., Ohashi, K., & Onuma, M. (2004) RNA-interference silencing of the adenosine transporter-1 gene in *Trypanosoma evansi* confers resistance to diminazene aceturate. *Exp. Parasitol.*, **107**, 47-57.
- World Health Organisation. WHO Model Prescribing Information: Drugs Used in Parasitic Diseases. WHO. 2nd Edition. 1995. Geneva. WHO.
- World Health Organisation. Global Surveillance of Epidemic-prone Infectious Diseases. WHO/CDS/CSR/ISR/2000.1. 2001. Geneva: WHO.
- Zhou, M., Duan, H., Engel, K., Xia, L., & Wang, J. (2010) Adenosine transport by plasma membrane monoamine transporter: reinvestigation and comparison with organic cations. *Drug Metab Dispos.*, **38**, 1798-1805.